



Alfayez, Ibrahim Abdullah (2021) *An investigation of 5-fluorouracil resistance in Leishmania and Trypanosoma species*. PhD thesis.

<http://theses.gla.ac.uk/82057/>

Copyright and moral rights for this work are retained by the author

A copy can be downloaded for personal non-commercial research or study, without prior permission or charge

This work cannot be reproduced or quoted extensively from without first obtaining permission in writing from the author

The content must not be changed in any way or sold commercially in any format or medium without the formal permission of the author

When referring to this work, full bibliographic details including the author, title, awarding institution and date of the thesis must be given

Enlighten: Theses

<https://theses.gla.ac.uk/>
research-enlighten@glasgow.ac.uk

An Investigation of 5-Fluorouracil Resistance in *Leishmania* and *Trypanosoma* species

Ibrahim Abdullah Alfayez

Institute of Infection, Immunity and Inflammation
College of Medical, Veterinary and Life Sciences

This thesis is submitted in fulfilment of the requirements for the
Degree of Doctor of Philosophy

University of Glasgow

September, 2020

Abstract

Leishmaniasis is a parasitic vector-borne disease caused by the *Leishmania* parasite, which resides in female sandflies. African sleeping sickness or African trypanosomiasis is also a parasitic disease but it is spread by the tsetse fly (*Glossina* species). Chagas disease or American trypanosomiasis is a tropical disease caused by *Trypanosoma cruzi* and spread by insects called kissing bugs, *Triatominae*. Drug resistance has been one of the most important obstacles to the treatment of leishmaniasis and trypanosomiasis. For example, there has been evidence of resistance to melarsoprol and pentamidine for gHAT, and eflornithine for late stage HAT particularly in the *T. b. rhodesiense*, and pentavalent antimonials for leishmaniasis. This has limited the treatment options for these diseases. This has limited the treatment options for these diseases. Recent evidence has shown that pyrimidine metabolism is an excellent anti-protozoan drug development target, with multiple enzymes that are genetically essential. Pyrimidine nucleobase and nucleoside analogues have shown promising activity against *Leishmania* and *Trypanosoma* spp. Drugs like 5-fluorouracil and 5-fluoro-2'deoxyuridine are rapidly metabolized by the parasites into metabolic intermediates such as 5F-UDP-glucose, 5F-2'dUMP, 5F-UDP-galactose and 5F-UDP-N-acetylglucosamine, and incorporated into RNA. Pyrimidine analogue 5-FU was found to be a good inhibitor of high-affinity uracil transporters in *T. b. brucei* (TbU1 and TbU3) and *Leishmania* (LmajU1 and LmexU1).

Although the transporters for therapeutically active nucleobase allopurinol and antiparasitic nucleoside analogues have been identified, the transporter for 5-FU is still unknown. However, following the exclusion method, it is concluded that the 5-FU transporter is not an ENT transporter in *Trypanosoma* and *Leishmania* spp. as their ENT transporters have all been cloned and characterised. Hence, our main interest is identifying the transporter gene (family) of kinetoplastids for pyrimidine nucleobases, using the antimetabolite 5-FU as a probe. It is expected that the 5-FU transporter is not of a gene family that has been previously associated with that activity. Resistance to 5-FU was generated in both *T. b. brucei* s427-wild type BSF and *L. mexicana* promastigotes, producing clonal lines *Tbb-5FURes* and *Lmex-5FURes*, respectively. RNA-seq and RIT-seq

analyses of 5-FU resistant cell lines have identified candidate genes for pyrimidine transporters, including genes annotated as cation transporters (*Tbb-CAT1-4*), fatty acid desaturase (*Tbb-FAD* and *Lmex-FAD*) and glucose transporters. Apart from some of the glucose transporters, none of these potential transport genes have been previously characterised in protozoa and as such they are of interest in their own right as well.

Using the Alamar blue assay, the sensitivity to 5-FU in a single knockout of *Tbb-CAT1-4* genes in *T. b. brucei* s427 WT cells was determined, and found to have no significant difference. Also, the results showed that [³H]-uracil uptake in *T. b. brucei* s427 WT + *Tbb-CAT1-4*^{+/-} was almost the same as in wild type cells. Further, according to our results, the overexpression of *Lmex-FAD* gene in *Lmex-5FURes* and *Tbb-FAD* gene in *Tbb-5FURes* did not cause increased sensitivity to 5-FU *in vitro*, and similarly, did not change the rate of transport of [³H]-uracil. Following a full knockout of glucose transporter genes, their sensitivity to 5-FU was determined, revealing a significantly reduced sensitivity of the *LmexGT1-3* double knockout genes in *L. mexicana* to 5-FU, in comparison to the wild type cell lines. Our results also revealed that the *Lmex-GT1-3* KO cells do not accumulate 5-FU and uracil. In the re-expression of single *LmexGT* in *Lmex-GT1-3* KO cells, the sensitivity to 5-FU increased significantly, but not quite back to the level of wild-type cells. After the introduction of the glucose transporter genes, all the three genes did appear to have a very similar ability of functioning with regards to the (regulation of) uptake of 5-FU and uracil, restoring uptake to ~50% of 5-FU and ~30% of uracil uptake of wild type, respectively. It was also discovered that 5-FU and uracil did not have any measurable effects on the transport of glucose by *LmexGT1*, *LmexGT2* and *LmexGT3*, an indication that none of them inhibits the transport of 0.1 μM of [³H]-2-deoxy-D-glucose up to 2.5 mM and therefore, the GTs are not themselves transporting uracil.

We successfully expressed and characterized the FurD transporter in the 5-FU resistant cell lines (*Tbb-5FURes* and *Lmex-5FURes*) in order to investigate whether the sensitivity to 5-FU *in vitro* resistant strains could be restored by the introduction of a confirmed uracil/5-FU transporter. This would allow a functional screening of potential transporter genes. However, we found that the EC₅₀ values of 5-FU of the 5-FU resistant cell lines and the FurD-expressing cell

lines were not significantly different, although the expression of FurD in *Lmex-5FURes* induced a very high level of [³H]-uracil/5-FU uptake, even much above the wild type activity. We also characterised the transport activity of FurD in *Lmex-5FURes* promastigotes, and found FurD to be a highly selective and high-affinity transporter for uracil with K_m of $0.97 \pm 0.17 \mu\text{M}$. Interestingly, our results confirmed that the anticancer drug 5-FU was as good a substrate as uracil for FurD in *Lmex-5FURes*, with a K_i of $0.76 \pm 0.25 \mu\text{M}$.

Using a targeted CRISPR-Cas9 gene knockout strategy, we show that deletion of the *LmexNT1* locus in *L. mexicana-Cas9* promastigotes completely abolished adenosine and thymidine uptake. Moreover, it became highly resistant to tubercidin (and its analogues) and to 5-fluoro-2'-deoxyuridine. We also tested the possibility of using *L. mexicana-Cas9^{ΔNT1}* promastigotes as a surrogate system for the expression of TcrNT2 and TcrNB2 transporters of *T. cruzi*. We found TcrNT2 to be a high-affinity thymidine transporter with a K_m $0.156 \pm 0.017 \mu\text{M}$, while TcrNB2 could not be characterised despite our efforts.

To conclude, the results obtained in this study provide significant contributions to the identification of the pyrimidine transporter genes. The results also increase our understanding of the cytotoxic activity of 5-FU in kinetoplastid parasites, gaining insight into the complex pyrimidine metabolism that occurs in these parasites. In addition, the study shows that pyrimidine transport mechanisms could potentially be exploited as drug carriers against kinetoplastid parasites.

Table of Contents

Abstract	1
Table of Contents.....	4
List of Figures	8
List of Tables	15
Acknowledgement.....	17
Publications and presentations	18
Author's declaration	19
List of abbreviations	20
1 General Introduction	25
1.1 <i>Leishmania</i> and leishmaniasis.....	27
1.1.1 Morphology and life cycle	27
1.1.2 Geographical distribution.....	29
1.1.3 The genome.....	31
1.1.4 Pathology and clinical manifestation	32
1.1.5 Diagnosis	34
1.1.6 Treatment and control of leishmaniases	35
1.1.7 Drug resistance mechanisms	41
1.2 Trypanosomes and trypanosomiasis.....	43
1.2.1 Morphology and life cycle	44
1.2.2 Geographical distribution.....	46
1.2.3 The genome.....	48
1.2.4 Pathology and clinical manifestation	48
1.2.5 Diagnosis	49
1.2.6 Treatment.....	50
1.2.7 Drug resistance mechanisms	56
1.3 Pyrimidine biosynthesis and metabolism in Kinetoplastids.....	58
1.3.1 <i>De novo</i> biosynthesis of uridine monophosphate	58
1.3.2 Pyrimidine salvage and interconversion	60
1.3.3 Classification of membrane transporter proteins	62
1.3.4 Nucleoside and nucleobase transporters in Kinetoplastids	65
1.4 The current understanding of mode of action of 5-FU in Kinetoplastid parasites	73
1.5 The applications of RNA sequencing (RNA-seq) and RNA interference target-sequencing (RIT-seq).....	75
1.6 Metal ion transporters	79
1.7 Glucose transporters	81
1.8 Uracil transporter families in other species	84

1.9	Aims of the study	87
2	Material and Methods.....	89
2.1	Materials	90
2.1.1	Media and media components.....	90
2.1.2	Chemicals including nucleoside and nucleobase analogues	90
2.1.3	Radiolabelled compounds.....	91
2.2	Culturing of kinetoplastid cells.....	91
2.2.1	Culturing of <i>T. b. brucei</i> BSF and PCF	91
2.2.2	Culturing of <i>L. mexicana</i> promastigote form	92
2.2.3	Growth curves	92
2.2.4	Preparation of stabilates	93
2.3	Molecular techniques	93
2.3.1	Polymerase chain reactions PCR.....	93
2.3.2	List of primers for PCR	95
2.3.3	Isolation of genomic DNA	96
2.3.4	Plasmid construction and transfection.....	97
2.3.5	Quantitative real-time PCR (qRT-PCR).....	105
2.4	Drug sensitivity assays using Alamar blue dye.....	107
2.5	Transport assays	109
2.6	Statistics	111
3	Assessment of the role of the <i>T. b. brucei</i> cation transporters in toxicity of 5-FU and heavy metals.....	112
3.1	Introduction	113
3.2	Results.....	115
3.2.1	Knockout of Tbb-CAT1-4 by homologous recombination into <i>T. b. brucei</i> s427-BSF	115
3.2.2	Over-expression of Tbb-CAT1, Tbb-CAT2, Tbb-CAT3, and Tbb-CAT4 in the <i>Tbb-5FURes</i> strain BSF.....	121
3.2.3	Effect of heavy metal ions, ion chelators and a TAO inhibitor on <i>T. b. brucei</i> BSF	127
3.3	Discussion	130
4	Assessment of the role of fatty acid desaturase in <i>T. brucei</i> BSF and <i>L. mexicana</i> promastigotes in 5-FU sensitivity	136
4.1	Introduction	137
4.2	Results.....	138
4.2.1	Over-expression of Tbb-FAD in <i>Tbb-5FURes</i> and <i>Tbb-s427</i> WT BSF ..	138
4.2.2	Over-expression of <i>Lmex</i> -FAD in <i>Lmex-5FURes</i> and <i>L. mexicana</i> -WT promastigotes	145

4.3	Discussion	153
5	Heterologous expression of the <i>Aspergillus nidulans</i> uracil transporter (FurD) in <i>T. b. brucei</i> BSF and <i>L. mexicana</i> promastigotes	156
5.1	Introduction	157
5.2	Results.....	159
5.2.1	Heterologous expression of FurD in <i>Tbb-5FURes</i> BSF	159
5.2.2	The heterologous expression of FurD in <i>Lmex-5FURes</i> promastigotes	164
5.2.3	The heterologous expression of FurD in <i>L. mexicana</i> WT promastigotes	173
5.3	Discussion	176
6	Investigation of glucose transporters in <i>L. mexicana</i> promastigotes in the sensitivity to 5-FU.....	180
6.1	Introduction	181
6.2	Results.....	183
6.2.1	The assessment of growth rate of <i>Lmex-GT1-3</i> KO in the presence and absence of 5 mM L-proline.....	183
6.2.2	Drug sensitivity assay with 5-FU in the presence and absence of 5 mM L-proline.....	184
6.2.3	Transport assays with 5-fluorouracil, uracil, 2-deoxy-D-glucose and pentamidine	186
6.2.4	The evaluation of 5-FU EC ₅₀ of <i>L. mexicana</i> in normal and glucose free medium.....	190
6.2.5	Re-expression of <i>LmexGT1</i> , <i>LmexGT2</i> and <i>LmexGT3</i> into <i>Lmex-GT1-3</i> KO promastigotes	191
6.2.6	<i>Trypanosoma brucei brucei</i> s427-WT procyclic form	201
6.3	Discussion	204
7	Cloning and functional expression of <i>T. cruzi</i> ENT in <i>L. mexicana-Cas9^{ΔNT1}</i> promastigotes.....	209
7.1	Introduction	210
7.2	Results.....	212
7.2.1	PCR and qRT-PCR confirmation of knockout of NT1 in <i>L. mexicana-Cas9</i> by using CRISPR technique	212
7.2.2	Confirmation of tubercidin resistance phenotype in <i>L. mexicana-Cas9^{ΔNT1}</i>	215
7.2.3	Confirmation of the abolition of adenosine and thymidine uptake in <i>L. mexicana-Cas9^{ΔNT1}</i>	216
7.2.4	The heterologous expression of <i>TcrNT2</i> in <i>L. mexicana-Cas9^{ΔNT1}</i>	218
7.2.5	The heterologous expression of <i>TcrNB2</i> in <i>L. mexicana-Cas9^{ΔNT1}</i>	229

7.2.6 The introduction of the <i>T. cruzi</i> NB2 in <i>Lmex-5FURes</i> promastigotes	237
7.2.7 The introduction of TcrNB2 transporter in the <i>T. b. brucei</i> B48 strain	239
7.3 Discussion	243
8 General discussion	248
Appendices	261
References	272

List of Figures

Figure 1.1: Classification of the kinetoplastids.	26
Figure 1.2: Schematic representation of promastigotes (left) and amastigotes (right) of <i>Leishmania</i> parasites.	28
Figure 1.3: Life cycle of <i>Leishmania</i> parasites. Image taken from.....	29
Figure 1.4: Worldwide geographic distribution of leishmaniasis. A) Visceral leishmaniasis and B) Cutaneous leishmaniasis.	31
Figure 1.5: The genomic distribution of 36 chromosomes that have been assembly from <i>L. donovani</i>	32
Figure 1.6: Morphology of <i>Trypanosoma brucei</i>	45
Figure 1.7: The life cycle of Africa trypanosomes in insect vector and mammalian host.	46
Figure 1.8: Epidemiology of Human African trypanosomiasis.....	47
Figure 1.9: Schematic representation showing some of the structures and the main transport proteins involve in the uptake of the commonly available anti-trypanosomal drugs for the <i>T. brucei</i>	58
Figure 1.10: Pyrimidine biosynthesis pathways	60
Figure 1.11: Pyrimidine salvage pathways.....	61
Figure 1.12: Interconversions of pyrimidines.....	62
Figure 1.13: Transmembrane topologies of mammalian members of the CNT and ENT families.....	65
Figure 1.14: Possible biochemical linkages between 5-FU toxicity and damage to RNA and DNA in A) <i>T. brucei</i> and B) <i>Leishmania</i> spp.	75
Figure 1.15: Predicted topology and subcellular localisation of the metal ion transporter proteins of the ZIP family	81
Figure 1.16: The structure of the <i>E. coli</i> uracil transporter UraA.....	87
Figure 2.1: Linear map of pHD1336 plasmid.	99
Figure 2.2: Linear plasmid map of pNUS-HcN.	100
Figure 2.3: The plasmid construct for the knockout of four cation transporter genes (CATs) in <i>T. b. brucei</i> s427-WT.	101
Figure 2.4: The plasmid maps of (A) pTBlast and (B) pTPuro constructs for the knockout of the target locus of NT1 in <i>L. mexicana</i> -Cas9 promastigotes by using CRISPR technique.....	105

Figure 3.1: Knockout strategy used for the replacement of the genomic locus on chromosome 11 containing a tandem array of four cation transporter genes (<i>Tbb-CAT1-4</i>).	116
Figure 3.2: Confirmation for single KO of CATs integration by PCR after transfection into <i>T. b. brucei</i> WT s427 cell line by amplification of the antibiotic resistance genes.	117
Figure 3.3: The expression levels of sKO of <i>Tbb-CAT1-4</i> genes with three antibiotic cassettes in <i>Tbb-s427</i> WT determined by qRT-PCR and compared to the control.	118
Figure 3.4: The growth curve of <i>Tbb-s427</i> WT and <i>Tbb-WT + TbbCAT1-4 sKO</i> with three antibiotic cassettes on HMI-9 medium supplemented with 10% FBS.....	119
Figure 3.5: The averages of EC ₅₀ values of <i>Tbb-s427</i> WT and <i>Tbb-s427WT + Tbb-CAT1-4 sKO</i> with three antibiotic cassettes to A) 5-fluorouracil, B) 6-Azauracil and C) Pentamidine determined by using the alamar blue assay.	120
Figure 3.6: [³ H]-Uracil transport by <i>Tbb-s427</i> WT and <i>Tbb-s427WT + Tbb-CAT1-4^{+/-}</i>	121
Figure 3.7: Schematic representations of pHDK199, pHDK200, pHDK201 and pHDK202 plasmids.	122
Figure 3.8: PCR confirmation for the linearity of pHDK199, pHDK200, pHDK201 and pHDK202 plasmids and the present of <i>Tbb-CAT1</i> , <i>Tbb-CAT2</i> , <i>Tbb-CAT3</i> and <i>Tbb-CAT4</i> genes into <i>Tbb-5FURes</i> strain after transfection.	123
Figure 3.9: The expression levels of <i>Tbb-CAT1</i> , <i>Tbb-CAT2</i> , <i>Tbb-CAT3</i> , and <i>Tbb-CAT4</i> in <i>Tbb-5FURes</i> strain (BSF) and compared to the <i>Tbb-5FURes</i> determined by qRT-PCR.....	124
Figure 3.10: The growth assay of <i>Tbb-5FURes</i> , <i>Tbb-5FURes + Tbb-CAT1^{0.e}</i> , <i>Tbb-5FURes + Tbb-CAT2^{0.e}</i> , <i>Tbb-5FURes + Tbb-CAT3^{0.e}</i> and <i>Tbb-5FURes + Tbb-CAT4^{0.e}</i> on HMI-9 medium supplemented with 10% FBS.	125
Figure 3.11: Effect of overexpression of <i>Tbb-CAT1</i> , <i>Tbb-CAT2</i> , <i>Tbb-CAT3</i> and <i>Tbb-CAT4</i> on sensitivity of <i>Tbb-5FURes</i> strain to A) 5-fluorouracil, B) 6-Azauracil and C) Pentamidine determined by using the alamar blue assay.	126
Figure 3.12: [³ H]-Uracil uptake in <i>T. brucei</i> strains. The uptake of 0.1 μM of [³ H]-uracil over 10 minutes by <i>Tbb-s427WT</i> , <i>Tbb-5FURes</i> and <i>Tbb-5FURes + Tbb-CAT1^{0.e}</i> , <i>Tbb-5FURes + Tbb-CAT2^{0.e}</i> , <i>Tbb-5FURes + Tbb-CAT3^{0.e}</i> and <i>Tbb-5FURes + Tbb-CAT4^{0.e}</i>	127
Figure 4.1: Plasmid map of pHDK219 vector for the homologous expression of <i>Tbb-FAD</i> gene in <i>Tbb-5FURes</i> and <i>Tbb-s427WT</i> strain.	140
Figure 4.2: Digestion of pHDK219 plasmid by <i>MluI</i> and <i>BamHI</i> restriction enzymes to drop out <i>Tbb-FAD</i> gene from the pHDK219 plasmid.	140
Figure 4.3: PCR confirmation for the linearity of pHDK219 vector and the integration of <i>Tbb-FAD</i> gene into <i>Tbb-5FURes</i> strain after transfection.	140

Figure 4.4: PCR confirmation for the linearity of pHDK219 vector and the integration of <i>Tbb-FAD</i> gene into <i>Tbb-s427WT</i> strain after transfection.	141
Figure 4.5: Quantitative RT-PCR of <i>Tbb-FAD</i> gene expression in the <i>Tbb-5FURes</i> and <i>Tbb-s427WT</i> strains.	142
Figure 4.6: The growth rates of <i>Tbb-5FURes</i> and <i>Tbb-s427WT</i> strains expressing <i>Tbb-FAD</i>	143
Figure 4.7: Alamar blue drug sensitivity assay of overexpression of <i>Tbb-FAD</i> gene in <i>Tbb-5FURes</i> clones 1-3 and <i>Tbb-5FURes</i> by using 5-fluorouracil (A), 6-azauracil (B) and pentamidine (C).	144
Figure 4.8: Alamar blue drug sensitivity assay of overexpression of <i>Tbb-FAD</i> gene in <i>Tbb-s427WT</i> clones 1-3 and <i>Tbb-s427WT</i> by using 5-fluorouracil (A), 6-azauracil (B) and pentamidine (C).	144
Figure 4.9: Transport of 0.1 μ M of [³ H]-uracil by <i>Tbb-s427 WT</i> , <i>Tbb-5FURes</i> , <i>Tbb-s427WT + Tbb-FAD^{o.e}</i> and <i>Tbb-5FURes + Tbb-FAD^{o.e}</i> was measured over 3 min .	145
Figure 4.10: Plasmid map of pHDK220 vector for the homologous expression of <i>Tbb-FAD</i> gene in <i>Lmex-5FURes</i> and <i>L. mexicana</i> WT strains.	147
Figure 4.11: Digestion of pHDK220 plasmid by <i>NdeI</i> and <i>BglII</i> restriction enzymes to drop out <i>Lmex-FAD</i> gene from the pHDK220 plasmid.	147
Figure 4. 12: PCR Confirmation of the presence of <i>Lmex-FAD</i> gene into <i>Lmex-5FURes</i> and <i>L. mexicana</i> WT after transfection.	147
Figure 4.13: The expression levels of <i>Lmex-FAD</i> gene in <i>Lmex-5FURes</i> and <i>L. mexicana</i> -WT.	148
Figure 4.14: Alamar blue drug sensitivity assay for overexpression of <i>Lmex-FAD</i> gene in <i>Lmex-5FURes</i> clones 1-3 using 5-fluorouracil (A) and pentamidine was used as a positive control (B).	149
Figure 4.15: Alamar blue drug sensitivity assay of <i>L. mexicana</i> wild type and overexpression of <i>Lmex-FAD</i> gene in <i>L. mexicana</i> WT clones 1-3 using 5-fluorouracil (A) and pentamidine was used as a positive control (B).	150
Figure 4.16: The drug sensitivity assay of <i>Lmex-5FURes</i> and <i>Lmex-5FURes + Lmex-FAD</i> clones 1-3 to Amphotericin B (A) and Miltefosine (B).	151
Figure 4.17: The drug sensitivity assay of the <i>L. mexicana</i> wild type and <i>L. mexicana</i> WT + <i>Lmex-FAD^{o.e}</i> clones 1-3 to mphotericin B (A) and Miltefosine (B).	152
Figure 4.18: Transport of 0.1 μ M of [³ H]-uracil by <i>L. mexicana</i> -WT, <i>Lmex-5FURes</i> , <i>Lmex-WT + Lmex-FAD^{o.e}</i> and <i>Lmex-5FURes + Lmex-FAD^{o.e}</i> was measured over 8 minutes.	153
Figure 5.1: Plasmid map of pHDK069 vector for the heterologous expression of <i>Aspergillus nidulans</i> uracil transporter gene (<i>FurD</i>) in <i>Tbb-5FURes</i>	160
Figure 5.2: PCR confirmation for the linearity of pHDK069 plasmid and the integration of <i>FurD</i> gene into <i>Tbb-5FURes</i> strain after transfection.	160

Figure 5.3: The expression levels of <i>FurD</i> gene in <i>Tbb-5FURes</i> and compared to the control (<i>Tbb-5FURes</i>) determined by qRT-PCR.	161
Figure 5.4: The growth curve of <i>Tbb-5FURes</i> and <i>Tbb-5FURes</i> expressing <i>FurD</i> clones 1, 2 and 3 on HMI-9 medium supplemented with 10% FBS.	161
Figure 5.5: Alamar blue drug sensitivity assay of expression of <i>FurD</i> gene in <i>Tbb-5FURes</i> using 5-fluorouracil (A), 6-azauracil (B) and pentamidine (C).	163
Figure 5.6: [³ H]-Uracil transport by <i>Tbb-s427WT</i> , <i>Tbb-5FURes</i> and <i>Tbb-5FURes</i> expressing <i>FurD</i>	164
Figure 5.7: Plasmid map of pHDK254 vector for the heterologous expression of <i>Aspergillus nidulans</i> uracil transporter <i>FurD</i> in <i>Lmex-5FURes</i> and <i>L. mexicana</i> wild-type.	165
Figure 5.8: Restriction digest products for pHDK254 plasmid with <i>XhoI</i> and <i>BglII</i> to release <i>FurD</i>	166
Figure 5.9: Confirmation of the presence of <i>FurD</i> gene into <i>Lmex-5FURes</i> strain after transfection.	166
Figure 5.10: The expression levels of <i>FurD</i> gene in <i>Lmex-5FURes</i> and compared to the control (<i>Lmex-5FURes</i>) determined by qRT-PCR.	167
Figure 5.11: Alamar blue drug sensitivity assay of expression of <i>FurD</i> gene in <i>Lmex-5FURes</i> by using 5-fluorouracil (A), 6-azauracil (B) and pentamidine (C).	168
Figure 5.12: Radiolabelled uracil transport by <i>L. mexicana</i> -WT and <i>Lmex-5FURes</i>	169
Figure 5.13: [³ H]-Uracil and [³ H]-5-Fluorouracil transport by <i>Lmex-5FURes</i> and <i>Lmex-5FURes</i> expressing <i>FurD</i>	170
Figure 5.14: [³ H]-Uracil and [³ H]-5-Fluorouracil transport by <i>Lmex-5FURes</i> expressing <i>FurD</i> over 10 minutes and 60 seconds.	171
Figure 5.15: Inhibition of 0.1 μ M of [³ H]-uracil over 10 seconds.	172
Figure 5.16: Confirmation of the presence of <i>FurD</i> gene into <i>L mexicana</i> -WT strain after transfection.	174
Figure 5.17: The expression levels of <i>FurD</i> gene in <i>L mexicana</i> -WT and compared to the control (<i>L mexicana</i> -WT) determined by qRT-PCR.	174
Figure 5.18: Alamar blue drug sensitivity assay of expression of <i>FurD</i> gene in <i>L mexicana</i> -WT by using 5-fluorouracil (A), 6-azauracil (B) and pentamidine (C).	175
Figure 5.19: [³ H]-5-Fluorouracil transport by <i>L mexicana</i> -WT and <i>L mexicana</i> -WT expressing <i>FurD</i>	176
Figure 6.1: Knockout strategy used for the replacement of the genomic <i>locus</i> on chromosome 20 containing a <i>tandem</i> array of three glucose transporter genes (<i>LmexGT1-3</i>).	183

Figure 6.2: The growth curves of <i>L. mexicana</i> WT, <i>Lmex-5FURes</i> and <i>L.mex-1-3</i> KO on HOMEM medium supplemented with 10% FBS and incubated at 25 °C. ..	184
Figure 6.3: The biphasic inhibition curve of <i>L. mexicana</i> WT promastigotes against 5-fluorouracil by using the Alamar blue fluorescent dye as a proxy for the cell number.....	186
Figure 6.4: The Alamar blue drug sensitivity assay of <i>L. mexicana</i> WT, <i>Lmex-5FURes</i> , <i>L.mex-GT1-3</i> KO using 5-fluorouracil (A) and pentamidine (B).	186
Figure 6.5: [³ H]-Uracil and [³ H]-5-Fluorouracil transport were performed in parallel on the same day by <i>L. mexicana</i> -WT and <i>Lmex-GT1-3</i> KO.	188
Figure 6.6: [³ H]-Pentamidine transport by <i>L. mexicana</i> -WT and <i>Lmex-GT1-3</i> KO.	188
Figure 6.7: [³ H]-2-deoxy-D-glucose transport by <i>L mexicana</i> -WT, <i>Lmex-5FURes</i> and <i>Lmex-GT1-3</i> KO.	190
Figure 6.8: The Alamar blue drug sensitivity assay of <i>L. mexicana</i> -WT, <i>Lmex-5FURes</i> and <i>L mexicana</i> -WT in glucose free medium using 5-fluorouracil (A) and pentamidine (B).	191
Figure 6.9: Alamar blue drug sensitivity assay of re-expression of glucose transporter genes (<i>LmexGT1</i> , <i>LmexGT2</i> and <i>LmexGT3</i>) in <i>Lmex-GT1-3</i> KO by using 5-fluorouracil (A) and pentamidine (B).....	192
Figure 6.10: [³ H]-Uracil and [³ H]-5-Fluorouracil transport by <i>L mexicana</i> -WT, <i>Lmex-GT1-3</i> KO and re-expression of each glucose transporter genes (<i>LmexGT1</i> , <i>LmexGT2</i> and <i>LmexGT3</i>) in <i>Lmex-GT1-3</i> KO.....	194
Figure 6.11: Inhibitory effect of various concentrations of unlabelled glucose, unlabelled uracil and unlabelled 5-fluorouracil on the uptake of 0.1 µM of [³ H]-2-deoxy-D-glucose over 30 seconds by <i>Lmex-GT1-3</i> KO + <i>LmexGT1</i> (A), <i>Lmex-GT1-3</i> KO + <i>LmexGT2</i> (B) and <i>Lmex-GT1-3</i> KO + <i>LmexGT3</i> (C).	196
Figure 6.12: Confirmation of the presence of <i>FurD</i> gene into <i>Lmex-GT1-3</i> KO strain after transfection.....	198
Figure 6.13: The expression levels of <i>FurD</i> gene in <i>Lmex-GT1-3</i> KO and compared to the control (<i>Lmex-GT1-3</i> KO) determined by qRT-PCR.	199
Figure 6.14: Alamar blue drug sensitivity assay of expression of <i>FurD</i> gene in <i>Lmex-GT1-3</i> KO and <i>L. mexicana</i> by using 5-fluorouracil (A) and pentamidine (B).	200
Figure 6.15: [³ H]-5-Fluorouracil transport by <i>L. mexicana</i> -WT, <i>Lmex-GT1-3</i> KO and <i>Lmex-GT1-3</i> KO + <i>FurD</i>	201
Figure 6.16: The growth rate of <i>T. b. brucei</i> -s427 wild type PCF on SDM-79 medium supplemented with 10% FBS, 0.6 g/L proline, and 1 g/L glucose 'standard condition', 0.2 g/L D-glucose and D-glucose free.	202
Figure 6.17: The biphasic inhibition curve of <i>T. b. brucei</i> -s427 wild type PCF against 6-azauracil by using the Alamar blue fluorescent dye as a representative for the cell number.	203

Figure 6.18: The Alamar blue drug sensitivity assay of <i>T. b. brucei</i> -s427 wild type PCF on SDM-79 medium supplemented with 10% FBS, 0.6 g/L of proline and three different growth conditions for glucose using 5-fluorouracil (A), 6-azauracil (B) and pentamidine (C).	204
Figure 7.1: Workflow of CRISPR-Cas9 rapid gene knockout used for the replacement of the <i>NT1</i> locus on chromosome 15 containing a <i>tandem</i> array of two nucleoside transporter 1 genes in <i>L. mexicana</i> -Cas9.	213
Figure 7.2: PCR amplification of 5' sgRNA-NT1 and 3' sgRNA-NT1 templates for knockout of <i>NT1</i> locus in <i>L. mexicana</i> -Cas9; and PCR amplification of blasticidin and puromycin resistance markers.....	214
Figure 7.3: PCR validation of knockout of <i>NT1</i> region in <i>L. mexicana</i> -Cas9 by using CRISPR-Cas9 system.	215
Figure 7.4: The expression levels of NT1 in <i>L. mexicana</i> -Cas9 ^{ΔNT1} compared to the control (<i>L. mexicana</i> -Cas9) determined by qRT-PCR.....	215
Figure 7.5: Alamar blue drug sensitivity assay of the deletion of LmexNT1 in <i>L. mexicana</i> -cas9 by using tubercidin (A) and pentamidine (B) as positive control.	216
Figure 7.6: [³ H]-Adenosine and [³ H]-Thymidine transport by <i>L. mexicana</i> -cas9 and <i>L. mexicana</i> -Cas9 ^{ΔNT1}	218
Figure 7.7: Plasmid map of pHDK270 vector for the heterologous expression of <i>T. cruzi</i> high-affinity thymidine transporter (TcrNT2) in <i>L. mexicana</i> -Cas9 ^{ΔNT1} cells.	219
Figure 7.8: Restriction digest products for pHDK270 plasmid and confirmation of the presence of <i>TcrNT2</i> gene into <i>L. mexicana</i> -Cas9 ^{ΔNT1} cells after transfection.	219
Figure 7.9: The growth rate of <i>L. mexicana</i> -Cas9 and <i>L. mexicana</i> -Cas9 ^{ΔNT1} and <i>L. mexicana</i> -Cas9 ^{ΔNT1} expressing <i>TcrNT2</i> on HOMEM medium supplemented with 10% FBS at 25° C.....	220
Figure 7.10: [³ H]-Adenosine transport was by <i>L. mexicana</i> -Cas9, <i>L. mexicana</i> -Cas9 ^{ΔNT1} and <i>L. mexicana</i> -Cas9 ^{ΔNT1+TcrNT2}	223
Figure 7.11: [³ H]-Thymidine transport was by <i>L. mexicana</i> -cas9, <i>L. mexicana</i> -Cas9 ^{ΔNT1} and <i>L. mexicana</i> -Cas9 ^{ΔNT1+TcrNT2} over 3 and 10 minutes.....	224
Figure 7.12: <i>K_m</i> and <i>V_{max}</i> measurement for <i>TcrNT2</i> upon expression by <i>L. mexicana</i> -Cas9 ^{ΔNT1} cell lines.	225
Figure 7.13: Affinity of <i>TcrNT2</i> for thymidine and adenosine analogues.....	227
Figure 7.14: Plasmid map of pHDK271 vector for the expression of <i>T. cruzi</i> NB2 transporter (TcrNB2) in <i>L. mexicana</i> -Cas9 ^{ΔNT1} cell lines.	230
Figure 7.15: Restriction digest products for pHDK271 plasmid and confirmation of the presence of <i>TcrNB2</i> gene into <i>L. mexicana</i> -Cas9 ^{ΔNT1} cells after transfection.	230

Figure 7.16: The growth rates of <i>L. mexicana</i> -Cas9, <i>L. mexicana</i> -Cas9 ^{ΔNT1} and three clones of <i>L. mexicana</i> -Cas9 ^{ΔNT1} expressing <i>TcrNB2</i> on HOME medium supplemented with 10% FBS.	231
Figure 7.17: The expression levels of <i>TcrNB2</i> gene in <i>L. mexicana</i> -Cas9 ^{ΔNT1} compared to the control (<i>L. mexicana</i> -Cas9 ^{ΔNT1}) determined by qRT-PCR.....	232
Figure 7.18: Alamar blue drug sensitivity assay of expression of <i>TcrNB2</i> in <i>L. mexicana</i> -Cas9 ^{ΔNT1} clones 1-3 using 5-fluorouracil (A) and pentamidine (B).	235
Figure 7.19: [³ H]-Adenosine, [³ H]-Adenine and [³ H]-Uracil transport by <i>L. mexicana</i> -Cas9, <i>L. mexicana</i> -Cas9 ^{ΔNT1} and <i>L. mexicana</i> -Cas9 ^{ΔNT1+TcrNB2}	236
Figure 7.20: Confirmation of the presence of <i>TcrNB2</i> gene into <i>Lmex-5FURes</i> strain after transfection.....	238
Figure 7.21: The expression levels of <i>TcrNB2</i> gene in <i>Lmex-5FURes</i> and compared to the control (<i>Lmex-5FURes</i>) determined by qRT-PCR.....	238
Figure 7.22: Alamar blue drug sensitivity assay of expression of <i>TcrNB2</i> gene in <i>Lmex-5FURes</i> clones 1-3 by using 5-fluorouracil (A), pentamidine (B) and diminazene aceturate (C).	239
Figure 7.23: Plasmid map of pHDK223 vector for the heterologous expression of <i>TcrNB2</i> gene in <i>B48</i>	240
Figure 7.24: PCR conformation for the linearisation of the circular pHDK223 plasmid and the integration of <i>TcrNB2</i> gene into <i>B48</i> strain after transfection.	240
Figure 7.25: The expression levels of <i>TcrNB2</i> gene in <i>B48</i> cells and compared to the control (<i>B48</i>) determined by qRT-PCR.....	241
Figure 7.26: The growth curve of <i>B48</i> cell lines and <i>B48</i> expressing <i>TcrNB2</i> clones 1-3 on HMI-9 medium supplemented with 10% FBS.	242
Figure 7.27: Alamar blue drug sensitivity assay of expression of <i>TcrNB2</i> gene in <i>B48</i> clones 1-3, <i>B48</i> strain and <i>Tbb-s427WT</i> by using pentamidine (A) and diminazene aceturate (B).	243

List of Tables

Table 1.1: Kinetic parameters of <i>Leishmania</i> species purine and pyrimidine transporters.	67
Table 1.2: Kinetic parameters of <i>T. brucei</i> purine and pyrimidine transporters.	71
Table 1.3: Kinetic parameters of <i>T. cruzi</i> purine and pyrimidine transporters.	72
Table 2.1: The PCR master mix for Phusion High-Fidelity DNA Polymerase.	94
Table 2.2: The PCR condition for Phusion High-Fidelity DNA Polymerase.	94
Table 2.3: The PCR master mix for GoTaq DNA Polymerase.	94
Table 2.4: The PCR condition for GoTaq DNA Polymerase.	94
Table 2.5: Oligonucleotides designed and used in this project.	95
Table 2.6: The list of primers that are designed and used to generate <i>NT1</i> KO in <i>L. mexicana-Cas9</i>	102
Table 2.7: The PCR reaction that was prepared for the amplification of 5' and 3' sgRNA.	102
Table 2.8: The programme that was used for the amplification of 5' and 3' sgRNA by using PCR.	103
Table 2.9: The PCR reaction that was prepared for the amplification of pTBlast and pTPuro plasmids.	103
Table 2.10: The programme that was used for the amplification pTBlast and pTPuro plasmids by using PCR.	103
Table 2.11: The list of primers that designed and used in qRT-PCR.	107
Table 3.1: Annotation of cation transporter genes in the genome of <i>T. b. brucei</i> s427 wild type.	114
Table 3.2: Amino acid sequence identity calculated between Tbb-CAT1, Tbb-CAT2, Tbb-CAT3, Tbb-CAT4, hZIP2 and zntA.	114
Table 3.3: Effect of Heavy metal ions, Salicylhydroxamic acid (SHAM) and Deferoxamine (DFOA) on <i>Trypanosoma brucei brucei</i> (BSF).	129
Table 4.1: Annotation of fatty acid desaturase genes in the genome of <i>T. b. brucei</i> s427 WT BSF and <i>L. mexicana</i> M379 promastigote form.	138
Table 5.1: The amino acid sequence identity of the FurD uracil transporter of <i>A. nidulans</i> with uracil transporters in other species.	158
Table 5.2: Transport of uracil in <i>Lmex-5FURes</i> expressing <i>Aspergillus nidulans</i> FurD.	172

Table 6.1: K_i for various concentrations of glucose, uracil and 5-fluorouracil on the uptake of 0.1 μM of [^3H]-2-deoxy-D-glucose over 30 seconds by *Lmex-GT1-3* KO + *LmexGT1*, *Lmex-GT1-3* KO + *LmexGT2* and *Lmex-GT1-3* KO + *LmexGT3* ..197

Table 7.1: Annotation of the nucleoside transporter 1 (*LmexNT1*) in the genome of *L. mexicana* M379 promastigote form.....212

Table 7.2: The EC_{50} of different adenosine analogues and 5-fluoro-2'-deoxyuridine (pyrimidine analogue) on *L. mexicana-Cas9*, *L. mexicana-Cas9 ΔNT1* and *L. mexicana-Cas9 $\Delta\text{NT1+TcrNT2}$* promastigotes, obtained from drug sensitivity assay.....221

Table 7.3: K_i for pyrimidine nucleosides and adenosine analogues on the transport of [^3H]-thymidine by *TcrNT2* into *L. mexicana-Cas9 ΔNT1*228

Table 7.4: The EC_{50} sensitivity values of *L. mexicana-cas9*, *L. mexicana-Cas9 ΔNT1* and *L. mexicana-Cas9 $\Delta\text{NT1+TcrNB2}$* promastigotes to various adenosine analogues, obtained from drug sensitivity assay233

Acknowledgement

Before all, all thanks and praises are due to Allah (SWT) whom without his mercy and constant support, this work would have never been possible.

I would like to express my sincere gratitude to my supervisor **Prof. Harry de Koning** for valuable advice and endless support throughout the entire project. Through his guidance, support, motivation, encouragement, attention and patience, I have learned valuable skills to produce the outcomes of this thesis. I am proud to have worked under his supervision.

I would like to thank my assessors, Prof. Mike Barrett and Dr. Lisa Ranford-Cartwright, for their advice and support. Special thanks to Dr. Richard Burchmore for your help during this work.

Big thanks to the members of the Harry de Koning group and Mike Barrett group (previous and current members) who contribute to this project for their collaboration and support.

Thank you to all office staffs, technicians and Lab groups of the Institute of Infection, Immunity and Inflammation of the School of Life Sciences at University of Glasgow. Further to this, I would also like to thank the Ministry of Health and Ministry of Education in Saudi Arabia for the provision of the grant to support my studies.

Last, but not least, from my heart with love, I would like to thank my mother Hessa (RIP) and my father Abdullah for their pray and encouragements throughout my life. These thanks also go to my beautiful kids, my son Abdullah, and my daughter Danah for their patience. Also, many thanks to my wife's family for their help and support during my study and writing-up my thesis.

Finally, I would like to acknowledge my wonderful wife, Mshael (may Allah be merciful to her), for her support over the last years. She was my rock, and always supported my decisions, helped me in every possible way, and created a peaceful and loving atmosphere at home. I was hoping that my wife still lives to proudly see her husband get his PhD before she passed away this year.

Publications and presentations

Publications:

Hulpia, F., Bouton, J., Campagnaro, G. D., **Alfayez, I. A.**, Mabile, D., Maes, L., de Koning, H. P. , Caljon, G. and Van Calenbergh, S. (2020) C6-O-alkylated 7-deazainosine nucleoside analogues: Discovery of potent and selective anti-sleeping sickness agents. *European Journal of Medicinal Chemistry*, 188, 112018. (doi: 10.1016/j.ejmech.2019.112018) (PMID:31931339).

HULPIA, F., CAMPAGNARO, G. D., ALZHRANI, K. J., **ALFAYEZ, I. A.**, UNGOGO, M. A., MABILLE, D., MAES, L., DE KONING, H. P., CALJON, G. & VAN CALENBERGH, S. 2020. Structure-activity relationship exploration of 3'-deoxy-7-deazapurine nucleoside analogues as anti-*Trypanosoma brucei* agents. *ACS Infectious Diseases*. (DOI: 10.1021/acsinfecdis.0c00105) (PMID: 32568511).

Nvau, J.B., Alenezi, S., Ungogo, M.A., **Alfayez, I.A.**, Natto, M.J., Gray, A.I., Ferro, V.A., Watson, D.G., De Koning, H.P. and Igoli, J.O., 2020. Antiparasitic and cytotoxic activity of bokkosin, a novel diterpene-substituted chromanyl benzoquinone from *Calliandra portoricensis*. *Frontiers in Chemistry*, 8.

Presentations:

Alfayez, I. A., & De Koning, H. P. (2019) Investigation of glucose transporters in *L. mexicana* promastigotes in the sensitivity to 5-Fluorouracil (**Oral presentation**), Research Update Meeting (RUM), Wellcome Centre for Integrative Parasitology, Institute of Infection, Immunity & Inflammation, University of Glasgow, Scotland, UK, 4th October 2019.

Alfayez, I. A., Alzahrani, K. J., Ali, J. A & De Koning, H. P. (2018) An Investigation of 5-Fluorouracil Resistance in Kinetoplast Parasites (**Poster presentation**), British Society for Parasitology Spring meeting, University of Aberystwyth, Aberystwyth, Wales, UK, 8th April -11th April 2018.

Alfayez, I. A., Alzahrani, K. J., Ali, J. A & De Koning, H. P. (2018) An Investigation of 5-Fluorouracil Resistance in *T. b. brucei* and *L. mexicana* 5FU-resistant cell lines (**Poster presentation**), Scottish Universities Life Sciences Alliance (SULSA), SULSA's Antimicrobial Resistance Conference, University of Strathclyde, Glasgow, Scotland, UK, 26th - 27th April 2018.

Alfayez, I. A., G. Diallinas, & De Koning, H. P. (2019) Functional expression of *Aspergillus nidulans* uracil transporter gene in *T. b. brucei* and *L. mexicana* 5FU-resistant cell lines (**Poster presentation**), British Society for Parasitology Spring meeting, University of Manchester, Manchester, England, UK, 15th April -18th April 2019.

Author's declaration

I hereby declare that this thesis and the results presented here are my own work, except where otherwise stated and acknowledged. This work contains no material submitted to obtain any other degree at any University.

Ibrahim Abdullah Alfayez

List of abbreviations

× g	Relative centrifugal force (RCF)
°C	Degree Celsius
³ H	Tritium
AAT	Animal African Trypanosomiasis
AB	Assay buffer
ABC	ATP-binding cassette transporters
ACT	Aspartate carbamoyltransferase
Ado	Adenosine
ADE	Adenine
ADP	Adenosine diphosphate
AU	Azauracil
AmB	Amphotericin B
AMP	Adenosine monophosphate
ATP	Adenosine triphosphate
bp	Base pair
BSF	Bloodstream form
CATT	Card Agglutination Test for Trypanosomiasis
CAT	Cation transporter
CDP	Cytosine diphosphate
Ci/mmol	Curies per millimole
CL	Cutaneous leishmaniasis
CNS	Central nervous system
CNT	Concentrative nucleoside transporter
CPS II	Glutamine dependent Carbamoylphosphate Synthase II
CSF	Cerebrospinal fluid
DFOA	Deferoxamine
DFMO	D,L-α-difluoromethyl ornithine
dH ₂ O	distilled water
DNA	Deoxyribonucleic acid
dNTP	Deoxynucleotide triphosphates
DMSO	Dimethyl Sulfoxide
DHO	Dihydroorotase

DHOH	Dihydroorotate Dehydrogenase
<i>E. coli</i>	<i>Escherichia coli</i>
EC ₅₀	Half maximal effective concentration
ENT	Equilibrative nucleoside transporter
FAD	Fatty acid desaturase
FBS	Fetal bovine serum
FDA	Food and Drug Administration Agency
FU	Fluorouracil
FurD	<i>Aspergillus nidulans</i> uracil transporter
FURes	Resistant line to 5-fluorouracil
gDNA	Genomic DNA
GDP	Guanosine diphosphate
GFP	Green Fluorescent Protein
GPI	Glycophosphatidylinositol
h	Hour
HAPT	High affinity pentamidine transporter
HAT	Human African Trypanosomiasis
HIV	Human immunodeficiency virus
HMI-9	Hirumi's medium 9
HOMEM	Eagle's minimal essential medium
<i>HYG</i>	Hygromycin resistance gene
IC ₅₀	50% inhibitory concentration
Kb	Kilobase
Kg	Kilo gram
K_i	Inhibitor constants
K_m	Michaelis constant
KO	Knockout
L	Litter
LB	Luria broth
LdNT	<i>Leishmania donovani</i> nucleoside transporter
LHPT	Low affinity pentamidine transporter
LmajNT	<i>Leishmania major</i> nucleoside transporter
LmajU	<i>Leishmania major</i> uracil transporter
<i>Lmex-FAD</i>	<i>Leishmania mexicana</i> fatty acid desaturase gene

LmexNT	<i>Leishmania mexicana</i> nucleoside transporter
LmexU	<i>Leishmania mexicana</i> uracil transporter
LmexGT1	<i>Leishmania mexicana</i> glucose transporter 1 gene
LmexGT2	<i>Leishmania mexicana</i> glucose transporter 2 gene
LmexGT3	<i>Leishmania mexicana</i> glucose transporter 3 gene
M	Molar
MCL	Mucocutaneous leishmaniasis
mg	Milligram
µg	Microgram
min	Minute
mL	millilitre
µL	Microlitre
mM	Millimolar
µM	Micromolar
MFS	Major Facilitator Superfamily
mRNA	Messenger ribonucleic acid
NAT	Nucleobase-Ascorbate Transporter Family
NCS	Nucleoside Cation Symporter Family
NEO	Neomycin resistance gene
ng	Nanograms
No.	Number
NTDs	Neglected Tropical Diseases
OMP	Orotate monophosphate
OMPDC	Orotidine Monophosphate Decarboxylase
OPRT	Orotate phosphoribosyl transferase
ORF	Open reading frame
P2	Amino purine transporter
PAC	puromycin resistance gene
PBS	Phosphate buffered saline
PCF	Procyclic form
PCR	Polymerase chain reaction
PPTs	Protozoan pyrimidine transporter genes
pmol	picomol
PYR6-5 ^{-/-}	Pyrimidine auxotrophic-double knockout

PYR6-5 ^{+/-}	Pyrimidine auxotrophic-single knockout
qRT-PCR	Quantitative Reverse Transcription PCR
RIT-seq	RNA-interference target sequencing
RNA	Ribonucleic acid
RNAi	Ribonucleic acid interference
rpm	Revolutions per minute
RRNA	ribosomal ribonucleic acid
RT	Reverse transcriptase
s	Second
SbV	Pentavalent antimonials
SDS	Sodium dodecyl sulphate
SEM	Standard error of mean
sKO	Single knockout
SHAM	Salicylhydroxamic acid
TAO	Trypanosome Alternative Oxidase
<i>T. b. b.</i>	<i>Trypanosoma brucei brucei</i>
T7RNAP	T7 RNA polymerase
Tb427	<i>Trypanosoma brucei</i> strain 427
<i>TbAQP2</i>	<i>Trypanosoma brucei</i> aquaporin-2 gene
<i>TbAQP3</i>	<i>Trypanosoma brucei</i> aquaporin-3 gene
TbAT1	<i>Trypanosoma brucei</i> adenosine transporter
<i>Tbb-CAT1</i>	<i>Trypanosoma brucei</i> cation transporter-1 gene
<i>Tbb-CAT2</i>	<i>Trypanosoma brucei</i> cation transporter-2 gene
<i>Tbb-CAT3</i>	<i>Trypanosoma brucei</i> cation transporter-3 gene
<i>Tbb-CAT4</i>	<i>Trypanosoma brucei</i> cation transporter-4 gene
<i>Tbb-FAD</i>	<i>Trypanosoma brucei</i> fatty acid desaturase gene
<i>TgAT1</i>	<i>Toxoplasma gondii</i> adenosine transporter 1
THT1	Hexose transporter genes 1
THT2	Hexose transporter genes 2
TbU	<i>Trypanosoma brucei</i> uracil transporter
TK	Thymidine kinase
TM	Transmembrane
TMP	Thymidine monophosphate
TS	Thymidylate synthase

TTP	Thymidine triphosphate
UDP	Uridine diphosphate
UMP	Uridine monophosphate
UP	Uridine phosphorylase
UPRT	Uracil phosphoribosyl transferase
UTP	Uridine triphosphate
UTR	Un-translated region
UTRs	Untranslated regions
UV	Ultraviolet
VL	Visceral leishmaniasis
V_{max}	Maximal velocity
VSG	Various Surface Glycoprotein
WHO	World Health Organization
WT	Wild type
ΔG^0	Gibbs free energy

1 General Introduction

Kinetoplastida is a widespread order of flagellated protozoan pathogens and the defining feature of these parasites is the presence of a large mitochondrial DNA region known as the kinetoplast (Stuart et al., 2008). Members of this order have the potential to parasitise virtually every animal group as well as several plant groups (Maslov et al., 2001). The taxonomic hierarchy of Kinetoplastida is: Phylum Euglenozoa, order Kinetoplastida, suborder Trypanosomatina and family Trypanosomatidae. The order Kinetoplastida may be biflagellate Bodonidae or uniflagellate Trypanosomatidina. Bodonidae includes free living species whilst the latter are extremely parasitic. Trypanosomatidae family consists of parasitic flagellated protozoans which have the potential to cause pathologies in both humans and animals. The most important genus of the Trypanosomatidae family are *Trypanosoma* and *Leishmania*. The most important species of these two genera are *Trypanosoma brucei*, *Trypanosoma cruzi*, *Trypanosoma congolense*, *Leishmania mexicana*, *Leishmania major*, *Leishmania donovani* and *Leishmania infantum* (Figure 1.1) (Lukeš et al., 2014; Maslov et al., 2001; Maslov et al., 2013; Dolezel et al., 2000). Some kinetoplastida can cause common parasitic diseases in humans. These include *Trypanosoma brucei* which causes sleeping sickness (or Human African trypanosomiasis, HAT), *Trypanosoma cruzi* which causes Chagas' disease (or American trypanosomiasis), and *Leishmania* spp. which causes leishmaniasis. These all have a major global impact on health (Maslov et al., 2001; Barrett and Croft, 2012).

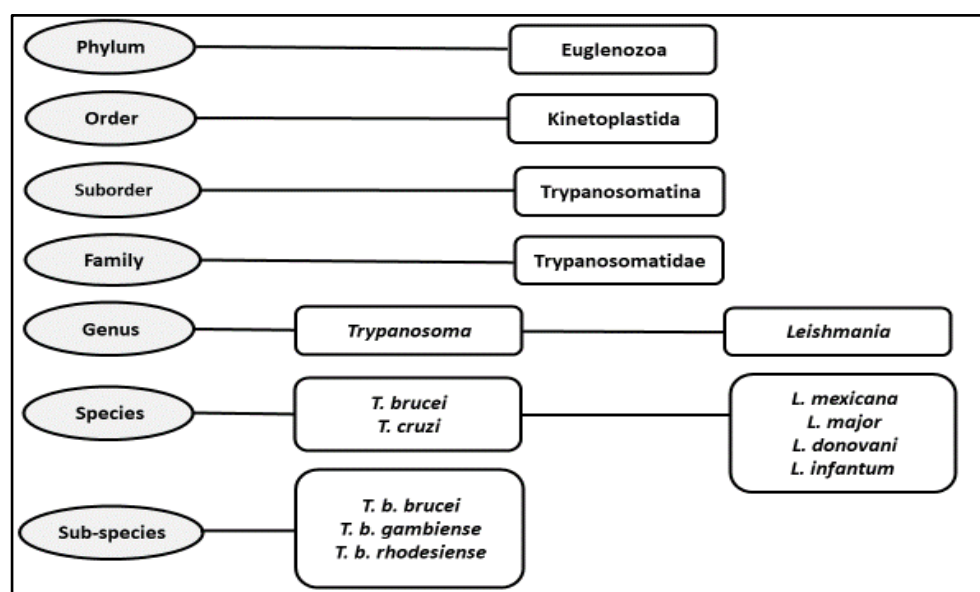


Figure 1.1: Classification of the kinetoplastids.

1.1 *Leishmania* and leishmaniasis

The protozoan parasites belonging to genus *Leishmania* cause infections that lead to a group of diseases known as leishmaniasis. More than 90 species of female phlebotomine sandflies (the genus of *Phlebotomus* in the old world and *Lutzomyia* in the new world) bites transmit the leishmaniasis infection (Desjeux, 1996; Boelaert and Sundar, 2014; W.H.O., 2020c). Charles Donovan and William Leishman in 1903 independently described the *Leishmania* parasites. However, they had previously been observed by Peter Borovosky in 1898 and David D. Cunningham in 1885. It was easy to mistake these parasites for other protozoa, but James Wright proposed *Leishmania* in 1903 (Vannier-Santos et al., 2002). *Leishmania* species are digenetic parasitic protozoans belonging to the order Kinetoplastida and the family Trypanosomatidae (Van der Auwera and Dujardin, 2015). There are two subgenera of the genus *Leishmania*, *Leishmania* and *Viannia* based on how they are developed in the sandfly vector. A number of factors determine how the subgenera are specified like the geographical distribution, clinical presentation and the epidemiology of the animal reservoir and the vector (Marfurt et al., 2003; Leprohon et al., 2015). According to the World Health Organization (WHO), one of the most Neglected Tropical Diseases (NTD) is human leishmaniasis, caused by twenty species of the obligate intracellular protozoan *Leishmania* (W.H.O., 2020c).

1.1.1 Morphology and life cycle

Morphology of protozoan parasites like *Leishmania* are often directly connected to the pathogenicity and evolutionary pressures that establish, maintain and transmit an infection within the host organism (Lipa, 2012). It has crosslinked sub pellicular microtubules with a single copy of each organelle like mitochondrion and Golgi apparatus. The kinetoplast or mitochondrial DNA is directly associated with the basal body from which the flagellum arises (Neto et al., 2011). *Leishmania* exists in two basic body forms: promastigote form (infective stage) and amastigote form (vertebrate tissue stage) (Figure 1.2). Promastigotes are extracellular forms in the sandfly vector, elongated and motile, with dimensions ranging from 15 to 20 μm in length and 1.5 to 3.5 μm in width. The kinetoplast is elongated and perpendicular to the nucleus. In

contrast, amastigotes are intracellular forms in the vertebrate host, oval or rounded shape, no free flagellum, with dimensions ranging from 2.5 to 6.5 μm in length and 1.5 to 3 μm in width (Ambit et al., 2011; Rodriguez et al., 2018; Akpunarlieva and Burchmore, 2017).

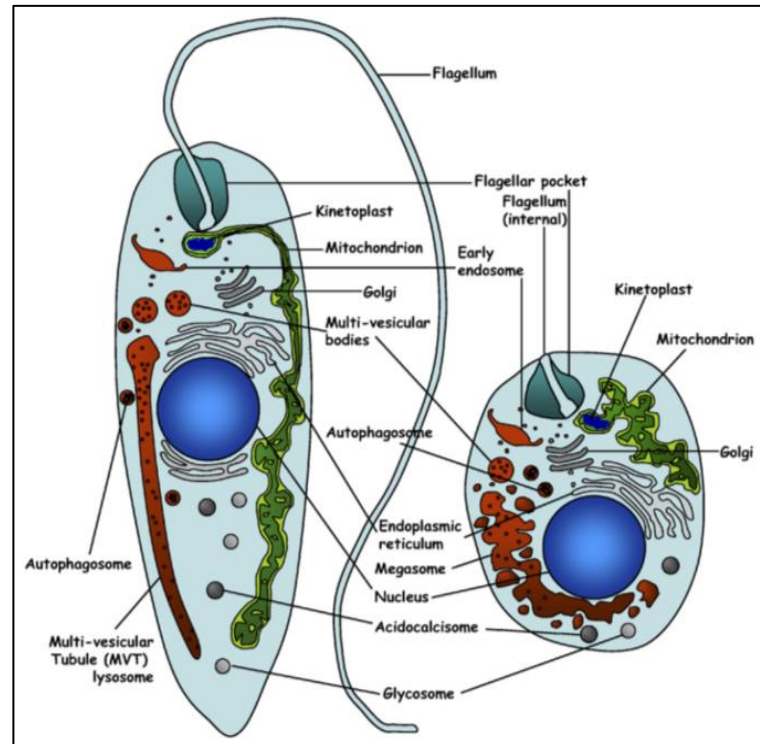


Figure 1.2: Schematic representation of promastigotes (left) and amastigotes (right) of *Leishmania* parasites (Besteiro et al., 2007).

Leishmania parasite undergo a complex life cycle which includes being hosted by both vertebrates and invertebrates in addition to two developmental stages which are: promastigotes, this is the proliferative type present in the lumen of the sandfly, and amastigotes which represent the proliferative form present in a number of mammalian host cells (Teixeira et al., 2013). The bite of an infected female phlebotomine sandfly on the skin of a mammalian host is where the lifecycle of *leishmania* transmits infective metacyclic promastigote forms. Phagocytes are mostly macrophages and some mononuclear phagocytic cells. The differentiation process (amastigogenesis) of the parasite happens inside the host cell. This leads to the emergence and multiplication of rounded amastigotes inside a parasitophorous vacuole (PV) which may continue to infect other phagocytic cells even after death of the host cell. The blood meal of the sandfly is when the amastigotes are ingested and changed in its midgut to procyclic promastigotes that multiply through binary fission. There is then migration of

procyclic-derived forms towards the anterior midgut where they differentiate to metacyclic forms (metacyclogenesis), which then has capacity to infect another mammalian host (Figure 1.3) (Bates, 2007; De Pablos et al., 2016).

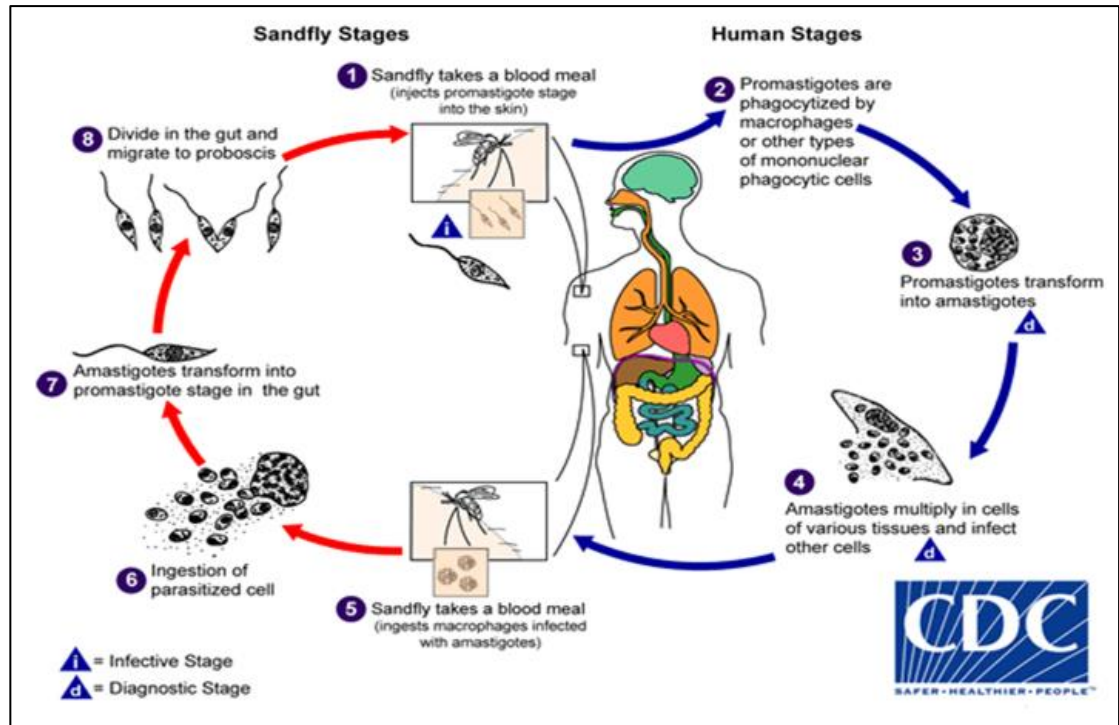


Figure 1.3: Life cycle of *Leishmania* parasites. Image taken from .

1.1.2 Geographical distribution

Leishmaniasis is a vector-borne disease caused by the parasite *Leishmania*, which lives in a variety of sand fly species. This insect is most active in warm and humid environments. Thus, the parasite is found in tropical and subtropical regions such as the rainforests of Central and South America, some parts of Mexico, the Mediterranean basin, deserts of Western Asia and the Middle East (Pratlong et al., 2009). Though environment and climate are one of the determining factors of spreading of the disease, according to WHO, poverty also heavily influences the spreading of leishmaniasis. In addition to poverty, socio-economic factors like malnutrition, lack of financial resources, famine, migration of people in large numbers caused by urbanisation, emergency situations such as war, etc. influence the disease's epidemiology (Peterson and Shaw, 2003; W.H.O., 2020b). Thus, leishmaniasis is found in the countries where the above-mentioned conditions are common. WHO classifies leishmaniasis as an NTD, and out of the 200 countries and territories that report to WHO, 98

countries and territories are endemic for this disease and over 350 million people are at the risk of getting infected with the disease. In 2014, over 90 percent of all cases that were reported to WHO, were from six countries: Brazil, Ethiopia, India, Somalia, South Sudan and Sudan. This disease is found in people of almost every continent in the world except Australia and Antarctica. Cutaneous leishmaniasis occurs mostly in Afghanistan, Brazil, Iran, Peru and Saudi Arabia (90 percent of total cases) (Figure 1.4B) (W.H.O., 2020b; Tiuman et al., 2011). The muco-cutaneous form occurs in Brazil, Bolivia and Peru, which account for more than 90 percent of the total cases. India, Bangladesh, Brazil, Nepal and Sudan account for 90 percent of global incidence of visceral leishmaniasis (Figure 1.4A). Leishmaniasis is predominantly found in developing countries rather than in developed countries and is more likely to occur in rural areas than in urban areas but can be found in the outskirts of some cities (Chakravarty and Sundar, 2010).

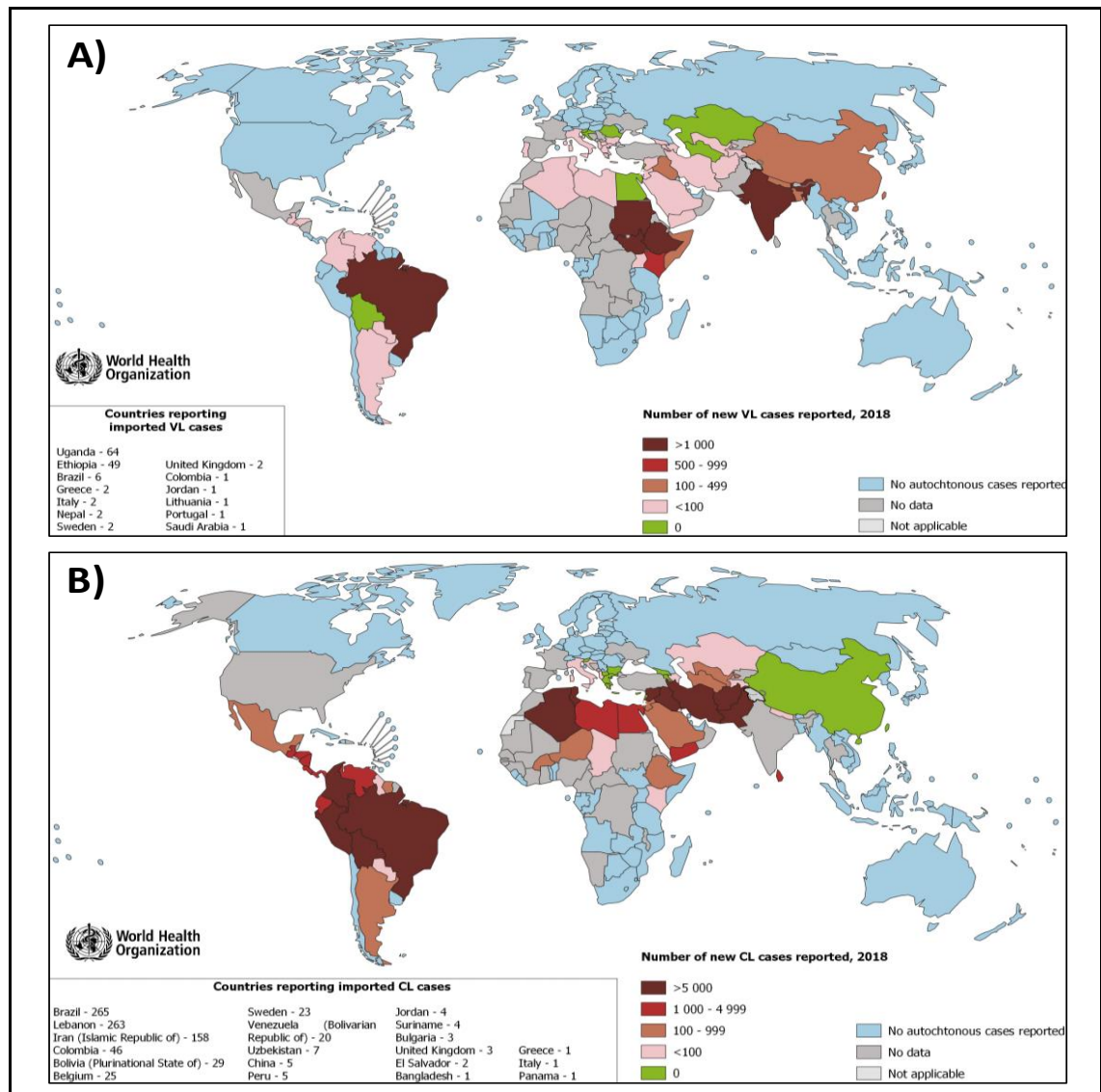


Figure 1.4: Worldwide geographic distribution of leishmaniasis. A) Visceral leishmaniasis and B) Cutaneous leishmaniasis (Image taken from (W.H.O., 2020b)).

1.1.3 The genome

L. major, *L. infantum* and *L. donovani* have their genetic information in 36 chromosomes (Figure 1.5). However, *L. mexicana* has 34 chromosomes while *L. braziliensis* possesses 35 chromosomes. *Leishmania* species have unique gene distributions as a consequence of chromosome fusion events. *Leishmania* commonly have genetic variation resulting from single gene expansion during multi-copy array or whole genome replication (Llanes et al., 2015; Fiebig et al., 2015; Rogers et al., 2011; Real et al., 2013). A study from Zhang et al. (2008b) demonstrated that the genetic variation and their expression levels affects the virulence and tissue tropism of the organism. The structure of the chromosome is similar to that of other pathogenic protozoa. It has a central conserved core

with a single or low copy number sequences and extensive repeated telomeric and sub-telomeric sequences. The sizes of telomeric and sub-telomeric sequences are highly diverse even among the homologous chromosomes which make every other isolate of *Leishmania* distinct from each other. The 36 chromosomes contain 32,816,678 bp of DNA. 8272 genes within the genome code for proteins, 911 for RNA and 39 genes are pseudo genes (Llanes et al., 2015; Real et al., 2013). Apart from the nuclear chromosomes the independently replicating mitochondrial genome is present within the kinetoplast. . In 1998, RNA interference (RNAi) was discovered and accepted as a critical element of studying the functions of genes and anatomise the biological processes of organisms that carry them (Fire et al., 1998). From the discovery, *T. brucei* was identified as the first protozoan parasite to have a functional RNAi system (Oberholzer et al., 2007). Nonetheless, *T. cruzi* and most *Leishmania* species do not have the RNAi pathway (Peacock et al., 2007; Downing et al., 2011; Fire et al., 1998).

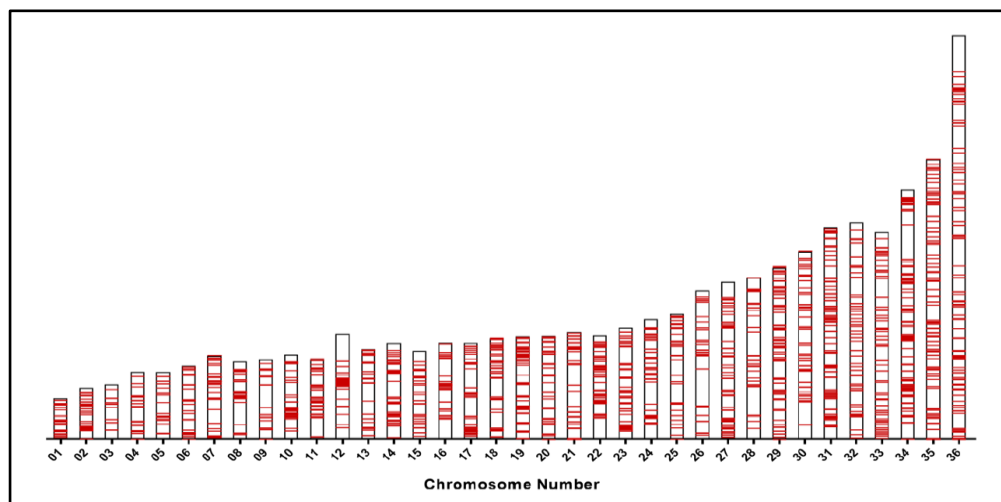


Figure 1.5: The genomic distribution of 36 chromosomes that have been assembly from *L. donovani* (Lypaczewski et al., 2018).

1.1.4 Pathology and clinical manifestation

The leishmaniases are known to affect the poorest people and are commonly linked with lack of financial resources, weak immune system, poor housing, population displacement and malnutrition. There are approximately 700,000 to 1 million new cases every year in addition to around 20,000 to 30,000 death occur annually (W.H.O., 2020c). Amastigotes are the obligate intracellular stage of the

parasites inside macrophages and they multiply and survive within a compartment known as the phagolysosome. Human leishmaniasis exists in three main forms (Reithinger et al., 2007).

1.1.4.1 Visceral leishmaniasis

Visceral leishmaniasis (VL), also known as kala azar, is the most deadly form of leishmaniasis (Elarabi et al., 2020). Visceral leishmaniasis is caused by two *Leishmania* species, *L. infantum* and *L. donovani*, based on the respective geographical region. Children and immunosuppressed individuals are the ones mostly affected by *L. infantum* whereas *L. donovani* can infect any age group. VL has an incubation period of between 2 and 6 months. Symptoms reported by visceral leishmaniasis patients include persistent systematic infection (loss of appetite, weight loss, weakness, fatigue and fever), reticulo-endothelial system and parasitic invasion of the blood which causes enlargement of lymph nodes, liver and spleen (Chappuis et al., 2007; Desjeux, 2004). This parasitic disease has attracted increased attention with the emergence of *Leishmania*/HIV co-infection in many areas of the world (Vannier-Santos et al., 2002). The potential origin of the rise of anti-leishmanial drug resistance is the HIV/VL co-infected patients. The reason is these patients have a weak immune response and high parasite burden, making it hard to clear the infection with standard drug dosages. In addition, it can be fatal if there is delayed diagnosis of visceral leishmaniasis (Singh, 2014).

1.1.4.2 Cutaneous leishmaniasis

Cutaneous leishmaniasis (CL) is the most common form of the disease. Cutaneous leishmaniasis is common in more than seventy countries in the world (Desjeux, 2004). Multiple species of *Leishmania* produce cutaneous leishmaniasis in adults and children such as *L. tropica*, *L. major* and *L. (L) aethiopica* (Old World); *L. chagasi* and *L. infantum* (Mediterranean and Caspian Sea Regions); and *L. (V) guyanensis*, *L. (V) peruviana*, *L. (V) panamensis*, *L. braziliensis*, *L. (L) amazonensis* and *L. mexicana* (New World). The sandfly bite is where the papule begins; it then grows to a nodule and ulcerates for almost 3 months (Dowlati, 1996; Magill, 2005). Cutaneous leishmaniasis patients often have more

than one lesion on the skin, usually without fever. *L. major* infections are characterized by superficial satellite papules found in the periphery of the main lesion, usually healing after 4 - 6 months in an estimated 50 - 70% of the cases. *L. tropica* is characterised by the dry form of its ulcers on the skin which take a year or longer to heal. HIV-linked cutaneous leishmaniasis is not that common, but prevalence might increase in the future (Wajihullah and Zakai, 2014; Couppie et al., 2004; Romero et al., 2005).

1.1.4.3 Mucocutaneous leishmaniasis

Mucocutaneous leishmaniasis (MCL) is most common in the new world relative to the old world. Most 90% cases of mucocutaneous leishmaniasis are reported in Peru, Brazil and Bolivia. Mucocutaneous leishmaniasis is referred to as *espundia* in Latin America and is as a result of several *Viannia Leishmania* subgenera such as *panamensis*, *braziliensis* and sometimes (but rare) *guyanensis* and *amazonensis*. Most cases of mucocutaneous leishmaniasis are attributed to *L. braziliensis* (Chappuis et al., 2007; Chakravarty and Sundar, 2010; Crovetto-Martínez et al., 2015). Mucocutaneous leishmaniasis is not that common in the old world. It is caused by *L. tropica*, *L. major* and *L. infantum*, which normally affects immunosuppressed patients and older adults. Mucocutaneous leishmaniasis causes patients to go through progressive destructive ulcerations of the mucosa which extends from the nose, mouth to the pharynx and larynx. The lesions do not heal on their own and can remain for months or years after colonization of the macrophages of the naso-oropharyngeal mucosa. The metastatic spread is not common and is vulnerable to parasitic factors, geographic factors and the immune status of the host (Chappuis et al., 2007; Crovetto-Martínez et al., 2015).

1.1.5 Diagnosis

Several laboratory methods are used to diagnose leishmaniasis to detect the parasite and identify its species. The diagnosis of the visceral form is done by performing a physical examination to look for enlarged spleen or liver followed by a bone marrow biopsy or blood sample examination. Also, visceral leishmaniasis is diagnosed through PCR to detect the parasite DNA in the blood,

which is highly specific and sensitive. Serological testing can provide supportive evidence for the diagnosis (Chakravarty and Sundar, 2010; Handler et al., 2015; Reithinger et al., 2007). For diagnosis of cutaneous leishmaniasis, skin biopsy is done from the lesion area to look for the DNA of the parasite (Sundar and Rai, 2002). Diagnosis is based on the production of antibodies by cutaneous leishmaniasis patients against *Leishmania* antigens that are detected through normal serologic approaches like the immunoenzymatic assay (ELISA) and the indirect immunofluorescent assay (IFA) (Couppie et al., 2004; Romero et al., 2005). A variety of specialised tests that are available only in reference laboratories, are also performed. It is necessary to mention here that since the manifestations take years in some cases, the condition becomes hard to diagnose. In such cases, a history of living or travelling to an area where leishmaniasis is highly endemic is helpful for the diagnosis.

1.1.6 Treatment and control of leishmaniases

The approach to treatment of leishmaniasis partly depends on the host and parasite species and partly on the geographical region. Some treatment approaches are effective against a particular species of *Leishmania* in a particular geographical region. In fact, the data from a well-conducted clinical trial in a particular setting cannot always be generalised to other settings. All cases of visceral and muco-cutaneous leishmaniasis require treatment, however not all cases of the cutaneous form require treatment (Khare et al., 2016). Antileishmanial effects have been established for approximately 25 compounds; however only a few of them are used as antileishmanial drugs for humans and these are mostly parenteral. Urea-stibamine was the initial effective drug, which was discovered in 1912. Brahmchari of India first reported it as effective against *L. donovani* in 1922. Millions of poor lives in India were saved by this discovery which led to the nomination of Prof Brahmchari for a Nobel Prize in 1929 (Singh and Sivakumar, 2004; Papadopolou et al., 1998).

Anti-parasitic drugs such as pentavalent antimonials (sodium stibogluconate and meglumine antimonate), amphotericin B, paromomycin, pentamidine, miltefosine, and orally administered 'azoles' (ketoconazole, itraconazole, and fluconazole) are effective for the treatment of all three clinical forms of

leishmaniasis (Khare et al., 2016). In some settings, local therapies such as cryotherapy, thermotherapy, intralesional administration of Sb^V , and topical application of particular paromomycin formulations are used as effective treatment approaches. Different medications and dosages may be needed for young children, pregnant or lactating women, elderly persons, and persons who have a compromised immune system or other co-morbidities. There is no available vaccine or prophylactic medication to prevent the disease. The best way of prevention is to protect oneself from sand fly bites. Protective measures include wearing clothes that cover as much skin as possible, application of insect repellent on exposed skin, spraying of insecticides, reducing nocturnal activities and the use of bed nets tucked into the mattress (Kobets et al., 2012). In general, the preventive measures must be tailored to the geographical area one lives in and, though difficult, must be sustained for the effective control of leishmaniasis (Otranto and Dantas-Torres, 2013).

1.1.6.1 Pentavalent antimonials

Pentavalent antimonials (Sb^V s) are a group of compounds used extensively for more than 50 years as a treatment for parasitic leishmaniasis. Although they are still the first line of drugs often used for the disease their use is becoming highly reduced due to adverse side effects, drug resistance and a need for daily parenteral administration (Lawn et al., 2003). The gradual development and improvement of Sb^V s has decreased its side effects hence being a major component of the anti-leishmaniasis drugs. The most common organic compounds of Sb^V s used are pentostam or sodium antimony gluconate (SAG) and glucantime or meglumine antimoniate (MG) (Chakravarty and Sundar, 2010; Singh and Sivakumar, 2004). These drugs are available for intravenous or intramuscular use only. 100 mg of the active ingredient, pentavalent antimony, is present in 1 mL of sodium stibogluconate and 85 mg is found in meglumine antimoniate. The half-lives of the two variants differ hugely, the first having a half-life of just about 2 h and the second having a half-life of about 33 h (Vouldoukis et al., 2006).

The mechanism of action of pentavalent antimonials is still highly debated. Some studies claim that the drug initially acts as a prodrug and the more active

as well as more toxic trivalent form acts as the active ingredient against leishmaniasis. Hence, there are several proposed models for the mechanism of action of pentavalent antimonials. The first model suggests that the pentavalent antimonials are converted into trivalent antimonials by the action of various thiols like cysteine and cysteinyl-glycine that are predominant in lysosomes, glutathione in cytosol and trypanothione in parasites (Frézard and Demicheli, 2010). The trivalent compounds are the active ingredient. The second model proposes that sodium stibogluconate inhibits the DNA unwinding enzyme DNA Topoisomerase I (TOPI). TOPI plays a crucial role in the maintenance aspect during the replication of DNA. Another model proposes that the drug acts by activating the host's innate and adaptive immune system, which also protects the host from future infections (Walker and Saravia, 2004; Oliveira et al., 2012). Also, the distinct thiol metabolism of *Leishmania* is believed to be essential in the mechanism action of Sb^V drugs (Chakravarty and Sundar, 2010).

Several side effects of the drug have been identified including headache, abdominal pain, anaemia, cardiotoxicity and reversible kidney failure. In the history of use of the drug, little of clinical resistance was observed. However, clinical resistance has been a threat during the past 15 years, yet it remains the primary choice of treatment in most parts of the world (Basu et al., 2005). *L. donovani* remains the only species identified as being drug resistant in several parts of India. Resistance of the drug in Indian state of Bihar was as a result of the high misuse of the drug and trivalent arsenic contamination of the drinking water, in addition to leishmaniasis having zoonotic transmission exception in East Africa and the Indian subcontinent where the transmission is highly anthroponotic (Chakravarty and Sundar, 2010; McConville and Ralph, 2013; Perry et al., 2013). Pentavalent antimonial resistance is accompanied by some of these common factors (i) aquaglyceroporin 1 (AQP1) (ii) an unknown efflux system (iii) thiols and (iv) Multidrug resistance protein A (MRPA) (Singh, 2006; Plourde et al., 2015). For instance, Plourde et al. (2015) reported that the susceptibility of an *L. major* promastigote *AQP1* null mutant to antimonyl tartrate (Sb^{III}) was very significantly reduced (60-fold).

1.1.6.2 Amphotericin B

Amphotericin B (AmB) is a polyene antibiotic and antifungal utilised since the 1960s in the second line treatment for leishmaniasis. This compound performs selective actions against fungi in addition to *Trypanosoma cruzi* and *Leishmania*. The drug is used for various fungal infections like candidiasis, cryptococcosis, blastomycosis and most importantly pentavalent antimony-resistant cutaneous and visceral leishmaniasis (Kovacic and Cooksy, 2012; Croft et al., 2006). The mechanism of action of AmB is not fully understood but AmB has a high affinity for ergosterol, the prevalent sterol in many microbes including *Leishmania*, over cholesterol, the prevalent sterol for the mammalian host cells, hence the selective action. Amphotericin B causes an increase in membrane permeability of leishmanial parasites through interference of sterol metabolism and shifting construction of the cell membrane (Croft et al., 2006; Purkait et al., 2012; Balaña-Fouce et al., 1998). Excretion of the drug from the body may take up to several weeks to months (Kovacic and Cooksy, 2012).

Many countries have adopted liposomal AmB (Ambisome) as the standard treatment however it is still expensive for single-course treatments and needs intravenous administration (Leprohon et al., 2015). Adverse side effects of the drug include fever, weight loss, hypotension, nausea, diarrhoea, anaemia and localised pain with or without phlebitis (Purkait et al., 2012). Clinical resistance to amphotericin B is not common; however shifting of the plasma membrane sterol profile may lead to substantial drug resistance for AmB, particularly in *L. infantum*/HIV co-infected individuals (Leprohon et al., 2015; Chakravarty and Sundar, 2010). Studies performed recently by Mwenechanya et al. (2017) explain how a single mutation, changing an amino acid from asparagine to isoleucine (N176I) in Sterol 14 α -demethylase, results in resistance to amphotericin B in *L. mexicana* promastigotes.

1.1.6.3 Miltefosine

Hexadecyl phosphocholine, the chemical name of miltefosine (MLF), was originally intended to be used as an antitumor drug. The antileishmanial potential of the drug was discovered in the 1980s and it was the first oral

antileishmanial drug available for treatment (Vélez et al., 2010). With other drugs such as pentavalent antimonials and amphotericin B having various disadvantages such as reduced and variable efficacy, adverse side effects and parenteral administration, miltefosine is becoming the first choice of drug for effective treatment of leishmaniasis (Vélez et al., 2010). The actual antileishmanial mode of action of MLF has not been revealed yet. In Kinetoplastid parasites, miltefosine is shown to act via inhibition of lipid biosynthesis. Biosynthesis of Phosphatidylcholine, one of the structural components of the plasma membrane is found to be inhibited in the parasites by the drug which is much higher potency than that of in mammalian cells; thus explaining the high level of specificity of the of miltefosine as an antiparasitic drug (Canuto et al., 2014). The major step of its action may be linked with its intracellular accumulation. The following steps are included in its intracellular accumulation; connection to plasma membrane, internalization in the parasite cell (two proteins, the beta subunit LdRos3 and the *L. donovani* miltefosine transporter 'LdMT'), in addition to intracellular targeting and metabolism (Chakravarty and Sundar, 2010; Maltezou, 2009).

Adverse effects associated with miltefosine includes vomiting, diarrhoea and ocular side-effects (Singh, 2006). Although the drug has showed a high cure rate in visceral leishmaniasis, some cases of resistance have been reported in various parts of the world, primarily in India. The main reason behind the drug resistance has been proposed to be the very long period of treatment and a long half-life of the drug in humans. Although the exact mechanism of resistance remains to be discovered, the role of integral membrane proteins that are responsible for the uptake of the drug have been indicated (Srivastava et al., 2017).

1.1.6.4 Paromomycin

Paromomycin (PRM) is an aminoglycoside aminocyclitol antibiotic that is synthesised by *Streptomyces riomus* var *Paromomycinus* and PRM exhibits both anti-leishmanial and antibacterial activity (Sundar and Chakravarty, 2013). . This drug is used to treat visceral leishmaniasis parenterally, either as a single drug or combined with SbV, against cutaneous leishmaniasis it is used either as

topical or parenteral formulation (Sundar and Chakravarty, 2013). In India, Phase III of clinical trials with PRM proved to be 93-95% efficacy, whereas, in Africa, it proved to be 64-85% efficacy with the dose of 15 mg/kg for 21 days; hence this drug was considered in 2006 for the treatment of VL in India (Barrett and Croft, 2012; Altamura et al., 2020). The drug is being marketed as paromomycin sulphate capsule with a brand name Humatin. With high efficacy rate, shorter duration of administration and limited side effects the drug has the potential to be used as the first line of treatment for leishmaniasis (Fernández et al., 2011). Studies indicate involvement of the drug in interfering with the translation mechanism of the cells. Ribosomal proteins are involved in such mode of action. The drug also interferes with membrane fluidity and mitochondrial membrane potential establishment, eventually leading to inhibition of respiration (Fernández et al., 2011).

The most prominent adverse effects of the drug include diarrhoea, abdominal cramps, nausea, vomiting and heartburn. Prolonged use of the drug may lead to fungal or bacterial superinfection. Patients with renal diseases and ulcerative bowels are strictly recommended to avoid intake of the drug (Chawla et al., 2011). The drug has not been widely used and therefore clinical resistance with visceral leishmaniasis is still unknown. As is the case for amphotericin B and miltefosine, there are geographical variations associated with variable efficacy of paromomycin against visceral leishmaniasis. For example, it is seen to be less effective in East Africa (such as Sudan), relative to India; the reasons for this remain currently unclear (Leprohon et al., 2015). Paromomycin-resistant strains of *Leishmania* show reduced accumulation of the drug within the organism due to a significant reduction in the initial binding of the drug (Chawla et al., 2011). A recent study by Bhattacharya et al. (2019) reported a significant reduction in PRM sensitivity after the heterozygous knockout of protein kinase CDPK1 in *L. infantum* promastigotes to paromomycin compared to the wild type cells.

1.1.6.5 Pentamidine

Pentamidine salts represent an antileishmanial drug that was first used for patients refractory to pentavalent antimonials (Chakravarty and Sundar, 2010). This drug is used for several parasitic and bacterial infections including

trypanosomiasis, leishmaniasis, pneumonia and babesiosis for patients with compromised immune systems. It is an aromatic diamidine, the active ingredient being its isethionate salt, used for prophylaxis. It can be given as injection via the veins or into the muscles (Lai A Fat et al., 2002). 99% of the patients were cured at first, however its efficacy dropped in the next two decades to curing 70% of the patients. It stopped being used for visceral leishmaniasis after the decrease in its efficacy. It has however been utilised effectively in the treatment of new world and old world mucocutaneous leishmaniasis and cutaneous leishmaniasis. Fewer injections, based on short periods, leads to minimum toxicity and a high cure rate (Chakravarty and Sundar, 2010).

There is still no clarity to the antileishmanial mechanism of action of pentamidine; however, it is thought to include effects on the mitochondrial inner membrane and to be a DNA minor groove binding. Also, it is believed to act by interfering with DNA replication, RNA transcription and metabolism of phospholipids and proteins in the target cell (Lai A Fat et al., 2002; Chakravarty and Sundar, 2010). Parenteral administration of the drug is associated with adverse side effects; however, they are less severe than pentavalent antimonials. Some of the adverse effects involve nephrotoxicity, damage to the pancreatic islet cells, anorexia, nausea, cardiac arrhythmias and localised necrosis (Hellier et al., 2000). Drug resistant strains of *L. donovani* and *L. amazonensis* show reduced uptake (18-fold and 75-fold, respectively) of the drug which is carrier-mediated and at the same time the efflux rate of the accumulated drug is much higher compared to wild type strains (Mukherjee et al., 2006; Chakravarty and Sundar, 2010).

1.1.7 Drug resistance mechanisms

Drug resistance hinders the treatment of infections caused by microbes and creates a threatening situation for the patient's health and safety. Several therapeutic strategies are facing failure due to the emergence of drug resistant microorganisms (Serenio et al., 2019). Drug therapy is unsuccessful and insufficient in such circumstances and the disease persists longer (Freitas-Junior et al., 2012). Some researches focused on how the most parasites have developed resistance to drugs (de Koning, 2008). Irregular and incomplete drug

intake often results in resistance to drugs in patients with leishmaniasis. Other than explicitly acquired resistance several parasite-associated factors play a major role in development of drug resistance. There is currently no vaccine for human use of leishmaniasis but there are prospective vaccines in development. There are alternative strategies to control drug resistance in leishmaniasis such as management of HIV/VL co-infection, monitoring drug resistance, combination therapy, free distribution of the drugs and monitoring therapy (Leprohon et al., 2015; Chakravarty and Sundar, 2010; Croft et al., 2006).

Drug combination has been used for the treatment of a number of infectious diseases (such as tuberculosis, HIV, Human African trypanosomiasis and malaria) and is now being considered for treatment of neglected diseases like leishmaniasis. There are two major reasons behind the establishment of combination therapies: reduction of the length of treatment for improvement of compliance (for instance, the miltefosine regimen includes drug intake two times a day for 4 weeks) and delaying the emergence of resistance for protection of the few available molecules (Leprohon et al., 2015; Chakravarty and Sundar, 2010; Croft et al., 2006). Therefore, a combination therapy is suggested in order to cope with this phenomenon, which improves the drug efficacy, shortens the course of treatment and reduces the resistance. Administration of sodium stibogluconate along with paromomycin is reported as effective and safe (Cobo, 2014; Croft and Coombs, 2003).

In the case of pentavalent antimonials the more potent trivalent form is produced in the host macrophages and enters the parasite via membrane carriers. Gene deletion of such protein carriers is found in the resistant strains rendering reduced number of the carrier on the parasite. Over-expression of ATP binding cassette transporters, which have a prominent role in efflux of the drug, have also being linked to drug resistance (Chakravarty and Sundar, 2010). Parasite physiology also can influence resistance by changing macrophage biochemistry, leading to increased efflux of the pentavalent form of the drug (Croft et al., 2006). Miltefosine-resistant *Leishmania* promastigotes could be created by point mutations in the miltefosine transporter, LdMT, which is considered as a drug resistance mechanism that causes a decrease in drug

uptake and inhibits miltefosine uptake into the cell. It is indicative of the importance and involvement of this transporter in resistance of the *Leishmania* parasite to miltefosine. Another suggested mechanism could be the upregulation of ABC transporters and hence, a rise in drug efflux (Ghorbani and Farhoudi, 2018; Laffitte et al., 2016).

1.2 Trypanosomes and trypanosomiasis

Human African trypanosomiasis (HAT), also known as sleeping sickness, is a vector-borne parasitic disease and is caused by protozoan parasites of the species *Trypanosoma brucei* (three subspecies: *Trypanosoma brucei brucei*, *Trypanosoma brucei gambiense* and *T. b. rhodesiense*). It is transmitted by the bite of an infected tsetse fly (*Glossina* species) that has acquired their infection from human beings or animals infected with pathogenic parasites. This disease is predominant in some regions of sub-Saharan Africa and only certain species of the fly transmits the disease (Aksoy et al., 2017; Mulenga et al., 2019; Wamwiri and Changasi, 2016; Hulpia et al., 2020a). According to WHO, about 10000 new cases are reported each year however many cases go undiagnosed and unreported. Sleeping sickness can be fatal if left untreated and is usually curable with medication, especially in the first stage of the disease (W.H.O., 2020d).

The disease can take two forms depending on the parasite: East African trypanosomiasis caused by the parasite *T. b. rhodesiense*, and West African trypanosomiasis caused by *T. b. gambiense*. West African trypanosomiasis accounts for 98 percent of all reported cases and leads to a chronic infection whereas East African trypanosomiasis accounts for only 2 percent cases and causes an acute infection. The symptoms for the West African trypanosomiasis takes months or even years to appear whereas East African trypanosomiasis develops rapidly and the symptoms are observed within a few weeks or, at the most, months after infection (Maseleno and Hasan, 2012; Mulenga et al., 2019; Wamwiri and Changasi, 2016). Both forms of HAT can affect the central nervous system and eventually lead to coma and death if left untreated. The rural population, who are involved in agriculture, fishing and animal husbandry, are most exposed to the tsetse fly and thus to the disease of sleeping sickness (Thuita et al., 2008).

Another form of the disease, known as Animal African trypanosomiasis (AAT), is caused by other species and sub-species of *Trypanosoma* than those affecting human beings. *T. b. brucei*, *T. congolense*, *T. equiperdum*, *T. evansi* and *T. vivax*, as well as *T. b. rhodesiense* (which is a zoonosis), are some of the species that causes disease in wild and domestic animals (Morrison et al., 2016). This acts as a major hindrance to the development of agriculture in Africa. All the diseases have different local names such as Nagana, Dourine and Surra, names that are mostly associate with disease in cattle, horses and camels, respectively (Wamwiri and Changasi, 2016; Büscher et al., 2019). A different form of human trypanosomiasis is known as American trypanosomiasis or Chagas' disease, and occurs mainly in rural areas of Latin America where there is widespread poverty. The disease was discovered by Brazilian physician Carlos Chagas in 1909 and hence the name (Rassi Jr et al., 2010; Pérez-Molina and Molina, 2018). It is transmitted by insect vectors called triatomine bugs that are infected with the parasite *Trypanosoma cruzi*. The triatomine bugs live in poor housing conditions such as houses made of mud, straw and palm thatch. They are active at night and during daytime hide themselves in crevices of walls and roofs. In people who have suppressed immune system (e.g. HIV-AIDS) if get infected with Chagas disease, the parasites can be reactivated in the circulating blood and this reactivation can potentially cause severe disease (Coura and De Castro, 2002; Pérez-Molina and Molina, 2018).

1.2.1 Morphology and life cycle

Trypanosomes are polymorphic parasites showing morphological variation under different conditions. They are characterised by the presence of a single flagellum and the specialised DNA containing Kinetoplast. There are numerous circular DNAs, which makes up the mitochondrial genome (kDNA). Trypanosomes have thin, flat bodies, tapered at both ends, the pointed end being anterior and the blunt end being the posterior end (Figure 1.6). Length varies from 15 to 30 μm and breadth at the middle is around 2.5 μm (Elias et al., 2007; Wheeler et al., 2019). It extends towards the anterior portion of the cell in a left-handed helical manner coiled around the cell body. The distal end of the flagellum is detached from the cell body, forming an overhang over the anterior portion of

the cell. It is involved in ingestion of nutrients from the surroundings (Ooi and Bastin, 2013; Kohl et al., 2003).

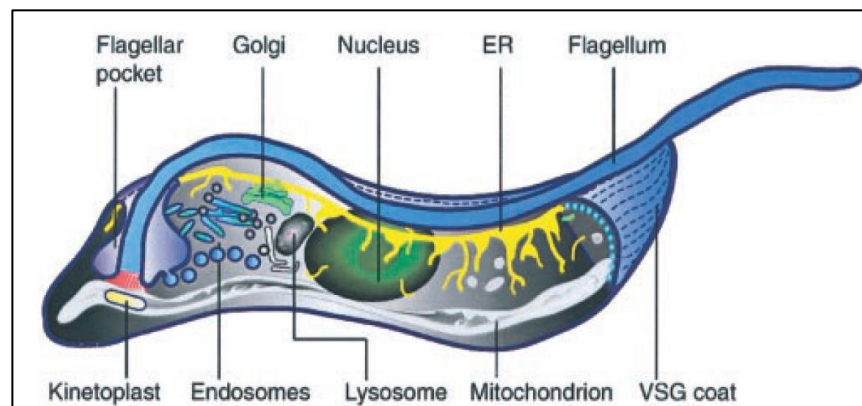


Figure 1.6: Morphology of *Trypanosoma brucei* (Grunfelder et al., 2003).

T. brucei has two hosts, an insect vector (tsetse fly) and a mammalian host (human or other mammal). When an uninfected tsetse fly bites an infected vertebrate host, it ingests trypomastigotes circulating in the bloodstream (Wheeler et al., 2019). The bloodstream trypomastigotes transform into procyclic trypomastigotes in the vector's midgut and then multiply by longitudinal binary fission. In the next stage, the procyclic trypomastigotes leave the midgut and migrate to the salivary glands of the vector, transforming into epimastigotes. Here they multiply for several generations. In the salivary glands, epimastigotes transform back into metacyclic trypomastigotes that are the infective stage. When the infected tsetse fly bites a human or an animal; it injects the metacyclic trypomastigotes into their bloodstream. The metacyclic trypomastigotes transform into bloodstream trypomastigotes and are carried to various body fluids such as blood, lymph, and in some cases the cerebro-spinal fluid (Figure 1.7) (Kennedy, 2004; Tyler and Engman, 2001). Here the trypomastigotes continue to replicate by binary fission and continue to circulation (Mortara et al., 2008).

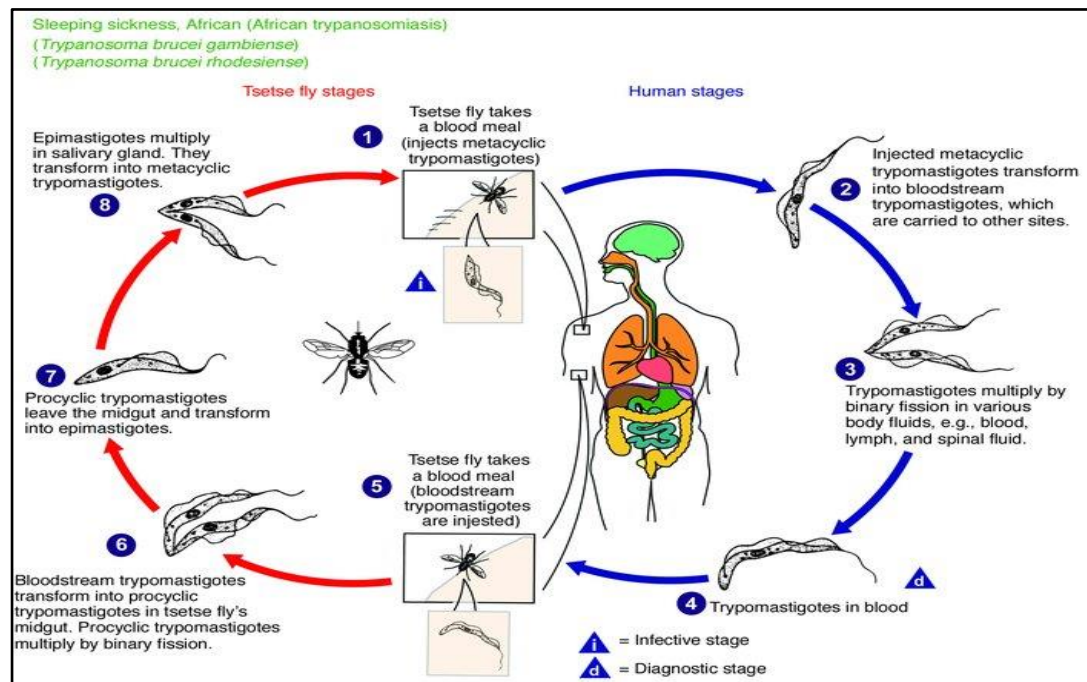


Figure 1.7: The life cycle of Africa trypanosomes in insect vector and mammalian host (Kennedy, 2004).

1.2.2 Geographical distribution

There are two subspecies of *T. brucei*: *T. b. rhodesiense* and *T. b. gambiense*. These two subspecies are morphologically undistinguishable but cause distinct diseases in humans namely the acute East African trypanosomiasis (rHAT), which is caused by *T. b. rhodesiense*, and the chronic West African trypanosomiasis (gHAT) is caused by the parasite *T. b. gambiense* (Figure 1.8) (Brun et al., 2010; Burri and Blum, 2017). There is a third subspecies, *T. b. brucei*, which infects cattle and other animals and under normal conditions does not infect humans (Desquesnes et al., 2013). Sleeping sickness is a threat to millions of people in the countries of sub-Saharan Africa. During the last epidemic, which started in 1970 and lasted until the late 1990s, the prevalence reached to Angola, the Democratic Republic of Congo, Central African Republic, Chad, northern Uganda, and South Sudan. According to WHO, the West African trypanosomiasis accounts for 98 percent of the reported cases and over the last 10 years, over 75 percent of the cases occurred in the Democratic Republic of Congo. Sleeping sickness was one of the major causes of mortality among the communities living here even of HIV-AIDS (W.H.O., 2020d; Franco et al., 2014). Though there has been a significant decline in the number of sleeping sickness cases as fewer than 1000 cases were reported in 2018, the estimated population currently at risk is 65

million people. Since then, but the incidence has decreased by 95% between 2000-2018. The world health organisation is working towards it elimination as a public health problem by the end of 2020, at least for *T. b. gambiense* HAT, and zero cases by 2030 (W.H.O., 2020d; Krishna et al., 2020).

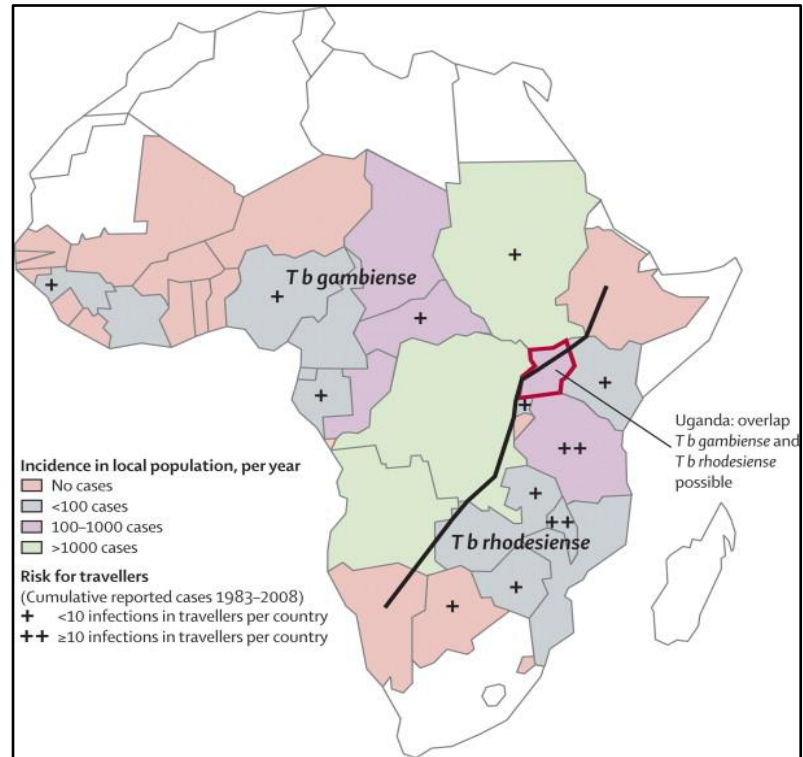


Figure 1.8: Epidemiology of Human African trypanosomiasis (Brun et al., 2010).

The transmission of Chagas disease by the parasite *T. cruzi* through triatomine bugs mainly occurs in the Americas, in rural areas of Mexico, central America, and South America. Some rare cases are found in the southern regions of the United States. An estimated 6 to 7 million people are infected in America (Rassi Jr et al., 2010). Moreover, emigration of millions of people from endemic countries to non-endemic countries leads to spreading of the disease in the United States and Europe (W.H.O., 2020a; Rassi Jr et al., 2010). The countries where this disease burden is highest are Bolivia, Argentina, El Salvador, Honduras, Paraguay, Guatemala, Ecuador, French Guyana, Guyana and Surinam, Venezuela, Nicaragua, Brazil, and Mexico. In recent years, due to the implementation of screening of blood banks and vector-control programmes, the epidemiology of *T. cruzi* infection has improved remarkably in many endemic countries (Prata, 2001; López-Vélez et al., 2020).

1.2.3 The genome

Among the subspecies of *T. brucei*, *T. b. gambiense* has the smallest genome with only 71-82% of the highest DNA content found in the species (Jackson et al., 2010; Kennedy, 2013). The diploid genome of *T. brucei* is 35 megabase (Mb) in size. *T. brucei* has 11 Mb sized chromosome and an unspecified number of small and intermediate sized chromosomes of about 30-700 kb, which are responsible for the coding of subtelomeric regions of the chromosomes (Romero-Meza and Mugnier, 2019; Berriman et al., 2005). It has been reported that about 50% nuclear genome comprises of coding sequences (Donelson, 2002).

The region between the telomere and the first housekeeping genes contains most of the assembled chromosome sequences. Long non-overlapping gene clusters are observed and are transcribed as polycistrons and undergo trans-splicing and polyadenylation (Berriman et al., 2005). Gene families are expanded by means of tandem duplication which compensate for their lack of transcriptional control. The major families of proteins encoded by the genome include kinesins, kinesin-like proteins, protein kinases and adenylate cyclases (Berriman et al., 2005). The genes in the subtelomeric regions are responsible for the antigenic variation in the parasite which aid in escaping the host immune system. Variant surface glycoproteins (VSG) are encoded by the genes that express surface proteins; they are activated in a clonal manner during infection (Jackson et al., 2010; Berriman et al., 2005). Unexpressed telomere linked VSG genes are also found in about 100 linear mini-chromosomes of 50-150 kb (Donelson, 2002).

1.2.4 Pathology and clinical manifestation

The two *T. brucei* subspecies causing sleeping sickness are morphologically undistinguishable. Sleeping sickness evolves through clinically distinct stages. The initial symptoms occur after a period of 5-6 days of the bite of the tsetse fly (Burri and Blum, 2017). There is reaction on the area of bite of the skin, which is called the trypanosomal chancre. This symptom is more common in East African trypanosomiasis. The disease then progresses from local symptom to the first (early) stage of infection (hemolymphatic stage) *i.e.* irregular pattern of fever,

headache, muscle, joint pain and enlarged lymph nodes (Krishna et al., 2020; Kennedy and Rodgers, 2019). In the second (late) stage the infection progresses to the central nervous system (meningoencephalitic stage) which is manifested by headache and mental changes. Patient may have problem in higher mental functions, with partial paralysis and hormonal imbalances, difficulty in concentration and adaptation to their surroundings and eventually a terminal somnolent state (Rodgers et al., 2019; Krishna et al., 2020). If left untreated, death ensues usually within 6 months (Burri and Blum, 2017).

American trypanosomiasis or Chagas' disease has an acute and a chronic phase. The acute phase occurs immediately after infection and can last up to a few weeks or months. In this phase the infection is mild with almost no symptoms. Following the acute phase, most infected people enter the chronic phase which is for a prolonged period, initially still with almost no symptoms. Most of the people who are infected are unaware of their infection as there are no severe or specific symptoms noticed. If left untreated, the infection remains lifelong and can also be fatal (Pérez-Molina and Molina, 2018; Rassi Jr et al., 2010). Chagas disease can have symptoms such as headache, painless swelling around the eye, palpitations, skin rash. If left untreated, it can cause congestive heart failure, megacolon and the weakening of other internal organs (Rassi Jr et al., 2000).

1.2.5 Diagnosis

Early diagnosis of the disease is difficult because there are no specific signs or symptoms of the infection in the first stage (Büscher et al., 2017). Human African trypanosomiasis generally progresses in two stages and thus the diagnosis requires the confirmed presence of the parasite in any body fluid such as in the blood and lymph system or any other tissues which confirms the early stage of the infection. In the late stage known as the meningoencephalitic stage, the trypanosomes invade the central nervous system (CNS). For both the stages of the disease, an examination of the cerebrospinal fluid is done to confirm the second stage (Krishna et al., 2020; Mitashi et al., 2012). Serological tests can be done as a form of clinical diagnosis; this may include the card agglutination test for trypanosomiasis (CATT). This is a reliable way of testing a large population that is at risk. CATT recognises antibodies to *T. b. gambiense* but this is not the

recommended tool for screening *T. b. rhodesiense* because of the high level of parasitemia, which allows direct microscopical observation of the parasite in blood samples. The *T. b. gambiense* (gHAT) is not easy to detect with microscopy alone because of the low level of parasitemia except when the blood sample is highly concentrated. . (Büscher et al., 2013; Checkley et al., 2007; Kennedy, 2013). For the diagnosis of the second stage HAT, the criteria for CNS involvement include increased protein in the cerebrospinal fluid and a white blood cell (WBC) count of more than 5 cell/ μ L (Bonnet et al., 2015). However, sleeping sickness can be diagnosed through several laboratory methods, including enzyme-linked immunosorbent assay (ELISA), immunofluorescence (IF), indirect haemagglutination (IHA) (Burri and Blum, 2017). In addition, laboratory blood testing is also done to diagnose HAT with a polymerase chain reaction (PCR) test, which detects the DNA of the *T. brucei* in the blood sample (Migchelsen et al., 2011).

1.2.6 Treatment

The largest impediment to treating African and American trypanosomiasis is the absence of any vaccine, this is because of the organism's high antigenic variation which helps it to effectively evade the host immune system (Kennedy and Rodgers, 2019). Currently, the only viable method by which to treat the disease is chemotherapy. However, chemotherapy, especially when the disease is in its second stage, can result in the patient experiencing severe adverse side effects. Pentamidine, suramin, melarsoprol and eflornithine are the only drugs used to treat HAT, with nifurtimox and benznidazole being used to treat Chagas' disease (Kennedy, 2013). A recent breakthrough in treating trypanosomiasis is by using the Nifurtimox-eflornithine combination treatment (NECT) (Kennedy and Rodgers, 2019; Franco et al., 2012; Priotto et al., 2009). The most advanced drug available against the disease is fexinidazole which is an orally-delivered nitroimidazole that has demonstrated high safety and efficacy against *T. b. gambiense* HAT over a 10-day treatment (Büscher et al., 2017). Fexinidazole was authorized as a drug for treating sleeping sickness in November 2018 by the European Medicines Agency (EMA) (under Article 58). Fexinidazole is expected to improve the treatment management and the epidemiology of the gHAT

infections. Its main drawback is that resistance to it will result in cross-resistance with nifurtimox (Lindner et al., 2020; P De Koning, 2020).

The most viable preventive measure useful for African trypanosomiasis is to avoid being bitten by tsetse flies. This includes wearing long sleeved tops and pants of medium-weight material as tsetse flies cannot bite through them, avoiding going near bushes and use of insect repellent (Krishna et al., 2020). Vector control is the primary strategy to be used, and can be done with traps and screens in combination with pesticides and insecticides. To prevent Chagas' disease, spraying of insecticides inside housing is effective to eliminate the triatomine bugs (Lidani et al., 2019; Legros et al., 2002). Blood donation screening can also be used to prevent the disease spreading through blood transfusions. The early detection and treatment of new cases will also be helpful in reducing the burden of the disease (Brun et al., 2001).

1.2.6.1 Pentamidine

Pentamidine was registered in 1950 but has been used against trypanosomiasis since 1937 and as pentamidine mesylate against leishmaniasis since 1940. Later in 1987 it was reevaluated and commercialised as pentamidine isethionate (Steverding, 2010; Bray et al., 2003). It is a positively charged aromatic diamidine compound that is soluble in water. The drug is administered parenterally since absorption from the gastrointestinal tract is usually ineffective. The drug can cross the blood-brain barrier and enter the cerebrospinal fluid (Sanderson et al., 2009; Sekhar et al., 2017), also trace amounts can be found in the liver and kidneys long after treatment because of selective binding on the respective organs (Bray et al., 2003). It is primarily used for the treatment of the early stage of *T. b. gambiense* African trypanosomiasis but almost never for *T. b. rhodesiense* sleeping sickness. The normal dose of the drug is 4 mg/kg body weight every day for a total period of 7 days (Dorlo and Kager, 2008; Barrett and Croft, 2012). The drug acts by selectively accumulating in the parasite's cells; pentamidine is extremely effective with EC₅₀ values of 1-10 nM in drug sensitivity assays (Barrett and Croft, 2012).

Certain membrane transport proteins are utilised for this purpose and loss or mutation of the transporter proteins can render the parasite resistant to pentamidine. *T. brucei* parasites are reported to take up pentamidine by three different transporters: P2 aminopurine transporter (TbAT1), the high affinity pentamidine transporter (HAPT1) and the low affinity pentamidine transporter (LAPT1) (de Koning and Jarvis, 2001; Matovu et al., 2003; Bridges et al., 2007). HAPT1 activity has recently seemed to be primarily the result of loss or mutation of aquaglyceroporin 2 (TbAQP2) in *T. brucei* (Baker et al., 2012; Munday et al., 2014; Alghamdi et al., 2020). Aquaglyceroporins (AQPs) are members of the major intrinsic protein family (MIP). AQP helps to move water, glycerol, urea, dihydroxyacetone and ammonia in *T. brucei* (Uzcategui et al., 2004; Zeuthen et al., 2006). Three genes encode the aquaglyceroporins (AQP1-3) in the *T. brucei* genome (Jeacock et al., 2017). An RNAi library screen shows that the loss of TbAQP2, but not of TbAQP3, leads to resistance to both pentamidine and melarsoprol (Alsford et al., 2012; Baker et al., 2012), and mutant alleles of TbAQP2 have been found in pentamidine- and melarsoprol-resistant strains (reviewed by P De Koning (2020)).

Many other modes of action are also suggested by various studies which include binding and inhibition of nucleic acids and phospholipids of the cell membrane, disruption of kinetoplast DNA, inhibition of messenger RNA trans-splicing and interfering with correct protein production (Chakravarty and Sundar, 2010; Dorlo and Kager, 2008). Pentamidine treatment has several disadvantages, among which: it is ineffective against infection from *T. b. rhodesiense* and against stage II of *T. b. gambiense*. As the drug cannot sufficiently cross the blood brain barrier it is not very effective in cases where the parasite has infected the CNS. Some adverse effects of the drug are nephrotoxicity, which is reversible upon proper medical care. It may also cause hypoglycaemia due to increased secretion of insulin from the pancreas. Hypotension and cardiac arrhythmias are also observed in some patients (Krishna et al., 2020; Pohlig et al., 2016).

1.2.6.2 Melarsoprol

Melarsoprol was introduced in 1949 and is a melaminophenyl-based organic arsenic compound (Nok, 2003). Until 2009 it was the most commonly used drug

for HAT, until the nifurtimox-eflornithine combination was introduced, which can treat the disease more effectively (Burri and Blum, 2017; Krishna et al., 2020). This is still the only available drug for the treatment of stage II *T. b. rhodesiense* and the only generally affordable compound for the treatment of stage II *T. b. gambiense*. It is administered as a 3.6% solution dissolved in propylene glycol and distributed in 5 mL ampoules for intravenous injection (Nok, 2003; Baker et al., 2013). The major advantage of the drug is that it can be used in stage II of trypanosomiasis infection where the parasite has crossed the blood brain barrier of the host. It can also be used on both the *T. b. gambiense* and *T. b. rhodesiense* sub-species of the parasite (Gregus and Gyurasics, 2000).

The exact mode of action of how arsenical compounds kill trypanosomes is still unknown. However, cell lysis occurs rapidly on application of the drug. The assumption is that the ATP supply of the cell is highly depleted by inhibition of glycolysis, ultimately leading to cell death. The drug interacts with low molecular weight thiols found in trypanosomes, yet this does not occur in mammalian cells. However, how this interaction reacts against the parasite remains unknown (Denise and Barrett, 2001; Nok, 2003). The mechanism of resistance has been intensively studied in recent years; the loss of both the P2 and HAPT1 transporters are responsible for melarsoprol resistance. Moreover, drug resistance to melarsoprol and cross-resistance between pentamidine and melarsoprol has increased (Barrett et al., 2011; de Koning et al., 2000; Baker et al., 2013; Munday et al., 2014). The drug is highly toxic to the human body because of the presence of the arsenic group. In 5-10% of patients post treatment reactive encephalopathy has been observed, the symptoms of which include seizures, high fever, headaches and nausea. 50% of patients affected by encephalopathy die within 48 hours of treatment (Gehrig and Efferth, 2008; Checkley et al., 2007).

1.2.6.3 Suramin

Suramin was discovered in 1920 and is a polysulfonated, symmetrical naphthalene derivative of urea first used for treating stage I *T. b. rhodesiense* infection in 1922. However, it does not significantly cross the blood-brain barrier

and therefore is administered only for the first stage of sleeping sickness. It derives from naphthalene-based dyes such as trypan red and trypan blue. Initially, trypan blue was described as having trypanocidal activities but was not permitted for human use since it is a coloured dye. Later the drug was synthesised as a naphthalene derivative which had colourless properties and was subsequently accepted for human use (Wiedemar et al., 2020; Docampo and Moreno, 2003; Sanderson et al., 2007). Treatment is usually by intravenous administration of 20 mg/kg, every 3-7 days for 4 weeks (Krishna et al., 2020). The drug has an extended half-life of approximately 41-78 days and binds effectively to serum proteins of human blood. It also binds with invariant surface glycoprotein 75 (ISG75) for which the parasites have a receptor, which is the main reason behind the drug accumulating within the parasitic cells via receptor mediated endocytosis (Barrett et al., 2011; Zoltner et al., 2016; Zoltner et al., 2020). The RNAi library screen revealed that the suramin receptor is ISG75 (Alsford et al., 2012). A recent study performed by (Wiedemar et al., 2018) proposed a link between antigenic variations and suramin resistance in *T. brucei* BSF. The connection between expression of a specific glycoprotein (VSG) and suramin resistance was identified by reverse genetics, which included the re-introduction of the original VSG to suramin resistant parasites, which fully restored susceptibility to suramin *in vitro* (Wiedemar et al., 2018).

In spite of a lot of speculation the exact mechanism of action of the drug remains to be discovered. Suramin bears six negative charges which participate in electrostatic interactions with several enzymes, causing inhibition of their activities. Glycolysis is thought to be a potent target of the drug since some of the enzymes suramin binds to participate in the glycolytic pathway (Nok, 2003; Wiedemar et al., 2020). However, it is unclear how suramin would enter the glycosomes (Zoltner et al., 2020). Drug resistance to suramin is rare because the drug simultaneously targets various enzymes. Observed side effects include stomal ulceration and fatigue. Less adverse symptoms include dermatitis, anaemia, peripheral neuropathy, and bone marrow toxicity (Wiedemar et al., 2020; Nok, 2003; McCarthy et al., 2015).

1.2.6.4 Nifurtimox-eflornithine combination therapy (NECT)

Eflornithine, also known as α -difluoromethyl ornithine (DFMO), derives from the amino acid ornithine and acts by inhibiting the polyamine enzyme ornithine decarboxylase. It was first developed as an antineoplastic drug but as yet has not been used for cancer therapy, as it is not effective enough. The drug is, however, effective even during the later stages of *T. b. gambiense* infection but is ineffective against *T. b. rhodesiense* (Priotto et al., 2009; Barrett and Croft, 2012; Kuemmerle et al., 2020). The drug deprives trypanosomes of polyamine synthesis for an extended period in comparison to mammalian cells (Priotto et al., 2009). In addition, it increases cellular levels of S-adenosyl methionine which causes unwanted methylation of proteins, lipids and nucleic acids within the cell (Willert and Phillips, 2012). The amino acid transporter (TbAAT6) mediates the uptake of eflornithine in *T. brucei* (Vincent et al., 2010), the loss of this transporter causes eflornithine resistance (Baker et al., 2011). Nifurtimox, a derivative of nitrofurantoin is used for melarsoprol failure, especially in combination with other therapies, particularly eflornithine. Its trypanocidal activity was empirically discovered and since 1967 it has been used for the treatment of Chagas' disease caused by *T. cruzi* in Latin America. Nitrogen is the key active element during its action against the parasite trypanosome. The free nitrogen radical generated on single electron reduction of the drug interacts with cellular components and generates reactive oxygen species, resulting in cell death of the parasites (Steverding, 2010; Wilkinson et al., 2008).

The combined efforts of the WHO and pharmaceutical corporations to shorten and simplify eflornithine-based therapy led to nifurtimox-eflornithine combination therapy (NECT) being developed in 2009 (Malvy and Chappuis, 2011). Using nifurtimox and eflornithine combined is now the first line of treatment for patients in the second stage of *T. b. gambiense* infection (Lindner et al., 2019). In comparison with previous treatments, NECT is known to be cheaper and easier to administer than eflornithine, and less toxic than melarsoprol (Simarro et al., 2012). The NECT treatment is a 10-day regime with a 5 mg/kg oral administration of nifurtimox every 8 hours for 10 days and 200 mg/kg of eflornithine in slow IV infusion every 12 hours for 7 days (Priotto et al., 2007). In patients treated with eflornithine, mortality rates are much lower

compared to those treated with melarsoprol (Chappuis et al., 2005). NECT treatment has less serious adverse reactions, including nausea, headache, abdominal pain and anorexia (Priotto et al., 2009; Franco et al., 2012).

1.2.6.5 Benznidazole

Benznidazole is a broad-spectrum antibiotic used for its antiprotozoal activities. Chemically, it is a nitroimidazole with a close similarity to metronidazole. The nitroheterocyclic compound is a prodrug which must be activated so that its potent cytotoxic effects are mediated (Trochine et al., 2014; Arrúa et al., 2019). Currently, the treatment of Chagas' disease is based on two drugs: benznidazole and nifurtimox. Benznidazole is primarily used to treat American trypanosomiasis in the disease's acute phase, however, it can also be effective in its chronic phase for cardiovascular disease patients (Arrúa et al., 2019; Bern et al., 2019). The mechanism of action of benznidazole is still being studied, indicates current hypothesis being that benznidazole reduction leads to the formation of glyoxal and a cytotoxic compound. Unfortunately, it has been reported over the past few years that some kind of resistance of *T. cruzi* to benznidazole has developed. The resistance mechanism to benznidazole includes the mutation of a nitroreductase that activates the drug by producing the nitro radical, and a P-glycoprotein efflux pump (Arrúa et al., 2019; Müller Kratz et al., 2018). Benznidazole displays high toxicity; frequent side effects include hypersensitivity reactions, anorexia, vomiting, polyneuritis, and depression of cell production by the bone marrow (Caldas et al., 2019; Bern et al., 2019).

1.2.7 Drug resistance mechanisms

Drug resistance was first discovered in trypanosomes by Paul Ehrlich and co-workers (Ehrlich, 1907). Human African trypanosomiasis (HAT) is still considered a neglected tropical disease (Hulpia et al., 2020b). Despite there being a moderately long list of available drugs to treat the disease, over time many drugs have shown signs of resistance, limiting treatment options. Drug resistance is one of the factors that makes trypanosomiasis difficult to be treated effectively. *T. brucei* has been extensively used in scientific research for decades and is the model organism for researching cellular and molecular

mechanisms of the order of Kinetoplastida (P De Koning, 2020; Dickie et al., 2020). Drug resistance in trypanosomes has been linked to changes in several transporters, including an amino acid transporter (TbAAT6) for eflornithine (Vincent et al., 2010), the P2 aminopurine transporter (TbAT1) for diamidines and melarsoprol (de Koning et al., 2004; Munday et al., 2015) and the high affinity pentamidine transporter (HAPT1/AQP2) for pentamidine and arsenic (Figure 1.9) (P De Koning, 2020; Munday et al., 2014).

The failure rate of melarsoprol treatment began to increase in the 1990s. This has been attributed to the failure of drug uptake by the P2 and HAPT1 transporters. The same transporters mentioned above also transport pentamidine and other diamidines. The AQPs are also known to have a major role in melarsoprol/pentamidine cross-resistance (MPXR) in *T. brucei* (Baker et al., 2012; Munday et al., 2014). Because of its resistance eflornithine has replaced melarsoprol as the first line of treatment in many areas of the world. However, it has been reported that there are some very rare cases of suramin and pentamidine resistance. Eflornithine monotherapy treatment failure has emerged in anecdotal accounts (Baker et al., 2013; Fairlamb, 2003; de Koning, 2008). New drugs, to which the parasites will not yet have developed resistance, must be developed to overcome resistance to the current drugs.

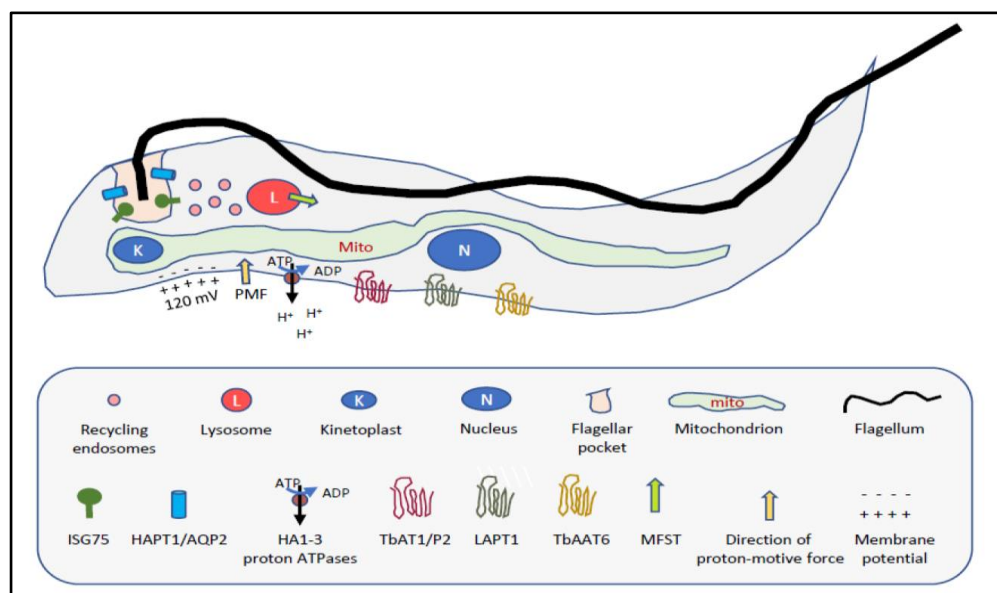


Figure 1.9: Schematic representation showing some of the structures and the main transport proteins involve in the uptake of the commonly available anti-trypanosomal drugs for the *T. brucei* (P De Koning, 2020).

1.3 Pyrimidine biosynthesis and metabolism in Kinetoplastids

1.3.1 *De novo* biosynthesis of uridine monophosphate

Pyrimidines and purines are the two types of nucleotides in the cell; they are aromatic compounds which are heterocyclic and nitrogenous in nature (De Koning et al., 2005; Peeters et al., 2005). These nucleotides are the major components of the nucleic acids (RNA and DNA), act as donors of nucleotide in second messenger molecules (cAMP and cGMP) and also act as modulators of enzyme activities. Most parasitic protozoa are able to synthesise pyrimidines *de novo* and also salvage the pyrimidine rings, except for *Trichomonas vaginalis*, *Tritrichomonas foetus* and *Giardia lamblia*, which acquire pyrimidines by use of their hosts. On the other hand, parasitic protozoa are all incapable of purine ring synthesis and they depend only on their host to salvage purine rings (Hulpia et al., 2020a; De Koning et al., 2005; Hulpia et al., 2020b).

The enzymes glutamine-dependent carbamoylphosphate synthetase II (CPS II), aspartate carbamoyltransferase (ACT), dihydroorotase (DHO), dihydroorotate dehydrogenase (DHOD), orotate phosphorybosyltransferase (OPRT) and orotidine monophosphate decarboxylase (OMPDC) perform a sequence of reactions that results in uridine monophosphate (UMP) synthesis (Hammond and Gutteridge, 1984; Carter et al., 2008).

The pyrimidines *de novo* pathway biosynthesis process begins with the use of simple substrates (ATP, water, Glutamine and HCO_3) to form carbamoyl phosphate. The enzyme CPS II catalyses this reaction. The next reaction is catalysed by enzyme ACT and occurs in the pathway between carbamoyl aspartate and carbamoyl phosphate. In the next step, the ring of the pyrimidine closes via the use of the enzyme DHO to remove a molecule of water from carbamoyl aspartate resulting in the formation of dihydroorotate. The enzyme DHOD is then used to produce orotate from dihydroorotate during the fourth step. The next step involves addition of the orotate to a 5-carbon ribose ring by

use of the OPRT enzyme, resulting in formation of orotidine-5-monophosphate (OMP). OMP is then decarboxylated by enzyme OMPDC during the final stage, to produce UMP (Figure 1.12: 1.10) (Berens et al., 1995; Hassan and Coombs, 1988; French et al., 2011).

Pyrimidine *de novo* pathway for kinetoplastid parasites are different from the mammalian ones in different ways (Carter et al., 2008). For mammals, the pathways for the first three enzymes are encoded by a single gene while for kinetoplastid parasites the encoding is by use of different genes resulting in a multifunctional protein. Uridine diphosphate inhibits the enzyme CPS II in kinetoplastid parasites while uridine triphosphate inhibits the mammalian enzyme. In parasites the localization of the enzyme dihydroorotate dehydrogenase is cytosolic while it is mitochondrial in mammals (Carter et al., 2008; Berens et al., 1995; Annoura et al., 2005).

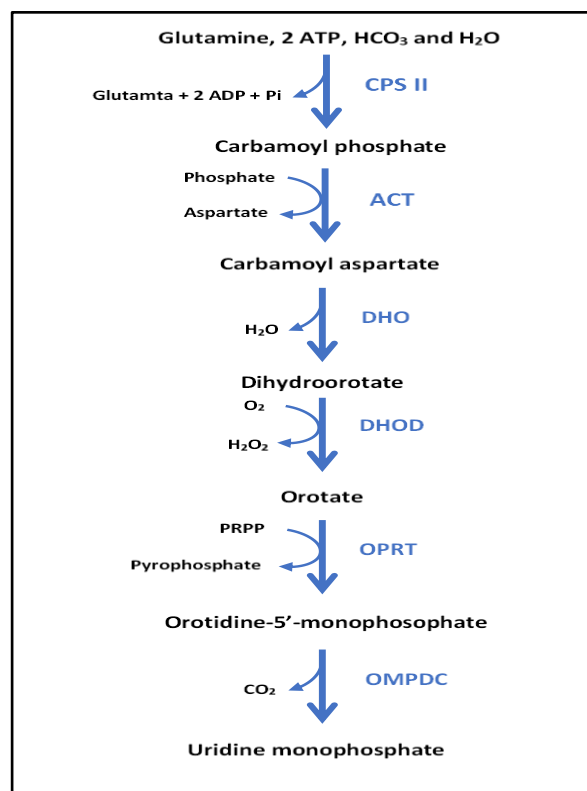


Figure 1.10: Pyrimidine biosynthesis pathways. Adapted from (Hammond and Gutteridge, 1984; Carter et al., 2008); Abbreviations are described in the text.

1.3.2 Pyrimidine salvage and interconversion

Generally, parasites are capable of synthesising pyrimidines *de novo*; in contrast, they are also able to salvage pyrimidines as nucleobases or nucleosides. It is for this reason that it becomes difficult to comprehend the separate importance of biosynthesis and salvage of pyrimidine, thus pyrimidine chemotherapy planning becomes complicated (Ali et al., 2013a). Pyrimidine nucleoside kinase or pyrimidine nucleoside phosphorylase are capable of converting pyrimidine nucleosides to their respective nucleotides and nucleobases forms (Hassan and Coombs, 1988). The beginning of pyrimidine pathway salvage takes place through pyrimidine nucleobases or nucleosides uptake into the cells of the parasites through transporters in the cell membrane. All pyrimidines with exemption of thymine and thymidine are transformed into uracil and later into UMP after being incorporated within the cell, this occurs through action uracil phosphoribosyl transferase enzyme (Figure 1.12: 1.11) (Gudin et al., 2006). Thus, UMP, the end product of salvage pathways and *de novo* biosynthesis, uses non-redundant pathways to act as an immediate precursor to every pyrimidine deoxyribonucleotide and ribonucleotide (Ali et al., 2013b).

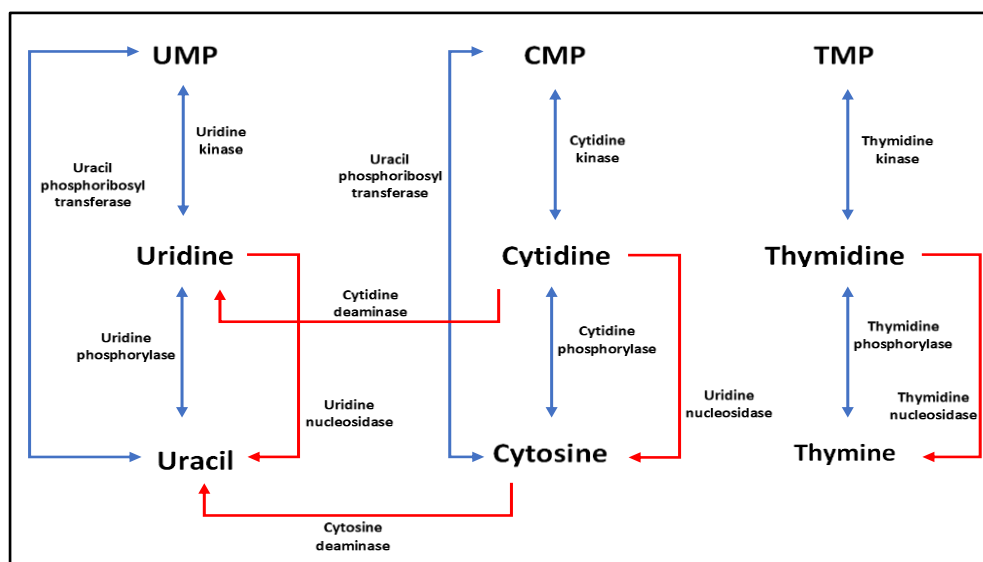


Figure 1.11: Pyrimidine salvage pathways. Red arrows indicate that the reaction occurs in one direction, whereas blue arrows indicate that the reaction occurs in both directions. Abbreviations are described in the text. Adapted from (Hammond and Gutteridge, 1984; Ali et al., 2013a).

Using ATP as the phosphate donor, the enzyme uridine nucleoside kinase is able to phosphorylate UMP into uridine triphosphate (UTP) through uridine diphosphate (UDP) in a two-step reaction (Carter et al., 2008). Three specific reactions are required for thymidine nucleotides, deoxycytidine and cytidine synthesis from UMP (Berens et al., 1995). After conversion of UMP to UTP through double phosphorylation, cytidine triphosphate synthase converts UTP to CTP (Carter et al., 2002; Fijolek et al., 2007; Hofer et al., 2001). In the second reaction, deoxyribonucleotides are synthesised from ribonucleoside diphosphates (GDP, UDP, CDP and ADP) through the enzyme ribonucleotide reductase (RR) (Berens et al., 1995). The third reaction involves production of deoxy-thymidine monophosphate (dTMP) from dUMP, a conversion process involving the enzyme thymidine synthase (TS), coupled to the folate cycle (Figure 1.12: 1.12) (Carter et al., 2002).

In addition, UDP and CDP can also be transformed into dUDP and dCDP through ribonucleotide reductase, and the enzyme nucleotide diphosphokinase is then used to convert them into dUTP and dCTP, respectively. Furthermore, cytidine deaminase in kinetoplastid protozoa converts deoxycytidine and cytidine to deoxyuridine and uridine, respectively (Carter et al., 2008). 2'-deoxycytidine and uridine are also important in synthesis of dUMP and UMP respectively (Hassan and Coombs, 1988); first, uridine phosphatase is used to convert uridine to uracil. This is an important step in obtaining UMP since uridine kinase (UK) activity is absent in kinetoplastids (Gudin et al., 2006; Hammond and Gutteridge, 1982). Some studies disagree with the UK activity argument since they consider salvage of uridine in a more direct path. The *Leishmania* genome database has been used to identify a potential UK activity (Carter et al., 2008).

According to (LaFon et al., 1982), salvage of thymidine is poor and thymidine kinase (TK) can be used to phosphorylate it to thymidine monophosphate (TMP), its genes are present in *Leishmania* and *Trypanosoma* spp. Thymine and thymidine can reversibly be converted via thymidine phosphorylase to give out

thymidine and thymine, respectively (Hammond and Gutteridge, 1984; Ali et al., 2013b).

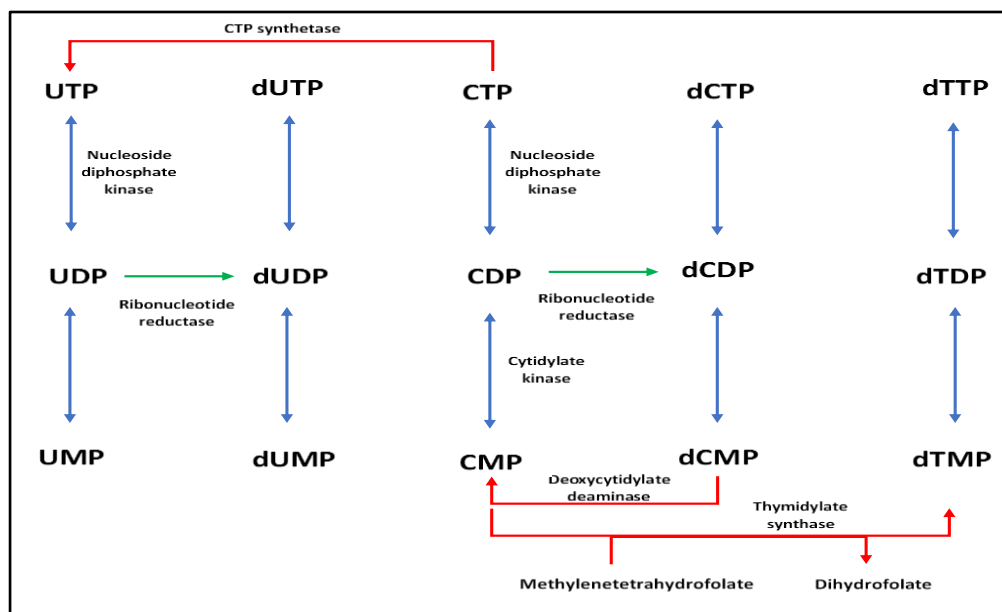


Figure 1.12: Interconversions of pyrimidines. Green and red arrows indicate that the reaction occurs in one direction, whereas blue arrows indicate that the reaction occurs in both directions. Abbreviations are described in the text. Adapted from (Hammond and Gutteridge, 1984; Ali et al., 2013a).

1.3.3 Classification of membrane transporter proteins

There are five mechanisms involved in molecule movements across the plasma membrane: exocytosis, facilitated diffusion, simple diffusion, endocytosis and active transport (Caspary, 1992). All biological membranes mediate compound movements across them via membrane protein transporters. Such integral membrane transport proteins are numerous in kinetoplastid protozoa where they help them in exportation and importation of drugs, uptake of nutrients, translocation of various molecules, regulate physiological concentrations and efflux of metabolites (Majumder, 2008; Kirk and Saliba, 2007; Rodriguez-Contreras et al., 2007; de Koning and Diallinas, 2000). Since purine and pyrimidine nucleobases and/or nucleosides have a hydrophilic profile, their movement into the cell relies on the transportation through such transmembrane proteins (Molina-Arcas et al., 2009; Carter et al., 2008).

There are two transport protein families in mammalian cells that aid in movement of nucleosides and nucleobases through the plasma membranes; these

include Equilibrative Nucleoside Transporters (ENT) and the Concentrative Nucleoside Transporters (CNT) (Baldwin et al., 1999; King et al., 2006; Young et al., 2013). Other gene families have also been described, however, including those in fungi, yeasts and bacteria (de Koning and Dhalluin, 2000; Campagnaro and de Koning, 2020). However, only members of the ENT family have, to date, been found in protozoa (De Koning et al., 2005). In addition to the nucleoside salvage role played by the ENT transporters, they have also been shown to play an important function in protozoan pharmacology; this is particularly common in African trypanosomes as well as in *Leishmania* (Carter et al., 1999; Geiser et al., 2005; Al-Salabi and de Koning, 2005; Rodenko et al., 2007; Kazibwe et al., 2009; Stewart et al., 2010; Ali et al., 2013a; Vodnala et al., 2013; Munday et al., 2015; Ranjbarian et al., 2017; Campagnaro and de Koning, 2020). Pyrimidine (5-fluorouracil) nucleobases and purine nucleobases (allopurinol) as well as pyrimidine and purine nucleoside analogues are among the chemotherapeutic compounds.

1.3.3.1 Concentrative nucleoside transporters

The family of CNTs, SLC28, encodes for the symporters that depend on an inward directed sodium gradient for its energy. For every import cycle, these electrogenic carriers import positive charge (Choudhuri and Chanderbhan, 2016; Baldwin et al., 2004). The CNT family in humans is made up of 3 members (CNT1, 2 and 3); each is made up of thirteen transmembrane domains (TMD) (Figure 1.12: 1.13). The selection of substrate depends on TMD7-9 (Baldwin et al., 2004; King et al., 2006). Eukaryotes and prokaryotes have been found to contain CNT family members, with mammalian members being sodium-dependent and the prokaryotic being proton symporters. Protozoa have been found not to contain CNT family members (De Koning et al., 2005; Campagnaro and de Koning, 2020). Transportation of adenosine and pyrimidine nucleosides is through CNT1, transportation of uridine and purine nucleosides is through CNT2, while CNT3 moves both pyrimidine and purine nucleosides. Renal epithelial and intestinal cells contain localised CNT transporters (Gray et al., 2004; Choudhuri and Chanderbhan, 2016; Young et al., 2008).

1.3.3.2 Equilibrative nucleoside transporters

The ENT or SLC29 family are trans-membrane glycosylated proteins that are localised to the plasma membranes and mitochondria, and act as pyrimidine and purine nucleosides transportation modulators (it can also play a role in nucleobases uptake), as well as therapeutic analogues associated with them. There are eleven TMD in ENT transporters (Figure 1.12: 1.13). They are expressed in mammary glands, placenta, brain, liver, erythrocytes, spleen and heart and probably other cell types. Human beings have three best known ENTs; hENT1, hENT2 and hENT3. In mammalian cells, the ENT1 and ENT2 isoforms are widely distributed and well characterised (King et al., 2006; Pastor-Anglada and Pérez-Torras, 2018). ENTs makes it possible for molecules to move in and out of cells down concentration gradients (facilitated diffusion) (Landfear et al., 2004; King et al., 2006). Investigation of the ENT family in protozoans has also been carried out. *Trypanosoma* and *Leishmania* are examples of active ENT transporters that are driven by the protonmotive force (De Koning et al., 2005; Young et al., 2008). A good number of nucleobase and nucleoside drugs consider ENTs as their primary conduits. There is still scarce information concerning their mechanism of action and their molecular mechanisms. An older classification of the mammalian ENTs divides them into *es* transporters, which are nM concentrations sensitive to the nitrobenzyl mercaptopurine riboside (NBMPR) inhibitor, and the *ei* transporters, unaffected by NBMPR or needs higher concentrations for inhibition. The detailed structure of human Equilibrative Nucleoside Transporter (hENT1) has recently been reported (Young et al., 2013; Campagnaro and de Koning, 2020; Wright and Lee, 2019).

ENT 1 and 2 are involved in the uptake of various pyrimidine and purine nucleosides. On the other hand, ENT3 transports adenine as well as pyrimidine and purine nucleosides (King et al., 2006). In addition, ENT4 plays an important role in regulating transportation of adenosine based on the pH level. ENT4 is also called the monoamine plasma membrane transporter (PMAT) since it is able to transport organic cations like neurotoxins, cationic drugs and biogenic amines (Barnes et al., 2006; King et al., 2006; Young et al., 2008). They control the efficacy of some drugs selectively through enhancing transportation across the cell membrane to their active sites and may also lead to transporter inhibition

when used as direct drug targets (Boswell-Casteel and Hays, 2017). The genome of *T. brucei* contains twelve ENT family members (Ortiz et al., 2009b), while the genome of *Leishmania* encodes five ENT transporters (Ortiz et al., 2009a). The large complement of ENT transporters in protozoa would make it highly challenging to target them by inhibitors with the aim of depriving the parasite of nucleosides. However, some of the protozoan ENT transporters are involved in the selective uptake of cytotoxic nucleosides and other therapeutics (Carter et al., 1999; Geiser et al., 2005; Al-Salabi and de Koning, 2005; Rodenko et al., 2007; Kazibwe et al., 2009; Stewart et al., 2010; Ali et al., 2013a; Vodnala et al., 2013; Munday et al., 2015; Ranjbarian et al., 2017; Campagnaro and de Koning, 2020).

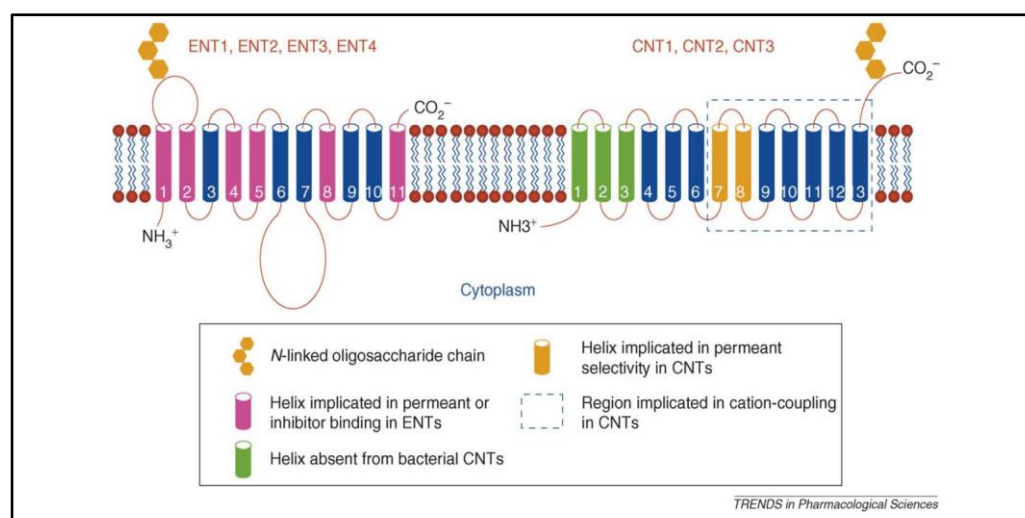


Figure 1.13: Transmembrane topologies of mammalian members of the CNT and ENT families (King et al., 2006).

1.3.4 Nucleoside and nucleobase transporters in Kinetoplastids

The uptake of pyrimidine/purine nucleobases or nucleosides plays a major role in the metabolism of parasitic protozoa like *Trypanosoma* and *Leishmania*. Due to their inability to synthesise *de novo* purine on their own, parasitic protozoa depend on their hosts for salvaged purines (De Koning et al., 2005; Campagnaro and de Koning, 2020). Protozoa however, show contrasting characteristics since they appear to carry out pyrimidine ring *de novo* synthesis on their own, and, therefore, do not have to depend entirely on uptake from the host (De Koning et al., 2005).

1.3.4.1 *Leishmania* spp.

Preformed purine nucleobases and nucleosides are initially translocated through the cell membrane of *Leishmania*. These nucleobases and nucleotides are unable to diffuse via the hydrophobic lipid bilayer since they are hydrophilic in nature. Thus, the selective transport process requires an advanced transport system (Carter et al., 2001; De Koning et al., 2005; Campagnaro and de Koning, 2020). The transportation of pyrimidines and purines in parasitic *Leishmania* spp. is dependent of a four-part mechanism. The parts are; NT1 (consisting of NT1.1 and NT1.2), NT2, NT3 and NT4 (Aronow et al., 1987; Campagnaro and de Koning, 2020; Carter et al., 2008). Studies of the genome of *L. donovani* have shown that it contains the genes for LdNT1, LdNT2, LdNT3 and LdNT4. Transporter proteins show considerable amino acid sequence homology to each other and also ENTs transporters in mammals (Carter et al., 2001).

NT1 is selective for the pyrimidine nucleosides (cytidine, thymidine and uridine) and adenosine (Vasudevan et al., 1998), whereas NT2 transports the 6-oxopurine nucleosides xanthosine, guanosine and inosine (Carter et al., 2001; Boitz et al., 2012). Specifically, the two similar genes NT1.1 and NT1.2 are used in encoding NT1. Alzahrani et al. (2017) recently found out that NT1.1 obtained from *L. mexicana* and *L. major* has greater sensitivity to uracil inhibition, due to this, it is referred to as uridine-uracil transporter 1 (UUT1). NT1.2 would be named NT1. The transporters NT2 and NT1 are also used as the major transporters of the inosine analogue formycin B and adenosine analogue tubercidin, respectively (Landfear, 2013; Ortiz et al., 2007). In the recent past, it has been found that the various *Leishmania* species appear to contain conserved NT1 activity. The expression of NT2 from *L. major* and *L. mexicana* in *T. brucei* showed that it is a transporter of oxopurines that has no affinity for uridine or adenosine (Alzahrani et al., 2017). On the other hand, the transporters NT3 and NT4 are purine nucleobase carriers in nature (Landfear, 2011). At neutral pH, purine nucleobases are mainly carried by NT3, which demonstrates high rates of xanthine, adenine, hypoxanthine and guanine transport. In addition to being the main transporter for purine nucleobases in intracellular amastigotes, it is involved in low affinity adenine transportation (Ortiz et al., 2007; Ortiz et al., 2009b). NT4 seems to have optimal functionality at acidic ranges of pH (Ortiz et

al., 2009a). Parasitic *Leishmania* survival seems to be essentially linked to NT3 and NT4 uptake of nucleobases. This is because it was difficult to create NT3 and NT4 simultaneous knockout (Ortiz et al., 2007).

First pyrimidine nucleobase transporter in *Leishmania* was discovered in 2005 and named as U1. It showed similar substrate binding and selectivity like U1 transporter in *T. brucei*, which means that, like purine nucleobase transport, pyrimidine nucleobase transport activity and mechanism has similarity in *Leishmania* and *Trypanosoma* (Papageorgiou et al., 2005). Papageorgiou et al. (2005) showed that U1 had a high affinity for uracil with a K_m value of 0.32 μM . The anti-metabolite 5-fluorouracil was found to be a good inhibitor for U1 with K_i value of 0.66 μM . Uracil and 5-fluorouracil are transported by the U1 transporter in *L. mexicana* and *L. major* (Papageorgiou et al., 2005; Alzahrani et al., 2017). A summary of the purine and pyrimidine transport activities in *Leishmania* spp. is shown on Table 1.1.

Table 1.1: Kinetic parameters of *Leishmania* species purine and pyrimidine transporters.

Substrate	Transporter					
	NT1 (NT1.2) ^{a*}	UUT1 (NT1.1) ^{a*}	NT2 ^b	NT3 (NBT1)	NT4 ^{e#}	U1 ^f
ADE	>1000	288; 5.14 ⁺		4.6^c; 8.5^d	39	NE ²
ADO	0.81	1.93 ⁺		5150 ^c		
GUA				2.8 ^c ; 8.8 ^d		NE ³
GUO			1.7	68 ^c		
HYP	>1000	>500		0.71 ^c ; 16.5^d ; 0.72 ^d	420	NE ²
INO	>500		0.3	125 ^c		
XAN				23 ^c ; 8.5^d ; 115.2 ^d		
CTS		>5000		NE ^{1,c}		NE ²
CTD	78.6					NE ²
TMN		560		NE ^{1,c}		237
TMD	11.2			NE ^{1,c}		NE ²
URA	>2500	29.7 ; 2.6 ⁺		NE ^{1,c}		0.32
URD	13.3 ; 33.5⁺	2 ; 3.12⁺				10.9
HPP				54.3^c		
5-FU		56.3				0.66

Values in bold represent K_m values; all others are K_i values. All K_m and K_i values * from *L. mexicana*, except were stated otherwise; ⁺ from *L. major*; [#] at pH 5.5. ADE, adenine; ADO, adenosine; GUA, guanine; GUO, guanosine; HYP, hypoxanthine; INO, inosine; XAN, xanthine; CTS, cytosine; CTD, cytidine; TMN, thymine; TMD, thymidine; URA, uracil; 5-FU, 5-fluorouracil; URD, uridine; HPP, allopurinol. NE, no effect at ¹1 mM, ²500 μM , ³250 μM , ⁴100 μM , ⁵25 μM . ^a(Alzahrani et al., 2017), from *L. mexicana*; ^b(Carter et al., 2000); ^c(Al-Salabi et al., 2003); ^d(Sanchez et al., 2004); ^e(Ortiz et al., 2007), at pH 5.5; ^f(Papageorgiou et al., 2005). Source: Table adapted from Campagnaro and de Koning (2020).

1.3.4.2 *Trypanosoma brucei*

The life cycle of *T. brucei* is complex and it involves many different hosts and environments. It also involved different tissues, the bloodstream and the cerebrospinal fluid in the case of vertebrates, and the gut, salivary glands, haemolymph, cardia in case of invertebrates. In order to adapt to dynamic and continually changing environments, it has developed a complex mechanism for the acquisition of nutrients such as purine uptake (Campagnaro and de Koning, 2020). There are 12 ENT transporters expressed by *T. brucei*. The family are designated as TbAT1 and TbNT2-TbNT12 (Ortiz et al., 2009b). African BSF trypanosomes express the P1, P2, H2, H3, HXT1, ADET1 purine transporters. Transporters in the *T. brucei* PCF, which are found in tsetse fly midgut, express P1, H1, H4 and ADET1 (Campagnaro and de Koning, 2020).

The P1 type is known as a adenosine/inosine/guanosine high affinity transporter (Carter and Fairlamb, 1993). Its substrate interactions including bonds with the N3, N7, 3'OH, 5'OH functional groups of nucleosides (de Koning and Jarvis, 1999). BSF of *T. brucei* expresses multiple P1 transporters. *T. brucei* genome contains eight P1 genes these are NT2, NT3, NT4, NT5, NT6, NT7, NT9 and NT10 (Sanchez et al., 2002; Al-Salabi et al., 2007; Sanchez et al., 2004). Chromosome 2 contains a cluster of related six genes encoding type P1 transporters. These are NT2-NT7 (Landfear et al., 2004). These six transporters are involved in the uptake of adenosine and inosine, sometimes they also take up hypoxanthine (Sanchez et al., 2002). In BSF and PCF of *T. brucei*, NT9 and NT10 were expressed (Al-Salabi et al., 2007; Sanchez et al., 2004), NT9 and NT10 are also in mitochondrial membrane hence indicating the role it plays in transportation of nucleoside into this organelle from the cytosol (Acestor et al., 2009; van Hellemond et al., 2005). The TbAT1 or P2 transporter is known as a transporter of adenine and adenosine. It is encoded by *TbAT1* which is just one gene as expressed by BSF (de Koning and Jarvis, 1999; Matovu et al., 2003). Antitrypanosomal drugs such as arsenical melarsoprol and the diamidine pentamidine are also carried by P2 in BSF *T. brucei* (Munday et al., 2013; Carter et al., 1999; Baker et al., 2013). Although *T. brucei* AQP2 is the major transporter of melarsoprol and pentamidine, P2 is also involved the transport of these drugs (Munday et al., 2014). The activity of NT11 and NT12, which are the

two last members of the ENT family in *T. brucei*, is not clearly known. There are suggestions that they encode adenine and pentamidine transporters (Ortiz et al., 2009b). TbNT11.1 and TbNT11.2 are two similar genes that composes TbNT11 region, meanwhile TbNT12 locus is composed by TbNT12.1 and TbNT12.2 (De Koning et al., 2005). The report of them transporting adenine and pentamidine could not be reproduced in the De Koning lab.

The H1 and H4 transporters mediate the transportation of nucleobases in the procyclic form of *T. brucei*. H1 has no affinity to pyrimidine nucleobase or to purine or pyrimidine nucleosides, and specifically mediates the uptake of purine nucleobases (De Koning and Jarvis, 1997a; De Koning et al., 2005). H4, also known as NT8.1, shows a high affinity for purine nucleobases and a low uracil affinity. H4 is encoded by one of three nucleobase transporter genes on chromosome 11 on a *tandem* repeat (Burchmore et al., 2003a). H2 and H3 are the two purine nucleobase transporters identified in the BSF of *T. brucei* for transporting nucleobases (De Koning and Jarvis, 1997a). The uptake of some pyrimidine nucleobase and purine nucleobases is mediated by H2, meanwhile H3 is specific for the uptake of nucleobases and has no affinity for pyrimidines, or for purine nucleosides (De Koning and Jarvis, 1997a).

Nucleoside and pyrimidine nucleobases require a transport protein to facilitate its entry in the plasma membrane; this is because they do not diffuse at an efficient rate through the plasma membrane. The genes encoding these transporters have not been identified fully in protozoans (Bellofatto, 2007; De Koning, 2007). The U1 carrier in procyclic forms was the first pyrimidine activity in *T. brucei* to be identified. U1 has a high uracil affinity and is selectively permeable to uracil with a K_m value of 0.46 μM , and is inhibited by uridine and the cytotoxic analogue 5-fluorouracil with K_i values of 48 μM for uridine and 3.2 μM for 5-fluorouracil. U1 has no affinity for pyrimidine nucleosides other than low affinity for uridine, nor for any purines (de Koning and Jarvis, 1998). Gudin et al. (2006) identified cytosine (C1) and uridine (U2) transport activities in PCF of *T. brucei*. C1 is inhibited by cytidine and uracil and has a high affinity with low capacity for cytosine. U2 has high affinity for uridine with a K_m of 4.1 μM , and U2 also shows high and moderate affinity towards thymidine and cytidine,

respectively (Gudin et al., 2006). (Ali et al., 2013a) reports indicate that BSF of *T. brucei* has 2 transport mechanisms that are used to transport pyrimidines. These two transporters are for thymidine (T1) and uracil (U3). The U3 transporter has a high uracil affinity with a K_m of 0.54 μM and extremely low uridine affinity with K_i value of $>1000 \mu\text{M}$. None of the genes encoding pyrimidine-specific transporters have been identified. A summary of the purine and pyrimidine transport activities in *T. b. brucei* is presented in Table 1.2.

Table 1.2: Kinetic parameters of *T. brucei* purine and pyrimidine transporters.

Transporter	Substrate														
	ADE	ADO	GUA	GUO	HYP	INO	XAN	CTS	CTD	TMN	TMD	URA	URD	5-FU	HPP
P1/NT2	NE ^{3,c}	0.15^a; 0.26^b; 0.38^c		1.8 ^c	NE ^{1,c}	0.44 ^c	>250 ^c		NE ^{3,c}	NE ^{2,c}	44 ^c	NE ^{2,c}	830 ^c		>500 ^c
P2/AT1	0.38 ^a ; 0.30 ^c	0.59^a; 0.92^c		NE ^{3,c}	>500 ^c	NE ^{4,c}	110 ^c		NE ^{3,c}	NE ^{2,c}	NE ^{2,c}	NE ^{2,c}	NE ^{2,c}		260 ^c
NT5 ^d		2	2.2		49.4										
NT6 ^d		1.4	4.3												
NT7 ^d		0.3	1.8												
NT9 ^e	148	0.068		6.2	320	2.75					510		235		
NT10 ^e		0.41				0.53									
NT11 ^f	2.7; 8	266	651		141		7.2	NE ¹				NE ²			67
H1 ^g	3.6	348	1.8	>1000	9.3	>1000	7.2	NE ¹	NE ¹	1300	NE ¹	NE ¹	NE ¹		5
H2 ^h	3.2	590	0.36	10.9	0.123	167	8.8	>500	NE ¹	82	>1000	60	>500		4
H3 ^h	8.8	NE ¹	5.6	NE ¹	4.7	NE ¹	28.8	NE ¹	NE ³	NE ¹	NE ³	NE ¹	NE ³		194
NT8/H4 ⁱ	2.6	860	2.6	4.7	0.55	20	5						95		2.5
U1	NE ^{1,j}	NE ^{1,j}	NE ^{5,j}	NE ^{1,j}	NE ^{1,j}	NE ^{1,j}		NE ^{1,j}	NE ^{1,j}	NE ^{1,j}	NE ^{1,j}	0.46^j	48 ^j ; 33 ^k	3.0^m	
U2 ^k									0.04 1		0.38		4.1		
U3 ⁱ		NE ¹			NE ¹		NE ¹	>2500		>2500	>10000	0.54	9500	2.6^e	
C1 ^k								0.048	0.42			0.36			
ADET1 ⁿ	0.57	NE ¹	NE ⁵		NE ¹	NE ¹	NE ¹		NE ¹	NE ¹	NE ¹	NE ¹	NE ¹		
HXT1 ⁿ	NE ¹	NE ¹	NE ⁵		22	NE ¹	NE ¹		NE ¹	NE ¹	NE ¹	NE ¹	NE ¹		

Values in bold represent K_m values; all others are K_i values. ADE, adenine; ADO, adenosine; GUA, guanine; GUO, guanosine; HYP, hypoxanthine; INO, inosine; XAN, xanthine; CTS, cytosine; CTD, cytidine; TMN, thymine; TMD, thymidine; URA, uracil; 5-FU, 5-fluorouracil; URD, uridine; HPP, allopurinol. NE, no effect at ¹1 mM, ²500 μ M, ³250 μ M, ⁴100 μ M, ⁵25 μ M. ^a(Carter and Fairlamb, 1993); ^b(de Koning and Jarvis, 1998); ^c(de Koning and Jarvis, 1999); ^d(Sanchez et al., 2002); ^e(Al-Salabi et al., 2007); ^f(Ortiz et al., 2007); ^g(De Koning and Jarvis, 1997a); ^h(de Koning and Jarvis, 1997b); ⁱ(Burchmore et al., 2003b); ^j(de Koning and Jarvis, 1998); ^k(Gudin et al., 2006); ^l(Ali et al., 2013a); ^m(Papageorgiou et al., 2005); ⁿ(Campagnaro et al., 2018a). Source: Table adapted from Campagnaro and de Koning (2020).

1.3.4.3 *Trypanosoma cruzi*

The first information about the ability of *T. cruzi* to transport purines was available from the 1970s (Marr et al., 1978). The existence of at least 3 nucleoside transport mechanisms in a *T. cruzi* was reported in these initial studies. In one study the transport mechanism of *T. cruzi* was investigated in a tubercidin-resistant strain and reported one carrier for pyrimidines and tubercidin, one for thymidine with no affinity for tubercidin, and one for adenosine and inosine. The resistance was selected after exposure to ionized radiation; however, this ionization may have caused mutations in other transporter genes, creating some uncertainty about the report (Finley et al., 1988; Nozaki and Dvorak, 1993). Four genes encode ENT transporters in *T. cruzi*, of which at least 3 encode different purine and pyrimidine transport systems (Campagnaro et al., 2018b). This was found through their expression and cloning in PCF of *T. brucei*. TcrNB1 has high affinity for hypoxanthine and guanine, with a K_m value of 0.093 μM for hypoxanthine and K_i value of 0.122 μM for guanine. Secondly, TcrNT1 has affinity for inosine and guanosine, with K_m value of 1.0 μM for inosine and K_i value of 0.97 μM for guanosine. The third is TcrNT2 which has affinity for thymidine (K_m value of 0.223 μM). TcrNB2 is the fourth one it is an ENT with unknown function (Campagnaro et al., 2018b). These 4 ENT genes that are found in a *T. cruzi* do not appear to transport adenine or adenosine (Campagnaro and de Koning, 2020). A summary of the purine and pyrimidine transport activities in *T. cruzi* is shown in Table.1.3.

Table 1.3: Kinetic parameters of *T. cruzi* purine and pyrimidine transporters.

Substrate	Transporter		
	TcrNB1	TcrNT1	TcrNT2
ADE	3.73	>1 mM	NE
ADO	NE	38.9	1556
GUA	0.122	NE	
GUO	17.1	0.97	NE
HYP	0.093	23.9	NE
INO	314.8	1.0	NE
XAN	18.36	410.3	NE
CTS	>1 mM	NE	NE
CTD	>500 μM	NE	728
TMN	>1 mM	>1 mM	>1 mM
TMD	>1 mM	>1 mM	0.223
URA	>1 mM	NE	NE

URD	>1 mM	>1 mM	65.5
2'-deoxyURD			1.11
Tubercidin			695.7

Values in bold represent K_m values; all others are K_i values. NE, no effect at ^a, 1 mM; ^b, 250 μ M; ^c, 25 μ M. Abbreviations: ADE, adenine; ADO, adenosine; CTD, cytidine; CTS, cytosine; GUA, guanine; GUO, guanosine; HPP, allopurinol; HYP, hypoxanthine; INO, inosine; TMD, thymidine; TMN, thymine; URA, uracil; URD, uridine; XAN, xanthine. The substrate affinity of TcrNB2, the fourth ENT identified in *T. cruzi* genome has not been identified yet. Source: Table taken from Campagnaro and de Koning (2020).

1.4 The current understanding of mode of action of 5-FU in Kinetoplastid parasites

Most nucleobase and nucleoside analogues are hydrophilic molecules and thus need specific membrane transporter proteins to enter cells. When they arrive in the cell, they are activated by intracellular metabolic steps to triphosphate derivatives (Galmarini et al., 2002; P De Koning, 2020). Cytotoxic fluoropyrimidine nucleobase and nucleoside analogues, for example, 5-FU and 5F-2'dUrd are antimetabolites that interfere with the synthesis of nucleic acids. These agents could exert cytotoxic action by being integrated into and changing the RNA and DNA macromolecules or by interfering with numerous enzymes involved in the production of nucleic acids such as thymidylate synthase (TS), or by altering the metabolism of physiological nucleobases or nucleosides. These activities result in the disruption of RNA or DNA synthesis and/or structure, and apoptotic cell death (Galmarini et al., 2002; Longley et al., 2003).

Pyrimidine nucleotide metabolism instead is more varied in kinetoplastid parasites. The metabolism and mode of action of the pyrimidine analogue 5-FU was studied using metabolomic evaluation of *T. brucei* and *Leishmania* 5-FU resistant cell lines and the sensitive parental strains (Ali et al., 2013a; Alzahrani et al., 2017). In *T. brucei*, 5-FU was a substrate for uracil phosphoribosyl transferase (UPRT) and assimilated into a large number of metabolites for example precursors for the biosynthesis of lipids (e.g. CDP-ethanolamine and CDP-choline) and sugar metabolism (e.g. UDP-N-acetylglucosamine, UDP-galactose and UDP-glucose), hypothetically affecting variant surface glycoprotein (VSG) glycosylation or GPI anchors, both of which are essential functions to trypanosomes (Ali et al., 2013a; Donelson, 2003), 5-FU may exert its toxicity via integration into RNA (Figure 1.14A). Ali et al. (2013a) mentioned that

sugar nucleotide metabolism contributes significantly to 5-FU mode of action in *T. brucei*, and that changes in this pathway could make major contributions to 5-FU resistance.

In contrast, the pyrimidine analogue 5-FU in *L. major* and *L. mexicana* is not a substrate for UPRT as no fluorinated ribonucleotides or 5F-UMP can be detected by metabolomic evaluations of the sensitive parental strain and *Leishmania* 5-FU resistant cells. The mechanism of action of 5-fluoro-pyrimidines such as 5-FU in *Leishmania* species have largely the same mechanism of action (Alzahrani et al., 2017). In general, promastigotes of *Leishmania* converted 5-FU to 5F-2'dUrd, which was phosphorylated by thymidine kinase (TK) to produce 5F-dUMP. 5F-2'dUrd could be transformed into 5-FU, the reaction, mediated by uridine phosphorylase (UP), the reaction evidently being reversible. Consequently, 5-FU has a general mechanism of anti-leishmanial activity via inhibiting TS by accumulation of 5F-dUMP, and secondly TK by 5F-2'dUrd and the consequent disruption of deoxynucleotide metabolism (Figure 1.14B) (Alzahrani et al., 2017).

The potent bactericidal impacts of 5-FU against numerous bacterial pathogens were described in the last thirty years. 5-FU was established to inhibit the growth of *Staphylococcus epidermidis* and *Staphylococcus aureus* with an MIC₅₀ below 0.8 mg/L. The MIC₅₀ represents the minimum inhibitory concentration (MIC) needed to prevent the growth of the organism by fifty percent. 5-FU was established to perform synergistically with β -lactams against gram-negative bacteria and hindering the formation of biofilm. 5-FU correspondingly applies its bactericidal impact through the inhibition of biosynthesis of the cell wall (Yssel et al., 2017). Another study, by Singh et al. (2015), has shown that 5-FU is incorporated into sugar nucleotides (for example, UDP-MurNAc-pentapeptide, UDP-GlcNAc and UDP-Gal) and results in the interruption of cell wall and nucleic acid biosynthesis.

While the pyrimidine analogue 5-FU is widely used to treat a wide array of cancers, which include colorectal cancer and breast cancer (Longley et al., 2003). There is now a clear understanding of how 5-FU induces cell death and

cytotoxicity; not merely in bacteria and cancer cells but also in protozoa, for example in *Leishmania* species and likewise in *T. b brucei* (Figure 1.14).

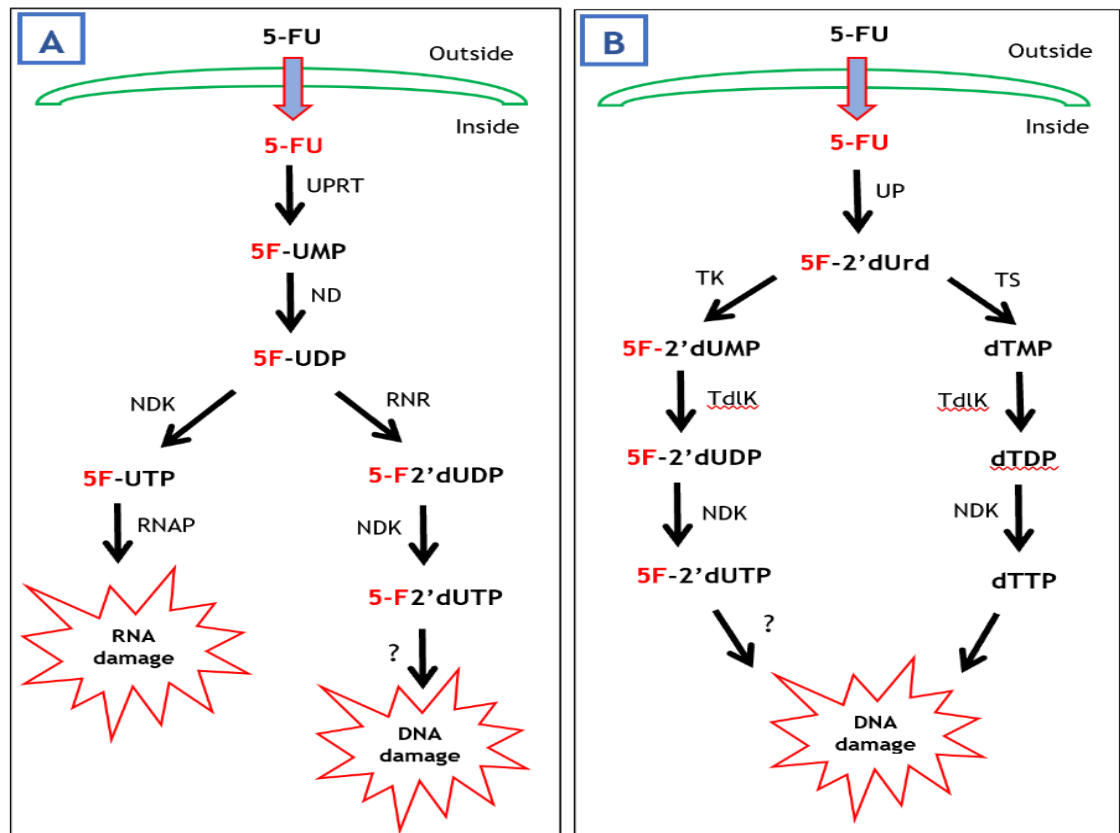


Figure 1.14: Possible biochemical linkages between 5-FU toxicity and damage to RNA and DNA in A) *T. brucei* and B) *Leishmania* spp. The curved green bar schematically represents the plasma membrane of the parasites. Abbreviations: FUMP, FUDP, FUTP: fluorouridine-5'-mono-, di-, and triphosphate, respectively; FdUMP, FdUDP, FdUTP: fluorodeoxyuridine-5'-mono-, di-, and triphosphate, respectively; dUMP: deoxyuridine-5'-monophosphate; dTMP, dTDP, dTTP: deoxythymidine-5'-mono-, di-, and triphosphate, respectively; 5-FU: 5-fluorouracil; 5F-2'dUrd: 5-fluoro-2'deoxyuridine; UPRT: uracil phosphoribosyl transferase; ND: nucleoside diphosphatase; NDK: nucleoside diphosphate kinase.; RNR: ribonucleoside-diphosphate reductase; RNAP: RNA Polymerase; UP: uridine phosphorylase; TdLK: thymidylate kinase; TS: thymidylate synthase; TK: thymidine kinase. Source: Adapted from (Ali et al., 2013a; Alzahrani et al., 2017).

1.5 The applications of RNA sequencing (RNA-seq) and RNA interference target-sequencing (RIT-seq)

In an effort to identify the gene(s) coding for kinetoplastid uracil transporters, a number of investigative avenues have been explored. Owing to the fact that the BLAST search for pyrimidine transporter genes using yeast, prokaryote, as well as fungal uracil transporter sequences has never yielded any candidate gene from any the available protozoan genomes, we have come to a conclusion that the genes cannot be identified by homology to known pyrimidine transporter

genes. For this reason, in an attempt to identify pyrimidine transporter genes of *L. mexicana* and *T. b. brucei*, RNA-seq and RIT-seq were undertaken in previous work in the De Koning laboratory (Ali, 2013; Alzahrani, 2017). In order to gain more details about pyrimidine salvage pathways in *Trypanosoma* and *Leishmania* species, 5-FU-resistant cell lines of *T. b. brucei* BSF and *L. mexicana* promastigotes were generated by subjecting cultures to an increasing concentration of 5-FU *in vitro* (Ali et al., 2013a; Alzahrani et al., 2017).

1.5.1 RNA-seq of WT and 5-FU resistant *T. brucei* BSF and *L. mexicana* promastigotes

According to (Wang et al., 2009; Kukurba and Montgomery, 2015), in order to determine the differential gene expression under varying environmental or physiological conditions, RNA-sequencing is taken as a prevailing method where deep-sequencing technologies are employed. The findings showed that first [³H]-5-FU rates in *Tbb-5FURes* reduced greatly, and 5-FU and uracil transport in *Lmex-5FURes* were completely eliminated (Ali et al., 2013a; Alzahrani et al., 2017). To find out changes in transcription between wild-type cells and 5-FU resistant cell lines of *L. mexicana* and *T. brucei*, analysis of RNA-seq was conducted. The RNA-seq, and parts of the analysis of the dataset, was carried out in the Glasgow Polyomics Facility, including the preparation of cDNA and Illumina sequencing. All the resistant strain genomes (*Tbb-5FURes* and *Lmex-5FURes*) were sequenced in parallel with their respective parental wild-type strains. The main reason for the screening was to find genes encoding pyrimidine-specific transporters in *L. mexicana* and/or *T. brucei*. A statistical analysis was conducted in order to find a group of genes that were expressed differentially between the resistant and sensitive strains.

For *L. mexicana* promastigotes, RNA-sequencing of the parental and 5-FU adapted strains of *L. mexicana* showed numerous changes in gene expression. There were 3967 differentially expressed genes in *L. mexicana* ($P < 0.05$), while the total number of down-regulated genes with a minimum of 3-TM domains in *Lmex-5FURes* was 100. When compared with *L. mexicana* M379 wild-type promastigotes, fatty acid desaturase gene (LmxM.10.1320; log₂ fold-change = -0.32; $P \leq 0.01$) was one of the most highly annotated differentially down-

regulated genes in *Lmex-5FURes* with 6 TMs, and the next was a glucose transporter gene (LmxM.32.0290; \log_2 fold-change = -0.52; $P \leq 0.01$) (Alzahrani, 2017).

Similarly, a large number of changes in gene expression were observed from comparative RNA-sequencing of the parental and 5-FU adapted *T. brucei* strains. There were 2828 differentially expressed genes in *T. brucei* ($P < 0.05$), while the total number of down-regulated genes with a minimum of 3-TM domains in *Tbb-5FURes* was 248. Compared to the reference *T. b. brucei* TREU 927 genome, 3 cation transporter genes (Tb11.v5.0514, Tb927.11.9000 and Tb927.11.9010; \log_2 fold-change = -1.2, -1.2 and -1.04; respectively; $P < 0.001$) were among the most down-regulated genes in *Tbb-5FURes*, with 6-14 TMs, followed by 2 glucose transporter genes (Tb927.10.8520 and Tb927.10.8530; \log_2 fold-change = -0.78 and -1.09; respectively; $P \leq 0.01$) and a fatty acid desaturase gene (Tb927.2.3080; \log_2 fold-change = -0.68; $P \leq 0.01$) (Alzahrani, 2017).

Thus, The RNAseq highlighted fatty acid desaturases and glucose transporters in both kinetoplastid species, and a cluster of cation transporters specifically in *T. b. brucei*.

1.5.2 RIT-seq of 2T1 PYR6-5^{-/-} selected with 5-FU and 6-AU

The genome-wide RNA interference (RNAi) library screen is a superior method for genetic screens for genes to be connected to function and accurate phenotypes, where knockdown confers resistant populations. The *T. b. brucei* PCF is the first organism used in the application of this method (Alsford et al., 2012; Chou et al., 2015; Mohr and Perrimon, 2012; Morris et al., 2002). The basic idea behind RIT-seq method is that every RNAi target fragment serves as barcode that can reveal the associated number of cells conveying the fragment in a mixed population (Glover et al., 2015). Over the past few years, identification of transporters of novel trypanosomal drug, including TbAQP2 as a determining factor for sensitivity of pentamidine (Baker et al., 2012; Munday et al., 2014); the aminopurine carrier TbAT1 as the melarsoprol transporter (Burkard et al., 2011); and amino acid carrier TbAAT6 as the eflornithine transporter (Baker et al., 2011; Burkard et al., 2011); all have been made possible by the use of RNAi-

libraries, sequencing the RNAi fragments in the cells growing out after challenge (RNAi Target sequencing; RITseq). Consequently, in order to identify the genes contributing to pyrimidine transport in *T. brucei* BSF, the genome-scale tetracycline-inducible RNAi library screens in *T. brucei* were implemented.

The RNAi library screen was carried out in London School of Hygiene and Tropical Medicine (LSHTM) at Dr Sam Alsford's laboratory and the library was set as per the established procedure (Glover et al., 2015). A pyrimidine-auxotrophic 2T1 PYR6-5^{-/-} cell line was generated by deleting both alleles of the *PYR6-5* gene that is required for pyrimidine biosynthesis from the 2T1 cell line (Ali et al., 2013b). The *NotI* restriction enzyme was used to digest pZJM RNAi plasmid library so as to produce the 2T1 PYR6-5^{-/-} RNAi library. Tetracycline was then used to induce the 2T1 PYR6-5^{-/-} cell lines (Alsford et al., 2011; Glover et al., 2015).

To generate Tet-inducible dsRNA expression, the pZJM-RNAi plasmid library was created from randomly sheared 600-bp genomic DNA fragments with approximately 11× genome-coverage (complexity of 500,000 fragments) (Alsford et al., 2011; Glover et al., 2015), which permits dsRNA expression for RNA interference knockdown (Glover et al., 2015). At the 14th day of incubation with 5-FU or at the 24th day of incubation with 6-AU, genomic DNA was extracted from the pyrimidine auxotrophic 2T1 PYR6-5^{-/-} cells. The resistant population was isolated from the rest of the samples and the remaining samples were sent to Beijing Genomics Institute (BGI; Hong Kong). In order to reveal the candidate pyrimidine transporter genes in *T. brucei*, RNAi target fragments were sequenced using an Illumina HiSeq platform. The RIT-seq data was analysed before applying a stringency cut off as >99 reads per kilobase per transcript. The results from sequencing runs with varying read depths were compared using barcoded reads expressed as kilobase of transcript per million mapped reads (RPKM) (Alzahrani, 2017; Alsford et al., 2011; Glover et al., 2015).

Genomic DNA from the 2T1 pyrimidine auxotrophic-PYR6-5^{-/-} cell lines challenged with 5-FU and 6-AU was isolated and sequenced at days 14 and 24, respectively. At the 14th day, the number of hits implicated from RIT-seq of 2T1 PYR6-5^{-/-} screened with 5-FU was 521, while the number of hits found in RIT-seq of 2T1 PYR6-5^{-/-} screened with 6-AU at 24th day was 290. Based on 5-FU selection

of 2T1 the PYR6-5^{-/-} RNAi library, genes Tb927.10.8530 (glucose transporter 2A) and Tb927.2.3080 (fatty acid desaturase) with a RPKM value of 6317 and 58392, respectively, were the most conspicuous hits. Glucose transporter 2A and fatty acid desaturase were also found in the RIT-seq data for 2T1 PYR6-5^{-/-} screened with 6-AU at the 24th day, with RPKM values of 4058 for glucose transporter 2A and 439 for fatty acid desaturase, respectively (Alzahrani, 2017).

1.6 Metal ion transporters

Metal ions participate in many different important metabolic functions in the body, gene regulation and in free radical homeostasis. Any anomalies in metal ion homeostasis are likely to lead to a severe illness or even death (Nelson, 1999; Rolfs and Hediger, 1999). Membrane proteins that are found in all living cells function as conduits for the regulated transport of solutes, metal ions, and other small molecules across the cell membranes (Neverisky and Abbott, 2016). The channels and ion transporters are proteins embedded with in a membrane and participate in many vital cell processes. These processes include the regulation of the electrochemical gradient across membranes, substrate transport, regulation of intracellular pH and energy generation. Even though both channels and ion transporters are membrane-bound proteins, there exists a few differences (Demirbilek et al., 2019; Akpunarlieva and Burchmore, 2017). Ion transport can either be active or passive transport. Active transport is aided by primary and secondary active transporters, while passive transport is facilitated by ion channels. The primary active transporters comprise ion pumps and secondary active transporters comprise ion co-transporters and exchangers (Neverisky and Abbott, 2016; Demirbilek et al., 2019). The key difference between channels and ion transporters is that some ion transporters act as ion pumps, facilitating the movement of ions (against the electrochemical gradient) across the membrane (Demirbilek et al., 2019).

The ZIP family of metal ion transporters are broad and can be found in all phylogenetic levels of living organisms. The solute carrier 39 (SLC39) proteins belong to this family of proteins (Eide, 2004). All ZIP/SLC39A proteins are thought to have the same topology, consisting of eight transmembrane (TM) domains, C-terminal and N-terminal extracellular on the cell surface or in the

lumen of cell organelles (see figure 1.15A) (Bowers and Srai, 2018). The human genome has 14 encoded ZIP/SLC39A transporters, with their genes designated SLC39A1-SLC39A14. The genes encode the proteins ZIP1-ZIP14. In the human genome, ZIP transporters are found within distinct sub-cellular compartments (see figure 1.15B) (Jeong and Eide, 2013; Takagishi et al., 2017; Bowers and Srai, 2018). It is still not clear how proteins in the ZIP family and other transporters or trafficking systems coordinate in an effort to regulate zinc homeostasis (Jeong and Eide, 2013). Transporters and channels for inorganic ions have been studied less extensively as potential targets for drugs in *T. brucei*. Conversely, transporters of organic nutrients such as sugars, amino acids, metabolites, nucleobases, and nucleosides have been widely studied (Steinmann et al., 2015).

According to Nyarko et al. (2002), heavy metals such as mercury and cadmium in drug sensitivity assays are extremely toxic to *T. b. brucei* parasites. Toxicity is also a key disadvantage of using heavy metals in drugs against kinetoplastid parasites for human use (Jeong and Eide, 2013; De Carvalho and de Melo, 2017). Many studies have shown that ion transporters are essential in the survival of *Leishmania* and *Trypanosoma* parasites. Steinmann et al. (2015) reported that calcium-activated potassium channels TbK1 and TbK2 are vital for *T. brucei* BSF to survive in culture. The reason for this is that RNAi-mediated downregulation of either of the proteins found in *T. brucei* BSF parasites causes growth defects followed by cell death. Although *Leishmania* iron transporter, LIT1, can transport divalent cations of zinc, manganese and cadmium, it exhibits increased affinity for ferrous iron. When the *LIT1* gene was deleted in *L. amazonensis* amastigotes, it made the parasites unable to proliferate within macrophages that would otherwise result in the development of lesions in mice (Richard et al., 2002; Flannery et al., 2011). Null mutants of the mitochondrial iron transporter, MIT1, in *Leishmania* were unsuccessfully generated. This further supports the crucial role played by this ion transporter in ensuring the survival of *L. amazonensis* promastigotes (Huynh et al., 2012).

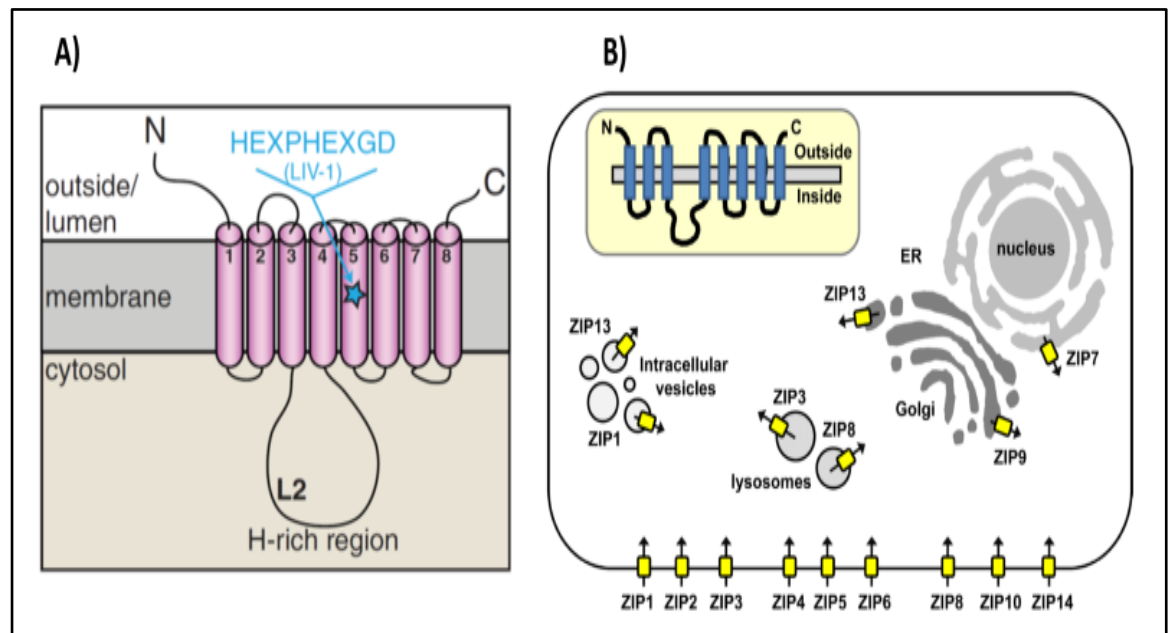


Figure 1.15: Predicted topology and subcellular localisation of the metal ion transporter proteins of the ZIP family. A) Predicted structures and transport mechanisms of ZIP family metal ion transporters. B) Subcellular localization of human ZIP transporters. Zinc transport directions are displayed as arrows, and the inset shaded in yellow depicts a ZIP transporter's predicted topology. Figures taken from (Bowers and Srail, 2018; Jeong and Eide, 2013).

1.7 Glucose transporters

During the metabolic activity of kinetoplastid parasites, glycosomes play a very important role. In kinetoplastid species such as *Trypanosoma* and *Leishmania*, the glycolytic pathway is different in the way that the enzymes of that metabolic pathway are present in a glycosome, a specialised organelle found in the cytoplasm (Opperdoes, 1987; Gualdrón-López et al., 2013; Bayele et al., 2000). Within this organelle in kinetoplastids, the compartmenting for glycolysis is different from other organisms whose glycolytic pathway occurs free in the cytosol, producing pyruvate, before proceeding to further oxidation within the mitochondria (Hannaert, 2011; Hart and Opperdoes, 1984). Glucose is a basic and important source of energy for different organisms, including *Trypanosoma* and *Leishmania* spp. However, hydrophilic glucose cannot pass through the cell membrane into the inside of a cell, and instead depends on glucose transporters embedded in cell membranes, which enable the passive transportation of hydrophilic glucose molecules intracellularly (Delrot et al., 2000; Akpunarlieva and Burchmore, 2017; Manolescu et al., 2007; Pereira and Silber, 2012). Once inside the cell, the glucose is broken down by glycolysis and the pentose phosphate pathway (Barrett, 1997; Landfear, 2011). In glycolysis, a molecule of

glucose is metabolised into two molecules of pyruvate, and yields two molecules of ATP (Saunders et al., 2011; Drew et al., 2003).

1.7.1 *Leishmania* glucose transporters

Glucose is an important source of energy for *L. mexicana* promastigote form. It is also an important nutrient for building blocks used in synthesising different biomolecules (Akpunarlieva and Burchmore, 2017; Rodriguez-Contreras et al., 2007). To this end, glucose transporters play a crucial role in the viability of a variety of pathogenic protozoa, where they have a great influence in both nutrition and metabolism. Considering *Leishmania* spp, the parasite experiences different stages of life cycle, which exposes the organism to different types of sugars in varying concentrations in their environments. The procyclic promastigotes depend on the catalysis of glucose and amino acids, and at the later stages of promastigote development, more amino acid is used, and less glucose (Inbar et al., 2017; Landfear, 2010; Rodriguez-Contreras et al., 2007). The glucose transporters in *L. mexicana* promastigote and amastigote forms have a high glucose affinity, with K_m values of 24 μM and 29 μM for promastigote and amastigote, respectively. The K_m values for the two transporters are closely comparable, suggesting that the same transporter is expressed in both stages of development (Burchmore and Hart, 1995).

There exists a cluster of three glucose transporters in the genome of *L. mexicana*, LmexGT1, LmexGT2 and LmexGT3 (Burchmore et al., 2003a). This cluster is part of the sugar transporter sub-family of the Major Facilitator Superfamily (MFS) (Deng et al., 2014; Dean et al., 2014). Although the three LmexGTs differ in terms of their hydrophilic domains at the carboxyl and amino terminal ends, their amino acid sequence is 90% similar (Burchmore and Landfear, 1998). Each of the three glucose transporters has twelve transmembrane domains, enabling them to transport glucose molecules through the plasma membrane via a passive transport mechanism (Burchmore et al., 2003a; Silber et al., 2009; Pereira and Silber, 2012). The cluster consisting of these three transporters in *L. mexicana* promastigotes was deleted by a targeted gene replacement. Following this technique, it was discovered that the transport

of radiolabelled 2-deoxy-D-glucose in *Lmex-GT1-3* KO cells ' $\Delta lmexgt$ ' was completely abolished (Burchmore et al., 2003a).

With the individual re-expression of the three transporters LmexGT1, LmexGT2 and LmexGT3 into complete knockout of LmexGT1-3 in *L. mexicana* promastigotes, the uptake of glucose, galactose, fructose and mannose is observed. LmexGT2 and LmexGT3 have K_m values of 109 μM and 208 μM respectively, which means that these two transporters are high affinity glucose transporters. On the other hand, LmexGT1 has a high K_m value of 1.22 mM, suggesting a relatively low glucose affinity. From fluorescent microscopy, LmexGT1 is mainly localised in the flagellum, while LmexGT2 and LmexGT3 are concentrated on the plasma membrane (Burchmore et al., 2003a; Rodriguez-Contreras et al., 2007). These observations are consistent with the lower glucose levels in the environments in which promastigotes are exposed to. LmexGT2 has mRNA levels in promastigotes approximately fifteen times higher compared to the amastigote form, while mRNA levels in both LmexGT1 and LmexGT3 are expressed at the same levels in both stages of life cycle (Burchmore and Landfear, 1998). In addition, there was a low growth rate of *Lmex-GT1-3* KO cells, suggesting a lower rate of infection to macrophages. This affirms that the survival of amastigotes is at least partly dependent on the expression of isoforms of LmexGT1-3 (Burchmore et al., 2003a).

1.7.2 Trypanosomes glucose transporters

The African trypanosomes that reside in the bloodstream depend entirely on the uptake of glucose to generate energy by glycolysis. The BSF that live in the mammalian blood express a broad specificity, high capacity hexose transporter. The absolute requirement for glucose uptake for the survival of these organisms makes the transporter and the glycolytic enzymes potential drug targets (Lamour et al., 2005; Landfear, 2010). Conversely, trypanosomes of procyclic form use amino acids (mainly proline) as their main source of energy using the Krebs cycle and the respiratory chain (Pereira and Silber, 2012; Tetaud et al., 1997). Glucose uptake by *T. brucei* BSF was studied by using an inhibitor for its transporter and it was found that the glucose transport mechanisms are very

distinct from that found in human erythrocytes and had 10 fold increased affinity for glucose (Seyfang and Duszenko, 1993).

The genome of *T. brucei* contains a cluster of the hexose transporter genes with 6 copies of the THT1 genes, and 5 copies of THT2 (Landfear, 2010). THT1 mRNA is mainly expressed in the parasite of the bloodstream form, while THT2 is entirely expressed in the procyclic form (Haanstra et al., 2011). Considering the amino acid sequence, THT1 and THT2 are about 80% identical (Borst and Fairlamb, 1998). The six genes encoding THT1 are >99.5% identical by amino acid sequence. The same is true for the THT2 isoforms and their amino acid sequence, which are also >99.5% identical. The functions of three glucose transporters 1B, 1E and 2A have been experimentally verified (Barrett et al., 1995; Feistel et al., 2008; Bringaud and Baltz, 1993). On the other hand, the functions of the other eight glucose transporter genes have been deduced from their amino acid sequences. In the previous studies, glucose transporter 1B was confirmed as a functional glucose transporter, heterologously expressed in *L. mexicana* for the uptake of glucose (Feistel et al., 2008). The glucose transporter 1E was expressed in *Xenopus oocytes*, and showed a significant increase in the uptake of radiolabelled 2-deoxy-D-glucose (Bringaud and Baltz, 1993). Also Barrett et al. (1995), cloned glucose transporter 2A from *T. brucei* PCF, which is expressed in *Xenopus oocytes*, a confirmation that the 2A is responsible for glucose transport in PCF of trypanosomes.

1.8 Uracil transporter families in other species

Uracil transport is a physiological activity of a cell present in the most organisms whether unicellular or multicellular. The molecular basis of uracil transport comes from microbiological studies, about half a century ago (de Koning and Diallinas, 2000) Further, previous studies on bacteria and fungi have shown the existence of uracil transport in those cells (Amillis et al., 2007). The uracil transporter from *Aspergillus nidulans* (FurD) belongs to the NAT/NCS2 family (nucleobase ascorbate transporters or nucleobase cation symporter family 2), whose function is to transport uracil and protons (Hamari et al., 2009). NAT transporters also participate in mediating the uptake of toxic pyrimidine analogues, for example, the 5-fluorouracil which is an anticancer analogue

(Kourkoulou et al., 2018; Byrne et al., 2016). It has been found that most of the uracil transport mutants are resistant to 5-fluorouracil. The uracil transport mutants were used as a guide in identifying and cloning the gene coding for uracil permeases in both bacteria and yeast (Andersen et al., 1995). The knockout of the *FurD* gene in *A. nidulans* contributed to a full phenotype of resistance to 5-fluorouracil and completely reduced uptake of radiolabelled uracil (Amillis et al., 2007). The K_m value of FurD is 0.45 μM , implying a high affinity of this transporter to uracil and its position 5-substituted analogues: 5-fluorouracil (K_i of 0.46 μM), 5-chlorouracil (K_i of 0.46 μM) and 5-aminouracil (K_i of 0.86 μM). However, FurD has no affinity for adenine, cytosine, guanine, hypoxanthine, thymidine or uridine ($K_i > 1500 \mu\text{M}$). FurD mediated radiolabelled uracil and was inhibited by xanthine (K_i value of 94 μM) and uric acid (K_i value of 99 μM) (Amillis et al., 2007). These findings suggest that FurD transporter has the capability to transport xanthine and uric acid (Hamari et al., 2009).

Given that BLAST analysis does not identify any FurD homologues in either metazoan or protozoan genome databases, the uptake of uracil must be mediated by a transporter from another family of genes (De Koning, 2007; Amillis et al., 2007). The closest homologues of FurD include the *Fur4p* gene, which encodes the *Saccharomyces cerevisiae* uracil transporter (Jund et al., 1977; JUND et al., 1988), the *PIUP* gene which encodes the *Paenibacillus larvae* uracil permease, and *UraA* gene which encodes the *Escherichia coli* uracil transporter. These genes have amino acid similarities 46.2% for *Fur4p*, 54.6% for *PIUP* and 37.1% for *UraA* with FurD (Jund et al., 1977; JUND et al., 1988; Andersen et al., 1995; Stoffer-Bittner et al., 2018). *Fur4p*, *UraA* and *PIUP* mutants in *S. cerevisiae*, *E. coli* and *P. larvae* respectively were found to be resistant to 5-fluorouracil and lacked radiolabelled uracil transport. *Fur4p* belongs to the NCS1 family, while *UraA* and *PIUP* are proton symporter and prototypical members of NAT, also known as the NCS2 family of proteins (Jund et al., 1977; Andersen et al., 1995; JUND et al., 1988; Stoffer-Bittner et al., 2018; Kryptou et al., 2015).

The *UraA/H⁺* symporters found in *S. cerevisiae*, *E. coli*, and *A. nidulans* belong to the NAT family of transporters. This symporter participates in the proton driven

uptake of uracil into the cells (Hamari et al., 2009; Kalli et al., 2015). UraA possesses a novel structural fold which consists of 14 transmembrane segments. These segments have their N terminal and C terminal domains located on the cytosolic side of the cells. An unwound fragment precedes two short, antiparallel β strands in UraA, followed by a short α helix. It is the unwound segment that differentiates UraA from other transmembrane proteins. The protein has 14 domains, which can further be divided into two main domains: core and gate domains. The core domain consists of TM1, TM2, TM3, TM4, TM5, TM8, TM9, TM10, TM11 and TM12, whereas the gate domain consists of TM5, TM6, TM7, TM12, TM13 and TM14. Between these two domains is an interface which accommodates residues that can either be protonated or deprotonated, meeting the requirement for symporters coupled with protons (see figure 1.16) (Kalli et al., 2015; Lu et al., 2011; Yu et al., 2017). The TM3 and TM10 transmembrane regions in uracil transporter is characterised by a pair of anti-parallel β -strands structure, which is crucial in the binding and transportation of substrate uracil. During the transport process, the core domain is responsible for substrate binding, while the gating domain becomes responsible for changing the conformation of the whole protein (Lu et al., 2011).

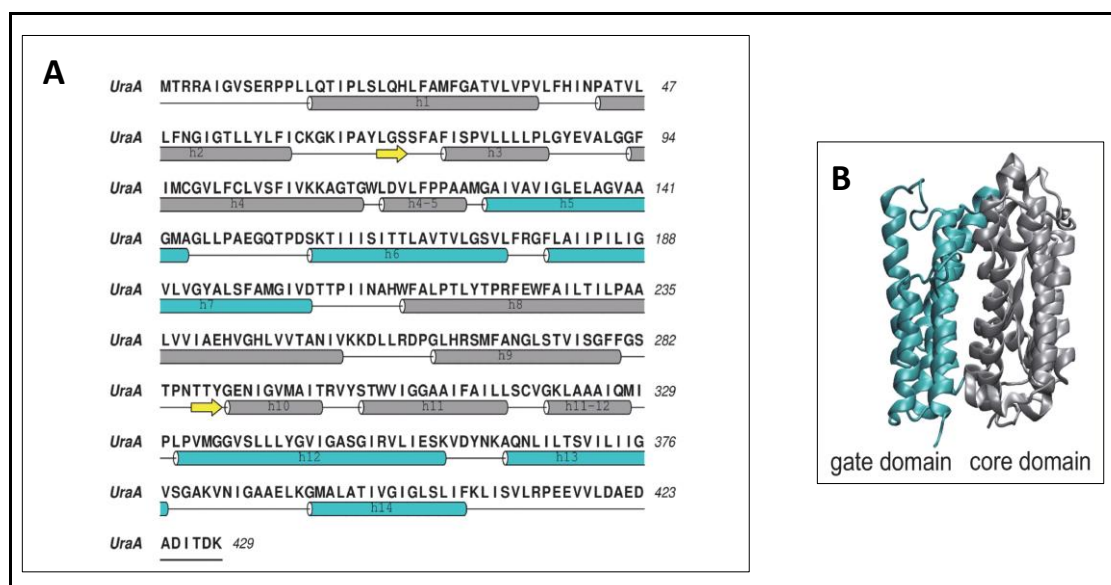


Figure 1.16: The structure of the *E. coli* uracil transporter UraA. A) The amino acid sequence of UraA; Grey colour indicates the core domain while cyan colour indicates the gate domain; h1 to h14 refer to the number of transmembrane helices. B) The crystal structure of UraA showing the gate (grey colour) and the core (cyan colour) domains. Figure modified from Kalli et al. (2015).

1.9 Aims of the study

The main aim of this research is to identify the gene family encoding the protozoan pyrimidine transporters and assess candidate genes potentially involved in the transport of, or sensitivity to, 5-fluorouracil. For this, we will use functional expression and reverse genetic approaches such as overexpression and knockout constructs of the target genes. The research described in this thesis had the following five specific aims:

1. To characterise the cation transporters of *T. b. brucei* BSF.

The purpose of this chapter is to continue working on the characterization of the CATs, which were among the few differentially expressed transporters in the 5FURes strain, and therefore must be considered as potential candidates for uracil transporter, or at least change something in the cellular biochemistry that changes susceptibility to 5-FU. Moreover, none of these potential transport genes have been previously characterised in protozoa and as such they are of interest in their own right as well. Here, we overexpress of CATs in the *Tbb-5FURes* cell lines and continue work on the characterization of CATs to attempt to acquire a double knockout for these genes in *T. b. brucei* s427 WT, aiming to determine their involvement, direct or indirect, in pyrimidine uptake and resistance to the pyrimidine analogues. As part of the characterisation efforts, we also assess the susceptibility of the overexpressing cell lines Tbb-CAT1-4 to heavy metal ions, as the analysis of Tbb-CAT1-4 protein sequences with Pfam (<http://pfam.xfam.org>) revealed that they belong to a family of Zip zinc transporter (PF02535).

2. To investigate the role of fatty acid desaturase in 5-FU resistant cells of *L. mexicana* and *T. brucei* that was clearly associated with 5-FU resistance for as yet unknown reasons.

The aim is to understand the role of the *Tbb-FAD* and *Lmex-FAD* genes in 5-FU resistance. We will investigate whether overexpression of these genes restores the sensitivity to 5-FU, or the transport of 5-FU/uracil *in vitro*.

3. To clone and functionally express the *A. nidulans* uracil transporter FurD in order to examine whether 5-FU resistant strains could restore the sensitivity to 5-FU, or the transport of 5-FU/uracil.

This would allow a functional screening of potential transporter genes. Moreover, it would expand knowledge of the mechanisms used by *T. brucei* and *L. mexicana* to transport pyrimidines.

4. To determine whether glucose transporters are associated with resistance to 5-FU in kinetoplastid parasites, as this possibility was prominently indicated in recent RITseq and RNAseq analyses.

The primary aim of this work is to determine the sensitivity to and transport of 5-FU after the full knockout of genes responsible for transportation of glucose in *L. mexicana* promastigotes. The chapter also focuses on examining the sensitivity/transport of *Lmex-GT1-3* KO cells that re-express individual glucose transporters to 5-FU/uracil. In addition, an investigation is conducted to ascertain whether, when the FurD uracil transporter is introduced, this is able to restore the sensitivity/transport to 5-FU in *Lmex-GT1-3* KO cells. Moreover, an assessment is carried out to find out the effects of the absence of glucose in the extracellular medium *T. b. brucei* s427 WT PCF in the sensitivity to 5-FU and the growth rate.

5. To characterise the TcrNT2 and TcrNB2 transporters and assess its transporter activity using the *L. mexicana-Cas9^{ΔNT1}* strain as a surrogate system.

This work is linked with the previous study by (Campagnaro et al., 2018b), who cloned TcrNT2 and TcrNB2 into the *L. mexicana-Cas9* nucleoside transporter 1 knockout cell line (*L. mexicana-Cas9^{ΔNT1}*). thereby enabling their transport activity to be assessed. Another objective of this study is to continue working on the characterisation of TcrNT2 and TcrNB2 transporters to establish if they can be used as drug delivery system.

2 Material and Methods

2.1 Materials

2.1.1 Media and media components

HMI-9 and SDM-79 medium powder for culturing *T. b. brucei* bloodstream form and *T. b. brucei* procyclic forms were bought from Gibco™ (Life Technologies, Paisley, UK). Heat-inactivated Fetal Bovine Serum (FBS) was from PAA Laboratories (Linz, Austria). Sodium bicarbonate (NaHCO₃) and β-mercaptoethanol were purchased from Sigma (Dorset, UK). HOMEM medium for culturing *L. mexicana* promastigote form was obtained from Gibco™ (Life Technologies, Paisley, UK). L-Proline was purchased from Sigma (Dorset, UK), whereas Penicillin-Streptomycin antibiotic was obtained from Gibco™ (Life Technologies, Paisley, UK).

2.1.2 Chemicals including nucleoside and nucleobase analogues

Promega (Madison, USA) supplied dNTPs, GoTaq DNA Polymerase and T4 DNA Ligase. Both the restriction enzymes and Phusion High-Fidelity DNA Polymerase were obtained from New England BioLabs (Hitchin, UK). The NucleoSpin® PCR and Gel extraction kit, and the NucleoSpin Plasmid purification kit were purchased from Macherey-Nagel® GmbH & Co. KG (Düren, Germany). Dimethyl Sulfoxide (DMSO) and glycerol were obtained from Merck (Sigma-Aldrich Company Ltd, Dorset, UK).

The Pentamidine, 6-Azauracil, 5-Fluorouracil, Amphotericin B, Miltefosine, Tubercidin, 5-Fluoro-2'-deoxyuridine, Deferoxamine, Salicylhydroxamate (SHAM), Diminazene aceturate, Cadmium(II) acetate, Mercury(II) chloride, Barium chloride, Lead(II) chloride, Copper(II) chloride, Zinc chloride and Iron(III) chloride hexahydrate compounds, and resazurin sodium salt were bought from Sigma-Aldrich® (Poole, UK). Novel adenosine analogues were designed and synthesised by Dr. Fabian Hulpia in the laboratory of Professor Serge van Calenbergh (University of Ghent, Belgium).

2.1.3 Radiolabelled compounds

The following radiolabelled compounds were used during the project: [³H]-Uracil (24.8 Ci/mmol), [³H]-Thymidine (56.6 Ci/mmol) and [³H]-Adenine (40.3 Ci/mmol) were obtained from Perkin-Elmer (Waltham, MA, USA). [³H]-5-Fluorouracil (20 Ci/mmol) and [³H]-2-deoxy-D-glucose (18.7 Ci/mmol) were from Moravek Inc (California, USA). [³H]-Adenosine (40 Ci/mmol) was purchased from American Radiolabelled Chemicals Incorporated (St Louis, MO, USA), while custom-made [³H]-Pentamidine (38.4 Ci/mmol) was purchased from Amersham Plc (Buckinghamshire, UK).

2.2 Culturing of kinetoplastid cells

2.2.1 Culturing of *T. b. brucei* BSF and PCF

In this project, six strains of bloodstream form (BSF) of *T. b. brucei* were used. 1) *Tbb-5FURes* was adapted to a high level of resistance to 5-Fluorouracil (Ali et al., 2013a), 2) from another strain, *T. b. brucei* Lister 427-WT. 3) B48, a multi-drug resistant strain that was generated by double knockout of the *TbAT1* gene (Matovu et al., 2003) and adaptation to growth in high levels of pentamidine *in vitro* (Bridges et al., 2007). 4) *T. b. brucei* MITat1.2, clone 221a (2T1) strain (Alsford et al., 2005). was generously donated by Prof. David Horn (University of Dundee). 5) The pentamidine-resistant Aquaporin 2/3 double null strain (*aqp2/aqp3 null*) and 6) Aquaporin 1-3 triple null strain (*aqp1/aqp2/aqp3 null*); *aqp1/aqp2/aqp3 null* were obtained by the knockout of the aquaporin genes specifically implicated in resistance to pentamidine in field isolates (Alsford et al., 2012; Jeacock et al., 2017).

The standard HMI-9 medium (Barrett and Croft, 2012; Hirumi and Hirumi, 1989) was used for culturing the six strains, complemented with 10% FBS, 3.0 g/L sodium hydrogen carbonate and 14 µl of β-mercaptoethanol per one litre of medium, with pH of 7.4 (*T. brucei* BSF cultures were not supplemented with Penicillin-Streptomycin antibiotic). A Millipore Express®PES Membrane Filter was used to filter-sterilise the medium inside the biosafety cabinet. The parasite cells in the vented flasks were cultured and incubated at 37 °C under 5% CO₂ and

the parasite cells were passaged three times for every week. One strain of procyclic forms (PCF) of *T. b. brucei-s427 WT* was used in this study. PCF of *T. b. brucei Lister s427* were maintained in non-vented plastic flasks with SDM-79 culture medium at 27 °C with pH of 7.4 and supplemented with 10% FBS and 7.5 µg/mL haemin.

2.2.2 Culturing of *L. mexicana* promastigote form

In this project, four strains of *L. mexicana* promastigote form were used: 1) *L. mexicana* wild type (MNY/BZ/62/M379 strain), 2) *L. mexicana* 5-FU resistant cells (*Lmex-5FURes*), a strain that was adapted to high levels of resistance to 5-Fluorouracil *in vitro* (Alzahrani et al., 2017). 3) Glucose transporter null mutant (*Lmex-GTs KO*) in *L. mexicana* promastigotes wild type from which all three glucose transporters *LmexGT1-3* have been deleted, and re-expression of each glucose transporter genes separately (*Lmex-GT1*, *Lmex-GT2* and *Lmex-GT3*) in the *Lmex-GTs KO* strain (Burchmore et al., 2003a) kindly gifted by Dr Richard Burchmore (University of Glasgow). 4) *L. mexicana-Cas9 T7* strain (derived from *L. mexicana WT* promastigotes by expression of the *Streptococcus pyogenes* Cas9 nuclease gene 'Cas9' and maintained on 32 µg/mL hygromycin (Beneke et al., 2017). As described by (Al-Salabi et al., 2003), HOMEM medium was used to culturing of *L. mexicana* cell lines in the unvented flask, supplemented with 10% of FBS and 1% Penicillin-Streptomycin antibiotic at 25 °C.

2.2.3 Growth curves

The standard HMI-9 medium added with 10% FBS was used to determine the growth rates of the *T. b. brucei* BSF strains, while the growth rates of the *T. b. brucei* PCF were determined in the SDM-79 medium supplemented with 10% FBS and either 1 g/L of glucose, 0.2 g/L of glucose or no glucose. The growth rates of the *L. mexicana* promastigotes were determined in the standard HOMEM medium supplemented with 10% FBS in the presence and absence of 5 mM of L-proline. After every 24 hours, cells were counted in a sample of the culture, using either a Neubauer haemocytometer chamber (Hawksley, UK) or by a coulter particle counter and size analyzer (Beckman, US) to count the cells in

triplicate. An average of the triplicate readings was taken and plotted using GraphPad PRISM 8 software to obtain the growth curves.

2.2.4 Preparation of stabilates

In order to prepare stabilates of *L. mexicana* promastigotes and *T. b. brucei* BSF/PCF, cell cultures were added to an equivalent volume of the corresponding culture medium (HMI-9, SDM-79 or HOMEM) containing 30% sterilized glycerol, in long-term storage cryogenic tubes. Before the cryogenic tubes were transferred to liquid nitrogen store, they were first frozen at a temperature of -80 °C for 72 h. For the recovery of stabilates, the cryogenic tubes were brought out from the liquid nitrogen store, and thawed at 25 °C and then cultivated to the suitable medium. In this project, the cells were renewed after 20 passages by bringing out fresh cells from the liquid nitrogen store.

2.3 Molecular techniques

The sequences of the nucleotide and amino acid for a gene of interest were obtained from GeneDB (genedb.org) and TritypDB (tritrypdb.org/tritrypdb) websites. The sequence alignments and the primers that were used in this project were created and designed by using the CLC Genomics Workbench version 7.0 software package (CLC bio, Qiagen).

2.3.1 Polymerase chain reactions PCR

All the primers used in this project were all synthesized by Eurofins MWG Operon (Ebersberg, Germany) and Sigma-Aldrich (Dorset, UK). PCR with specific primers was used to amplify the genomic DNA of *T. b. brucei*, *T. cruzi* and *L. mexicana*. In order to determine the best annealing temperature, a gradient PCR was performed. A gene of interest (GOI) from the genomic DNA in Table 2.1 and Table 2.2 was amplified by the Phusion High-Fidelity DNA Polymerase, whereas GoTaq DNA Polymerase was used for the PCR screening in Table 2.3 and Table 2.4. Upon completion of the PCR reaction, a 1% or 2% of agarose gel (1 g or 2 g of agarose in 100 mL of 1% TAE buffer) was run to visualise the PCR products with 5 µL of SYBR Safe DNA gel stain (Invitrogen) under UV light.

Table 2.1: The PCR master mix for Phusion High-Fidelity DNA Polymerase.

No.	Component	Volume
1	dd H ₂ O	34 µl
2	5x Phusion GC buffer	10 µl
3	10mM dNTP	1 µl
4	10 µM Forward primer	2 µl
5	10 µM Reverse primer	2 µl
6	Genomic DNA	0.5 µl
7	Phusion polymerase	0.5 µl
Total of reaction		50 µl

Table 2.2: The PCR condition for Phusion High-Fidelity DNA Polymerase.

Hot lid on 110°C
Temperature step: 98°C for 30 seconds
Start cycle (x35)
Temperature step: 98°C for 10 seconds
Temperature step: *°C for 40 seconds (*: Best melting temperature based on a gradient PCR)
Temperature step: 72°C for * seconds (*:30 sec/kb of DNA of interest)
End cycle
Temperature step: 72°C for 10 min
Store at 10°C - ∞

Table 2.3: The PCR master mix for GoTaq DNA Polymerase.

No.	Component	Volume
1	dd H ₂ O	34 µl
2	5x GoTaq reaction buffer	10 µl
3	10mM dNTP	1 µl
4	10 µM Forward primer	2 µl
5	10 µM Reverse primer	2 µl
6	Genomic DNA	0.5 µl
7	Go Taq polymerase	0.5 µl
Total of reaction		50 µl

Table 2.4: The PCR condition for GoTaq DNA Polymerase.

Hot lid on 110°C
Temperature step: 95°C for 3 min

Start cycle (x35)
Temperature step: 95°C for 30 seconds
Temperature step: *°C for 30 seconds (*: Best melting temperature based a gradient PCR)
Temperature step: 72°C for * seconds (*:1 min/kb of DNA of interest)
End cycle
Temperature step: 72°C for 10 min
Store at 10°C - ∞

2.3.2 List of primers for PCR

Table 2.5 displays the primers used in the genetic modification of *L. mexicana* and *T. b. brucei*. Suitable restriction sites were added onto particular primers so as to permit the cloned DNA fragment to be digested and then ligated into a suitable plasmid.

Table 2.5: Oligonucleotides designed and used in this project.

Primer name	Position	Restriction site	Sequence (5'UTR - 3'UTR)	Amplicon name
HDK1338	Forward	<i>MluI</i>	GGTTACGCGTATGTTGCCTAAGCAA CAGAT	<i>Tbb-FAD</i>
HDK1339	Reverse	<i>BamHI</i>	GGTTGGATCCTTAAGTGGGATAAAT GC	
HDK1344	Forward	<i>NdeI</i>	GGCCCATATGATGAGGTCCGTGCTC AA	<i>Lmex-FAD</i>
HDK1345	Reverse	<i>BglII</i>	AATCAGATCTTTACGCGCCCTTCCCG G	
HDK1427	Forward	<i>BglII</i>	GATTAGATCTATGCGTTTCGGTCGC TT	<i>FurD</i>
HDK1428	Reverse	<i>XhoI</i>	GGTTCTCGAGTCAGTAAACAGCAAA AC	
HDK1537	Forward	<i>BglII</i>	GGCCGGAGATCTATGCCTTTTTTCA GTTCC	<i>TcrNB2 in Leish</i>
HDK1538	Reverse	<i>XhoI</i>	CCGGCTCGAGCTATATGGCAAGCAC AATA	
HDK1551	Forward	<i>BglII</i>	AGATCTATGGGACTGGGCTTCGAAT TCT	<i>TcrNT2</i>
HDK1552	Reverse	<i>XhoI</i>	AAATTTCTCGAGCTACCCGCGCAAG GTCTG	
HDK1039	Forward	<i>MluI</i>	GGCTACGCGTATGGCTAACGTTAAT AACG	<i>Tbb-Cations 1-4</i>
HDK1040	Reverse	<i>BamHI</i>	GGCTGGATCCTTAGACCCATTTTCCT AAC	<i>Tbb-Cations</i>

				1-4
HDK1041	Reverse	<i>Bam</i> HI	CCGGGGATCCTTAGATCCACTTTCC AATA	<i>Tbb-Cations</i> 1-4
HDK1042	Reverse	<i>Bam</i> HI	CCGGGGATCCTTAGATCCATTTTCCA ATA	<i>Tbb-Cations</i> 1-4
HDK802	Forward	<i>Ap</i> al	GGGCCCATGCCTTTTTTCAGTTCC	<i>TcrNB2 in</i> <i>Tryp</i>
HDK803	Reverse	<i>M</i> lul	ACGCGTCTATATGGCAAGCACAATA GCC	
HDK535	Forward	-	CGGACAGGTATCCGGTAAGC	-
HDK335	Reverse	-	TGGCCACACAACCCGGTGT	-
HDK340	Reverse	-	CGTGGAGCAGCTGAAGGACA	-
HDK531	Forward	-	ATGCGTTTTCGGTCGCTTTCA	-
HDK532	Reverse	-	TCAGTAAACAGCAAAACCCT	-
HDK429	Forward	-	TTCGAGTTTTTTTTCTTTT	-
HDK1052	Forward	-	GCTGCTGTCCAAGTGGCACTAG	<i>Tbb-CAT 1-</i> <i>4 KO</i>
HDK1053	Reverse	-	CTGACGGTGGCGCTTAGGCAT	
HDK1523	Forward		TCCGCTGCAAAACAACTTCTGG	NT1 KO
HDK1524	Reverse		TACGCCGCTACGATGATCCAGC	
MB39	Forward	-	ATGAAAAAGCCTGAACTCAC	<i>Hygromycin</i>
MB40	Reverse	-	ACTCTATTCTTTGCCCTCG	
MB37	Forward	-	ATGATTGAACAAGATGGATTGC	<i>Neomycin</i>
MB38	Reverse	-	TCAGAAGAACTCGTCAAGAAG	
HDK282	Forward	-	CGAATTCATGGCCAAGCCTTTGTCT	<i>Blasticidin</i>
HDK283	Reverse	-	CGAATTCTTAGCCCTCCCACACATA	

2.3.3 Isolation of genomic DNA

The NucleoSpin Tissue kit (MACHEREY-NAGEL, Germany) was used to extract genomic DNA for the *T. b. brucei* and *L. mexicana*, according to the instructions given by the manufacturer. Firstly, the cells were centrifuged at $1000 \times g$ for 10 min. Thereafter, the cells were resuspended in 200 μ L Buffer T1, 200 μ L Buffer B3 and 25 μ L Proteinase K (provided with the kit). The mixture was vortexed vigorously and incubated at a temperature of 70 °C for a period of 10 to 15 min. Next, 210 μ L of pure ethanol was added and vortexed vigorously. The specimen was thereafter put into a NucleoSpin tissue column and centrifuged for 1 minute at $11,000 \times g$. The specimen was washed by using 500 μ L Buffer BW and

thereafter centrifuged for 1 minute at $11,000 \times g$. Then, the specimen was washed again by using 600 μ L Buffer B5 and centrifuged for 1 min at $11,000 \times g$. Subsequently, the specimen was centrifuged for 1 min at $11,000 \times g$. Lastly, buffer BE (50 μ L) was added to elute DNA from the membrane. The concentration of DNA was measured by using the NanoDrop-1000 spectrophotometer (Thermo Scientific, UK), and the specimens of the DNA were kept at a temperature of -20°C .

2.3.4 Plasmid construction and transfection

2.3.4.1 Expression plasmids in *T. b. brucei* and *L. mexicana*

2.3.4.1.1 Generation of plasmids for expression and transfection into *T. b. brucei* BSF

The fatty acid desaturase gene Tb427.02.3080 (*Tbb-FAD*), four cation transporter genes Tb427tmp.01.0725 (*Tbb-Cation1*), Tb427tmp.01.0730 (*Tbb-Cation2*), Tb427tmp.01.0760 (*Tbb-Cation3*) and Tb427tmp.01.0770 (*Tbb-Cation4*), and *Aspergillus nidulans* uracil transporter gene A6N844 (*FurD*) and *T. cruzi* NB2 TcCLB.506445.110 (*TcrNB2*) were expressed in the *Tbb-5FURes*, *Tbb-s427 WT* and B48 strains by using the pHD1336 plasmid that contains the *Blasticidin* resistance gene. The pHD1336 vector is constitutively expressed and integrates into the non-transcribed ribosomal RNA (rRNA) spacer (Figure 2.1) (Biebinger et al., 1997) and has been found to be very effective for the overexpression of genes in *T. b. brucei* BSF and PCF (Munday et al., 2013; Alzahrani et al., 2017; Campagnaro et al., 2018b). The suitable restriction enzymes were used to digest the pHD1336 plasmid and the gene of interest (GOI). Then, as explained by the manufacturer's protocol, the ligation of digested GOIs into the digested pHD1336 plasmid was performed, using the T4 DNA Ligase kit. After that, the pHD1336 plasmid including the GOIs was transformed into the XL1-blue cells (*E. coli*) using a heat shock approach according to the manufacturer's protocol (Appendix 3). PCR screening of bacterial colonies on the plate was used to detect the colonies containing the desired target gene by using HDK429 forward and HDK335 reverse primers of the plasmid. Briefly, after overnight incubation, pick bacterial colonies from the LB agar plate with a sterile 200 μ l pipette tip (green), and streak them onto a new

LB agar plate and then use the residual bacteria for a PCR reaction, dipping the tip into the PCR reaction mix. The new LB agar plate was then incubated at 37 °C overnight. For each plasmid, five colonies containing the GOI were grown overnight in 10 mL of 100 µg/mL of ampicillin at 37 °C. Cultures were centrifuged at 4,500 x g for 10 min, the supernatant discarded and the pellet used for the plasmid purification (miniprep) using the NucleoSpin Plasmid purification kit following the manufacturer's instructions. After PCR screening, the pHDK1336 plasmids having the GOIs were sent to Source Bioscience for Sanger sequencing (Livingston, United Kingdom). After the sequences of the target gene were verified, the produced plasmids were named as pHDK219 (*Tbb-FAD*), pHDK069 (*FurD*), pHDK199 (*Tbb-Cation1*), pHDK200 (*Tbb-Cation2*), pHDK201 (*Tbb-Cation3*), pHDK202 (*Tbb-Cation4*) and pHDK223 (*TcrNB2*).

For transfection, the linearization was set up by *NotI* restriction enzyme; 1×10^7 *T. b. brucei* BSF were washed with 100 µL of transfection buffer and mixed with 10 µg of ethanol-precipitated DNA of the expression construct. The cells were electroporated using Program X-001 of the Amaxa Nucleofector (Amaxa AG, Germany). Cells were then transferred to 20 mL of HMI-9 medium containing 10% FBS and allowed to recover overnight at 37 °C and 5% CO₂. After recovery, 5 µg/mL Blasticidin was added to the culture as a selective marker for the expression construct; using limiting dilution (1:10, 1:25 and 1:100) the cells were plated out in a 96-well plate to produce individual clones. PCR was used to screen the antibiotic resistant clones: 1) the forward primer of pHDK1336 plasmid HDK535 and the reverse primers of the GOI were used to confirm the linearity of the transfected vector, whereas, 2) the forward primers of the GOI and the reverse primer of the pHDK1336 plasmid 'HDK335' were used to confirm the presence of the GOIs into *Tbb-5FURes*, *Tbb-s427 WT* and B48 strains after transfection has occurred.

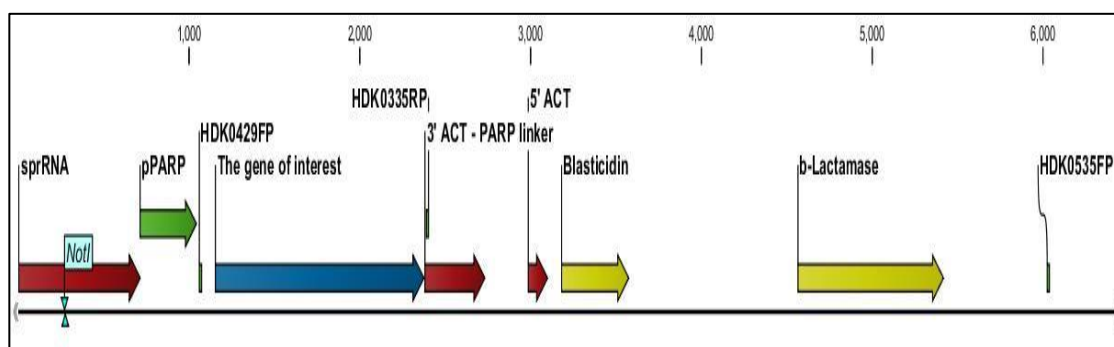


Figure 2.1: Linear map of pHDK1336 plasmid.

This plasmid was used to over-express *Tbb-FAD*, *Tbb-Cation1*, *Tbb-Cation2*, *Tbb-Cation3* and *Tbb-Cation4* genes into *Tbb-5FURes* and *Tbb-s427* WT strains, and heterologous expression of *FurD* gene in *Tbb-5FURes* strain and *TcrNB2* gene in *B48* strain.

2.3.4.1.2 Generation of plasmids for expression and transfection into *L. mexicana* promastigote form

The fatty acid desaturase gene *LmxM.10.1320* (*Lmex-FAD*) and the *Aspergillus nidulans* uracil transporter gene *A6N844* (*FurD*) were expressed in the *Lmex-5FURes*, *L. mexicana* WT and *Lmex-GTs* KO strains by using the pNUS-HcN plasmid which contains a *G418* resistance gene (Figure 2.2) (Tetaud et al., 2002). In addition, the pNUS-HcN plasmid was used to express the *T. cruzi* high-affinity thymidine transporter *TcCLB.506773.50* (*TcrNT2*) and *T. cruzi* NB2 *TcCLB.506445.110* (*TcrNB2*) in the *L. mexicana-Cas9-NT1* KO strain. The pNUS-HcN vector was used to heterologously express *TbAQP2* in *L. mexicana* promastigote form, causing a very large sensitisation to pentamidine (40-fold) and cymelarsan (~1000-fold) (Munday et al., 2014).

The appropriate restriction enzymes were used to digest the pNUS-HcN plasmid and the gene of interest (GOI). Thereafter, the T4 DNA Ligase kit was used to perform the ligation of the digested GOI into the digested pNUS-HcN plasmid. After ligation, the pNUS-HcN plasmid containing the GOI was transformed into the XL1-blue cells (*E. coli*) by heat shock as described in the manufacturer's protocol. The bacterial colonies that were on the plate were subjected to PCR screening using the forward primer of the GOI and the reverse primer of pNUS-HcN plasmid (HDK340), which was used to detect colonies having the desired target gene. After PCR screening, the pNUS-HcN plasmid containing the desired target gene was sent to Source Bioscience (Livingston, United Kingdom) for Sanger sequencing. Once the correct sequences were verified, 25 µg of the generated plasmids (pHDK220 '*Lmex-FAD*', pHDK245 '*FurD*', pHDK270 '*TcrNT2*'

and pHDK271 'TcrNB2') were precipitated by ethanol and resuspended in 15 μ L sterile water.

The plasmid DNA was not digested before transfection since it was designed for episomal expression. *L. mexicana* promastigotes (5×10^7 cells) were washed with 100 μ L transfection buffer and mixed with 10 μ g DNA of the expression construct. The cells were electroporated with the Amaxa Nucleofector Device (Amaxa AG, Germany), using Program U-033. Cells were then transferred to 20 mL HOMEM medium containing 10% FBS and allowed to recover overnight at 25 °C. After recovery, 50 μ g/mL of G418 was added to the culture as a selection agent for the expression construct. After that, the cells were plated out in a 96-well plate to produce individual clones by limiting dilution (1:10, 1:25 and 1:100). PCR was used to screen the positive clones, the forward primer of the GOI and the reverse primer of pNUS-HcN plasmid (HDK340) were used to confirm the presence of the target gene into *Lmex-5FURes*, *Lmex-WT*, *Lmex-GTs KO* and *L. mex-Cas9-NT1 KO* strains after transfection.

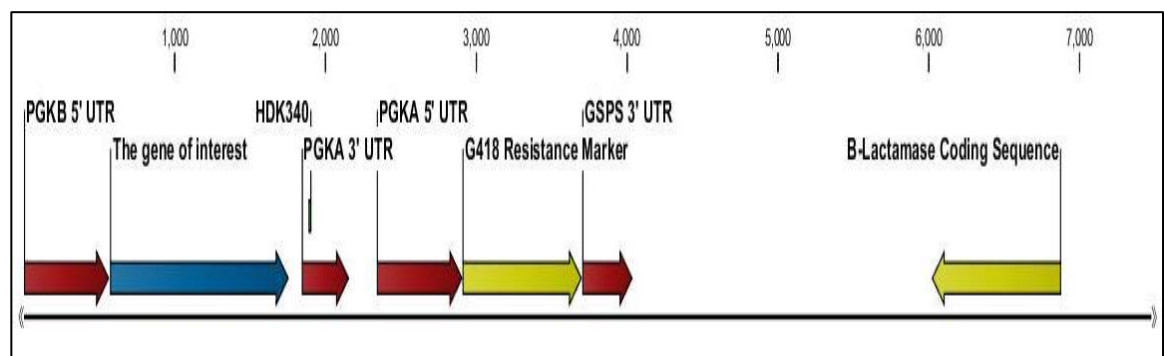


Figure 2.2: Linear plasmid map of pNUS-HcN.

This plasmid was used to express *Lmex-FAD* and *FurD* in *Lmex-5FURes*, *Lmex-WT* and *Lmex-GTs KO* strains, and heterologous expression of *TcrNT2* and *TcrNB2* in *L. mex-Cas9-NT1 KO* and *Lmex-5FURes* strains.

2.3.4.2 Gene knockout plasmids in *T. b. brucei* and *L. mexicana*

2.3.4.2.1 Targeted gene replacement plasmids

Dr. Khalid Alzahrani (Prof Harry de Koning Lab, University of Glasgow) has generated the plasmid constructs that are used for deleting the chromosomal locus containing the four cation transporter genes (CATs) in the *T. b. brucei* s427-WT. In this study, pHDK149 (with Blasticidin resistance cassette), pHDK150 (with Neomycin resistance cassette), and pHDK207 (with Hygromycin B

resistance cassette) are the three knockout constructs used to remove CATs from the genome of *T. b. brucei* s427 WT (Figure 2.3). The four CAT genes are located in tandem array on chromosome 11 and are annotated as cation transporters (Tb427tmp.01.0725, Tb427tmp.01.0730, Tb427tmp.01.0760 and Tb427tmp.01.0770) in the TritrypDB (tritrypdb.org/tritrypdb) website. Before transfection, *NotI* and *XhoI* restriction enzymes digested the knockout constructs so as to release the antibiotic resistance cassette between the 3'UTR and 5'UTR flanking regions of the four-CAT tandem array (Figure 2.3). These constructs were then transfected into *T. b. brucei* s427-WT as explained in section 2.3.4.1.1.

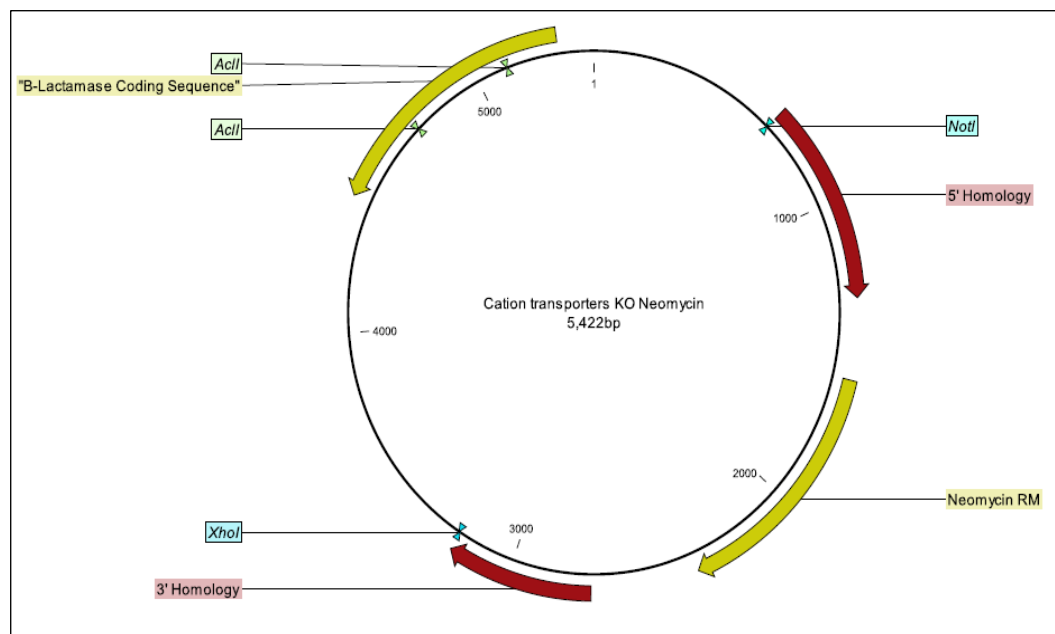


Figure 2.3: The plasmid construct for the knockout of four cation transporter genes (CATs) in *T. b. brucei* s427-WT.

2.3.4.2.2 Targeted CRISPR gene knockout plasmids

The Knockout strategy of nucleoside transporter 1 (NT1) containing the two nucleoside transporter genes (*NT1.1* and *NT1.2*) in *L. mexicana*-Cas9 was performed exactly as described previously (Beneke et al., 2017). *L. mexicana*-Cas9 T7 strain (Beneke et al., 2017) was generously donated by Professor Eva Gluenz (University of Oxford). Briefly, primers number 1 to 5 (Listed in Table 2.6) were used to produce *NT1* KO in *L. mexicana*-Cas9 and these primers were designed using an online platform named LeishGEdit (Beneke et al., 2017). The deletion of *NT1* locus requires the amplification of two single guide RNA (sgRNA)

by using primers 1 - 3 to direct *Cas9* (nuclease and typically derived from *Streptococcus pyogenes*) to cut immediately upstream (5') or downstream (3') of the target locus of *NT1* (Table 2.7 and 2.8). To create CRISPR plasmids specific to the target locus of *NT1*, pTBlast and pTPuro plasmids (with blasticidin and puromycin cassettes respectively (Figure 2.4)) were amplified using primers 4 and 5 (Table 2.9 and 2.10). These constructs were to integrate into the *NT1* locus after cutting with the two sgRNAs.

Table 2.6: The list of primers that are designed and used to generate *NT1* KO in *L. mexicana*-*Cas9*.

¹ 5' and 3' sgRNA primers: Low case indicates the T7 RNAP promoter (left), Upper case indicates the 20 nucleotides of the sgRNA target sequences (middle) and Low case indicates *Cas9*-backbone-start (right). ² Upstream forward and downstream primers (*NT1* KO): Upper case indicates the 30 nucleotides homology flanks for target-gene specific (left) and Lower case indicates primer binding sites for pTBlast and pTPuro (right).

No.	Primer name	Sequence (5' → 3')
HDK1502	G00 primer (sgRNA scaffold)	AAAAGCACCGACTCGGTGCCACTTTTTCAAG TTGATAACGGACTAGCCTTATTTTAACCTGC TATTTCTAGCTCTAAAC
HDK1508 ¹	5' sgRNA primer (<i>NT1</i> KO)	gaaattaatacgactcactataggTGCGACTTTGG ATGCACTGAgtttttagagctagaatagc
HDK1510 ¹	3' sgRNA primer (<i>NT1</i> KO)	gaaattaatacgactcactataggACGCATACACAA GCAAGGAGgttttagagctagaatagc
HDK1507 ²	Upstream forward primer (<i>NT1</i> KO)	TCGCACACATCTCTCGTCCACAAGGCCCTg tataatgcagacctgtgc
HDK1509 ²	Downstream reverse primer (<i>NT1</i> KO)	GCGATCAACAGCAGTGCGCGGGGCACGCAC ccaatttgagagacctgtgc

Table 2.7: The PCR reaction that was prepared for the amplification of 5' and 3' sgRNA.

No.	Component	Volume
1	dd H ₂ O	23.5 µl
2	Phusion HF buffer	5 µl
3	10mM dNTPs	1 µl
4	10 µM G00 primer	10 µl
5	10 µM of 5' or 3' sgRNA primers	10 µl
6	Phusion polymerase	0.5 µl
Total of reaction		50 µl

Table 2.8: The programme that was used for the amplification of 5' and 3' sgRNA by using PCR.

Temperature step: 98 °C for 30 seconds
Start cycle (x35)
Temperature step: 98 °C for 10 seconds
Temperature step: 60 °C for 40 seconds
Temperature step: 72 °C for 15 seconds
End cycle
Temperature step: 72 °C for 10 min
Store at 10 °C - ∞

Table 2.9: The PCR reaction that was prepared for the amplification of pTBlast and pTPuro plasmids.

No.	Component	Volume
1	dd H ₂ O	34 µl
2	Phusion HF buffer	8 µl
3	10mM dNTPs	1 µl
4	50% MgCl ₂	3 µl
5	3% DMSO	2.4 µl
6	10 µM Upstream forward primer	16 µl
7	10 µM Downstream reverse primer	16 µl
8	30 ng of pTBlast or pTPuro plasmids	0.5 µl
9	Phusion polymerase	0.5 µl
Total of reaction		80 µl

Table 2.10: The programme that was used for the amplification pTBlast and pTPuro plasmids by using PCR.

Hot lid on 110 °C
Temperature step: 94 °C for 5 min
Start cycle (x40)
Temperature step: 94 °C for 30 seconds
Temperature step: 65 °C for 30 seconds
Temperature step: 72 °C for 2.15 min
End cycle
Temperature step: 72 °C for 7.30 min
Store at 10 °C - ∞

After that, the two sgRNA templates and two resistance cassettes (pTBlast and pTPuro) were transfected into *L. mexicana* cas9 as described by (Beneke et al., 2017) into *L. mexicana-Cas9* and that cell line was maintained in the presence of 32 µg/mL of hygromycin. For the transfection, the two sgRNA templates and two KO resistance cassettes were heat-sterilised at 94 °C for 5 minutes. Then, 1×10^7 cells of *L. mex-Cas9* promastigotes was washed with 150 µL of transfection buffer and mixed with 100 µL of the heat-sterilised mixture of the two sgRNA templates and the two KO resistance cassettes. The mix was electroporated with the Amaxa Nucleofector Device, using Program X-001 (Amaxa AG, Germany). Cells were then transferred to 20 mL HOMEM medium containing 10% FBS and allowed to recover overnight at 25 °C. After recovery, 5 µg/mL of blasticidin and 20 µg/mL of puromycin were added to the culture as a selective marker for the knockout constructs. After that, the cells were plated out in the 96-well plate to produce individual clones by limiting dilution (1:10, 1:25 and 1:100). Thus, to yield the *NT1* KO, *L. mexicana-Cas9* was transfected once, with two sgRNA templates and two antibiotic resistance markers (pTBlast and pTPuro). The combination of two antibiotic resistance markers was used to eliminate any heterozygous cells that retain a copy of *NT1*.

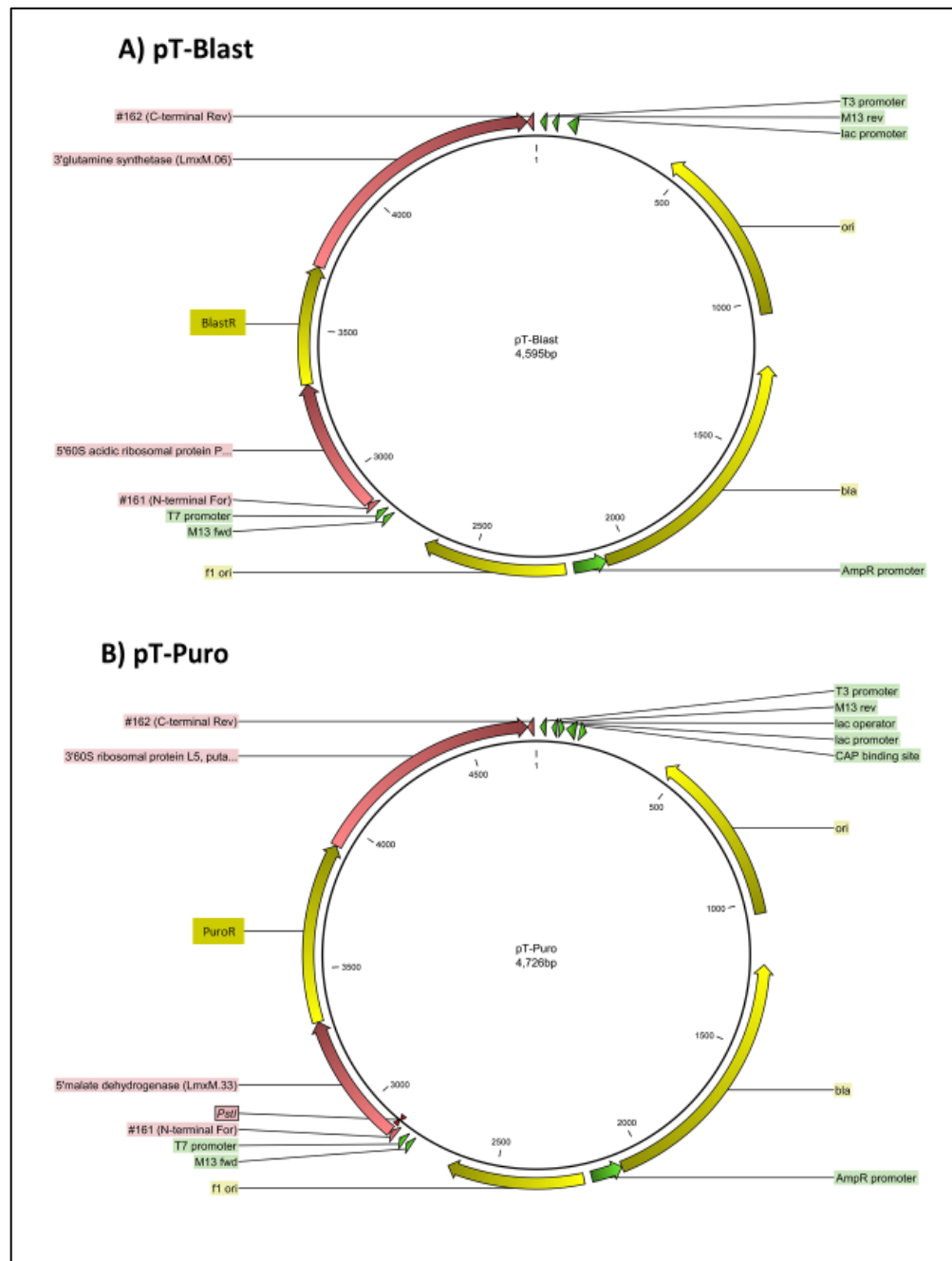


Figure 2.4: The plasmid maps of (A) pT-Blast and (B) pT-Puro constructs for the knockout of the target locus of NT1 in *L. mexicana*-Cas9 promastigotes by using CRISPR technique. pT plasmids serve as template DNA for PCR amplification of blastcidine and puromycin cassettes (Beneke et al., 2017).

2.3.5 Quantitative real-time PCR (qRT-PCR)

qRT-PCR enables the quantification of specific RNAs to be studied after the generation of the complementary DNA (cDNA) by using reverse transcriptase (Stephenson, 2016). An experiment was carried out as previously described (Ali et al., 2013b; Alzahrani et al., 2017), the expression levels of target genes that expressing in *T. b. brucei* and *L. mexicana* were measured and then comparison

with the control cell lines by the use of qRT-PCR. However, the quantification of the heterologous expression of a gene (such as FurD and TcrNB2 genes) relative to the house keeping gene (GPI8) is difficult as the gene was simply not present in the control cells (*L. mexicana* and *T. b. brucei*). However, the relative level of expression in multiple clonal cell lines expressing the gene of interest is possible and of value as a basis to select one of the clones for further experimentation. RNA was extracted for the *T. b. brucei* and *L. mexicana* using the NucleoSpin RNA kit (Macherey-Nagel, Germany) in accordance with the manufacturer's instructions. The NanoDrop ND-1000 spectrophotometer was used to quantify the RNA concentration and RNA samples were stored at a temperature of -80 °C until further use. The designing of the qRT-PCR primers was designed by use of Primer Express 3.0 software (Table 2.11). For each sample, 20 µL total volume was obtained by diluting 4 µg of RNA in RNase-free water, after which complementary DNA (cDNA) was synthesised using the Precision nanoScript™ 2 Reverse Transcription kit (PrimerDesign Ltd, UK) in accordance with the manufacturer's protocol. The cDNA was produced under the following conditions: 1) For annealing step: heat to 65 °C for 5 min and directly cool the tubes in ice. 2) For extension step: incubate at 42 °C for 20 min, followed by heat inactivation of the reaction by incubation at 75 °C for 10 min. Then, the cDNA samples were kept at -20 °C until further use. For each primer pair and the house keeping (GPI8) primers, the primer efficiency was measured by the previously described method of Pfaffl to ensure proper and efficient binding of primers (Pfaffl, 2001). The cDNA was amplified using the PrecisionPLUS OneStep RT-qPCR Master Mix kit (PrimerDesign Ltd, UK) in a 7500 Real-Time PCR System coupled to a desktop computer (Thermo Fisher Scientific, UK). To ensure that only one product at a time is being amplified, a dissociation curve was used. Samples without reverse transcriptase (RT) or cDNA were used in the experiment as negative controls, whereas the GPI8 of *T. b. brucei* and *L. mexicana* of which are constitutive genes expression were used as a house keeping control. In each case, the gene expression was normalised to GPI8 expression which is a standard reference gene in *T. b. brucei* and *L. mexicana* (Kang et al., 2002). Relative quantification was calculated using the delta delta ct method. Applied Biosystems 7500 Fast Real-Time PCR System Software

(Thermo Fisher Scientific, UK) was used for analysis of data. Each experiment was carried out with three independent determinations.

Table 2.11: The list of primers that designed and used in qRT-PCR.

Primer name	Position	Sequence (5'UTR to 3'UTR)	Gene
HDK1488	Forward	GCACTCACCATAAACACACCAATC	<i>Tbb-FAD</i>
HDK1487	Reverse	GCGCTGCACAGGTACGAA	
HDK1494	Forward	ACCAAATCCCCGCCAAGTA	<i>Lmex-FAD</i>
HDK1498	Reverse	TGTCGCGGAAGACGTAGTACA	
HDK1438	Forward	GTGGGCATTACCCCTTATCA	<i>FurD</i>
HDK1439	Reverse	CCTTACTGGGAAGCCATAACTC	
HDK1289	Forward	CACGGCGGGTGTGAAAGT	<i>Tbb-CAT 1-4 KO</i>
HDK1283	Reverse	AAAGATCGCCACAACATGCA	
HDK568	Forward	GCTTCTCGCCGTCGTTGA	<i>Lmex-NT1</i>
HDK569	Reverse	ATGATCCAGCGCTGCTTGT	
HDK1565	Forward	ACTTGCCCGCCCACTACTA	<i>TcrNB2</i>
HDK1566	Reverse	CGTCAGGGCACCAGAAACA	
GPI8FT	Forward	TCTGAACCCGCGCACTTC	<i>T. b. brucei GPI8</i>
GPI8RT	Reverse	CCACTCACGGACTGCGTTT	
GPI8FL	Forward	GGCTGTCATTGTCTCCTCCT	<i>L. mexicana GPI8</i>
GPI8RL	Reverse	GTACATGGTAAGCGCATTGG	

2.4 Drug sensitivity assays using Alamar blue dye

In this project, the Alamar blue assay (resazurin sodium salt) was used to determine the drug sensitivity of the *L. mexicana* promastigotes and *T. b. brucei* BSF/PCF strains *in vitro*. Alamar blue dye was used as a metabolic cell function indicator and based on the reduction of resazurin sodium salt (blue colour and non-fluorescent) to resorufin (pink colour and fluorescent) by live cells (Räz et al., 1997; Gould et al., 2008).

2.4.1 Drug sensitivity assay for *T. b. brucei* BSF

HMI-9 medium with 10% FBS (100 μ L) was added to all wells of a white 96-well plate apart from the first well. 200 μ L of a known concentration of test compounds were diluted in HMI-9 medium and placed in the first well. Compounds were tested in one plate and every compound was diluted over two rows (23 concentrations), leaving the last well of every dilution as a negative control having 100 μ L of HMI-9 medium. After that, 100 μ L of *T. b. brucei* culture at a density of 2×10^5 cells/mL was added into every well in the plate and incubated for 48 h at a temperature of 37 °C under 5% CO₂. After 48 h, Alamar blue dye (20 μ L of a solution of 12.5 mg resazurin sodium salt in 100 mL phosphate buffered saline PBS) was added and the plate was incubated under the same conditions for 24 h.

With the metal ion compounds, Alamar blue assay was performed as explained above with the exception that (8×10^5 cell per mL) were added in each well of HMI-9 culture medium containing the serially diluted tested drugs, and the incubation time before the addition of Alamar blue dye was 18 h at 37 °C and incubated with 20 μ L of Alamar blue dye for additional time of 24 h (Nyarko et al., 2002).

The FLUOstar OPTIMA plate reader (BMG Labtech, Germany) was used to read the fluorescence intensity at 544 nm wavelength for excitation and 620 nm wavelength for emission. The EC₅₀ values and fluorescence data were determined and plotted by the GraphPad Prism 8.0 Software. Pentamidine and Diminazene were used as positive control and every experiment was done on 3-4 independent times in this project.

2.4.2 Drug sensitivity assay for *T. b. brucei* PCF

In *T. b. brucei* procyclic forms, the drug sensitivity assay was done as described in section 2.4.1, with the exception that (4×10^5 cell per mL) were added in each well of SDM-79 culture medium containing the serially diluted tested drugs, and the incubation time before the addition of Alamar blue dye (20 μ L) was 72 h at

27 °C and incubation with resazurin sodium salt was for an additional period of 24 h.

2.4.3 Drug sensitivity assay for *L. mexicana* promastigote form

In *L. mexicana* promastigote form, Alamar blue was done as explained for *T. b. brucei* BSF (section 2.4.1), with the exception that 2×10^6 cells/mL of HOMEM culture medium complemented with 10% FBS were added in each well, the incubation time before the addition of Alamar blue dye (20 μ L) was 72 h at 25 °C, and the plates were incubated with Alamar blue dye for an additional period of 48 h.

2.5 Transport assays

For the study and characterization of the transporters of *L. mexicana* promastigotes and *T. brucei* BSF to be possible, the two species were subjected to transport assays. This can be achieved either by using dose-dependent assays or time course assays, using radiolabeled pyrimidines, purines, diamidines, and 2-deoxy-D-glucose as required.

The uptake assay protocol for *T. b. brucei* BSF and *L. mexicana* promastigotes has been described previously in detail (Al-Salabi et al., 2003; Al-Salabi and de Koning, 2005; Gudin et al., 2006; Wallace et al., 2002). The kinetoplastid parasite cultures were incubated for approximately 40-48 h to reach the mid to late logarithmic stage of growth. Cell pellets were then produced after centrifuging the culture medium at $1000 \times g$, 25 °C for 10 min. The assay buffer (AB; 33 mM HEPES, 98 mM NaCl, 4.6 mM KCl, 0.5 mM CaCl_2 , 0.07 mM MgSO_4 , 5.8 mM NaH_2PO_4 , 0.03 mM MgCl_2 , 23 mM NaHCO_3 , 14 mM D-glucose, pH 7.3, stored at 4 °C) was used to wash the pellets twice. The cells were resuspended in AB to a cell density of 1×10^8 cells/mL. The suspended cells were allowed to recover from centrifugation stress at room temperature for 30 min. A radiolabeled test compound, at a predetermined concentration in 100 μ L, is then incubated together with 100 μ L of the suspended cells for a time that is predefined but variable depending on the assay. The transport assay was stopped by the addition of 750 μ L ice-cold stop solution. The stop solution is usually comprised

of 2 mM unlabeled analogue of the radiochemical. The step is followed by prompt centrifugation through an oil layer (1:7 mixture of mineral oil and di-n-butyl phthalate) at $14800 \times g$ for 60 s. Liquid nitrogen was used to freeze the microfuge tubes quickly, and the cell pellets at the bottom of the tube were collected into scintillation vials after cutting off the tip of the Eppendorf tube. 500 μ L of 2% of sodium dodecyl sulfate (SDS; 10 g SDS in 500 mL H₂O) was used to lyse the pellets with shaking for 60 to 90 min at 40 rpm using a gyro rocker (GENEO BioTechProducts GmbH, Germany). To each vial 3 mL of scintillation solution (Optiphase Hisafe-2) was added, and the vials were incubated overnight at room temperature in the dark, followed by vigorous shaking. Scintillation was measured using a Hidex 300 SL liquid scintillation counter (LabLogic Systems Ltd, Sheffield, UK). The assays were carried out in triplicate and three repeated independent experiments.

With transport of radiolabeled 2-deoxy-D-glucose in *L. mexicana* promastigotes, the experiment was performed as described above apart from the fact that cells were washed twice with phosphate buffered saline (PBS, pH 7.4) and resuspended at a density of 1×10^8 cells/mL in PBS instead of AB. The stop solution of D-glucose, the solution of radiolabeled of 2-deoxy-D-glucose and saturation label of D-glucose were all prepared in PBS instead of AB (Seyfang and Landfear, 2000).

2.5.1 Time-course assay

T. brucei and *L. mexicana* cells were incubated with a radiolabeled substrate in a concentration below the K_m for every transporter to facilitate the evaluation of the transport of purine, pyrimidine, pentamidine, and 2-deoxy-D-glucose as a function of time. The experiment was conducted in triplicate for each time period. The cells were incubated with the same volume of radiolabeled test compounds to measure the radiolabel association with cells at the point of transporter saturation. To determine this, usually 2 mM of the corresponding unlabeled solution is used. The process mentioned above was followed after which the calculation of linear regression was conducted using Prism 8 GraphPad Software. The rate of uptake of the transport assay is considered to be linear if

$r^2 > 0.95$ and an F-test shows insignificant deviation from linearity ($P > 0.05$). All the procedures were performed triplicate in three independent successions.

2.5.2 Dose-dependent assay

The addition of increasing concentrations of unlabeled substrates in the presence of a radiolabeled substrate at a constant level was used to determine biochemical parameters such as K_m , K_i and V_{max} . This was performed for a preset time and well within the linear transport phase, as first determined by the time course assay. The experiment was conducted in triplicate for every concentration. Similar steps were followed as described above to obtain scintillation measurements. The lowered scintillation intensity caused by the increasing level of unlabeled substrate allowed for the determination of K_m and V_{max} through the application of the Michaelis-Menten equation $V_0 = V_{max}([substrate]/([substrate] + K_m))$, using Prism 8 GraphPad Software. The inhibition constant (K_i) of unlabeled substrates was determined by calculating the 50% Inhibitory Concentration (IC_{50}) through the fitting of an inhibition curve by a non-linear regression with variable slope using the Prism 8 GraphPad Software, and applying the Cheng-Prusoff equation: $K_i = IC_{50}/(1 + (L/K_m))$, where the K_m is that determined for the labeled permeant and L represents the radiolabel concentration (Cheng and Prusoff, 1973). Based on the obtained K_i , the Gibbs free energy of binding (ΔG^0) is calculated by: $\Delta G^0 = -RT \ln(K_i)$ in which R is the gas constant and T the absolute temperature (de Koning and Jarvis, 1999).

2.6 Statistics

In drug sensitivity assays, transport assays and quantitative RT-PCR statistical significance was determined using unpaired t-test significance indicated by * $P < 0.05$; ** $P < 0.01$; *** $P < 0.001$.

3 Assessment of the role of the *T. b. brucei* cation transporters in toxicity of 5-FU and heavy metals

3.1 Introduction

Kinetoplastid protozoa express many membrane transport proteins that enable them to take up nutrients, efflux metabolites, regulate physiological concentrations, translocate various molecules, and import or export drugs. Kinetoplastid parasites are capable of salvage as well as synthesis of pyrimidine nucleotides (Majumder, 2008; Kirk and Saliba, 2007; Rodriguez-Contreras et al., 2007; De Koning et al., 2005; Hammond and Gutteridge, 1984). The gene family encoding pyrimidine nucleobase transporters in kinetoplastid parasites has not yet been identified (De Koning, 2007; Ali et al., 2013a). In this study, the pyrimidine analogue 5-fluorouracil is used as a tool to try to identify the gene(s) encoding uracil transport functions in trypanosomes. Resistance to 5-fluorouracil was generated in *T. b. brucei* s427 BSF, yielding the clonal line *Tbb-5FURes* (Ali et al., 2013a). The rate of 5-FU transport is substantially reduced (> 65%) in this cell line. Likewise, the transport rate of [³H]-uracil in the *Tbb-5FURes* cells was also only partly reduced from the wild-type levels.

There are three cation transporter genes (CATs) in *T. b. brucei* BSF, that all could be considered as potential candidates for pyrimidine transporters, following an evaluation of the wild-type and the 5-FU resistant the *T. b. brucei* cell line (Ali et al., 2013a). That analysis, performed by former PhD student Khalid Alzahrani in the De Koning group, was done through RNA sequencing, which allows transcriptome analyses of genomes using deep-sequencing technologies, with the goal of studying the difference in gene expression between cell lines or conditions (Nagalakshmi et al., 2010). The results of this analysis found significant differences between the expression level of the genes Tb11.v5.0514, Tb927.11.9000 and Tb927.11.9010 in the *Tbb-5FURes* and the control strain (*T. b. brucei* Lister s427WT), as the three CATs were significantly down-regulated in the *Tbb-5FURes* strain (Alzahrani, 2017). The mRNA abundance of Tb11.v5.0514, Tb927.11.9000 and Tb927.11.9010 in the *Tbb-5FURes* was down-regulated with a log₂ fold-change of -1.2, -1.2 and -1.04, respectively ($P < 0.001$) compared to the parental wild-type strain. In *T. b. brucei* Lister 427 strain BSF, the corresponding cation transporter genes IDs are Tb427tmp.01.0725, Tb427tmp.01.0730, Tb427tmp.01.0760 and Tb427tmp.01.0770, named here as *Tbb-CAT1*, *Tbb-CAT2*, *Tbb-CAT3* and *Tbb-*

CAT4 respectively (Table 3.1). These four CATs are almost identical and located in tandem array on chromosome 11 and annotated as cation transporters in TriTrypDB website. The four cation transporter genes share an amino acid sequence identity ranging from 86.43% to 98.73% when compared with each (Table 3.2). The multiple sequence alignment result of the four CATs is presented in Appendix 5.

Table 3.1: Annotation of cation transporter genes in the genome of *T. b. brucei* s427 wild type.

Gene code	Chromosome	Transcript	Name
Tb427tmp.01.0725	11	1185 bp	<i>Tbb-CAT1</i>
Tb427tmp.01.0730	11	1185 bp	<i>Tbb-CAT2</i>
Tb427tmp.01.0760	11	1152 bp	<i>Tbb-CAT3</i>
Tb427tmp.01.0770	11	1164 bp	<i>Tbb-CAT4</i>

Table 3.2: Amino acid sequence identity calculated between *Tbb-CAT1*, *Tbb-CAT2*, *Tbb-CAT3*, *Tbb-CAT4*, *hZIP2* and *zntA*.

Gene name	GeneDB ID	<i>Tbb-CAT1</i>	<i>Tbb-CAT2</i>	<i>Tbb-CAT3</i>	<i>Tbb-CAT4</i>
<i>Tbb-CAT1</i>	Tb427tmp.01.0725	-	98.73%	90.36%	86.43%
<i>Tbb-CAT2</i>	Tb427tmp.01.0730	98.73%	-	91.62%	86.93%
<i>Tbb-CAT3</i>	Tb427tmp.01.0760	90.36%	91.62%	-	93.28%
<i>Tbb-CAT4</i>	Tb427tmp.01.0770	86.43%	86.93%	93.28%	-
<i>hZIP2</i> ^a	AAF35832.1	26.94%	26.46%	25.26%	30.72%
<i>zntA</i> ^b	A0A256LFN4	35.14%	35.14%	32.43%	32.43%

^a Zinc transporter *hZIP2* in Human; ^b Zinc/cadmium/lead-transporting P-type ATPase in *Escherichia coli* (strain K12).

The purpose of this chapter is to continue working on the characterization of the CATs, which were among the few differentially expressed transporters in the 5FURes strain, and therefore must be considered as potential candidates for uracil transporter, or at least change something in the cellular biochemistry that changes susceptibility to 5-FU. Moreover, none of these potential transport genes have been previously characterised in protozoa and as such they are of interest in their own right as well. Here, we overexpress of CATs in the *Tbb-5FURes* cell line (Ali et al., 2013a), and continue work on the characterization of

CATs to attempt to acquire a double knockout for these genes in *T. b. brucei* s427 WT, aiming to determine their involvement, direct or indirect, in pyrimidine uptake and resistance to the pyrimidine analogues. As part of the characterisation efforts, we also assess the susceptibility of the overexpressing cell lines *Tbb-CAT1-4* to heavy metal ions, as the analysis of *Tbb-CAT1-4* protein sequences with Pfam (<http://pfam.xfam.org>) revealed that they belong to a family of zinc and iron transporters.

3.2 Results

3.2.1 Knockout of *Tbb-CAT1-4* by homologous recombination into *T. b. brucei* s427-BSF

Previous work in our laboratories showed that the overexpression of the cation transporter genes (*Tbb-CAT1*, *Tbb-CAT2*, *Tbb-CAT3* and *Tbb-CAT4*) resulted in increased sensitivity to 6-Azauracil in the 5FU resistant cell lines (Alzahrani, 2017). Thus, we decided to try to delete the 4 cation transporter genes, which would lead to the complete deletion of CATs and thus give a stronger phenotype. Dr. Khalid Alzahrani (Prof Harry de Koning Lab, University of Glasgow) previously constructed the plasmids that can be used for deleting the chromosomal locus containing the four CATs, and named them as pHDK149 (with blasticidin resistance cassette), pHDK150 (with neomycin resistance cassette), and pHDK207 (with hygromycin B resistance cassette) (Figure 3.1).

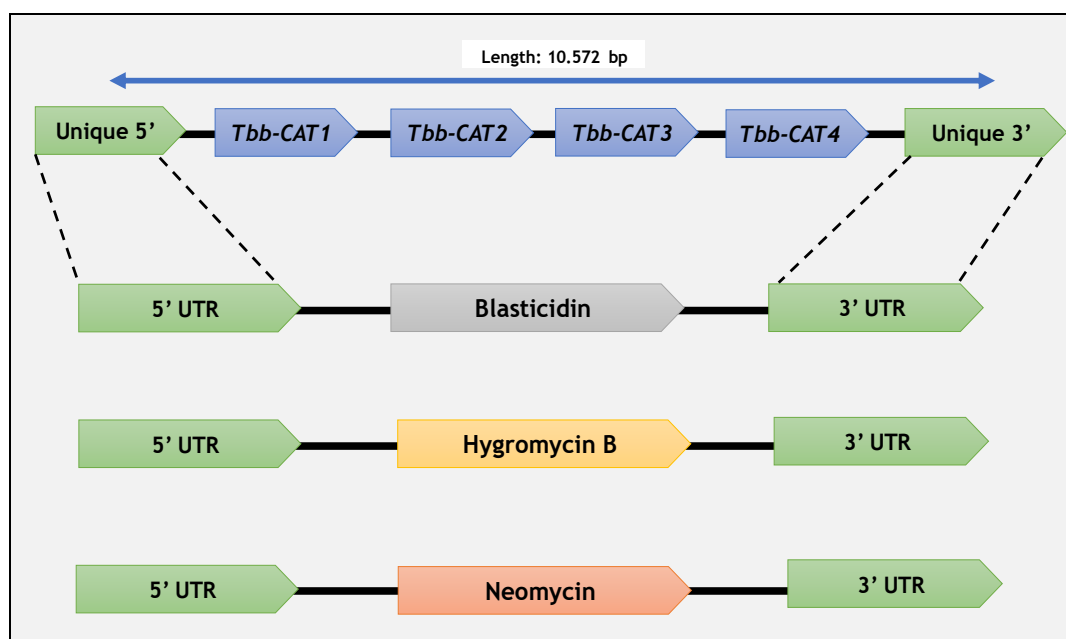


Figure 3.1: Knockout strategy used for the replacement of the genomic locus on chromosome 11 containing a tandem array of four cation transporter genes (*Tbb-CAT1-4*).

3.2.1.1 PCR confirmation for single knockout of *CAT1-4* in *T. b. brucei*

Following transfection, PCR screening was used to evaluate the integration of each antibiotic resistance cassette into *T. b. brucei* s427 WT. Since the genome of *T. b. brucei* is diploid, the complete deletion of CATs requires two rounds of deletion. For that reason, we used three antibiotic resistance cassettes (Neomycin, Blasticidin and Hygromycin B) to achieve double knockout for CATs from the genome of *T. b. brucei* s427 WT. After the transfection of three different selective markers into *T. b. brucei* s427 WT, a specific pair of primers for every antibiotic selective marker were used to amplify the 3'UTR and 5'UTR regions and ran on 1% of agarose gel to be observed visually. The correct integration of the constructs was confirmed with PCR, first pair with unique forward primer binding pre-5' UTR (HDK1052) with reverse primers to the antibiotic cassette (HDK283 for blasticidin, MB39 for hygromycin and MB37 for neomycin); and second pair with unique reverse primer binding post-3' UTR (HDK1053) and forward to the antibiotic cassette (HDK282 for blasticidin, HDK40 for hygromycin and MB38 for neomycin). The bands in Figure 3.2 corresponded to the expected sizes of ~1.8 kb for blasticidin, ~2.5 kb for hygromycin and ~2.4 kb for neomycin integrations into *T. b. brucei* s427 WT after transfection. This shows that all three constructs were able to delete the *TbCAT1-4* locus.

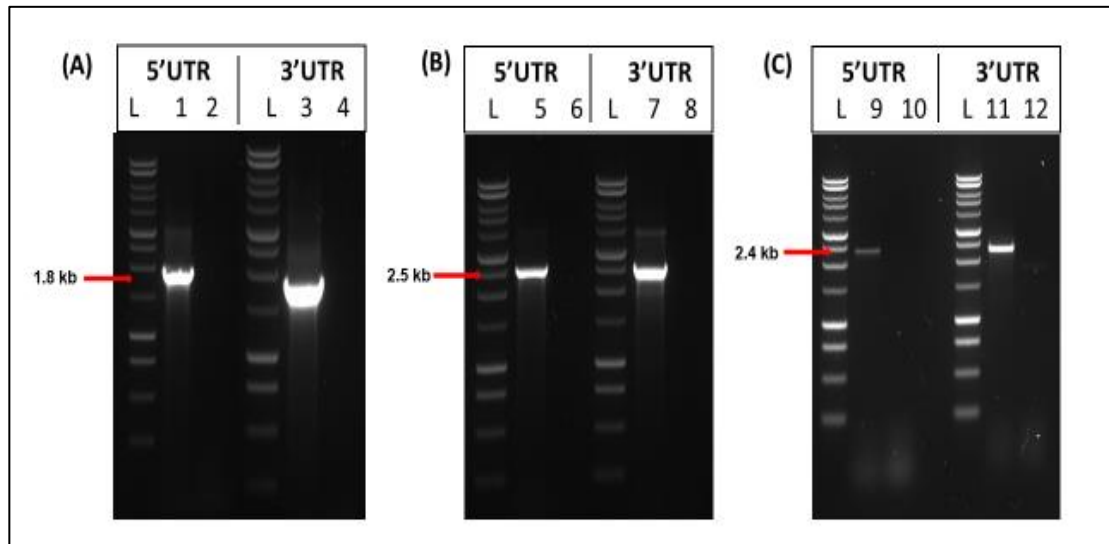


Figure 3.2: Confirmation for single KO of CATs integration by PCR after transfection into *T. b. brucei* WT s427 cell line by amplification of the antibiotic resistance genes.

A) with Blasticidin; B) with Hygromycin; C) with Neomycin. The bands at ~1.8 kb, ~2.5kb and ~2.4 kb represent the antibiotic resistance markers of Blasticidin, Hygromycin B and Neomycin respectively. L: 1kb DNA Ladder (Promega); 2,4,6,8,10,12: non-transfected control (gDNA from *Tbb-s427* WT); 1 and 3: *Tbb-sKO-CAT1-4^{+/-} blasticidin*; 5 and 7: *Tbb-sKO-CAT1-4^{+/-} hygromycin*; 9 and 11: *Tbb-sKO-CAT1-4^{+/-} neomycin*.

3.2.1.2 qRT-PCR confirmation and growth curve of single knockout of *Tbb-CAT1-4* in *T. b. brucei*

An analysis of the expression levels of single knockout of the CATs was performed and compared to the control of *Tbb-s427* WT through the use of qRT-PCR (Figure 3.3). The gene expression was normalised to GPI-8 expression which is a standard reference gene for qRT-PCR in *T. brucei* (Kang et al., 2002). The *Tbb-sKO-CAT1-4^{+/-} blasticidin* recorded the lowest level of mRNA expression (0.52-fold; $P < 0.001$) among the three antibiotic resistance cassettes, while *Tbb-sKO-CAT1-4^{+/-} neomycin* was also significantly decreased with 0.59-fold ($P < 0.01$). In contrast, there was no significant difference between the expression levels for *Tbb-sKO-CAT1-4^{+/-} hygromycin* and the control *Tbb-s427*WT ($P > 0.05$).

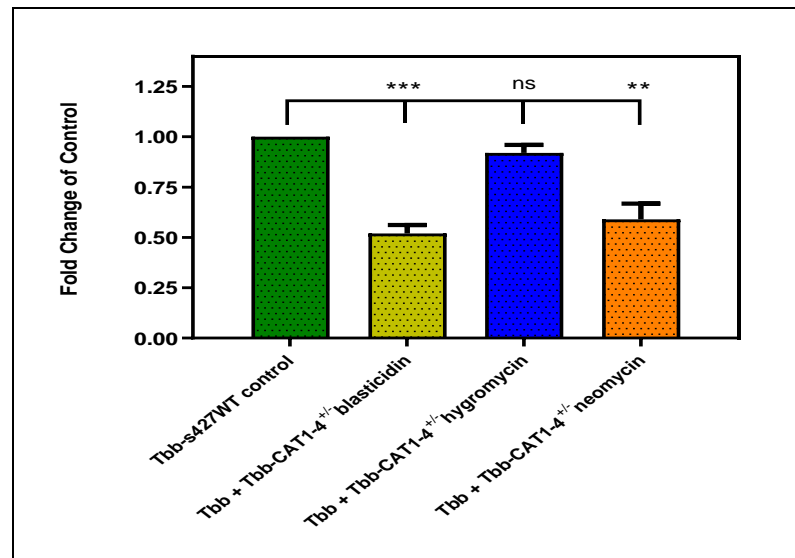


Figure 3.3: The expression levels of sKO of *Tbb-CAT1-4* genes with three antibiotic cassettes (blasticidin, hygromycin and neomycin) in *Tbb-s427* WT determined by qRT-PCR and compared to the control.

Levels were corrected against expression of the housekeeping gene (*T. b. brucei* GPI8). The presented results are the average and \pm SEM of 4 independent repeats. ** $P < 0.05$; *** $P < 0.001$.

The growth of single knockout of *Tbb-CAT1-4* genes and the control *Tbb-s427* WT was analysed in HMI-9 medium supplemented with 10% FBS, at 37 °C under 5% CO₂. The density of the cell culture was evaluated every 24 h and cells were passaged every 48 h once the growth has reached between 1.5 and 2 x 10⁶ cells/ml (Figure 3.4). The result of the study showed that there was no effect on growth following the deletion of the first allele of the *Tbb-CAT1-4* genes in *Tbb-s427* WT when compared to the control *Tbb-s427* WT.

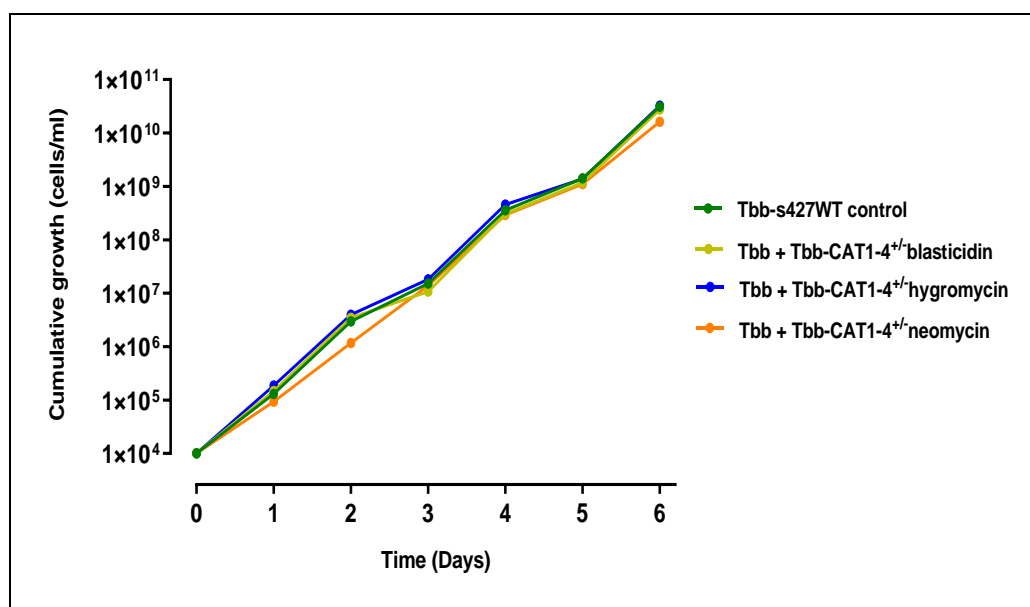


Figure 3.4: The growth curve of *Tbb-s427* WT and *Tbb-WT + TbbCAT1-4 sKO* with three antibiotic cassettes (blasticidin at 5 µg/ml, hygromycin at 2 µg/mL and neomycin at 1 µg/ml) on HMI-9 medium supplemented with 10% FBS.

The cells were seeded at the density of 1x10⁴ cells/mL, and cell densities were determined every 24h. Samples were and counted taken from three separate cultures of the same cell line and the average of these three determinations is shown. The error bars are too small to be visible in the graph. Cultures were grown in the respective antibiotics.

3.2.1.3 Drug sensitivity assay of heterozygote (*CAT 1-4*^{+/+}) in *Tbb-s427* WT

The alamar blue assay is a convenient technique that relies on the metabolic activity of living cells, as dead cells fail to convert the blue resazurin to the pink, fluorescent resorufin (Gould et al., 2008). Therefore, the alamar blue dye (resazurin sodium salt) was used to evaluate drug sensitivity of a single knockout of the CAT transport locus to 5-flourouracil and 6-azauracil compounds. Pentamidine was used as a positive control against *T. b. brucei* s427 WT and hemizygous knockout cells (Figure 3.5). The results show that the drug sensitivity of *T. b. brucei* s427-WT to these compounds was the same as the generated cell lines ($P > 0.05$), presumably because the CATs were still expressed, albeit at a lower level. Several attempts were made to produce a null mutant for *Tbb-Cation1-4* by replacing the second allele of *Tbb-CAT1-4* genes with all three antibiotics-resistance constructs (Neomycin, Blastocidin and Hygromycin) but were unable to remove both *Tbb-CAT1-4* alleles. However, we were not able to conduct a complete double knockout for the *Tbb-CAT1-4* genes as it resulted in the death of the cells and, as a result, showed the essentiality of their function for continued growth of the *T. b. brucei* BSF. Furthermore, Alzahrani (2017) showed that the genes encoding cation transporters are

essential for the cell viability of *T. brucei* BSF: RNAi-mediated downregulation of Tbb-Cation1-4 confirmed that these genes are essential, as a growth defect was observed after induction with tetracycline.

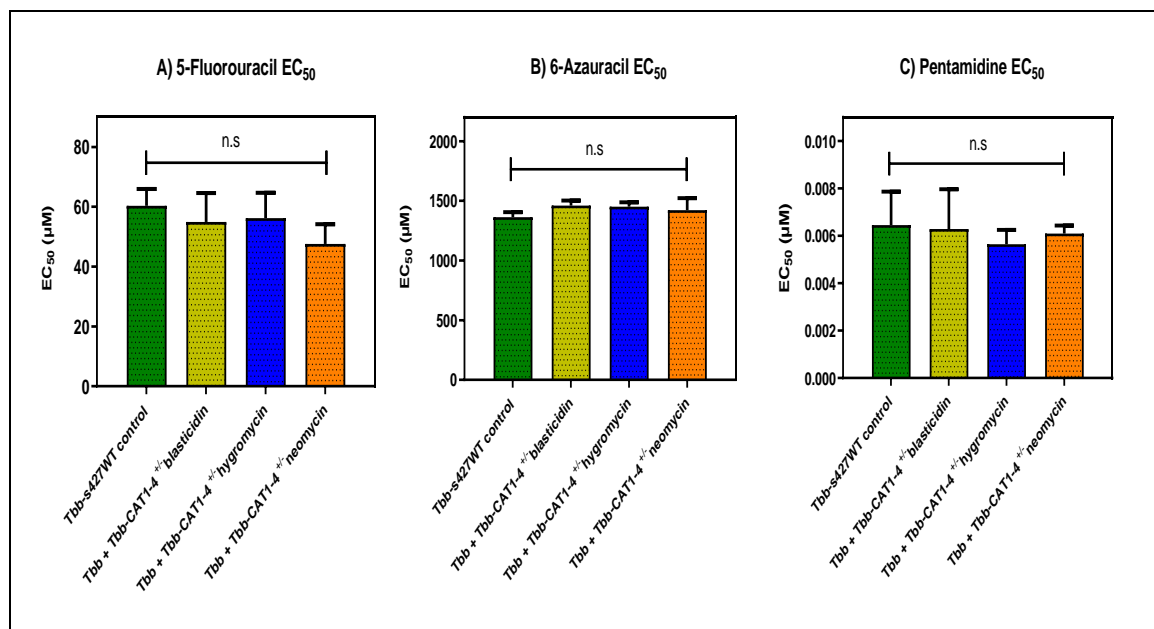


Figure 3.5: The averages of EC₅₀ values of *Tbb-s427 WT* and *Tbb-s427WT + Tbb-CAT1-4 sKO* with three antibiotic cassettes (blasticidin, hygromycin and neomycin) to A) 5-fluorouracil, B) 6-Azauracil and C) Pentamidine determined by using the alamar blue assay. Each bar represents the average of three independent repeats is shown \pm SEM in μ M.

3.2.1.4 Uptake of uracil by *Tbb-s427WT+sKO-CAT1-4^{+/-}* strain

The uptake of 0.1 μ M of [³H]-uracil in the *Tbb-s427 WT* and *Tbb-s427WT+sKO-CAT1-4^{+/-}* was investigated in order to check whether the single knockout of the CAT transport locus causes changes to the rate of uracil transport (Figure 3.6). [³H]-Uracil uptake was linear for 10 minutes in *Tbb-s427 WT* (Linear regression; $r^2 = 0.96$) with a rate of 0.317 ± 0.034 pmol. (10^7 cells)⁻¹.s⁻¹ (n=1), and was completely inhibited by 1 mM unlabelled uracil. The uptake of [³H]-uracil in *Tbb-s427WT + sKO-CAT1-4^{+/-}* was almost the same as the wild type cells, with a rate of 0.345 ± 0.045 pmol. (10^7 cells)⁻¹.s⁻¹ (Linear regression; $r^2 = 0.95$; n=1). The addition of 1 mM unlabelled uracil completely inhibited the uptake of [³H]-uracil in *Tbb-s427WT+sKO-CAT1-4^{+/-}*. This result confirmed that the sKO of the CAT transport locus does not change the rate of uracil uptake in comparison to the parental cell line *Tbb-s427 WT*.

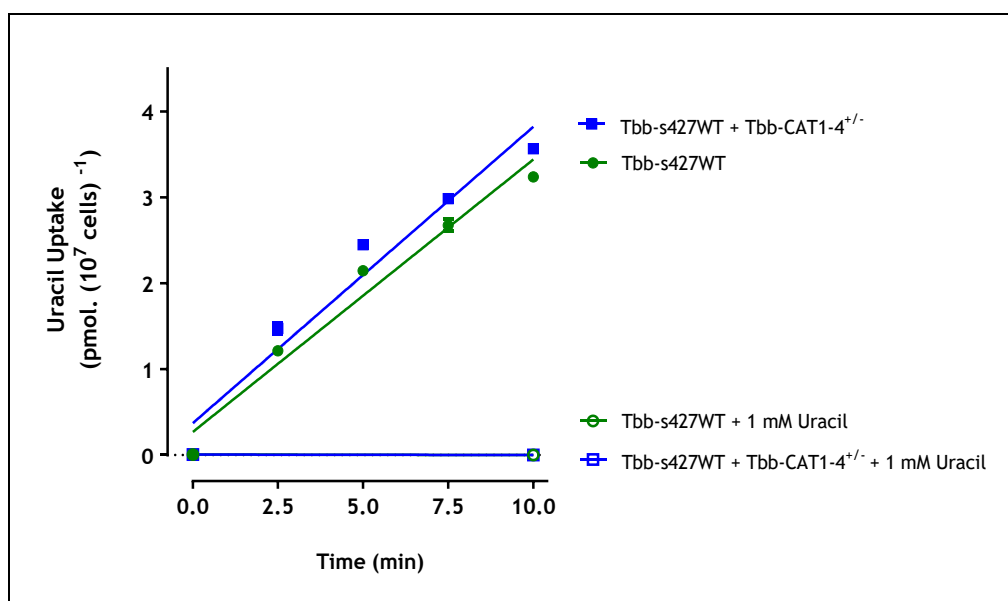


Figure 3.6: [³H]-Uracil transport by *Tbb-s427 WT* and *Tbb-s427WT + Tbb-CAT1-4^{+/-}*. Transport of 0.1 μ M [³H]-uracil by *Tbb-s427WT* and *Tbb-s427WT + Tbb-CAT1-4^{+/-}* was measured over 10 minutes in the presence (open symbols) or absent (closed symbols) of 1 mM unlabelled uracil. The graph shows one representative experiment in triplicate, and error bars represent \pm SEM.

3.2.2 Over-expression of *Tbb-CAT1*, *Tbb-CAT2*, *Tbb-CAT3*, and *Tbb-CAT4* in the *Tbb-5FURes* strain BSF

Dr. Khalid Alzahrani (Prof Harry de Koning Lab, University of Glasgow) has generated the plasmid constructs that are used for the individual overexpression of each of the four cation transporter genes in the *Tbb-5FURes* strain, based on the vector pHD1336 and named as pHDK199 (*Tbb-CAT1*), pHDK200 (*Tbb-CAT2*), pHDK201 (*Tbb-CAT3*) and pHDK202 (*Tbb-CAT4*) (Figure 3.7). The pHD1336 plasmid is constitutively expressed and integrates into the non-transcribed ribosomal RNA (RRNA) spacer.

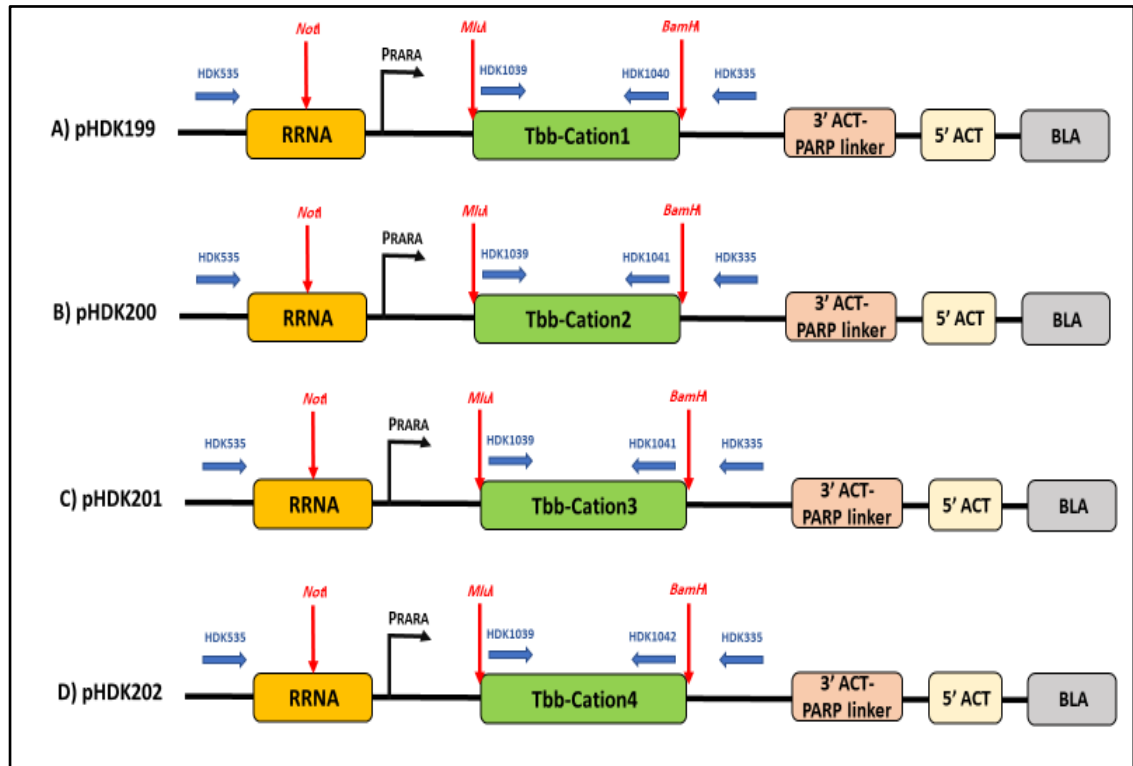


Figure 3.7: Schematic representations of pHDK199, pHDK200, pHDK201 and pHDK202 plasmids.

3.2.2.1 PCR confirmation of plasmid integration of *Tbb-CAT1-4* into *Tbb-5FURes*

The *Tbb-5FURes* + *Tbb-CAT1^{o.e}*, *Tbb-5FURes* + *Tbb-CAT2^{o.e}*, *Tbb-5FURes* + *Tbb-CAT3^{o.e}* and *Tbb-5FURes* + *Tbb-CAT4^{o.e}* cells were retrieved from liquid nitrogen storage and PCR was used to confirm the presence of an extra copy of each cation transporters in the *Tbb-5FURes* strain. These cell lines were generated by Dr Khalid Alzahrani and Ibrahim Alfayez at the De Koning laboratory. After genomic DNA extraction, PCR technique was performed to confirm the presence of *Tbb-CAT1* (1185 bp), *Tbb-CAT2* (1185 bp), *Tbb-CAT3* (1152 bp), and *Tbb-CAT4* (1164 bp) genes in the *Tbb-5FURes* strain by using HDK1039 as forward primer for *Tbb-CAT1-4* and HDK335 as reverse primer for the pHD1336 plasmid (Figure 3.8A). Also, PCR was used to confirm the linearization of the circular pHDK199, pHDK200, pHDK201 and pHDK202 plasmids into *Tbb-5FURes* strain by using HDK535 as forward primer for pHD1336 plasmid and the reverse primer for each gene (HDK1040 for *Tbb-CAT1*; HDK1041 for *Tbb-CAT2* and *Tbb-CAT3*; HDK1042 for *Tbb-CAT4*). It is expected that the four cell lines do not give bands (~2.6 Kb) as it is linearized by *NotI* before transfection (Figure 3.8B).

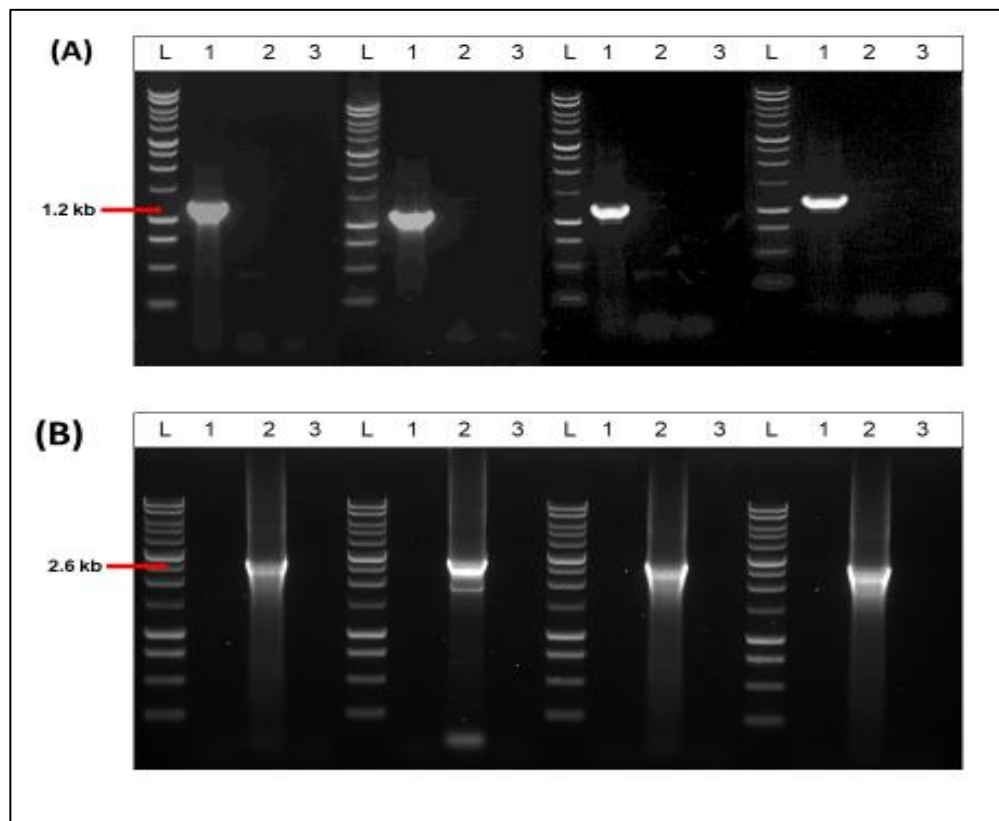


Figure 3.8: PCR confirmation for the linearity of pHDK199, pHDK200, pHDK201 and pHDK202 plasmids and the present of *Tbb-CAT1*, *Tbb-CAT2*, *Tbb-CAT3* and *Tbb-CAT4* genes into *Tbb-5FURes* strain after transfection.

A) Confirmation of the presence of *Tbb-CAT1*, *Tbb-CAT2*, *Tbb-CAT3* and *Tbb-CAT4* genes into *Tbb-5FURes* strain after transfection. L: 1kb DNA Ladder (Promega); 1: *Tbb-CAT1*, *Tbb-CAT2*, *Tbb-CAT3* and *Tbb-CAT4* (~1200 bp) respectively; 2: Non-transfected control (gDNA of *Tbb-5FURes* strain); 3: negative control. B) Confirmation of the linearization of pHDK199, pHDK200, pHDK201 and pHDK202 plasmids after transfection into *Tbb-5FURes* strain. L: 1kb DNA Ladder (Promega); 1: pHDK199, pHDK200, pHDK201 and pHDK202 plasmids respectively; 2: Undigested plasmids of pHDK199, pHDK200, pHDK201 and pHDK202 (~2.6 kb); 3: negative control.

3.2.2.2 qRT-PCR confirmation and growth curve of overexpression of *Tbb-CAT1-4* in *Tbb-5FURes*

The level of mRNA expression for *Tbb-5FURes* + *Tbb-CAT1*^{o.e}, *Tbb-CAT2*^{o.e}, *Tbb-CAT3*^{o.e} and *Tbb-CAT4*^{o.e} was analysed and compared to the control cell line by qRT-PCR (Figure 3.9). The *Tbb-5FURes* + *Tbb-CAT4*^{o.e} recorded the highest transcription level, amounting to a 2.80-fold increase ($P < 0.01$) compared to the control *Tbb-5FURes*. When compared to the control cell lines (*Tbb-5FURes*), the expression level of *Tbb-CAT1*^{o.e} and *Tbb-CAT2*^{o.e} in the *Tbb-5FURes* was recorded as 1.32 and 2.33-fold, respectively ($P < 0.01$), while, the expression of *Tbb-5FURes* + *Tbb-CAT3*^{o.e} increased approximately (2.53 -fold; $P < 0.05$).

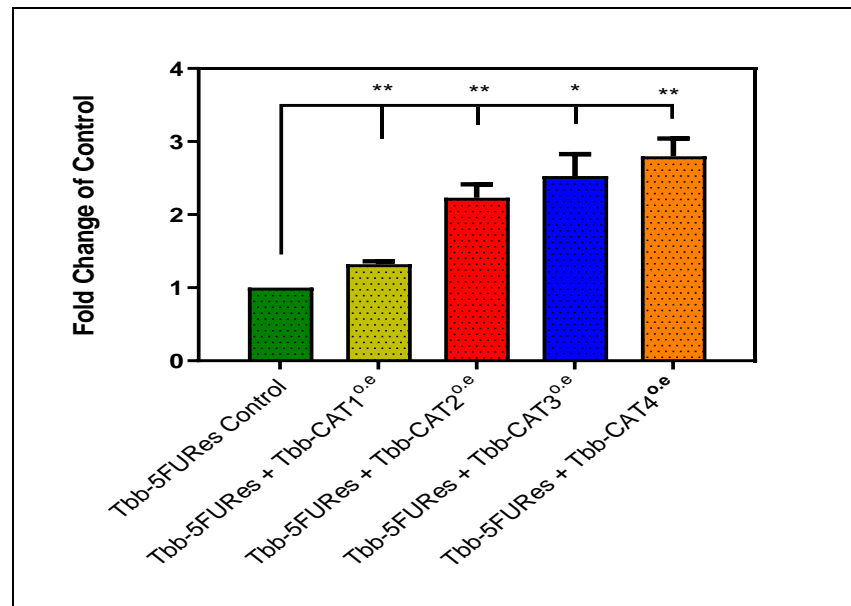


Figure 3.9: The expression levels of Tbb-CAT1, Tbb-CAT2, Tbb-CAT3, and Tbb-CAT4 in *Tbb-5FURes* strain (BSF) and compared to the *Tbb-5FURes* determined by qRT-PCR. Levels were corrected against expression of the housekeeping gene (GPI8). The presented results are the average and \pm SEM of 3 independent replicates. * $P < 0.05$; ** $P < 0.01$.

Figure 3.10 shows the analysis of the growth of the *Tbb-5FURes*, *Tbb-5FURes* + *Tbb-CAT1*^{0.e}, *Tbb-5FURes* + *Tbb-CAT2*^{0.e}, *Tbb-5FURes* + *Tbb-CAT3*^{0.e} and *Tbb-5FURes* + *Tbb-CAT4*^{0.e} was assessed in HMI-9 medium complemented with 10% FBS; cell densities were determined every 24 h. Cells were passaged every 48 h once the growth had reached between 1.5 and 2×10^6 cells/mL. The result show that there was no effect on the growth of *Tbb-5FURes* + *Tbb-CAT1*^{0.e}, *Tbb-CAT2*^{0.e}, *Tbb-CAT3*^{0.e} and *Tbb-CAT4*^{0.e} when *Tbb-CAT1*, *Tbb-CAT2*, *Tbb-CAT3*, and *Tbb-CAT4* genes were overexpressed in comparison with the control *Tbb-5FURes*.

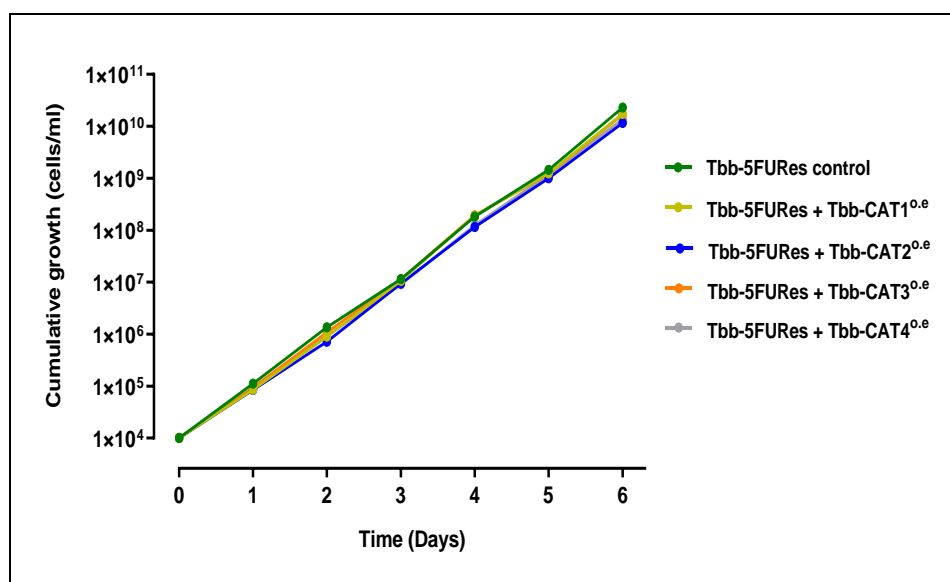


Figure 3.10: The growth assay of *Tbb-5FURes*, *Tbb-5FURes + Tbb-CAT1^{o.e}*, *Tbb-5FURes + Tbb-CAT2^{o.e}*, *Tbb-5FURes + Tbb-CAT3^{o.e}* and *Tbb-5FURes + Tbb-CAT4^{o.e}* on HMI-9 medium supplemented with 10% FBS.

3.2.2.3 The cells were seeded at the density of 1×10^4 cells/mL, and cell densities were determined every 24h. This result represents data from two similar independent determinations. **Drug sensitivity test of overexpression (*Tbb-CAT1-4*) in *Tbb-5FURes***

The Alamar blue assay was used to determine the EC_{50} of the *Tbb-5FURes* over-expressing *Tbb-CAT1*, *Tbb-CAT2*, *Tbb-CAT3*, and *Tbb-CAT4* in order to verify these clones are resistant to 5-FU and sensitisation to 6-Azauracil before performing any transport assays; the Alamar blue assay was performed in parallel with the wild-type strains. Pentamidine was used as control drug throughout the assessment (Figure 3.11). The sensitivity of *Tbb-5FURes* to 5-FU was strongly decreased (Resistance Factor (RF) = 92; $P < 0.0001$) in comparison with the *Tbb-s427* wild type. The Resistance Factor (RF), defined as the ratio of the EC_{50} values of the transgene parasite to that of the wild-type s427 strain, is calculated by $[RF; EC_{50}(Tbb-5FURes)/EC_{50}(427WT)]$. None of the 5-FU resistant cell lines that overexpressed *Tbb-CAT1*, *Tbb-CAT2*, *Tbb-CAT3* and *Tbb-CAT4* exhibited significant differences in the sensitivity to 5-FU when compared to the control cells ($P > 0.05$), although the overexpressing clones for each CAT trended towards higher sensitivity, consistent with the initial observation from RNAseq that CAT downregulation was associated with 5FU resistance. Interestingly, the *Tbb5-FURes* displayed increased sensitivity to 6-AU (5.8-fold more sensitive to 6-AU; $P < 0.001$) when compared to the wild type strain, probably indicating a reduced uracil salvage pathway and increasing reliance on *de novo* synthesis. 6-

AU is considered to be an inhibitor of pyrimidine *de novo* biosynthesis pathway; specifically, it is a known inhibitor of orotidylate decarboxylase in trypanosomes (Jaffe, 1961). However, *Tbb-5FURes* + *Tbb-CAT1*, *Tbb-CAT2*, *Tbb-CAT3* and *Tbb-CAT4* cells exhibited significantly reduced sensitivity to 6-AU (RF = 0.6, 0.55, 0.52 and 0.56, respectively) compared to the parental 5FURes line. Also, the sensitivity of *Tbb-s427* wild type and *Tbb-5FURes* overexpressing *Tbb-CAT1*, *Tbb-CAT2*, *Tbb-CAT3* and *Tbb-CAT4* to pentamidine was not significant different ($P > 0.05$).

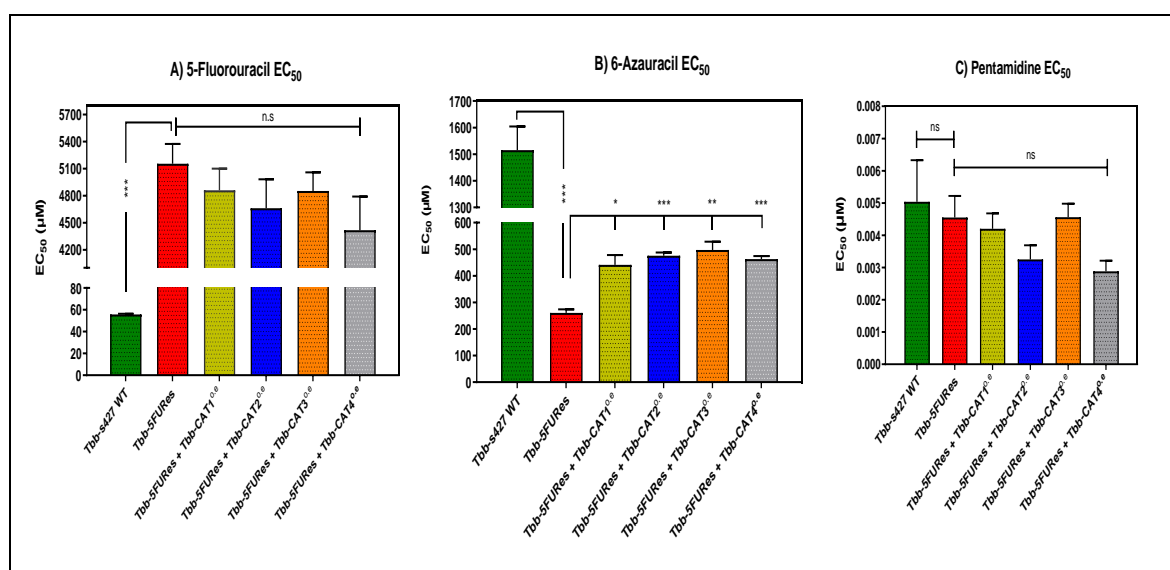


Figure 3.11: Effect of overexpression of *Tbb-CAT1*, *Tbb-CAT2*, *Tbb-CAT3* and *Tbb-CAT4* on sensitivity of *Tbb-5FURes* strain to A) 5-fluorouracil, B) 6-Azauracil and C) Pentamidine determined by using the alamar blue assay. Each bar represents the average of three independent repeats is shown \pm SEM in μ M. * $P < 0.05$; ** $P < 0.01$; *** $P < 0.001$.

3.2.2.4 Transport of uracil by overexpression of *CAT 1-4* in *Tbb-5FURes*

The transport of 0.1 μ M of [3 H]-uracil in the *Tbb-5FURes* expressing *Tbb-CAT1*, *Tbb-CAT2*, *Tbb-CAT3* and *Tbb-CAT4* was determined in order to check whether the overexpression of each cation transporter could cause changes in the rate of uracil transport (Figure 3.12). [3 H]-Uracil transport was linear for 10 min in *Tbb-s427* WT cells ($r^2 = 0.99$) with a rate of 0.237 ± 0.016 pmol.(10^7 cells) $^{-1}$.s $^{-1}$. Although the uptake of [3 H]-uracil was reduced by 26.4% in *Tbb-5FURes* cells, with a rate of 0.174 ± 0.021 pmol.(10^7 cells) $^{-1}$.s $^{-1}$ (not significantly different from wild type $P > 0.05$ by F-test; n=1), the uptake of [3 H]-uracil in all *Tbb-5FURes* over-expressing *Tbb-CAT1*, *Tbb-CAT2*, *Tbb-CAT3* and *Tbb-CAT4* was very similar

to that of the wild-type, with a rate of 0.247 ± 0.022 , 0.225 ± 0.04 , 0.264 ± 0.05 and 0.218 ± 0.027 pmol. $(10^7 \text{ cells})^{-1} \cdot \text{s}^{-1}$, respectively (n=1). This result confirmed that *Tbb-CAT1-4* does not transport uracil, but may (up) regulate uracil transport in some way. There was partial decline in transport rate of [^3H]-uracil in the *Tbb-5FURes* cells relative to the wild type. This is attributed to the high background generated from TbU3 transporter.

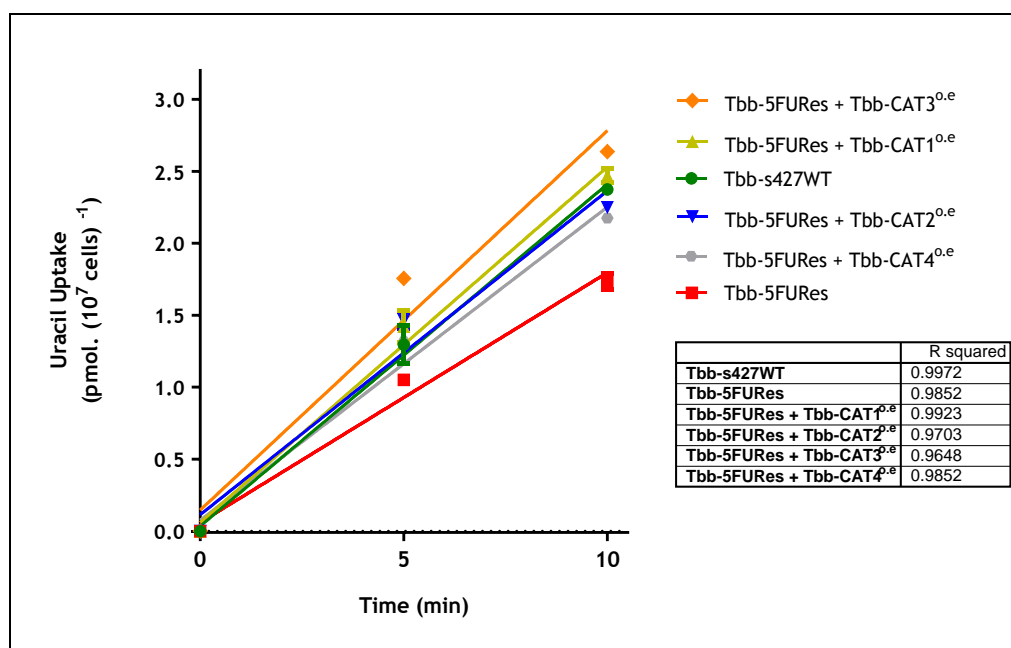


Figure 3.12: [^3H]-Uracil uptake in *T. brucei* strains. The uptake of $0.1 \mu\text{M}$ of [^3H]-uracil over 10 minutes by *Tbb-s427WT*, *Tbb-5FURes* and *Tbb-5FURes + Tbb-CAT1^{oe}*, *Tbb-5FURes + Tbb-CAT2^{oe}*, *Tbb-5FURes + Tbb-CAT3^{oe}* and *Tbb-5FURes + Tbb-CAT4^{oe}*. Linear regression correlation coefficients (r^2) for each line are given in the inset table.

Figure shows one representative experiment in triplicate, and error bars represent \pm SEM. F-test was determined by GraphPad Prism 8.

3.2.3 Effect of heavy metal ions, ion chelators and a TAO inhibitor on *T. b. brucei* BSF

According to a Pfam analysis (<https://pfam.xfam.org>) *Tbb-CAT1-4* protein sequences identified that the sequences can be part of the Zip Zinc transporter family (PF02535). For that reason, we conducted a test of single knockout of the cation transporters in *Tbb-s427* wild type and of the overexpressing clones for each of four cation transporter genes (*Tbb-CAT1*, *Tbb-CAT2*, *Tbb-CAT3* and *Tbb-CAT4*) in *Tbb-5FURes* to establish their susceptibility to heavy metal ions (Cd^{2+} , Hg^{2+} , Ba^{2+} , Pb^{2+} , Cu^{2+} , Zn^{2+} and Fe^{2+}), Salicylhydroxamic acid (SHAM) and Deferoxamine (DFOA). The experiments were carried out at least three times for

each compound tested, and pentamidine and diminazene aceturate were used as positive control in this assay (Table 3.3).

Table 3.3: Effect of Heavy metal ions, Salicylhydroxamic acid (SHAM) and Deferoxamine (DFOA) on *Trypanosoma brucei brucei* (BSF).
 All EC₅₀ Values were obtained using Alamar blue assay and are given as means in μM ($\pm\text{SEM}$), of 3 independent repeats. * $P < 0.05$; ** $P < 0.01$; *** $P < 0.001$ by unpaired Student's T-test. Pentamidine and Diminazene is a standard drug used as control in this assay.

Cell lines \ Compounds	Cadmium (Cd ²⁺)	Mercury (Hg ²⁺)	Barium (Ba ²⁺)	Lead (Pb ²⁺)	Copper (Cu ²⁺)	Zinc (Zn ²⁺)	Iron (Fe ²⁺)	DFOA	SHAM	Pentamidine (Penta)	Diminazene (DMZ)
<i>Tbb-s427WT</i> ^a	7.21 \pm 1.18	0.0438 \pm 0.0028	3760 \pm 114	1230 \pm 100	11.9 \pm 0.46	1077 \pm 43	215 \pm 50	14.6 \pm 2.7	54.1 \pm 6.4	0.0041 \pm 0.0007	N.D
<i>Tbb-sKO-CAT1-4</i> ^{+/-}	21.6 \pm 1.53**	0.0485 \pm 0.0034	3370 \pm 394	1280 \pm 93	12.7 \pm 0.44	1275 \pm 57	204 \pm 29	14.6 \pm 2.6	50.6 \pm 5.6	0.0053 \pm 0.0002	N.D
<i>Tbb-5FURes</i> ^b	8.2 \pm 0.38	0.0460 \pm 0.0008	4216 \pm 140	1166 \pm 38	13 \pm 1.2	1032 \pm 38	234 \pm 62	10.3 \pm 0.90	70.1 \pm 2.72	0.0039 \pm 0.0008	N.D
<i>Tbb-5FURes+Tbb-CAT1</i> ^{o.e}	2.80 \pm 0.54**	0.0427 \pm 0.0014	3500 \pm 98*	1121 \pm 17	13.4 \pm 0.39	1069 \pm 7	214 \pm 38	11.1 \pm 0.72	69.5 \pm 3.87	0.0037 \pm 0.0005	N.D
<i>Tbb-5FURes+Tbb-CAT2</i> ^{o.e}	3.3 \pm 0.87*	0.0443 \pm 0.0025	3545 \pm 31*	1157 \pm 23	14.1 \pm 0.36	1015 \pm 8	250 \pm 60	9.2 \pm 1.32	56.1 \pm 5.90	0.0032 \pm 0.0007	N.D
<i>Tbb-5FURes+Tbb-CAT3</i> ^{o.e}	1.9 \pm 0.46***	0.0420 \pm 0.0043	3183 \pm 164*	1180 \pm 91	13.9 \pm 0.08	973 \pm 18	175 \pm 19	9.9 \pm 2.58	58.7 \pm 7.35	0.0038 \pm 0.0011	N.D
<i>Tbb-5FURes+Tbb-CAT4</i> ^{o.e}	0.03 \pm 0.0049***	0.0391 \pm 0.0024	3361 \pm 36**	1082 \pm 14.4	13.1 \pm 0.49	978 \pm 52	226 \pm 17	10.8 \pm 0.46	62.1 \pm 5.99	0.0029 \pm 0.0006	N.D
<i>2T1</i> ^c	4.6 \pm 0.87	0.1013 \pm 0.0101	3315 \pm 229	1231 \pm 1267	10.2 \pm 0.23	952 \pm 92	65 \pm 8	8.9 \pm 1.22	30.9 \pm 1.80	0.0022 \pm 0.0004	0.0226 \pm 0.0044
<i>aqp2/aqp3 null</i>	4.2 \pm 0.53	0.1096 \pm 0.0014	3934 \pm 175	1035 \pm 8	13.5 \pm 1.05	1039 \pm 64	72 \pm 5	13 \pm 2.14	24.6 \pm 1.73	0.0540 \pm 0.0061***	0.0342 \pm 0.0101
<i>aqp1/aqp2/aqp3 null</i>	1.1 \pm 0.14*	0.125 \pm 0.006	3541 \pm 311	1040 \pm 7.4	10.2 \pm 1.86	1035 \pm 144	73 \pm 9	10.1 \pm 0.87	6.1 \pm 0.31***	0.0271 \pm 0.0015***	0.0091 \pm 0.0019

Tbb-s427 WT = wildtype strai, *2T1* = *T. b. brucei* *2T1* cell. (Alsford et al., 2005), *aqp2/aqp3 null* = Aquaporin2/3 double knockout and *aqp1/aqp2/aqp3 null* = aquaporin1-3 triple knockout BSF *T. brucei* *2T1*. SHAM = Salicylhydroxamic acid and DFOA = Deferoxamine. ND = not determined. *P* values were calculated statistically by unpaired t-test, using Microsoft Excel function (comparing two arrays with three readings each, 2-tailed and type-2: comparing one value with only one other 'its control' and not with every other in the table). Student's unpaired t-test, comparing ^a*Tbb-WT* vs *Tbb-sKO-CAT1-4*^{+/-}, ^b*Tbb-5FURes* vs *Tbb-5FURes*+overexpressing of each individual CATs and ^c*2T1* vs *aqp1/aqp2/aqp3 null*.

The analysis did not identify any significant differences in the sensitivity to Mercury, Barium, Lead, Copper, Zinc, Iron, SHAM and Deferoxamine for the *Tbb-sKO-CAT1-4^{+/-}* compared to the wild type control ($P > 0.05$). However, the outcome of the test showed a significant reduction in the sensitivity of *Tbbs427-sKO-CAT1-4^{+/-}* to Cadmium with $21.6 \pm 1.5 \mu\text{M}$ when compared to the control *Tbb-s427* wild-type, which displayed an EC_{50} of $7.2 \pm 1.2 \mu\text{M}$ (3-fold resistant to Cadmium; $P < 0.01$). Moreover, the EC_{50} of the overexpression of *Tbb-CAT1*, *Tbb-CAT2*, *Tbb-CAT3*, and *Tbb-CAT4* in *Tbb-5FURes* to Mercury, Lead, Copper, Zinc, Iron, SHAM and Deferoxamine did not exhibit any significant difference when compared to the parental cell line *Tbb-5FURes* ($P > 0.05$). Interestingly, the increased gene expression of either *Tbb-CAT1*, *Tbb-CAT2*, *Tbb-CAT3* or *Tbb-CAT4* in the *Tbb-5FURes* cell line significantly increased sensitivity to Cadmium compared to *Tbb-5FURes* ($8.2 \pm 0.4 \mu\text{M}$), with an average $2.8 \pm 0.5 \mu\text{M}$, $3.3 \pm 0.9 \mu\text{M}$, $1.9 \pm 0.4 \mu\text{M}$ and $0.03 \pm 0.004 \mu\text{M}$ respectively. Cell lines *Tbb-CAT1^{o.e}*, *Tbb-CAT2^{o.e}*, *Tbb-CAT3^{o.e}* and *Tbb-CAT4^{o.e}* were also more sensitive to Barium, with EC_{50} values of $3500 \pm 98 \mu\text{M}$, $3545 \pm 31 \mu\text{M}$, $3183 \pm 164 \mu\text{M}$ and $3361 \pm 36 \mu\text{M}$ respectively, compared to $4216 \pm 140 \mu\text{M}$ recorded for the *Tbb-5FURes*.

The activity of the above listed compounds against *2T1*, *aqp2/aqp3 null* and *aqp1/aqp2/aqp3 null* was also determined. The result showed that there was no significant difference between *2T1*, *aqp2/aqp3 null* and *aqp1/aqp2/aqp3 null* cell lines; only the *aqp1/aqp2/aqp3 null* showed approximately 4-fold increased sensitivity to Cadmium ($P < 0.05$), which may indicate that AQP1 can mediate the efflux of cadmium ions taken up by one or more of the CAT transporters. There were no significant differences in heavy metal ion sensitivity between CAT single knockout and AQP double knockout cell lines.

3.3 Discussion

Transport proteins are important for the movement of drugs in and out of the cell, making them special intermediaries in both therapy and drug resistance. Thus, the generation and characterization of drug resistant lines provides valuable information on resistance mechanisms, and can potentially be used to identify new drug transporters. For instance, multi-drug resistant *T. b. brucei*

line B48 was generated *in vitro* by stepwise increasing the concentration of pentamidine until these cells lost the transport activity known as the High Affinity Pentamidine Transporter (HAPT1) (Matovu et al., 2003; Bridges et al., 2007). Recently, the HAPT1 activity was found to be encoded by *T. brucei* aquaglyceroporin 2 (*TbAQP2*) (Baker et al., 2012; Munday et al., 2014). An essential role is played by purine and pyrimidine nucleotides in nucleic acid synthesis (DNA and RNA), as well as in prokaryotic and eukaryotic cell metabolism (de Koning and Diallinas, 2000; Rodriguez-Contreras et al., 2007; Campagnaro and de Koning, 2020). Pyrimidine analogue 5-fluorouracil was found to be a good inhibitor of high-affinity uracil transporters in *L. major* (LmajU1) and *T. b. brucei* (TbU1) (Campagnaro and de Koning, 2020). Apart from the chemotherapeutic potential of pyrimidine analogues, 5-FU can be used as a tool to identify a novel family of transporters in protozoa (Domin et al., 1993; de Koning and Diallinas, 2000; De Koning, 2007; Bellofatto, 2007).

Multiple lines of investigation have been followed to date to try to identify the gene(s) coding for kinetoplastid uracil transporters. The BLAST searches for pyrimidine transporter genes using fungal, yeast and prokaryote sequences have, until this day, not produced a single candidate gene from any of the available protozoan genomes, leading us to conclude that no genes can be identified by homology to known pyrimidine transporter genes. Therefore, previous work in our laboratory undertook whole genome sequencing, RNA-seq and RIT-seq and as a way of finding the pyrimidine transporter genes of *T. b. brucei* (Ali, 2013; Alzahrani, 2017). The generation of the 5-FU-resistant cell lines of *T. b. brucei* s427 WT was undertaken through exposure to increasing concentrations of 5-FU *in vitro* as a way of gaining additional insights into pyrimidine salvage pathways in *Trypanosoma* species (Ali et al., 2013a). RNA sequencing (RNA-Seq) is seen as a powerful technique where deep-sequencing technologies are utilised in sequencing RNA as a way of determining the differential gene expression under different physiological or environmental conditions (Wang et al., 2009; Kukurba and Montgomery, 2015). An attempt was made to identify the pyrimidine transporter genes by following up *Tbb-CAT1-4* genes. Overexpression and knockout strategies were utilised as investigative tools. Overexpression of a

candidate gene can be a powerful tool when the effect of a drug is reversed by overexpression and compensates for a reduced gene expression in the resistant line (Prelich, 2012). The knockout technique was utilised in deleting one allele of the *Tbb-CAT1-4* tandem-array locus in *T. b. brucei* wild-type BSF. It is possible to utilise these methods in studying either function gain or function phenotypes loss.

Subcellular localisation using an N-terminal tag showed that the putative cation transporter Tb927.11.9000 appeared to be localised in the cytoplasm; however with a C-terminal fusion the protein localised to the nuclear envelope and endoplasmic reticulum in PCF trypanosomes. As this transporter is an integral membrane protein, it cannot be localised free in the cytoplasm. The putative cation transporter Tb927.11.9010 was localised to the endocytic organelles of *T. b. brucei* PCF (TrypTag, 2020).

The hypothesis was that, if the TbCAT transporters had the capacity to transport uracil and 5-FU, their overexpression in *Tbb-5FURes* would lead to a significant rise in the sensitivity to 5-FU and a significant decline in the sensitivity to 6-AU which is an indication of a restored uracil salvage pathway and thereby reduced reliance on *de novo* synthesis, of which 6-AU is an inhibitor of pyrimidine *de novo* biosynthesis pathway in trypanosomes (Jaffe, 1961). In contrast, a significant reduction in the sensitivity to 5-FU and a significant rise in sensitivity to 6-AU would result from the knockout of *TbCAT* transporter genes and the thus abolished uracil salvage pathway, leading to an increasing reliance on *de novo* synthesis. We succeeded in utilising the expression plasmid pHD1336 to overexpress the *Tbb-CAT1-4* genes in *Tbb-5FURes*. This plasmid has been found to be very effective for overexpression of genes in *T. b. brucei* (Munday et al., 2013; Alzahrani et al., 2017; Biebinger et al., 1997; Campagnaro et al., 2018b). Munday et al. (2013) utilised the pHD1336 plasmid for the heterologous expression of *T. congolense* aminopurine transporter (*TcoAT1*) in multi-drug resistant *T. b. brucei* lines B48, which allowed its characterisation as a P1-type nucleoside transporter. Moreover, Alzahrani et al. (2017) identified that NT1.1 in *L. major* and *L. mexicana* is sensitive to inhibition by uracil and named as

uridine-uracil transporter 1 (UUT1), using this vector that expressed *NT1.1* gene in *T. b. brucei* B48 strain. Also, this vector was used to express and characterise the TcrNBT1, TcrNT1 and TcrNT2 ENT-family transporter genes in *T. brucei* procyclic TbNBT-KO cells showing that TcrNB1 is a high-affinity hypoxanthine transporter, TcrNT1 is a high-affinity inosine/guanosine transporter and TcrNT2 is a high-affinity thymidine transporter (Campagnaro et al., 2018b). PCR and qRT-PCR confirmed the overexpression of candidate pyrimidine transporter genes and the presence of knockout constructs, and their correct integration.

We determined the sensitivity of the 5-Fluorouracil and 6-Azauracil pyrimidine analogues in a single knockout of *Tbb-CAT1-4* genes in *T. b. brucei* s427 WT with the use of alamar blue method and found no significant difference; pentamidine was used as a control against the *T. brucei* s427 WT and heterozygous knockout cells. Further results showed that the uptake of [³H]-uracil in *Tbb-s427WT* + *Tbb-CAT1-4*^{+/-} was almost the same as the wild type cells. Similarly, the introduction of any cation transporters into *Tbb-5FUR*es did not significantly increase the rate of transport of [³H]-uracil of the 5-FU resistant cell lines, which was in any case only partly reduced from wild-type levels (F-test was determined by GraphPad Prism 8). However, this outcome does not mean that *Tbb-CAT1-4* genes are not involved in the 5-FU sensitivity or transport, for the reason that the first allele of these genes was deleted while the second allele still exists in the genome of hemizygous knockout cells. Unfortunately, we were unable to make a full double knockout for the *Tbb-CAT1-4* genes, as this led to the death of the cells, showing that their function is essential for the growth of the *T. b. brucei*. It has previously been shown that the deletion of both alleles of two other cation transporters, forming a heteromeric potassium channel, led to cell death through the elimination of ion conductance (Steinmann et al., 2015; Clayton, 1999).

Thus, it is possible for us to speculate that the double knockout of the *Tbb-CAT1-4* genes affected the viability of Tbb BSF by disrupting the intracellular ion distribution in *T. brucei* s427 WT. Consequently, it is possible that these CATs are iron transporters; iron ions are very important in mitochondrial metabolism,

as they are essential to the function of cytochromes and of Trypanosome Alternative Oxidase (TAO) (Saimoto et al., 2013; Shiba et al., 2013). However, this appears to rule out the possible involvement of CAT transporters in uracil uptake as we have reason to believe that the pyrimidine transporter genes are not essential in *T. b. brucei* BSF for two reasons. 1) The ability of pyrimidine prototrophic *T. b. brucei* cells to grow in pyrimidine-free HMI-9 media (Ali et al., 2013b). 2) There was a reduction of [³H]-5-FU uptake rate by greater than 65% when *T. b. brucei* WT adapted to high levels of 5-FU (*Tbb-5FURes*). Whereas transport of [³H]-uracil was only partly reduced in the *Tbb-5FURes* cells compared to s427-WT cells (Ali et al., 2013a). Moreover, an identical experiment using *L. mexicana* promastigotes totally eliminated (94.5%) [³H]-5-FU transport in the 5-FU resistant cell lines (*Lmex-5FURes*), thereby revealing that the uracil/5-FU transporters are not essential when it comes to these organisms although they are important when it comes to the anti-protozoal activity of 5-FU (Alzahrani et al., 2017).

On the other hand, the *Tbb-CAT1-4* protein sequences analysis with Pfam showed that they belong to the family of zinc and iron transport. That reason makes it of interest to conduct a test of single knockout of the *Tbb-CAT1-4* genes in *Tbb-s427WT* and also test the overexpressing of each of the four CAT transporter genes (*Tbb-CAT1*, *Tbb-CAT2*, *Tbb-CAT3* and *Tbb-CAT4*) in *Tbb-5FURes* by making a comparison of them with respect to sensitivity to heavy metal ions, ion chelators and a TAO inhibitor. We found that the effect of increased gene expression of *Tbb-CAT1*, *Tbb-CAT2*, *Tbb-CAT3* and *Tbb-CAT4* in *Tbb-5FURes* significantly increased the sensitivity to Cadmium and Barium. In addition, we observed a significant decrease in the sensitivity of single knockout clones of *Tbb-CAT1-4* in *Tbb-s427 wild-type* to Cadmium. The ZIP/SLC39A family of metal ion transporters have been identified at all phylogenetic levels and consist of fourteen transporters encoded in the human genome. These genes are designated SLC39A1-SLC39A14 and encoded 'protein ZIP1-ZIP14', respectively (Jeong and Eide, 2013; Eide, 2004). The ZIP proteins transport essential (e.g. zinc) as well as non-essential, toxic heavy metals (e.g. cadmium and mercury) (De Carvalho and de Melo, 2017; Jeong and Eide, 2013). It is still not clear how

proteins in the ZIP family, together with other transporters or trafficking systems coordinate in to regulate zinc homeostasis (Jeong and Eide, 2013). In the case of non-essential heavy metal ions such as cadmium, the main mechanism of entry into trypanosomes is through divalent metal ion transporters, mainly for calcium, due to its similar ionic radius (De Carvalho and de Melo, 2017). Although Cd^{2+} is obviously not the intended substrate for the TbbCAT transporters, we show here that they provide a potential point of entry for the heavy metal if there is a sufficient concentration of the ions in the parasite's immediate environment. Sensitivity to the metal ion, correlated to the level of TbbCAT expression is one method to assess the capacity of the carrier to take up that ion, especially if excess of that ion is deleterious to cell growth or survival. Alternatively, uptake of a radioactive isotope of the metal can be measured in an appropriate scintillation counter or gamma radiation counter, depending on the isotope. A further method would be to measure cellular content of the metal ion spectroscopically. Further, fluorescent probes (chelators) can serve as specific reporters for some of the dications including Ca^{2+} and Zn^{2+} (Eren and Argüello, 2004; Gee et al., 2002).

Studies by Nyarko et al. (2002) first reported that heavy metals such as cadmium and mercury in drug sensitivity assays are extremely toxic to *T. b. brucei* parasites. Toxicity is also a key disadvantage of using heavy metals in drugs against kinetoplastid parasites for human use (Jeong and Eide, 2013; De Carvalho and de Melo, 2017). To gain an insight into the possible resistance mechanism, cross-resistance between the *Tbb-s427WT* + *Tbb-CAT1-4^{+/-}* and *aqp1/aqp2/aqp3 null* cell lines for some heavy metal ions, ion chelators and a TAO inhibitor was assessed. The result showed that there was no cross-resistance pattern between the *Tbb-CAT1-4^{+/-}* and *aqp1/aqp2/aqp3 null* cell lines.

4 Assessment of the role of fatty acid desaturase in *T. brucei* BSF and *L. mexicana* promastigotes in 5-FU sensitivity

4.1 Introduction

Fatty acid desaturases are enzymes that convert saturated fatty acid to unsaturated fatty acid through the removal of two hydrogen atoms from fatty acids, introducing a double bond. The main function of fatty acid desaturases in the mammalian cell is to maintain the function and structure of biological membranes through balancing of the proportion of saturated and unsaturated fatty acids of phospholipids bilayer (Alloatti and Uttaro, 2011; Los and Murata, 1998). There are three classes of desaturases have been observed in Kinetoplastid parasites. Class one is Delta 'Δ' desaturases usually introduces a double-bond x-carbons from the carboxyl end. Class two Omega 'ω' comprises enzymes that introduce a double-bond x-carbons from the methyl end. Finally, class three groups Chi and nu 'ν + x' desaturases that add a double-bond x-carbons from an existing double bond (Alloatti and Uttaro, 2011; Petrini et al., 2004). *T. brucei* and *L. mexicana* cells can take up lipids from host environments by transportation of protein-bound fatty acids or receptor-mediated endocytosis of lipoprotein. Additionally, they can synthesise their own fatty acids *de novo* via a mitochondrial type II prokaryotic-type pathway (Smith and Bütikofer, 2010; Zhang and Beverley, 2010). In a screen for determinants for 5-FU resistance, fatty acid desaturases featured prominently, prompting speculation that they may have a role in uracil salvage or usage.

The gene family encoding pyrimidine nucleobase transporters in kinetoplastid parasites has not yet been identified (De Koning, 2007; Ali et al., 2013a). In this chapter, the pyrimidine analogue 5-fluorouracil is used as a tool to try to identify the uracil transporter in *T. b. brucei* BSF and *L. mexicana* promastigotes, or any other mechanism that may play a role in determining uracil salvage. Previous work in our laboratories (Alzahrani (2017); Ali (2013)) showed a fatty acid desaturase as one of the most promising candidate gene for a pyrimidine uptake determinant, following an evaluation of the wild-type and the 5-FU resistant cell lines of the *T. b. brucei* BSF (Tb427.02.3080) and *L. mexicana* promastigotes (LmxM.10.1320) by use of RNA Sequencing (RNA-seq) analyses of 5-FU resistant cell lines in *T. b. brucei* BSF and *L. mexicana* promastigotes, and by RNA Interference Target Sequencing (RIT-seq) analyses in *T. b. brucei* BSF. Analysis of this fatty acid desaturase in *T. b. brucei* s427 wild-

type BSF (*Tbb-FAD*) and the homologous fatty acid desaturase in *L. mexicana* M379 promastigotes (*Lmex-FAD*) showed a high level of identity (69.43%) (Table 4.1). The sequence alignment result of the *Tbb-FAD* in *T. b. brucei* s427 wild-type BSF and *Lmex-FAD* in *L. mexicana* M379 promastigotes is presented in Appendix 6.

The aim of this study is the role of *Tbb-FAD* and *Lmex-FAD* genes in 5-FU resistance. We will investigate whether overexpression of these genes is able to restore the sensitivity to 5-FU, or the transport of 5-FU/uracil *in vitro*.

Table 4.1: Annotation of fatty acid desaturase genes in the genome of *T. b. brucei* s427 WT BSF and *L. mexicana* M379 promastigote form.

Gene ID	Annotation	Chromosome	TM domains	Transcript	Name	Identity
Tb427.02.3080	Fatty acid desaturase, putative	2	6	1227 bp	<i>Tbb-FAD</i>	69.43%
LmxM.10.1320	Fatty acid desaturase, putative	10	6	1185 bp	<i>Lmex-FAD</i>	

4.2 Results

4.2.1 Over-expression of *Tbb-FAD* in *Tbb-5FURes* and *Tbb-s427* WT BSF

The fatty acid desaturase Tb927.2.3080 (*Tbb-FAD*) is a candidate gene that is potentially responsible for uracil transport following an analysis of the WT and 5-FU resistant lines for *T. b. brucei* by use of RNA sequencing. The expression level of Tb927.2.3080 was significantly decreased in *Tbb-5FURes* with a \log_2 fold-change of -0.68 compared to the reference *T. b. brucei* TREU 927 genome ($P \leq 0.01$) (Alzahrani, 2017). Moreover, this gene Tb927.2.3080 (fatty acid desaturase) has been identified to be a top hit in the RNAi library screening results whereby it leads to 58392 and 439 RPKM after analysis of the pyrimidine-auxotrophic 2T1 PYR6-5^{-/-} cell lines after selection with 5-FU at day 14 or 6-AU at day 24, respectively. (Alzahrani, 2017). The RIT-seq experiment was performed at the lab of Dr Sam Alsford at London School of Hygiene and Tropical Medicine. For *T. b. brucei* strain Lister 427, the correspondent fatty acid desaturase is

Tb427.02.3080 and will be referred to as *Tbb-FAD* throughout this study. *Tbb-FAD* is located in chromosome 2 and comprises six transmembrane domains and is annotated as fatty acid desaturase (TriTrypDB).

4.2.1.1 PCR confirmation for over-expression of *Tbb-FAD* in *Tbb-5FURes* and *Tbb-s427 WT*

The *Tbb-FAD* gene was amplified by PCR from the genome of *T. b. brucei* Lister 427 strain by using HDK1338 as forward and HDK1339 as reverse primers. The *Tbb-FAD* gene was expressed in the *Tbb-5FURes* and *Tbb-s427 WT* strains by using the pHD1336 plasmid. The pHD1336 plasmid and the *Tbb-FAD* gene were digested by the *MluI* and *BamHI* restriction enzymes respectively. The *Tbb-FAD* gene was then ligated into pHD1336 in order to generate plasmid pHDK219 (Figure 4.1). By inserting the gene into the pHDK219 vector, the *MluI* and *BamHI* restriction enzymes digested the vector, which helped in the identification of the relative sizes of the resulting DNA fragments. As shown in Figure 4.2, the *Tbb-FAD* gene is identified as the band at ~1.2 kb whereas the vector is represented by the band at ~6.5 kb. After the transfection of the linearized pHDK219 into the *Tbb-5FURes* and *Tbb-s427 WT* strains, PCR was used to confirm the linearity of the pHDK219 plasmid and integration of the *Tbb-FAD* gene in positive clones. The presence of the expected products (~1.2 kb for the integration while no band for the linearity of the circular of pHDK219 plasmid) was verified by running the PCR products on 1% agarose gel to be visualised under UV light (Figure 4.3 and Figure 4.4).

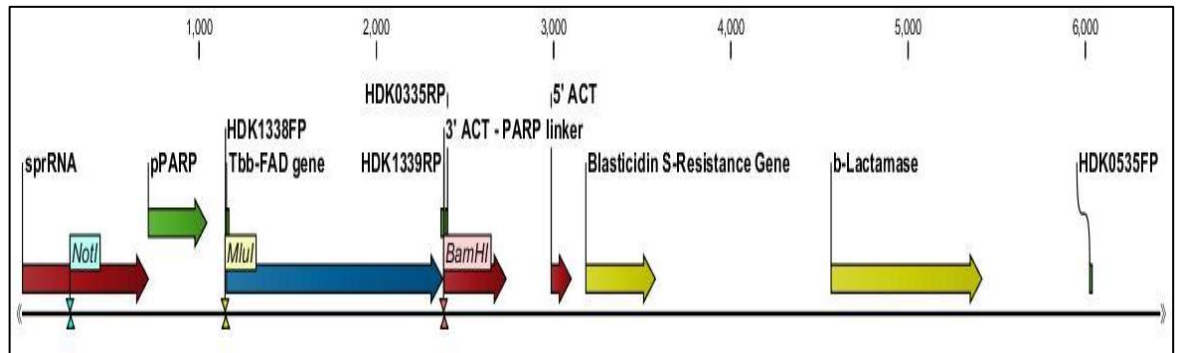


Figure 4.1: Plasmid map of pHDK219 vector for the homologous expression of *Tbb-FAD* gene in *Tbb-5FURes* and *Tbb-s427WT* strain.

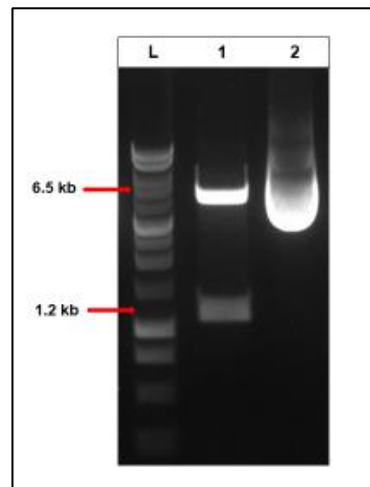


Figure 4.2: Digestion of pHDK219 plasmid by *MluI* and *BamHI* restriction enzymes to drop out *Tbb-FAD* gene (1227 bp) from the pHDK219 plasmid (6.5 kb). L: 1 kb DNA ladder (Promega); 1: Digested plasmid (*MluI* and *BamHI*); 2: Undigested plasmid for pHDK219.

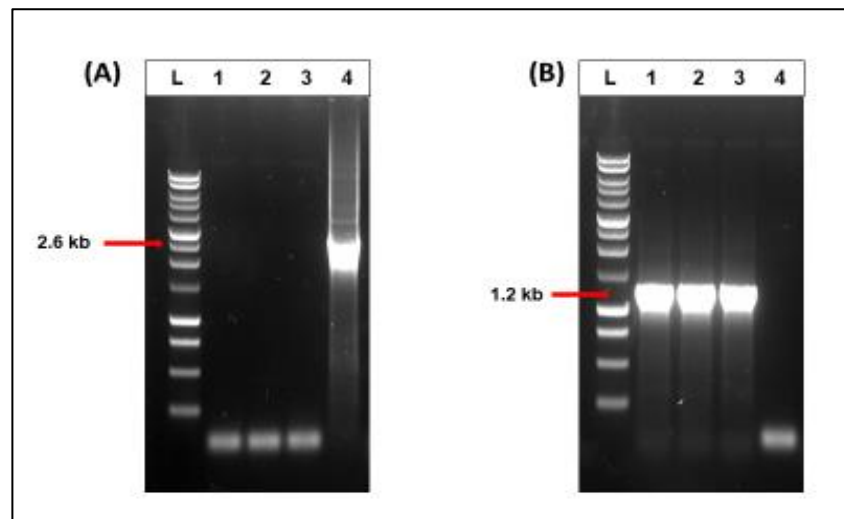


Figure 4.3: PCR confirmation for the linearity of pHDK219 vector and the integration of *Tbb-FAD* gene into *Tbb-5FURes* strain after transfection.

A) Confirmation of the linearization of pHDK219 vector into *Tbb-5FURes* strain after transfection by using HDK535 as forward primer for pHDK1336 plasmid and HDK1339 as reverse primer for *Tbb-FAD* gene. L: 1kb DNA Ladder (Promega); 1: Clone1; 2: Clone2; 3: Clone3; 4: Undigested PHDK219 (~2.6 kb). B) Confirmation of the integration of *Tbb-FAD*

gene into *Tbb-5FURes* strain after transfection by using HDK1338 as forward primer for *Tbb-FAD* gene and HDK335 as reverse primer for pHD1336 plasmid. L: 1 kb DNA Ladder (Promega); 1: Clone1; 2: Clone2; 3: Clone3; 4: Non-transfected control (gDNA from *Tbb-5FURes* strain).

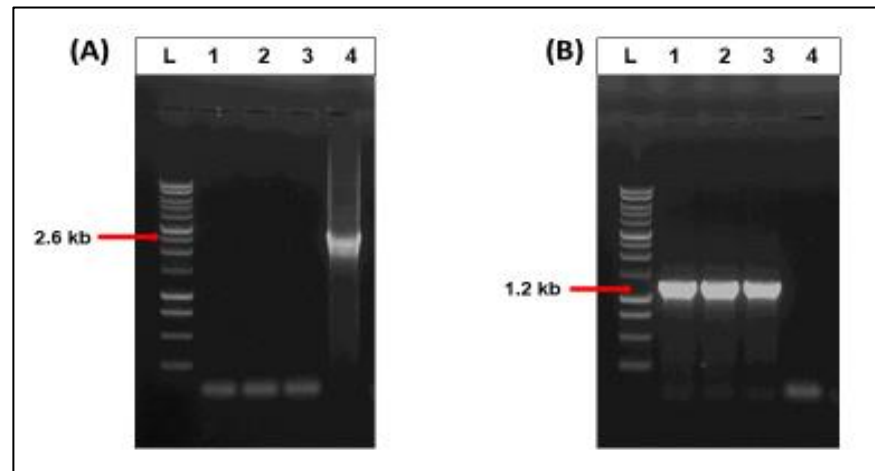


Figure 4.4: PCR confirmation for the linearity of pHDK219 vector and the integration of *Tbb-FAD* gene into *Tbb-s427WT* strain after transfection.

A) Confirmation of the linearization of pHDK219 vector into *Tbb-s427WT* strain after transfection by using HDK535 as forward primer for pHD1336 plasmid and HDK1339 as reverse primer for *Tbb-FAD* gene. L: 1kb DNA Ladder (Promega); 1: Clone1; 2: Clone2; 3: Clone3; 4: Undigested PHDK219 (~2.6 kb). B) Confirmation of the integration of *Tbb-FAD* gene into *Tbb-s427WT* strain after transfection by using HDK1338 as forward primer for *Tbb-FAD* gene and HDK335 as reverse primer for pHD1336 plasmid. L: 1kb DNA Ladder (Promega); 1: Clone1; 2: Clone2; 3: Clone3; 4: Non-transfected control (gDNA from *Tbb-s427WT* strain).

4.2.1.2 qRT-PCR confirmation and growth rate of *Tbb-FAD* in *Tbb-5FURes* and *Tbb-s427WT* strains

The assessment of the transcription level for the *Tbb-FAD* gene in *Tbb-5FURes* clones 1-3 and *Tbb-s427WT* clones 1-3 was conducted first and compared with the parental cell lines by the use of qRT-PCR. The *Tbb-5FURes* + *Tbb-FAD*^{o.e} clone 3 recorded the highest level of messenger RNA expression (3.7-fold; $P < 0.001$) compared with the control *Tbb-5FURes*. On the other hand, the expression level of the *Tbb-5FURes* + *Tbb-FAD*^{o.e} clone 2 amounted to 2.2-fold ($P < 0.01$), whereas the expression level in *Tbb-5FURes* + *Tbb-FAD*^{o.e} clone 1 increased 1.5-fold ($P < 0.001$) relative to the control cell line (Figure 4.5A). The further results showed that the *Tbb-s427WT* + *Tbb-FAD*^{o.e} clone 2 recorded the highest transcription level, amounting to a 2.9-fold increase ($P < 0.001$) compared to the control *Tbb-s427WT*. When compared to the control cell lines (*Tbb-s427WT*), the expression level of *Tbb-s427WT* + *Tbb-FAD*^{o.e} clone 1 and 3 were recorded as 2.7 and 2.5-fold, respectively ($P < 0.001$) (Figure 4.5B).

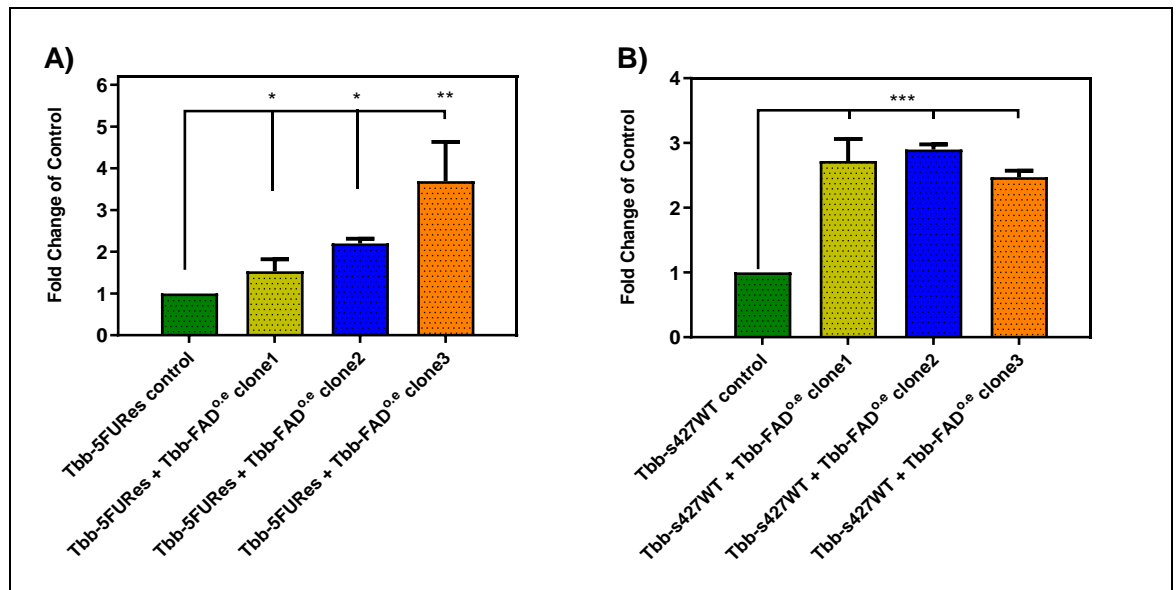


Figure 4.5: Quantitative RT-PCR of *Tbb-FAD* gene expression in the *Tbb-5FURes* and *Tbb-s427WT* strains.

A) The expression levels of *Tbb-FAD* gene in *Tbb-5FURes* and compared to the control (*Tbb-5FURes*) determined by qRT-PCR. **B)** The expression levels of *Tbb-FAD* gene in *Tbb-s427WT* and compared to the control (*Tbb-s427WT*) determined by qRT-PCR. Levels were corrected against the expression level of the housekeeping gene (*T. b. brucei* GPI8). The presented results are the average of 3 replicates \pm SEM. * $P < 0.05$; ** $P < 0.01$; *** $P < 0.001$.

For all the three clones of the *Tbb-5FURes* + *Tbb-FAD*^{o.e} and the *Tbb-s427WT* + *Tbb-FAD*^{o.e}, and its parental cell lines, the assessment was done on their growth in HMI-9 medium supplemented with 10% FBS and incubated at 37 °C under 5% CO₂, and the cell densities were determined every 24h (Figure 4.6A and B). The outcomes of the study demonstrated that there was no effect on the growth when the *Tbb-FAD* gene was overexpressed in the *Tbb-5FURes* and *Tbb-s427WT* for all three clones compared with the control cell lines.

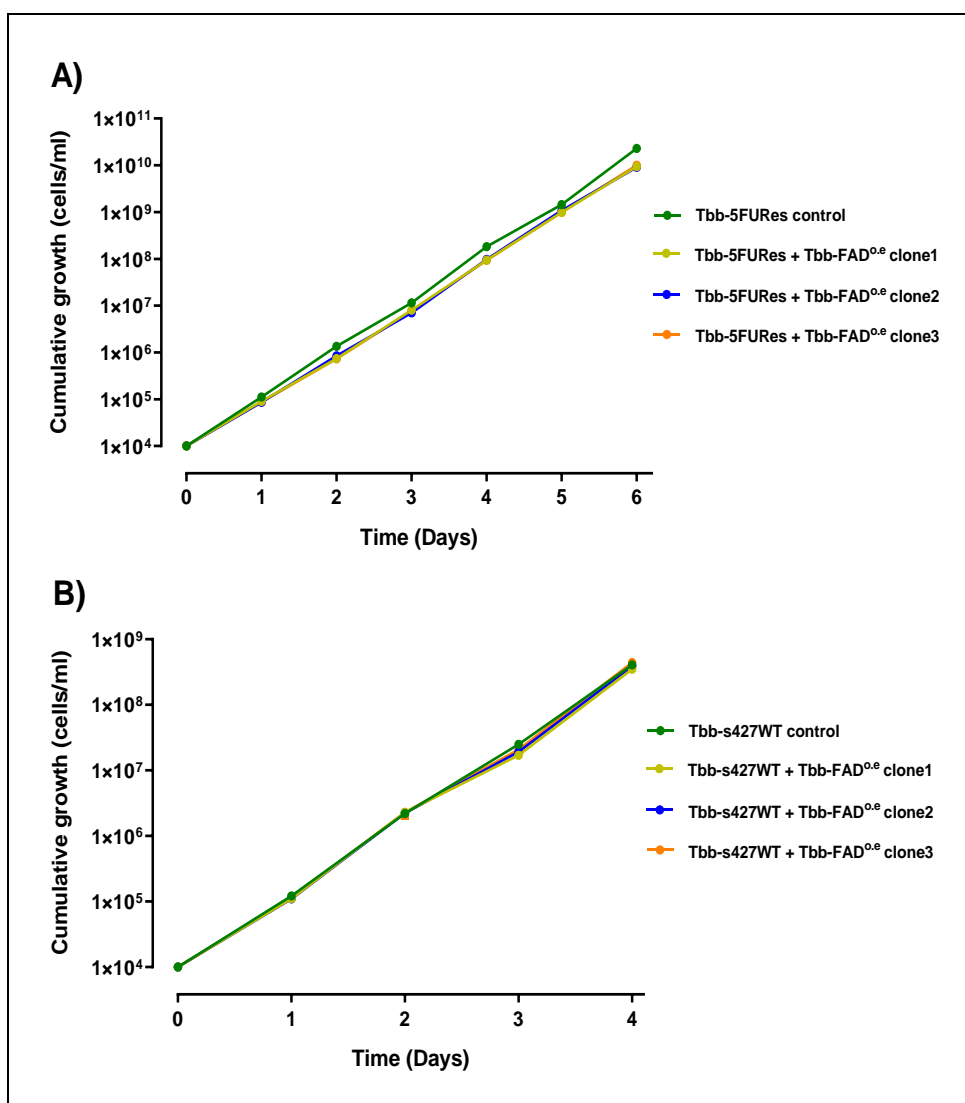


Figure 4.6: The growth rates of *Tbb-5FURes* and *Tbb-s427WT* strains expressing *Tbb-FAD*. A) The growth curve of *Tbb-5FURes* expressing *Tbb-FAD* clones 1-3 on HMI-9 medium supplemented with 10% FBS. B) The growth curve of *Tbb-s427WT* expressing *Tbb-FAD* clones 1-3 on HMI-9 medium supplemented with 10% FBS. The cells were seeded at the density of 1×10^4 cells/mL, and cell densities were determined every 24h. Cells were passaged every 48 hours, when the growth had reached between 1.5 and 2×10^6 cells/mL. Each data point in this result represents the mean of three similar independent repeats.

4.2.1.3 Drug sensitivity assay of overexpression of *Tbb-FAD* in *Tbb-5FURes* and *Tbb-s427WT* with pyrimidine analogues

The effects of increased gene expression of the *Tbb-FAD* gene for the three clones in the *Tbb-5FURes* and *Tbb-s427WT* strains on susceptibility to 5-FU and 6-AU were assessed through the use of the Alamar blue assay as shown in Figure 4.7 and Figure 4.8. The results of the study did not show any significant difference among the EC_{50} values of 5-FU and 6-AU when making a comparison between the over-expressing cell lines and the control cell lines (*Tbb-5FURes* and *Tbb-s427WT*) ($n=3$; $P > 0.05$). Pentamidine was applied as control compound

for the over-expressing cell lines and the control cell lines, and no significant difference was found with this drug either.

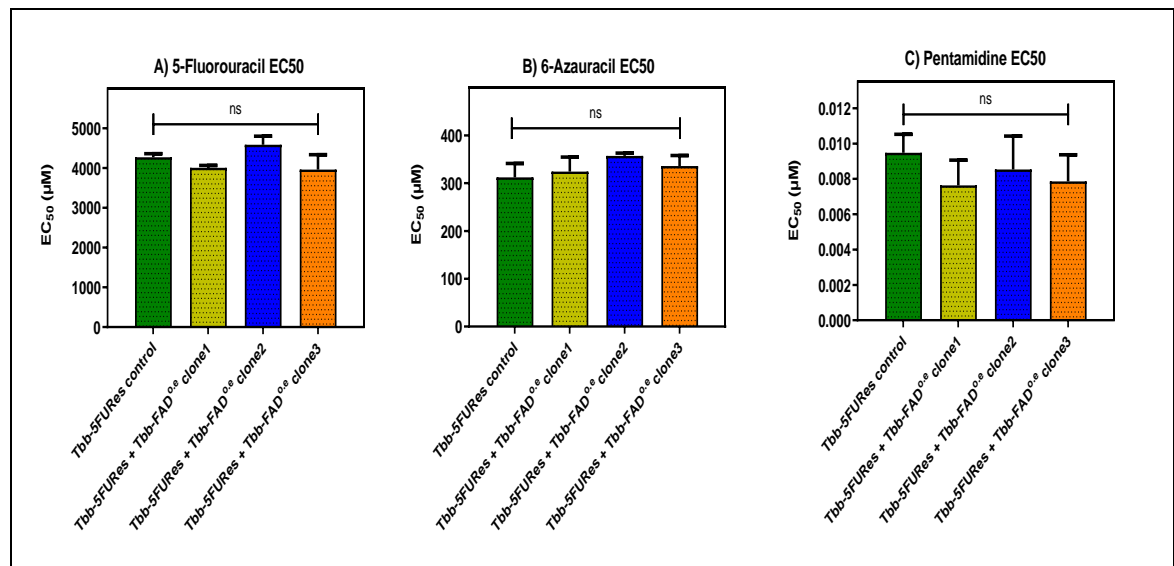


Figure 4.7: Alamar blue drug sensitivity assay of overexpression of *Tbb-FAD* gene in *Tbb-5FURES* clones 1-3 and *Tbb-5FURES* by using 5-fluorouracil (A), 6-azauracil (B) and pentamidine (C).

The mean of three independent repeats is shown \pm SEM in μ M. ns = not significant.

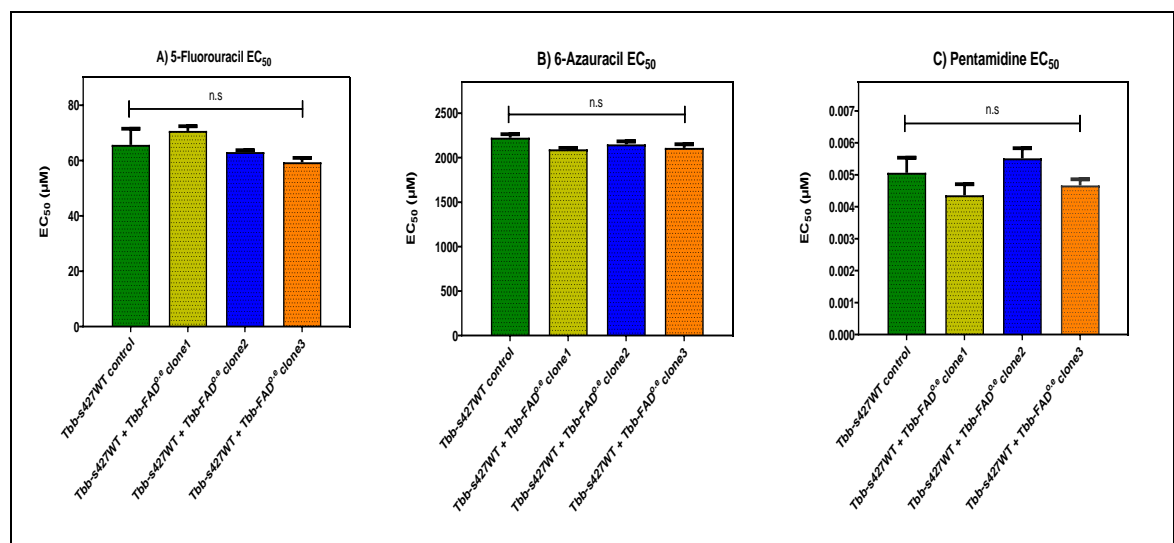


Figure 4.8: Alamar blue drug sensitivity assay of overexpression of *Tbb-FAD* gene in *Tbb-s427WT* clones 1-3 and *Tbb-s427WT* by using 5-fluorouracil (A), 6-azauracil (B) and pentamidine (C).

The mean of three independent repeats is shown \pm SEM in μ M. ns = not significant.

4.2.1.4 Uracil uptake for overexpression of *Tbb-FAD* in *Tbb-5FURES* and *Tbb-s427 WT*

Figure 4.9 shows that uptake of 0.1 μ M of [³H]-uracil in *Tbb-s427 WT*, *Tbb-5FURES*, *Tbb-s427WT + Tbb-FAD^{oe}* and *Tbb-5FURES + Tbb-FAD^{oe}* was linear over 3 minutes ($r^2 = 0.99, 0.98, 0.99$ and 0.99 respectively). The rates were $0.51 \pm$

0.03, 0.44 ± 0.030 , 0.47 ± 0.041 and 0.43 ± 0.006 pmol. $(10^7 \text{ cells})^{-1}.\text{s}^{-1}$ for *Tbb-s427WT*, *Tbb-5FURes*, *Tbb-s427WT + Tbb-FAD^{o.e}* and *Tbb-5FURes + Tbb-FAD^{o.e}* trypanosomes, respectively (n=1). However, the overexpression of *Tbb-FAD* in *Tbb-s427WT* and *Tbb-5FURes* did not change the rate of uracil uptake in comparison to the parental cell lines (*Tbb-s427 WT* and *Tbb-5FURes*). The addition of 1 mM unlabelled uracil completely inhibited the uptake of [³H]-uracil in all four cell lines. The transport rate of [³H]-uracil in the *Tbb-5FURes* cells was only partly reduced from the wild-type levels, as the measurement has the problem of high background of uracil generated by transport via TbU3.

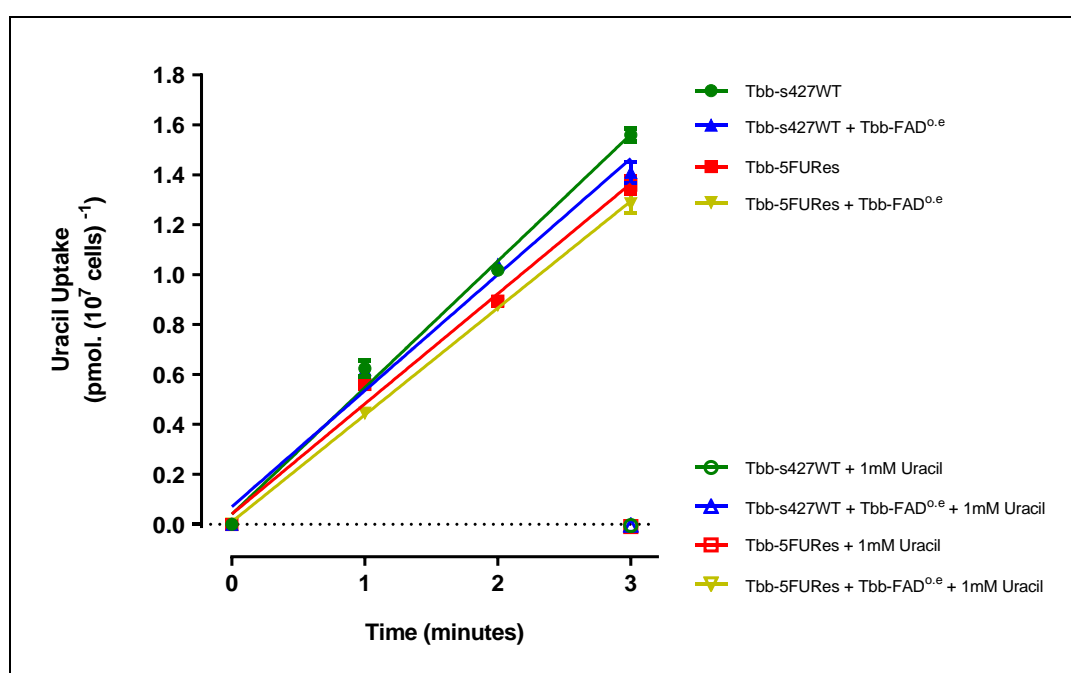


Figure 4.9: Transport of 0.1 μM of [³H]-uracil by *Tbb-s427 WT*, *Tbb-5FURes*, *Tbb-s427WT + Tbb-FAD^{o.e}* and *Tbb-5FURes + Tbb-FAD^{o.e}* was measured over 3 minutes in the presence (open symbols) or absent (closed symbols) of 1 mM unlabelled uracil. Symbols represent the average of triplicate determinations in a single representative experiment, and error bars represent \pm SEM.

4.2.2 Over-expression of *Lmex-FAD* in *Lmex-5FURes* and *L. mexicana*-WT promastigotes

Another gene that acts as a candidate for a determining influence on pyrimidine transport, following an analysis of the differences in the gene expression for the WT and 5-FU resistant line for *L. mexicana* promastigote form by using RNA-seq, is the fatty acid desaturase LmxM.10.1320 (*Lmex-FAD*). The gene exhibited a significant reduction in the transcription level by recording a change of Log₂ fold by -0.32 when comparing the *Lmex-5FURes* strain with *L. mexicana* wild-type (*P*

≤ 0.01) (Alzahrani, 2017). LmxM.10.1320 is located on chromosome 10 where it is known to comprise six transmembrane domains and it is also annotated as a fatty acid desaturase (TritypDB).

4.2.2.1 PCR conformation of plasmid presence of *Lmex-FAD* in *Lmex-5FURes* and *L. mexicana*-WT

The *Lmex-FAD* gene was amplified by PCR from genomic DNA of *L. mexicana* M379 strain by using HDK1344 as forward and HDK1345 reverse primers. The pNUS-HcN plasmid was used to express the *Lmex-FAD* gene in *Lmex-5FURes* and *L. mexicana*-WT. The pNUS-HcN plasmid and the *Lmex-FAD* gene were digested by the *Nde*I and *Bgl*II restriction enzymes and T4 DNA Ligase was used to perform the ligation, generating plasmid pHDK220 (Figure 4.10). The integration of *Lmex-FAD* gene into the pHDK220 was verified by a diagnostic restriction digest with restriction enzymes *Bgl*II and *Nde*I. As shown in Figure 4.11, the *Lmex-FAD* gene is represented by the band at ~1.2 kb, while the empty pHDK220 vector represented a band at ~6.4 kb. Following the transfection of the episomal plasmid pHDK220 into *Lmex-5FURes* and *L. mexicana* WT, PCR was used to verify the presence of pHDK220 in positive clones, using HDK1344 as forward primer for the *Lmex-FAD* gene and HDK340 as reverse primer for the pNUS-HcN plasmid (Figure 4.12).

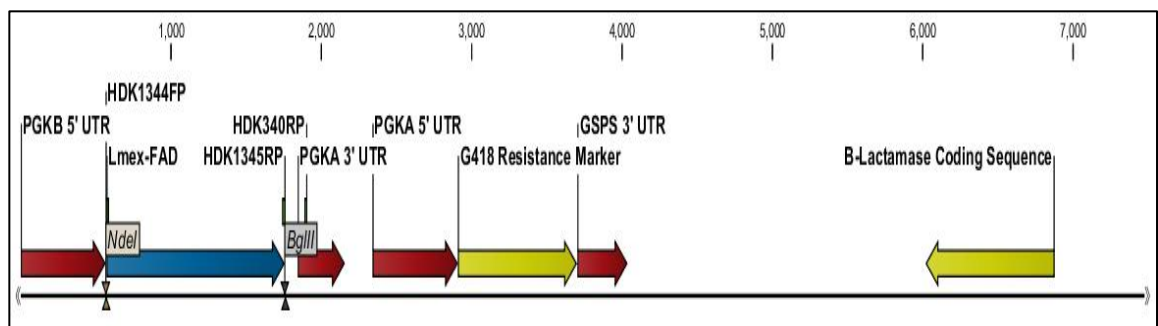


Figure 4.10: Plasmid map of pHDK220 vector for the homologous expression of *Tbb-FAD* gene in *Lmex-5FUR*es and *L. mexicana* WT strains.

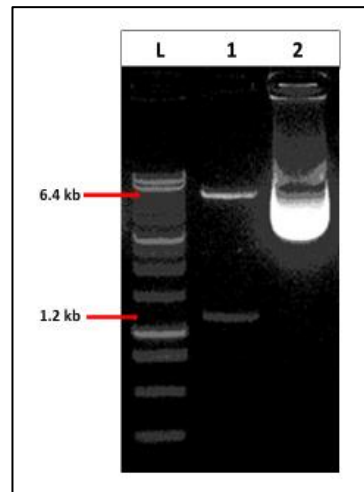


Figure 4.11: Digestion of pHDK220 plasmid by *Nde*I and *Bgl*II restriction enzymes to drop out *Lmex-FAD* gene (1185 bp) from the pHDK220 plasmid.

L: 1 kb DNA ladder (Promega); 1: Digested plasmid (*Nde*I and *Bgl*II); 2: Undigested plasmid.

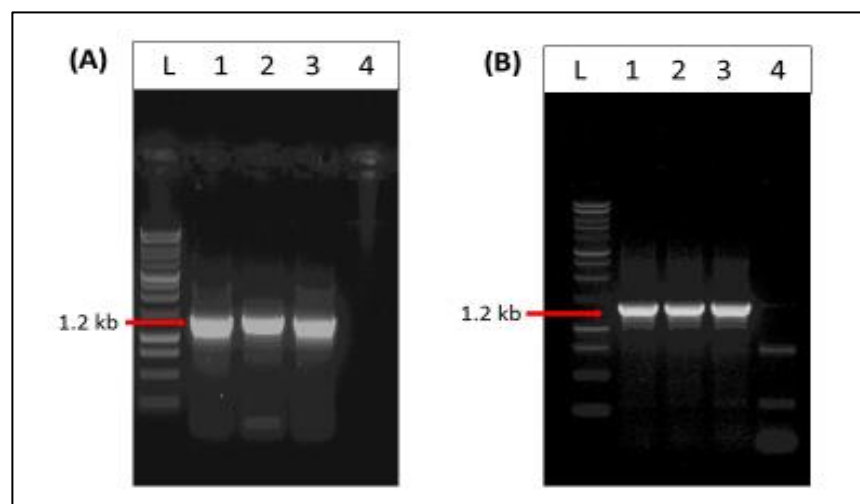


Figure 4. 12: PCR Confirmation of the presence of *Lmex-FAD* gene into *Lmex-5FUR*es and *L. mexicana* WT after transfection.

A) Confirmation of the presence of *Lmex-FAD* gene in the *Lmex-5FUR*es strain after transfection by using HDK1344 as forward primer for *Lmex-FAD* gene and HDK340 as reverse primer for pNUS-HcN plasmid. L: 1kb DNA Ladder (Promega); 1: Clone1; 2: Clone2; 3: Clone3; 4: Non-transfected control (gDNA of *Lmex-5FUR*es strain). B) Confirmation of the presence of *Lmex-FAD* gene in the *L. mexicana*-WT strain after transfection by using HDK1344 as forward primer for *Lmex-FAD* and HDK340 as reverse primer for pNUS-HcN plasmid. L: 1kb DNA Ladder (Promega); 1: Clone1; 2: Clone2; 3: Clone3; 4: Non-transfected control (gDNA of *L. mexicana*-WT strain).

4.2.2.2 Quantitative RT-PCR confirmation of *Lmex-FAD* overexpression in *Lmex-5FUR*es and *L. mexicana*-WT

Following the PCR confirmation of overexpressing of *Lmex-FAD* in *Lmex-5FUR*es and *L. mexicana*-WT, the gene expression level was determined using qRT-PCR. All three clones (1, 2 and 3) of overexpressing of *Lmex-FAD* gene in *Lmex-5FUR*es

significantly increased the mRNA levels compared to the control *Lmex-5FURes* (5.5-fold, 5.5-fold and 3.9-fold; $P < 0.001$, respectively) (Figure 4.13A). Also, the expression levels in *Lmex-WT* + *Lmex-FAD^{o.e}* clone 1, 2 and 3 significantly increased 2.9-fold, 4-fold and 2.9-fold, respectively ($P < 0.001$) compared with the control *L. mexicana*-WT (Figure 4.13B).

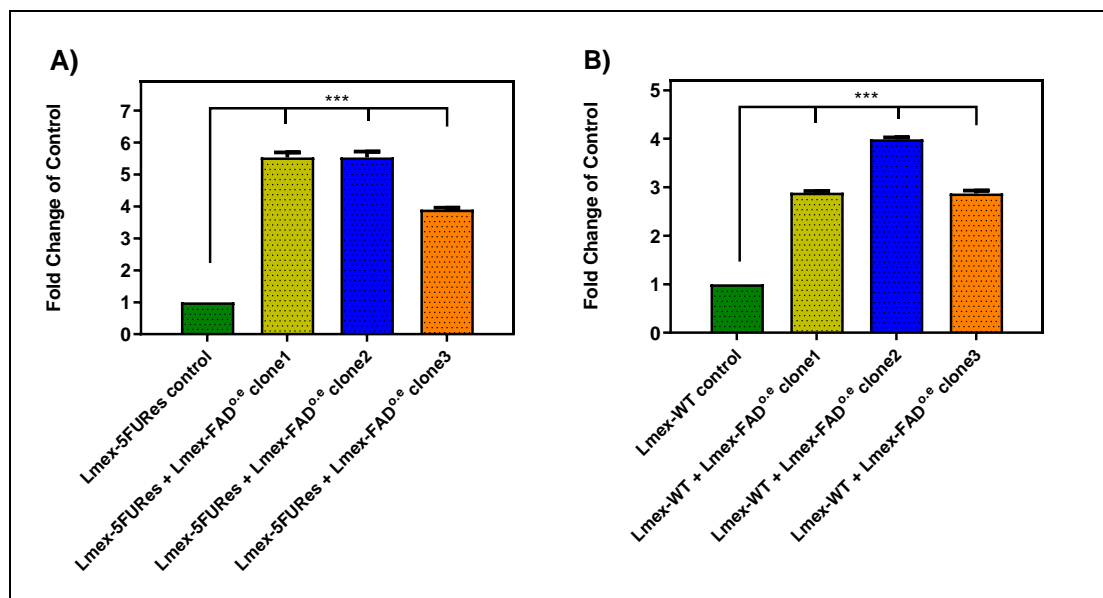


Figure 4.13: The expression levels of *Lmex-FAD* gene in *Lmex-5FURes* and *L. mexicana*-WT. **A)** The expression levels of *Lmex-FAD* gene in *Lmex-5FURes* and compared to the control (*Lmex-5FURes*) determined by qRT-PCR. **B)** The expression levels of *Lmex-FAD* gene in *Lmex-WT* and compared to the control (*L. mexicana*-WT) determined by qRT-PCR. Levels were corrected against the expression level of the housekeeping gene (*L. mexicana* GPI8). The presented results are the average of 4 replicates \pm SEM. *** $P < 0.001$.

4.2.2.3 Drug sensitivity assay with 5-Fluorouracil

As shown in Figure 4.14, the Alamar blue assay was used to help in the assessment of the susceptibility of the *Lmex-FAD* overexpressing *Lmex-5FU* resistant cell line. The results show that the sensitivities of *Lmex-5FURes* and the three *Lmex-FAD^{o.e}* clones in the *Lmex-5FURes* to 5-FU were almost identical to the *Lmex-5FU* resistant cell lines ($n=3$; $P > 0.05$). Additionally, there was no significant difference in the pentamidine EC_{50} values between the overexpressing cell lines and the control cell line ($P > 0.05$).

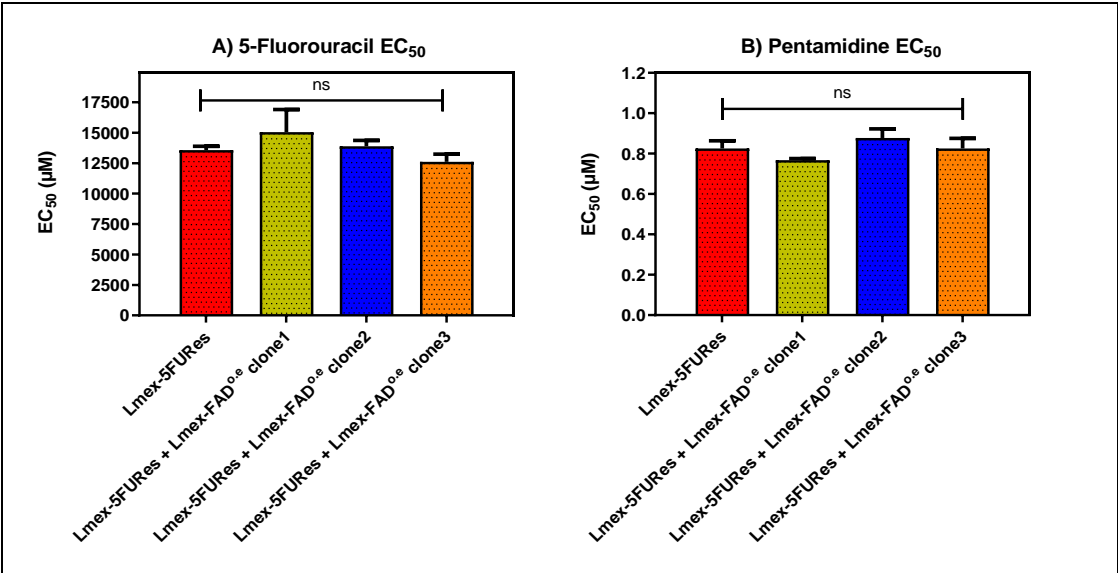


Figure 4.14: Alamar blue drug sensitivity assay for overexpression of *Lmex-FAD* gene in *Lmex-5FURES* clones 1-3 using 5-fluorouracil (A) and pentamidine was used as a positive control (B). The mean of three independent determinations in μM is shown ± SEM. ns = not significant.

In addition, the Alamar blue assay was used also to determine the EC₅₀ values for the overexpressing cell lines (*L. mexicana* WT + *Lmex-FAD*^{oe} clones 1-3) and the parental cell line (*L. mexicana* WT) (Figure 4.15). The result showed that there were no significant differences in the EC₅₀ values for 5-fluorouracil and pentamidine between the overexpressing cell lines and the parental control (n=3; *P* > 0.05).

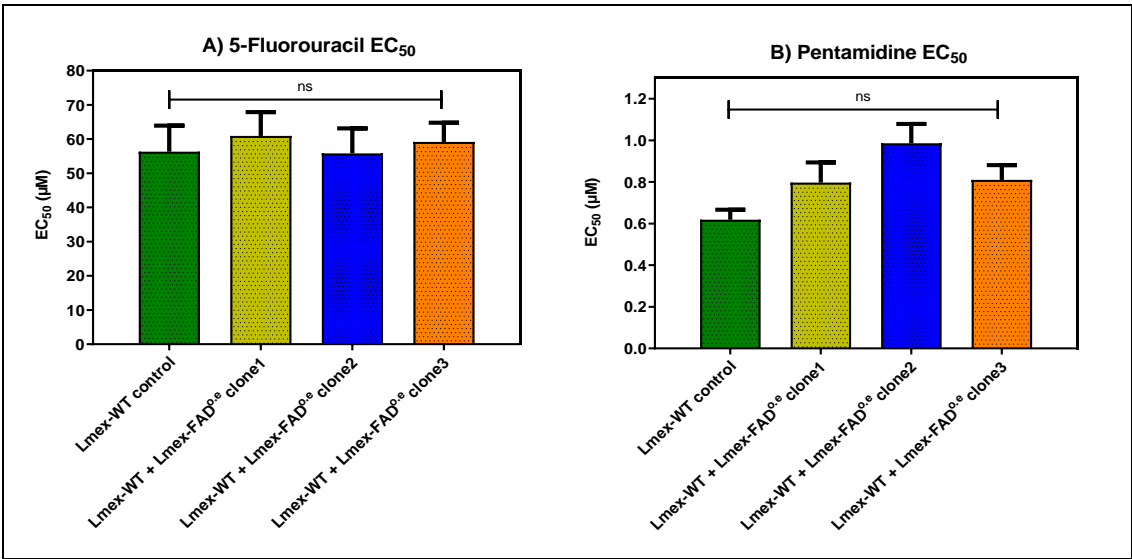


Figure 4.15: Alamar blue drug sensitivity assay of *L. mexicana* wild type and overexpression of *Lmex-FAD* gene in *L. mexicana* WT clones 1-3 using 5-fluorouracil (A) and pentamidine was used as a positive control (B).

The mean of three independent repeats is shown \pm SEM in μ M. ns = not significant.

4.2.2.4 Drug sensitivity assay with amphotericin B and miltefosine

Amphotericin B increases membrane permeability of leishmanial parasites, and miltefosine is has been shown to act by inhibiting lipid biosynthesis of *Leishmania* species (Kovacic and Cooksy, 2012; Canuto et al., 2014), making them excellent control drugs with modes of action that are unrelated to nucleoside transport or nucleoside metabolism. Thus, it is crucial to screen whether over-expression of the FAD gene in *L. mexicana* may cause any alteration in the sensitivity rates of amphotericin B and miltefosine, which would be indicative of a general effect on cellular fitness. Figure 4.16 presents a visual illustration of an evaluation of the sensitivity of the *Lmex-5FURes* and the three *Lmex-FAD^{o.e}* clones in the *Lmex-5FURes* to amphotericin B and miltefosine. The EC₅₀ values of the 5-FU resistant cell lines (*Lmex-5FURes*) to miltefosine significantly increased compared to the wild-type control (*L. mexicana* WT), with an average of $7.1 \pm 0.03 \mu$ M and $3.2 \pm 0.06 \mu$ M respectively. The *Lmex-5FURes* strain was found to have a 2.2-fold resistance to miltefosine when compared with the wild-type control (n=3; $P < 0.0001$). The results of the study identified a significant increase in the sensitivity of *Lmex-5FURes* + *Lmex-FAD^{o.e}* clone 3 to miltefosine ($3.3 \pm 0.15 \mu$ M) in comparison with the *Lmex-5FURes* ($7.1 \pm 0.03 \mu$ M; $P < 0.0001$). Also, the study identified that the sensitivity of *Lmex-5FURes* + *Lmex-FAD^{o.e}* clone 1 and clone 2 to miltefosine record significant difference from the outcomes of the *Lmex-5FURes* ($6.7 \pm 0.04 \mu$ M and $6.2 \pm 0.26 \mu$ M, respectively ($P > 0.05$). The study further identified that the sensitivity of *L. mexicana* WT, *Lmex-5FURes* and *Lmex-5FURes* + *Lmex-FAD^{o.e}* clones 1-3 to amphotericin B did not record any significant differences (n=3; $P > 0.05$).

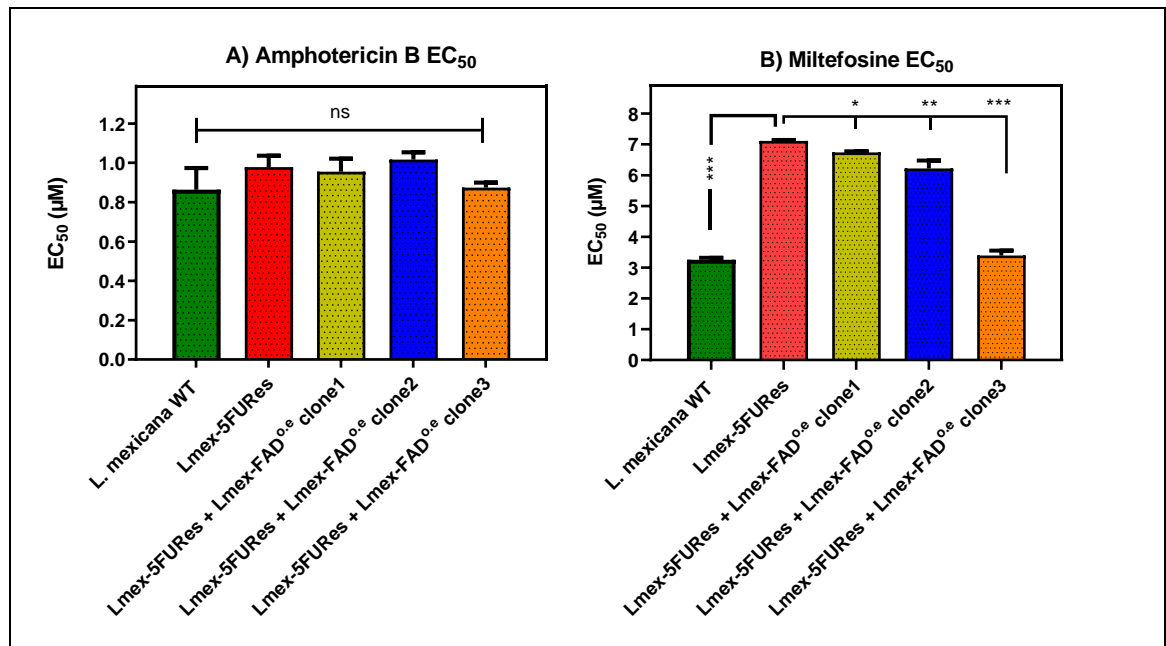


Figure 4.16: The drug sensitivity assay of *Lmex-5FURES* and *Lmex-5FURES + Lmex-FAD* clones 1-3 to Amphotericin B (A) and Miltefosine (B). The mean of three independent determinations in μM is shown \pm SEM. * $P < 0.05$; ** $P < 0.01$; *** $P < 0.001$.

In addition, a comparison was made between the effects of amphotericin B and miltefosine on the *L. mexicana* WT + *Lmex-FAD^{0.e}* clones 1-3 with the *L. mexicana* WT. The comparison is demonstrated in Figure 4.17 where it was identified that there was no significant difference between the EC_{50} values for the clonal lines when compared with the *L. mexicana* WT ($n=3$; $P > 0.05$), with the exception that the EC_{50} of the *Lmex-WT + Lmex-FAD^{0.e} clone 1* to amphotericin B significantly increased compared to the wild-type control (*L. mexicana* WT), with an average $0.75 \pm 0.08 \mu M$ and $1.1 \pm 0.04 \mu M$ ($n=3$; $P < 0.05$) respectively.

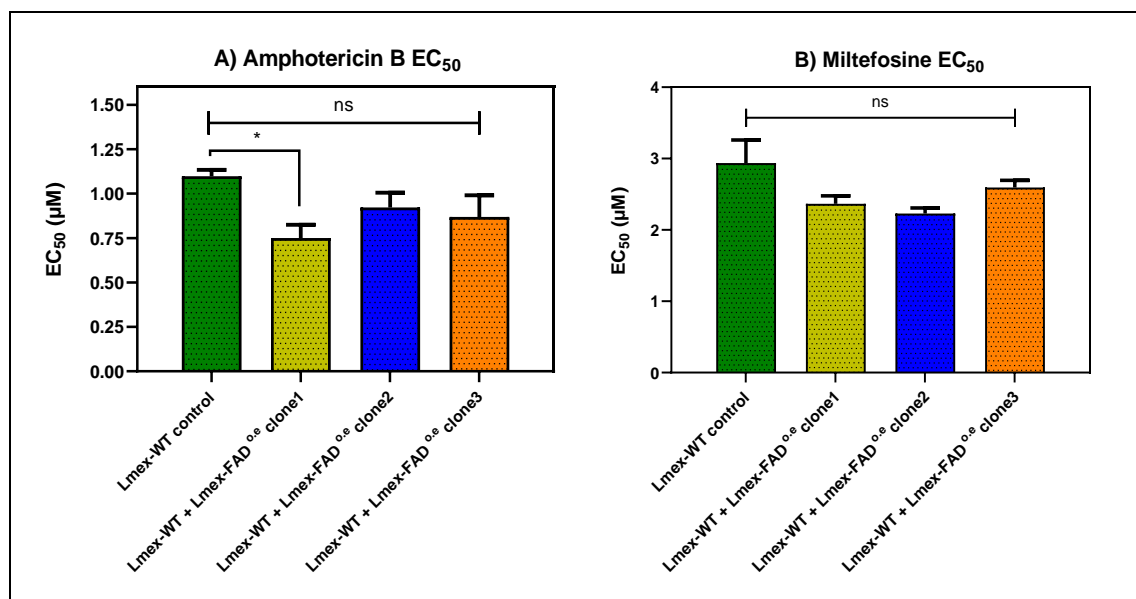


Figure 4.17: The drug sensitivity assay of the *L. mexicana* wild type and *L. mexicana* WT + *Lmex-FAD*^{o.e} clones 1-3 to amphotericin B (A) and Miltefosine (B). The mean of three independent determinations in μM is shown ± SEM. * $P < 0.05$.

4.2.2.5 Uracil transport for overexpression of *Lmex-FAD* in *Lmex-5FUR*es and *L. mexicana*-WT

The transport of 0.1 μM of [³H]-uracil in the *Lmex-5FUR*es and *L. mexicana*-WT expressing *Lmex-FAD* was determined in order to check whether the overexpression of *Lmex-FAD* could cause changes the uracil transport (Figure 4.18). The *L. mexicana*-WT and *Lmex*-WT + *Lmex-FAD*^{o.e} cell lines showed very similar high levels of uptake when incubated with 0.1 μM of [³H]-uracil, with a linear phase of at least eight minutes, (with a rate of 0.051 ± 0.0022 and 0.050 ± 0.0017 pmol.(10⁷ cells)⁻¹.s⁻¹, respectively; n=1). Moreover, the overexpression of *Lmex-FAD* gene in *Lmex-5FUR*es did not change the rate of uracil uptake in comparison to the parental cell line *Lmex-5FUR*es. The addition of 1 mM of unlabelled uracil completely abolished the transport of 0.1 μM of [³H]-uracil in all four cell lines, showing it is saturable.

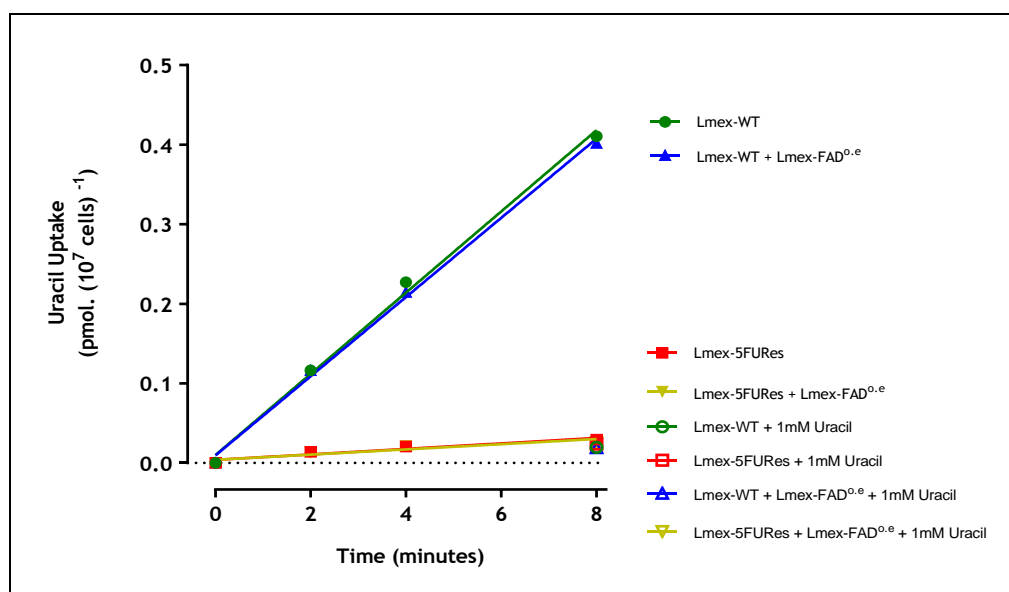


Figure 4.18: Transport of 0.1 μM of [^3H]-uracil by *L. mexicana*-WT, *Lmex-5FURes*, *Lmex-WT* + *Lmex-FAD^{0.e}* and *Lmex-5FURes* + *Lmex-FAD^{0.e}* was measured over 8 minutes in the presence (open symbols) or absent (closed symbols) of 1 mM unlabelled uracil.

Figure shows a representative experiment in triplicate, and error bars represent \pm SEM.

4.3 Discussion

Up to this moment, only ENT genes are identified as encoding purine and pyrimidine transporters in protozoans (De Koning et al., 2005; Campagnaro and de Koning, 2020), however, the involvement of other gene families has been proposed (Bellofatto, 2007; De Koning, 2007; Campagnaro et al., 2018a; Balcazar et al., 2017). A very strong technique for genetic screens for genes to be linked to function and precise phenotypes, where knockdown confers resistant populations, is the genome-wide RNA interference (RNAi) library screen. The first organism utilised in the application of this technique is *T. b. brucei* PCF (Alsford et al., 2012; Chou et al., 2015; Mohr and Perrimon, 2012; Morris et al., 2002). The utilisation of RNAi library screening helped to identify novel trypanosomal drug transporters in the last few years, including TbAQP2 as a determinant of pentamidine sensitivity (Baker et al., 2012; Munday et al., 2014), the aminopurine transporter TbAT1 as the carrier for melarsoprol (Burkard et al., 2011) and amino acid transporter TbAAT6 as the carrier for eflornithine (Baker et al., 2011; Burkard et al., 2011). Consequently, in order to identify the genes contributing to pyrimidine transport in *T. b. brucei* BSF, RNAi library screens in *T. b. brucei* lines exposed to 5-FU and 6-AU were implemented.

Both RNA-seq in (*Trypanosoma brucei* and *Leishmania*) and RIT-seq data revealed fatty acid desaturase (Tbb-FAD) as one of the most prominent hits to be linked to 5-FU resistance in *T. b. brucei* BSF (Ali, 2013; Alzahrani, 2017). We expected that RNAi knockdown of the candidate pyrimidine transporters in *T. b. brucei* cell lines would cause resistance for 5-FU as this could indicate the loss of an influx transporter for 5-FU/uracil in the *T. b. brucei* cells. From RNAi library screening results, it is seen that the downregulation of Tbb-FAD genes bestows a level of resistance to 5-FU/6-AU in 2T1 PYR6-5^{-/-} cells. Moreover, RNA-seq shows that fatty acid desaturase is an interesting hit also connected to 5-FU resistance in *L. mexicana* promastigotes (Alzahrani, 2017). The *T. b. brucei* and *L. mexicana* cells can take up lipids from host environments, and have their own lipid synthesising abilities *de novo* (Smith and Bütikofer, 2010; Zhang and Beverley, 2010).

The results in this chapter show that overexpression of *Tbb-FAD* gene in *Tbb-5FURes* and *T. b. brucei* s427 wild-type does not cause an increase in the sensitivity to 5-FU. Similarly, overexpression of the *Lmex-FAD* gene in *Lmex-5FURes* and *L. mexicana* wild-type had no effect on 5-FU sensitivity via using the Alamar blue assay. Additionally, the uptake rate of [³H]-uracil in *Tbb-5FURes* + *Tbb-FAD*^{0.e} and *Tbb-s427WT* + *Tbb-FAD*^{0.e} was almost identical to the parental cell lines (*Tbb-5FURes* and *Tbb-s427WT*). Likewise, overexpression of *Lmex-FAD* gene into *Lmex-5FURes* and *L. mexicana* wild-type did not increase the transport rate of [³H]-uracil. Therefore, it is still not clear how fatty acid desaturase (*Tbb-FAD* and *Lmex-FAD*) determines sensitivity to pyrimidine nucleobases or transport in *L. mexicana* and *T. b. brucei*. However, while it is clear that the regular expression of the FD gene is not limiting the sensitivity to 5-FU, it appears that a strong reduction in expression may cause resistance. We also recommend tagging *FAD* gene with GFP or Myc and transfecting the tagged genes in *T. brucei* and *L. mexicana*. Then, perform a conventional and fluorescent western blot to assess whether the proteins are expressed and quantify their expression. Fluorescence microscopy showed that putative fatty acid desaturase Tb927.2.3080 is localised in the endoplasmic reticulum of *T. b. brucei* PCF (TrypTag, 2020). Recent research has shown that the gene encoding cytochrome B5-dependent oleate desaturase Tb927.2.3080 is essential for the cell viability of

T. brucei procyclic form. This is because RNAi-mediated downregulation of fatty acid desaturase shows that this gene is essential for *T. brucei* PCF to survive, since the growth defect was noted after induction with tetracycline (Alloatti et al., 2010). In other research, Ali et al. (2013b) and Alzahrani et al. (2017) showed that uracil/5-FU transporters are not essential when it comes to these organisms (*T. b. brucei* and *L. mexicana*) although they are important when it comes to the anti-protozoal activity of 5-FU. A report from Ali et al. (2013a) showed that 5-FU, a substrate for uracil phosphoribosyltransferase (UPRT), is incorporated into precursors for lipid biosynthesis such as UDP-ethanolamine. Thus, it is possible to speculate on the possibility of downregulating fatty acid desaturase by *T. b. brucei* as a way of avoiding 5-FU's deleterious effects.

The overexpression of the *Tbb-FAD* gene in *Tbb-5FURes* and *Lmex-FAD* gene in *Lmex-5FURes* does not re-sensitise the parasites to 5-FU *in vitro*. Although, the over-expression of *Lmex-FAD* gene in *Lmex-5FURes* cells caused significant sensitisation to miltefosine compared to the parental cell line (*Tbb-5FURes*). Therefore, it is still not clear how FAD determines sensitivity to pyrimidine nucleobases or transport in *L. mexicana* and *T. b. brucei*. However, while it is clear that the regular expression of the FAD gene is not limiting the sensitivity to 5-FU, it appears that a strong reduction in expression may cause resistance, hence the observation that overexpression did not change susceptibility to 5-FU, but RNAi-mediated downregulation (RITseq) did. A further study of FAD knockdown phenotypes is thus recommended to understand the functional characterization of *Tbb-FAD* gene in *T. brucei* BSF using the RNAi technique.

5 Heterologous expression of the *Aspergillus nidulans* uracil transporter (FurD) in *T. b. brucei* BSF and *L. mexicana* promastigotes

5.1 Introduction

One of the defining characteristics of a cell is its ability to be selectively permeable. As such, very few molecules can cross the phospholipid bilayer that is the cell membrane. Transportation of most ions, nutrients and metabolites across the cell membrane is facilitated by transporters. Transporters are specialised membrane proteins that move molecules across the cell membrane, often regulated by various signalling pathways. Numerous membrane transporters have been identified in Kinetoplastid protozoa, and their functions include absorption of nutrients, regulation of ion gradients, excretion of metabolites, and transportation of drugs (Majumder, 2008; Kirk and Saliba, 2007; Rodriguez-Contreras et al., 2007; Akpunarlieva and Burchmore, 2017). Uracil transport is known to be an almost ubiquitous cellular activity that is found in cell types from free-living prokaryotes to eukaryote cells (de Koning and Dhalluin, 2000). Highly specific uracil transporters are described in mammalian cells (Baldwin et al., 1999; King et al., 2006). In protozoa, the *L. major* LmajU1 as well as *T. b. brucei* TbU1 and TbU3 transporters have been characterised by their kinetic characterisations, but the genes coding for these transporters have not been parameters (Amillis et al., 2007;; De Koning, 2007; Campagnaro and de Koning, 2020; Bellofatto, 2007), whereas in bacteria, yeasts and fungi multiple uracil transporter genes have been identified (de Koning and Dhalluin, 2000; Andersen et al., 1995; Jund et al., 1977; Stoffer-Bittner et al., 2018; Amillis et al., 2007). Uracil transporter mutants have been identified to be resistant to the toxic uracil analogue 5-fluorouracil in several instances, and have been shown to be deficient in the uptake of radiolabelled uracil (Palmer et al., 1975; Jund et al., 1977; Andersen et al., 1995; Amillis et al., 2007; Stoffer-Bittner et al., 2018). For example, the deletion of the *FurD* gene from *Aspergillus nidulans* has contributed to the phenotype of full resistance to 5-fluorouracil, and completely abolished the uptake of radiolabelled uracil (Amillis et al., 2007).

The *A. nidulans* FurD uracil transporter is classified as Nucleobase-Ascorbate Transporter or Nucleobase Cation Symporter family 2 (NAT/NCS2 family). This group of transporters are active, proton driven transporters specialised in transporting protons and nucleobase. Structurally, FurD consists of twelve transmembrane protein segments (Gournas et al., 2008; de Koning and Dhalluin,

2000; Kryptou et al., 2015). However, BLAST analysis does not identify any *FurD* homologues in any protozoan or metazoan genome databases and the uracil uptake must be mediated by a transporter from a different gene family (De Koning, 2007; Amillis et al., 2007). Although uracil transporters have been identified in other organisms as highlighted in Table 5.1, the degree of *FurD* homology observed for *S. cerevisiae* *Fur4p* (46.2%), *P. larvae* *PIUP* (54.6%) and *E. coli* *UraA* (37.1%) is relatively moderate (Amillis et al., 2007; JUND et al., 1988; Andersen et al., 1995; Stoffer-Bittner et al., 2018). Furthermore, Appendix 7 provides the results for the alignment of *FurD* amino acid sequences in *A. nidulans*, the *UraA* in *E. coli*, the *Fur4p* in *S. cerevisiae* and *PIUP* in *P. Larvae*.

Resistance to 5-fluorouracil was generated in *L. mexicana* promastigotes and *T. b. brucei* s427 BSF, which produced the *Lmex-5FURes* and *Tbb-5FURes* clonal lines, respectively. Uracil and 5-FU transport rates in these cell lines are strongly reduced, particularly in the *L. mexicana* cell lines (Ali et al., 2013a; Alzahrani et al., 2017). For that reason, it is of interest to clone and functionally express *FurD* into the 5-FU resistant cell lines (*Tbb-5FURes* and *Lmex-5FURes*) and *L. mexicana* wild-type in order to investigate whether the sensitivity to 5-FU, or the transport of 5-FU/uracil *in vitro* resistant strains could be restored by the introduction of a confirmed uracil/5-FU transporter. This would allow a functional screening of potential transporter genes. Moreover, it would expand knowledge into the mechanisms used by *T. brucei* and *L. mexicana* to transport pyrimidines. The importance of choosing *FurD* from *A. nidulans* is that the transporters of *FurD* have previously been characterized in detail (Prof George Diallinas Lab, National and Kapodistrian University of Athens, Greece). A study performed by Amillis et al. (2007) showed that the knockout of the *FurD* gene in *A. nidulans* contributed to a full phenotype of resistance to 5-FU and completely reduced uptake of radiolabelled uracil. The *A. nidulans* uracil transporter *FurD* is a confirmed uracil/5-FU transporter.

Table 5.1: The amino acid sequence identity of the *FurD* uracil transporter of *A. nidulans* with uracil transporters in other species.

Name	Accession number	Chromosome	Length (aa)	TMs	% Identity with <i>FurD</i>

FurD ^a	AN11247.3	3	544	12	-
Fur4p ^b	NP_009577.1	2	633	12	46.2%
UraA ^c	X73586.1	-	429	14	37.1%
PIUP ^d	PL1_0655	-	421	12	54.6%

^a *Aspergillus nidulans* uracil transporter; ^b *Saccharomyces cerevisiae* uracil transporter; ^c *Escherichia coli* uracil permease; ^d *Paenibacillus larvae* uracil transporter; aa: amino acids; TMs: transmembrane domains.

5.2 Results

5.2.1 Heterologous expression of FurD in *Tbb-5FURes* BSF

The aim of this section is to functionally express FurD in *Tbb-5FURes* in order to investigate whether the sensitivity/transport to 5-FU *in vitro* could be restored by the introduction of a confirmed uracil/5-FU transporter.

5.2.1.1 PCR confirmation of integration of FurD in *Tbb-5FURes*

A plasmid construct used to express *FurD* genes in *Tbb-5FURes*, pHDK069 (Figure 5.1) had previously been generated by Dr. Jane Munday (Prof Harry de Koning Lab, University of Glasgow). Following transfection of *NotI*-linearized pHDK069 plasmid, based on pH1336 plasmid (Biebinger et al., 1997), into the *Tbb-5FURes* strain, PCR was applied to verify the linearisation of the circular pHDK069 vector and the integration of the *FurD* gene in positive clones. The presence of the expected products (~1.6 kb for the integration, while no band for the linearity of the circular of pHDK69 plasmid) were verified by running the PCR products on 1% of agarose gel to be seen visually under UV light (Figure 5.2).

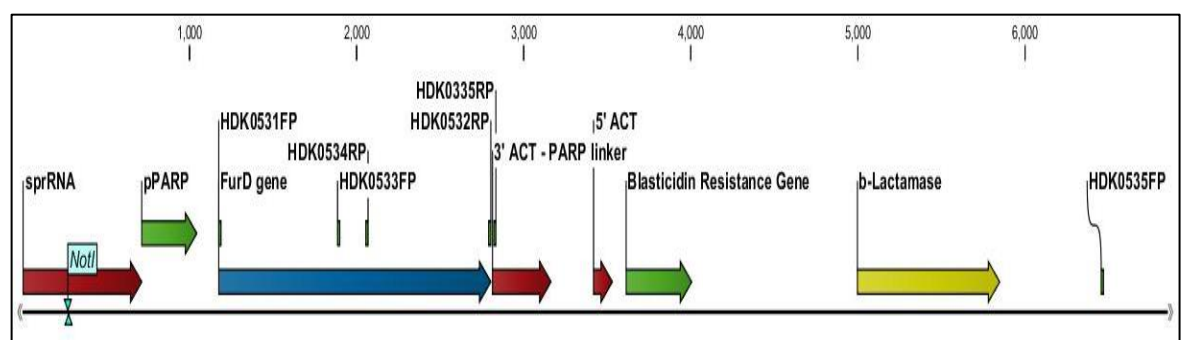


Figure 5.1: Plasmid map of pHDK069 vector for the heterologous expression of *Aspergillus nidulans* uracil transporter gene (*FurD*) in *Tbb-5FURes*.

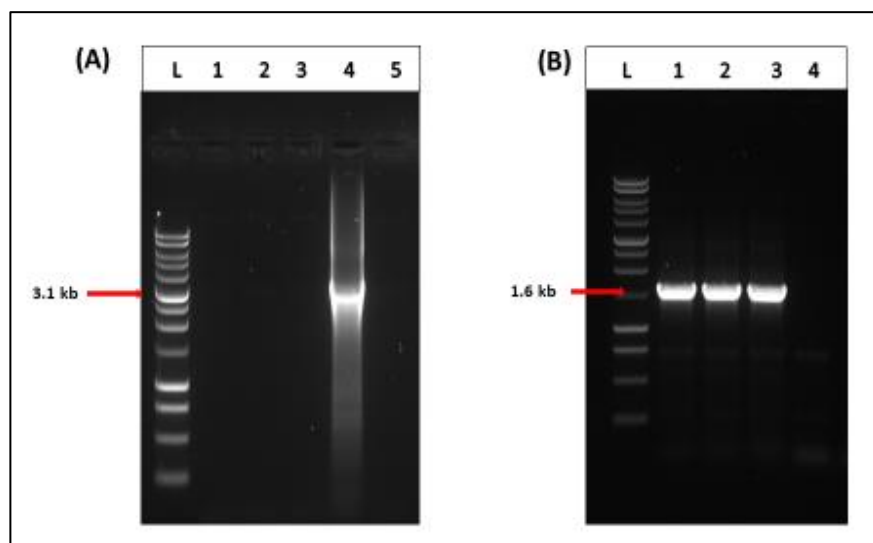


Figure 5.2: PCR confirmation for the linearity of pHDK069 plasmid and the integration of *FurD* gene into *Tbb-5FURes* strain after transfection.

A) Confirmation of the linearisation of pHDK069 vector into *Tbb-5FURes* strain after transfection by using HDK535 as forward primer for the pHDK069 plasmid and HDK532 as reverse primer for *FurD* gene. L: 1kb DNA Ladder (Promega); 1: Clone 1; 2: Clone 2; 3: Clone 3; 4: Undigested pHDK069; 5: Negative control (no DNA). **B)** Confirmation of the integration of *FurD* gene (~1.6 kb) into *Tbb-5FURes* strain after transfection by using HDK531 as forward primer for *FurD* and HDK335 as reverse primer for the pHDK069 plasmid. L: 1kb DNA Ladder (Promega); 1: Clone 1; 2: Clone 2; 3: Clone 3; 4: Non-transfected control (gDNA of *Tbb-5FURes*).

5.2.1.2 Growth rates and qRT-PCR confirmation of expression of *FurD* in *Tbb-5FURes*

The evaluation of the expression levels for *A. nidulans* uracil transporter in *Tbb-5FURes* + *FurD* clones 1-3 was compared with the control *Tbb-5FURes* by the use of qRT-PCR (Figure 5.3). The *FurD* gene in *Tbb-5FURes* + *FurD* clone 1 recorded the highest level of transcript expression (102-fold; $P < 0.001$) compared with the control, although the other two clones also appear to express the gene robustly: 94-fold for clone 2 ($P < 0.001$) and 101-fold for clone3 ($P < 0.001$). However, the quantification of fold-overexpression relative to the control is difficult as the gene was simply not present in the control cell line; either way, the experiment clearly showed the expression of *FurD* in all three clones.

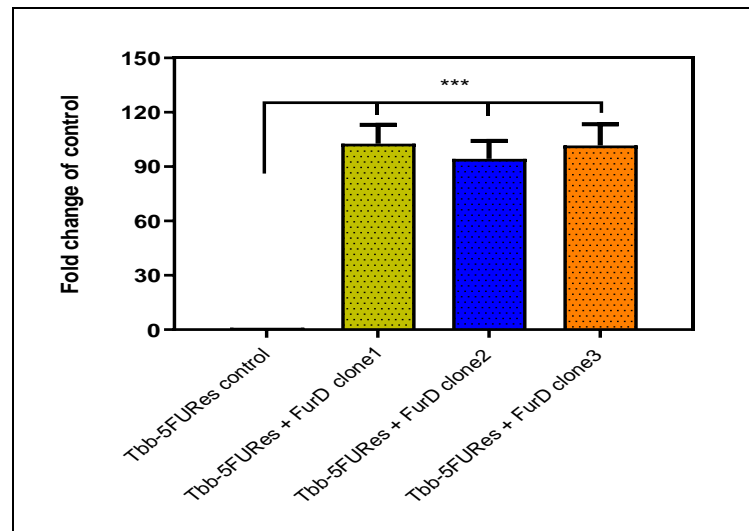


Figure 5.3: The expression levels of *FurD* gene in *Tbb-5FURes* and compared to the control (*Tbb-5FURes*) determined by qRT-PCR.

Levels were corrected against the expression level of the housekeeping gene (*T. b. brucei* GPI8). The presented results are the average of 4 replicates \pm SEM. *** $P < 0.001$ by Unpaired Student's T-test.

An assessment of the growth of *Tbb-5FURes* + *FurD*^{0.e} clones 1-3 and the control *Tbb-5FURes* was done in HMI-9 medium complemented by 10% FBS and incubated at 37 °C under 5% CO₂. The cell density was determined after every 24 h and cells were passaged every 48 hours once the growth has reached between 1.5 and 2 $\times 10^6$ cells/mL. (Figure 5.4). The result of the analysis identified that there was no effect on the growth of the *Tbb-5FURes* + *FurD* clone 1-3 when *FurD* gene was expressed and compared with the control *Tbb-5FURes*.

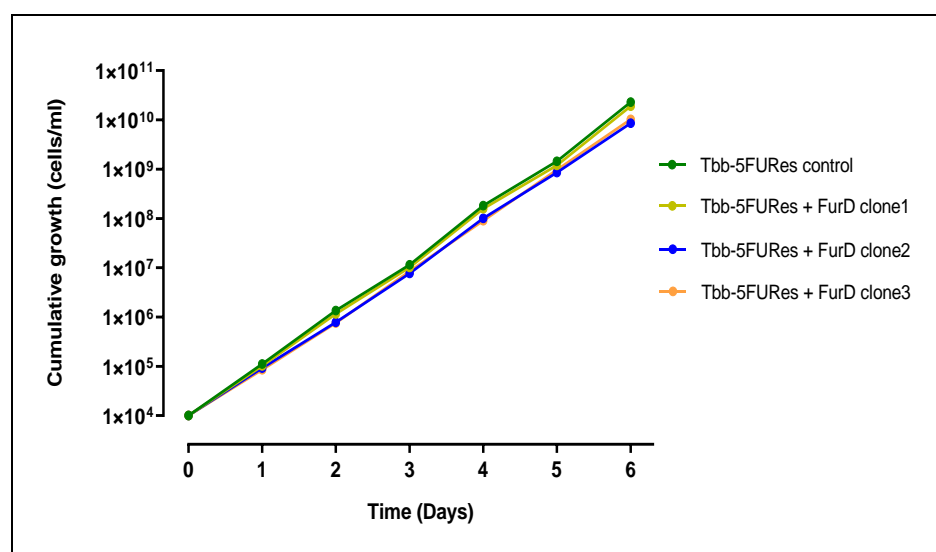


Figure 5.4: The growth curve of *Tbb-5FURes* and *Tbb-5FURes* expressing *FurD* clones 1, 2 and 3 on HMI-9 medium supplemented with 10% FBS.

The cells were seeded at the density of 1x10⁴ cells/mL, and cell densities were determined every 24h. Cells were passaged every 48 hours once the growth had reached between 1.5

and 2×10^6 cells/mL. Each data point in this result represents the mean of two similar independent repeats.

5.2.1.3 Drug sensitivity assay with 5-FU and 6-AU

An investigation into the sensitivity of *Tbb-5FURes* expressing *FurD* gene to 5-FU and 6-AU was conducted and a comparison made with the *Tbb-5FURes* as shown in Figure 5.5. The results showed that 5-FU had an average EC_{50} value of $4130 \pm 200 \mu\text{M}$ against *Tbb-5FURes*, compared to $70 \pm 6 \mu\text{M}$ for *Tbb-s427* WT, a 59-fold resistance ($n=3$; $P < 0.001$). The sensitivities of *Tbb-5FURes* + *FurD* clones 1, 2, and 3 to 5-FU were highly similar to the 5-FU resistant cell line ($P > 0.05$). Interestingly, the *Tbb-5FURes* demonstrated increased sensitivity to 6-AU, an inhibitor of pyrimidine biosynthesis, with an average EC_{50} value of $305 \pm 20 \mu\text{M}$, while *Tbb-s427* WT displayed EC_{50} value of $1849 \pm 86 \mu\text{M}$ (6.1-fold sensitisation to 6-AU; $n=3$; $P < 0.001$). However, there was no significant difference in the 6-AU EC_{50} values between three clones of the *Tbb-5FURes* + *FurD* and the *Tbb-5FURes* control ($P > 0.05$). The increased 6-AU sensitivity in the 5-FURes-based clones appears to indicate the much higher reliance on pyrimidine biosynthesis over salvage pathways. As expected, the analysis did not identify any significant difference in the susceptibility to pentamidine, included as internal control, for any of the strains ($P > 0.05$). The Alamar blue assay result indicated that expressing of *FurD* in *Tbb-5FURes* did not lead to an increase in the sensitivity to 5-FU in *Tbb-5FURes*. It therefore appears that the reduced uptake of 5-FU in 5-FU is likely to be just one of the adaptations to the drug, and reversing it does not significantly restore sensitivity. This hypothesis will need substantial follow-on for verification by using Western immunoblotting and immunofluorescence microscopy to confirm the expression and quantification of *FurD* in *T. b. brucei*.

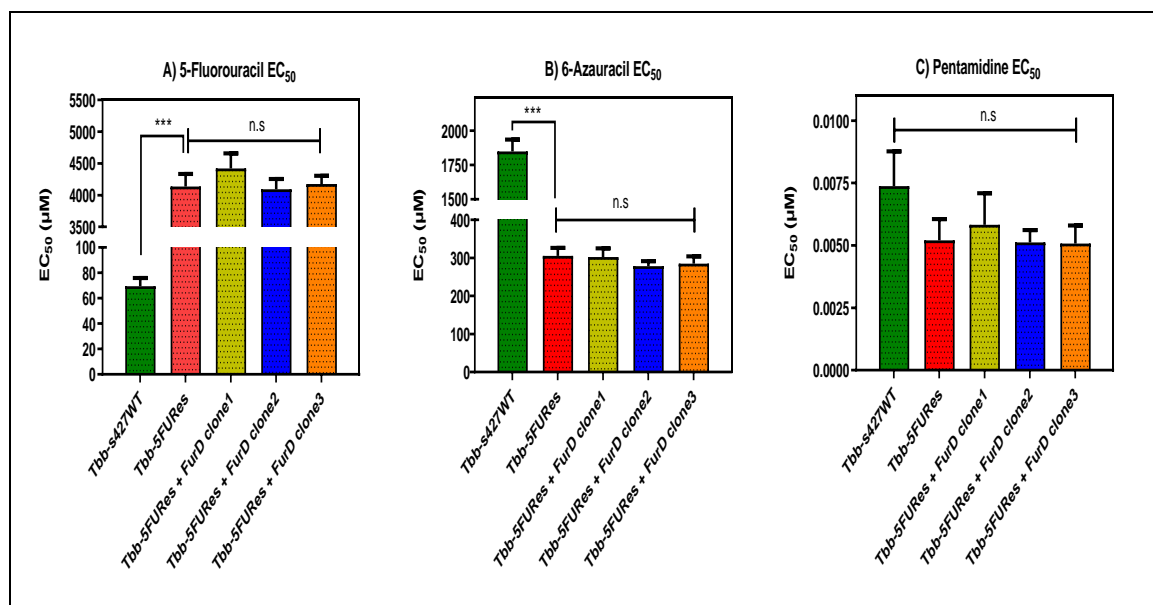


Figure 5.5: Alamar blue drug sensitivity assay of expression of *FurD* gene in *Tbb-5FURes* using 5-fluorouracil (A), 6-azauracil (B) and pentamidine (C). The mean of three independent repeats is shown \pm SEM. *** $P < 0.001$.

5.2.1.4 Uracil transport by *Tbb-5FURes* expressing *FurD*

The rate of transport of 0.1 μM of [³H]-uracil in *Tbb-5FURes* expressing *FurD* was investigated in order to check whether the expression of *FurD* could cause increases in uracil transport (Figure 5.6). [³H]-Uracil uptake was linear for 4 minutes in *Tbb-s427* wild-type (n=4), with a rate of 0.22 ± 0.082 pmol.(10⁷ cells)⁻¹.s⁻¹. When *Tbb-5FURes + FurD* cells were incubated with 0.1 μM of [³H]-uracil, we similarly observed a rate of transport of 0.24 ± 0.11 pmol.(10⁷ cells)⁻¹.s⁻¹ that was linear for at least four minutes (n=4), and was not significantly different from the parental cell lines *Tbb-5FURes*, with a rate of 0.17 ± 0.075 pmol. (10⁷ cells)⁻¹.s⁻¹ (n=4; $P > 0.05$), although the rate of uptake trended higher in cells expressing *FurD*. The addition of 1 mM of unlabelled uracil completely abolished the transport in all cell lines, showing the uptake is saturable. Thus, the expression of *FurD* in *Tbb-5FURes* caused no significant changes in the rate of uracil uptake compared with parental cell lines *Tbb-5FURes*, which was in any case only partly reduced from wild-type levels. When adapting *T. b. brucei* BSF to high levels of 5-FU, the rates of uptake of [³H]-5-FU is decreased by > 22%. A similar experiment using *L. mexicana* promastigotes strongly reduced 5-FU transport (> 98%) in the resistant cell line. It is thus clear that 5-FU resistance in this *T. brucei* cell line is not the (sole) result of reduced uptake of the drug. However, it was previously shown that uracil uptake was much more profoundly

impacted in 5-FU resistant *L. mexicana* (Alzahrani, 2017) and we next investigated whether this phenotype would be reversed by specifically increasing 5-FU transport.

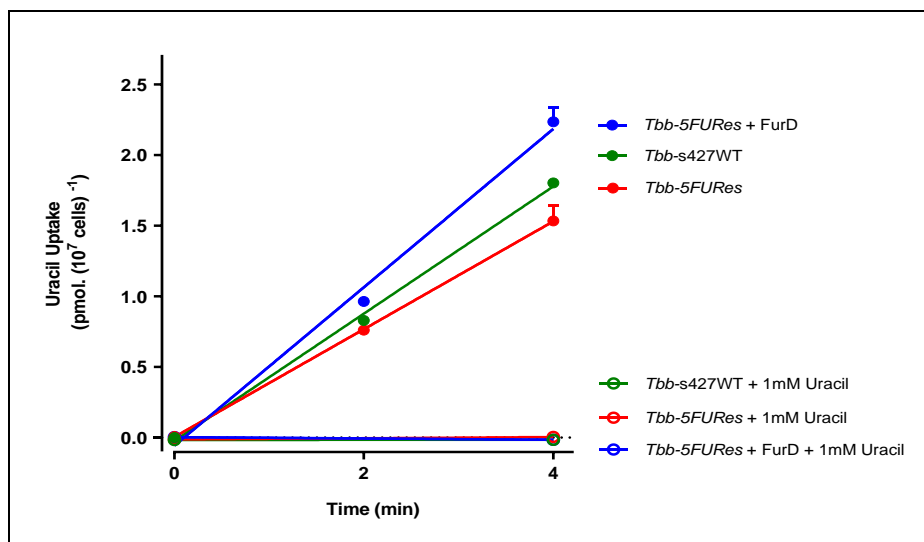


Figure 5.6: [³H]-Uracil transport by *Tbb-s427WT*, *Tbb-5FURes* and *Tbb-5FURes* expressing *FurD*.

Transport of 0.1 μ M of [³H]-uracil by *Tbb-s427WT*, *Tbb-5FURes* and *Tbb-5FURes* + *FurD* was measured over 4 minutes in the presence (open symbols) or absent (closed symbols) of 1 mM unlabelled uracil. Figure shows a representative out of four independent experiments. Symbols represent the average of triplicate determinations and error bars represent \pm SEM. $P > 0.05$ was determined by unpaired Student's T-test.

5.2.2 The heterologous expression of *FurD* in *Lmex-5FURes* promastigotes

The investigations described above have shown that heterologous expression of *FurD* in the *Tbb-5FURes* had no effect on the sensitivity of the cells to 5-FU. In the same way cloning of the *FurD* gene into the *Tbb-5FURes* could not increase the rate of transporting 0.1 μ M of [³H]-uracil significantly, yet it was only a slight reduction of the levels observed in wild types (see section 5.2.1). Hence, the objective of this section is to examine the effects that *Lmex-5FURes* could display towards the sensitivity of 5-FU following a heterologous expression of the *FurD* gene, and the transport of uracil/5-FU after a functional uracil/5-FU transporter is introduced.

5.2.2.1 PCR and qRT-PCR confirmation of the presence of *FurD* in *Lmex-5FURes*

PCR was used to amplify the *FurD* gene from plasmid pHDK069, using primers HDK1427 as forward and HDK1428 as reverse. The pNUS-HcN plasmid was used to express the *FurD* gene in the *Lmex-5FURes* (Tetaud et al., 2002). The *XhoI* and *BglII* restriction enzymes were used to digest the pNUS-HcN plasmid and *FurD* gene; the T4 DNA Ligase was used to ligate the digested *FurD* gene into the digested pNUS-HcN plasmid to generated plasmid pHDK254 (Figure 5.7). The *FurD* integration into pHDK254 was verified by diagnostic digest with *XhoI* and *BglII* restriction enzymes, which resulted in a band of ~6.5 kb for the plasmid, and a band at ~1.6 kb for *FurD* gene (Figure 5.8). After transfection of the pHDK254 plasmid into *Lmex-5FURes*, PCR was used to verify the existence of pHDK254 plasmid in positive clones using forward primer HDK531 for *FurD* gene and HDK340 as reverse primer for pNUS-HcN plasmid sequence (Figure 5.9).

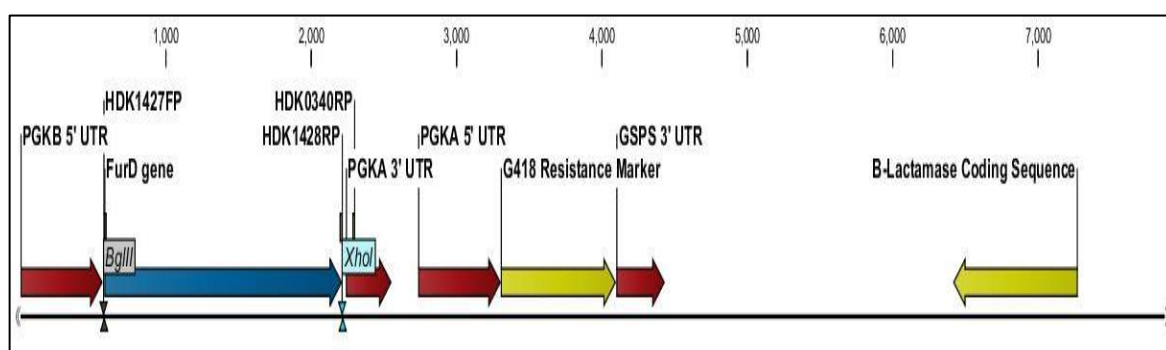


Figure 5.7: Plasmid map of pHDK254 vector for the heterologous expression of *Aspergillus nidulans* uracil transporter *FurD* in *Lmex-5FURes* and *L. mexicana* wild-type.

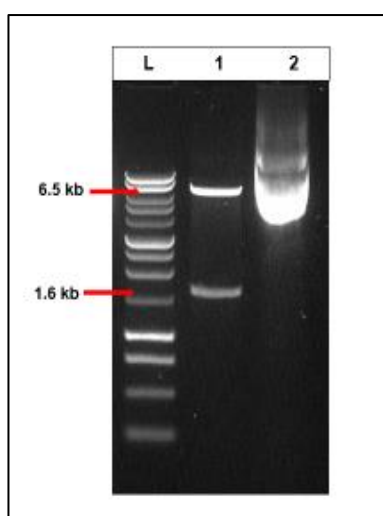


Figure 5.8: Restriction digest products for pHDK254 plasmid with *XhoI* and *BglII* to release *FurD*.

L: 1 kb DNA ladder (Promega); **1:** Digested plasmid by *XhoI* and *BglII* to release *FurD* gene (1635 bp) from pHDK254 (~6.5kb); **2:** Undigested plasmid for pHDK254.

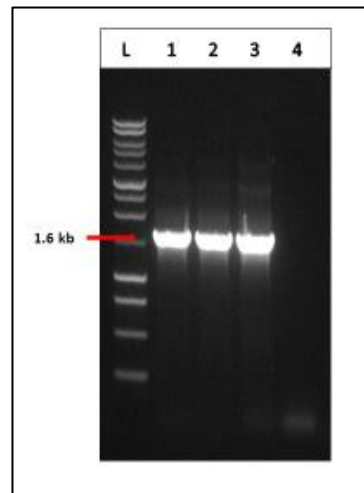


Figure 5.9: Confirmation of the presence of *FurD* gene into *Lmex-5FURes* strain after transfection by using HDK531 as forward primer for *FurD* gene and HDK340 as a reverse primer for pNUS-HcN plasmid.

L: 1kb DNA Ladder (Promega); **1:** Clone1; **2:** Clone2; **3:** Clone3; **4:** Non-transfected control (genomic DNA of *Lmex-5FURes*).

qRT-PCR was used to examine the level of expression for the *FurD* gene in *Lmex-5FURes* after cloning and the results were compared with those of the control lines of *Lmex-5FURes* as highlighted in Figure 5.10. Notably the results confirmed that the *Tbb-5FURes* + *FurD* clone 1 was at 30-fold ($P < 0.001$), while the results in *Tbb-5FURes* + *FurD* clone 3 increased to 69-fold ($P < 0.001$) in relation to the control cell lines, but *Tbb-5FURes* + *FurD* clone 2 recorded the highest expression level, amounting to a 232-fold increase ($P < 0.001$) compared to the control cell lines. Besides, there is a possibility of speculating the differences in expression levels of the cell lines reflected by the numbers of episomal plasmid pHDK254 that located in the genome of *Tbb-5FURes* parasites.

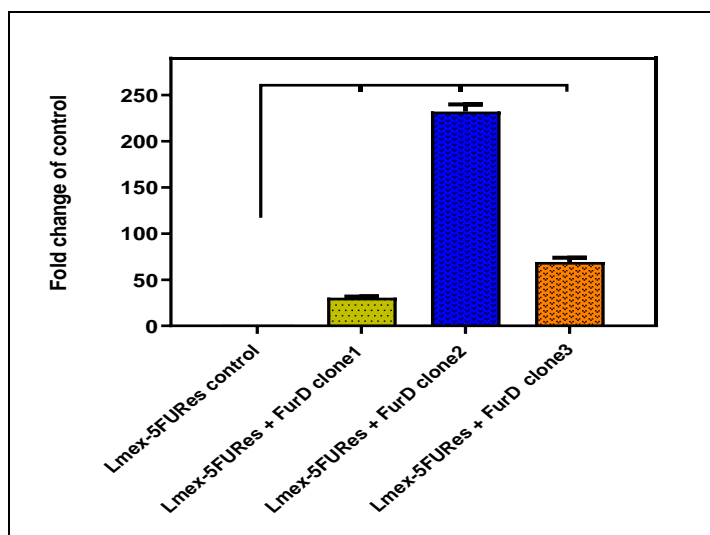


Figure 5.10: The expression levels of *FurD* gene in *Lmex-5FURes* and compared to the control (*Lmex-5FURes*) determined by qRT-PCR. Levels were corrected against the expression level of the housekeeping gene (*L. mexicana* GPI8). The presented results are the average of 4 replicates \pm SEM. *** $P < 0.001$ by unpaired Student's T-test.

5.2.2.2 Drug sensitivity assay with 5-FU and 6-AU

We investigated whether the expression of *FurD* in the *Lmex-5FURes* changed the sensitivity to 5-FU and 6-AU *in vitro*. This was assessed and compared with the *Lmex-5FURes* as shown in Figure 5.11, but no significant differences in the EC_{50} values against 5-FU were observed for the three *Lmex-5FURes* + *FurD* clones ($P > 0.05$). The results showed that 5-FU had an average EC_{50} value of 14 ± 0.45 mM against *Lmex-5FURes*, while *L. mexicana* WT displayed EC_{50} value amounting to 50 ± 9 μ M, a 284-fold resistance to 5-FU ($n=3$; $P < 0.001$). The sensitivities of *Lmex-5FURes* + *FurD* clones 1, 2, and 3 to 6-AU were highly similar to those of the 5-FU resistant cell line ($P > 0.05$). In addition, there were no significant differences in the EC_{50} values of pentamidine between the expressing cell lines and the control ($P > 0.05$). The EC_{50} values indicated that expressing of *FurD* in *Lmex-5FURes* did not lead to decreasing the EC_{50} value of 5-FU.

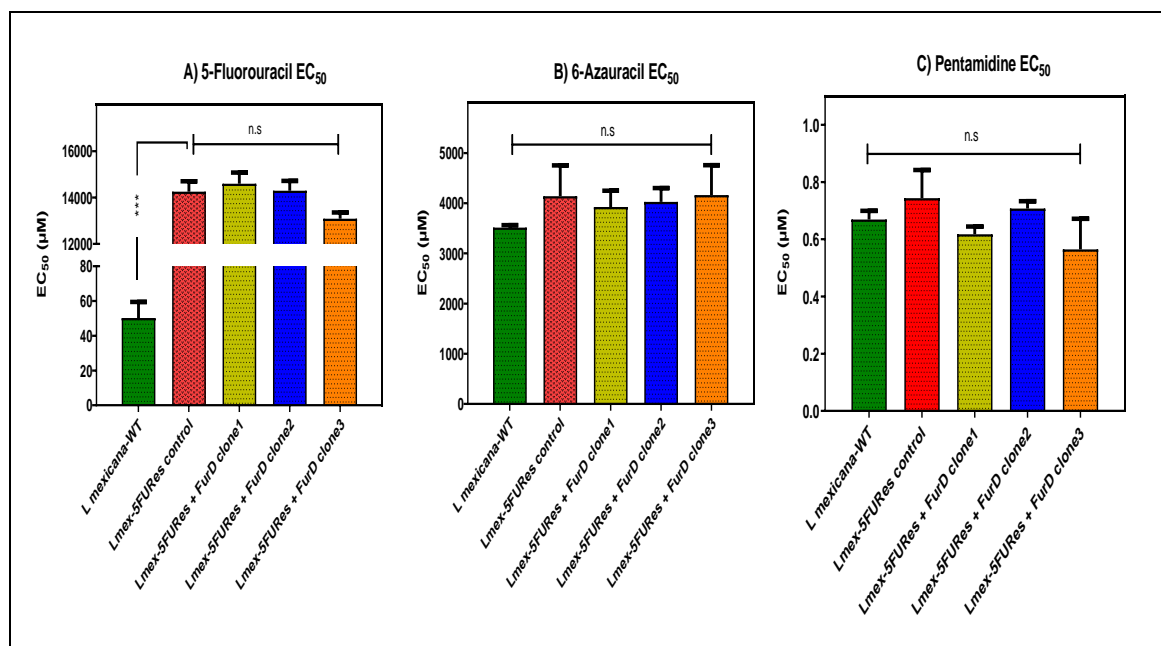


Figure 5.11: Alamar blue drug sensitivity assay of expression of *FurD* gene in *Lmex-5FURes* by using 5-fluorouracil (A), 6-azauracil (B) and pentamidine (C). The mean of three independent determinations is shown \pm SEM. * $P < 0.001$.**

5.2.2.3 Transport assay with uracil and 5-FU, and kinetic characterisation of FurD transporter

The results for *Lmex-5FURes* were significantly different from those observed in the *Tbb-5FURes* (Figure 5-6). As such, there appeared to be a completely loss of function of the LmexU1 as the rate of transportation of radiolabeled uracil was reduced by approximately 95% (Figure 5.12). The transport rate decreased from 0.068 ± 0.004 pmol. $(10^7$ cells) $^{-1}$.s $^{-1}$ to 0.009 ± 0.0002 pmol. $(10^7$ cells) $^{-1}$.s $^{-1}$, which made the *Lmex-5FURes* a more suitable expression system for the heterologous expression of the FurD transporter than *Tbb-5FURes*. A previous report indicated the rate of uptake of [3 H]-5FU *L. mexicana* promastigotes almost completely abolished 5-FU transport in the resistant cell lines (Alzahrani et al., 2017). Besides, the presence of TbU3 in *Tbb-5FURes* cells made it difficult to use *Tbb-5FURes* cells as expression system due to the high background of uracil transport (Ali et al., 2013a); there is no known equivalent of TbU3 in *L. mexicana*.

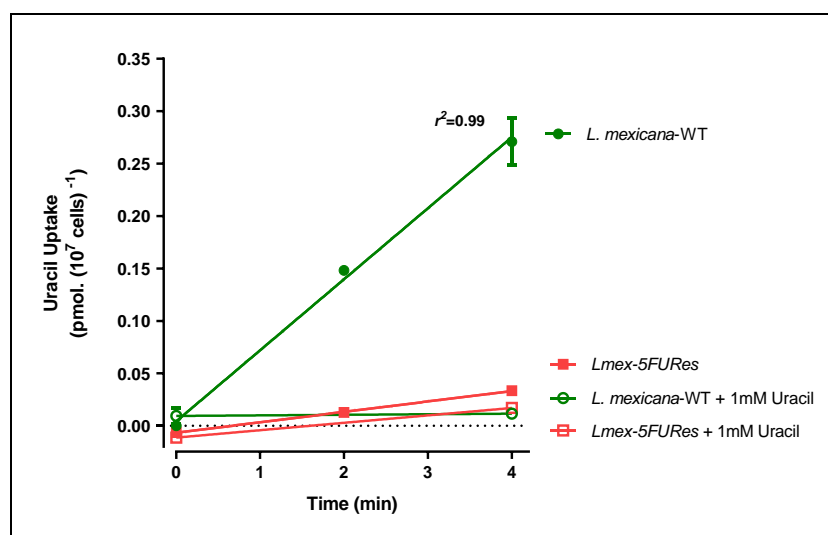


Figure 5.12: Radiolabelled uracil transport by *L. mexicana*-WT and *Lmex*-5FURes. Transport of 0.1 μM of [^3H]-uracil by *L. mexicana*-WT and *Lmex*-5FURes was measured over 4 minutes in the presence (open symbols) or absent (closed symbols) of 1 mM unlabelled uracil. Figure shows one representative experiment and error bars are \pm SEM of triplicate determinations.

Subsequent experiments were performed using 0.1 μM of [^3H]-uracil and [^3H]-5-fluorouracil to assess the transport rate of uracil and 5-FU in *Lmex*-5FURes expressing FurD in parallel with their 5-FU resistant cell line counterparts (Figure 5.13A and B). Indeed, the heterologous expression of FurD in *Lmex*-5FURes revealed a very high level of [^3H]-uracil transport, with a rate of uptake of $0.21 \pm 0.027 \text{ pmol. (10}^7 \text{ cells)}^{-1} \cdot \text{s}^{-1}$ and a linear phase over 45 seconds ($r^2=0.97$; Figure 5.13A). The addition of 1 mM of unlabelled uracil completely abolished the transport, showing that the uptake via FurD is saturable. The uptake rate of 0.1 μM [^3H]-5-fluorouracil over 20 seconds, in the presence or absence of 1 mM unlabelled 5-fluorouracil. However, under these conditions, the uptake of 0.1 μM of [^3H]-5-fluorouracil was much more quickly equilibrated than [^3H]-uracil, resulting in a non-linear rate of uptake after 10 seconds (Figure 5.13, blue dashed line), presumably because uracil is metabolised at a much higher rate than its fluorinated analogue. The heterologous expression of FurD in *Lmex*-5FURes revealed a very high level of [^3H]-5-fluorouracil uptake, with a rate of uptake of $0.14 \pm 0.008 \text{ pmol. (10}^7 \text{ cells)}^{-1} \cdot \text{s}^{-1}$ and a linear phase over 10 seconds (solid blue line; $r^2=0.99$; Figure 3.13B); in both strains [^3H]-5-fluorouracil transport was completely inhibited in the presence of 1 mM unlabelled fluorouracil. This result very much confirmed that uracil and 5-FU share the same transporter FurD, as transport of both substrates was very strongly increased upon expression of this carrier.

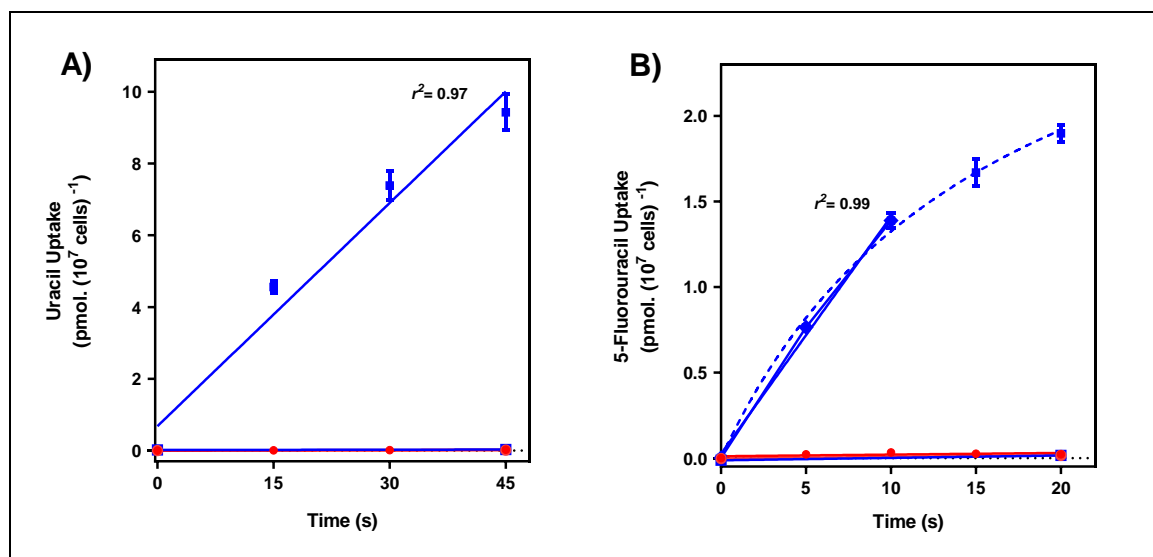


Figure 5.13: [³H]-Uracil and [³H]-5-Fluorouracil transport by *Lmex-5FURes* and *Lmex-5FURes* expressing *FurD*.

A) Transport of 0.1 μ M of [³H]-uracil by *Lmex-5FURes* (●) and *Lmex-5FURes* + *FurD* (■) was measured over 45 seconds in the presence or absent of 1 mM unlabelled uracil (○) and (□) respectively. **B)** Transport of 0.1 μ M of [³H]-5-fluorouracil by *Lmex-5FURes* (●) and *Lmex-5FURes* + *FurD* (■) was measured over 20 seconds in the presence or absent of 1 mM unlabelled 5-fluorouracil (○) and (□) respectively. The blue dashed line is showing the rate of uptake using a non-linear regression analysis (saturation plot). Symbols represent the average of triplicate determinations in a single representative experiment and error bars represent \pm SEM.

The transport of 0.1 μ M of [³H]-uracil was also investigated in *Lmex-5FURes* expressing *FurD* using longer incubations (Figure 5.14A). The result showed that the rate of 0.1 μ M of [³H]-uracil uptake in *Lmex-5FURes* + *FurD* became non-linear after 5 minutes (dashed green line). The linear phase of uptake (blue line), showed a rate of 2.1 ± 0.17 pmol.(10⁷ cells)⁻¹.s⁻¹ ($r^2=0.97$). The addition of 1 mM unlabelled uracil completely inhibited the *FurD* transporter. The uptake assay with 0.1 μ M of [³H]- 5-fluorouracil was also performed using longer incubations, which presented a non-linear uptake after 10 seconds (dashed green line), with a rate of 0.39 ± 0.04 pmol.(10⁷ cells)⁻¹.s⁻¹ ($r^2=0.98$) over the 9 seconds of the linear phase of uptake (blue line); the *FurD* transporter was completely inhibited by 1 mM unlabelled 5-fluorouracil (Figure 5.14B), showing that uracil and 5-fluorouracil uptake are mediated by a saturable transporter rather than by simple diffusion. These findings show very clearly that uracil and 5-fluorouracil is highly concentrated in *Lmex-5FURes* cells expressing *FurD*, but this saturates in less than 5 minutes and 9 seconds, respectively.

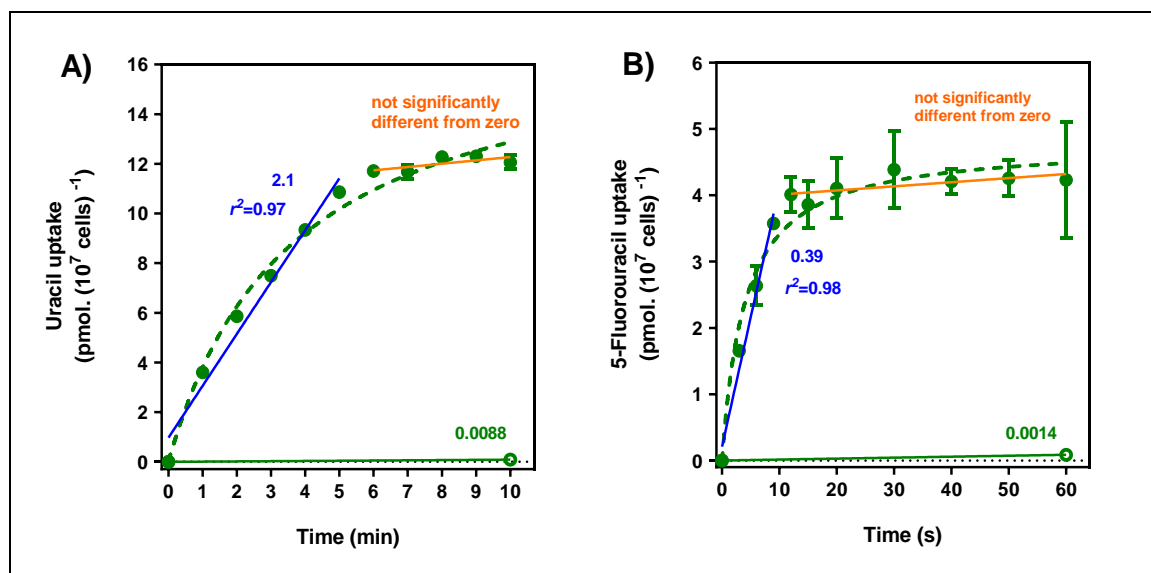


Figure 5.14: [³H]-Uracil and [³H]-5-Fluorouracil transport by *Lmex-5FURes* expressing FurD over 10 minutes and 60 seconds, respectively.

A) Transport of 0.1 μM of [³H]-Uracil by *Lmex-5FURes* + FurD (●) was measured over minutes in the presence (open symbols) or absent (closed symbols) of 1 mM unlabelled uracil (○). **B)** Transport of 0.1 μM of [³H]- 5-fluorouracil by *Lmex-5FURes* + FurD (●) was measured over 60 seconds in the presence (open symbols) or absent (closed symbols) of 1 mM unlabelled 5-fluorouracil (○). Symbols represent the average of triplicate determinations in a single representative experiment and error bars represent ± SEM.

Subsequent transport assays were performed using 0.1 μM of [³H]-uracil and incubations for 10 seconds as our time point - within the linear phase - in order to characterise uracil uptake in *Lmex-5FURes* expressing FurD. Figure 5.15A shows representative inhibition curves for the inhibition of 0.1 μM of [³H]-uracil transport by unlabelled uracil and 5-fluorouracil. Uracil and 5-fluorouracil were stronger inhibitors and, calculated from the Michaelis-Menten saturation plots (in competition with 0.1 μM of [³H]-uracil) (Figure 5.15B), an average K_m value of 0.97 ± 0.16 μM and V_{max} of 3.89 ± 0.25 pmol.(10⁷ cells)⁻¹.s⁻¹ for uracil (n=3) was calculated. This compared to a K_i value of 0.75 ± 0.24 (n=3) for 5-fluorouracil. Thus, FurD is a highly selective and high-affinity transporter for uracil and 5-fluorouracil when expressed in *Lmex-5FURes*.

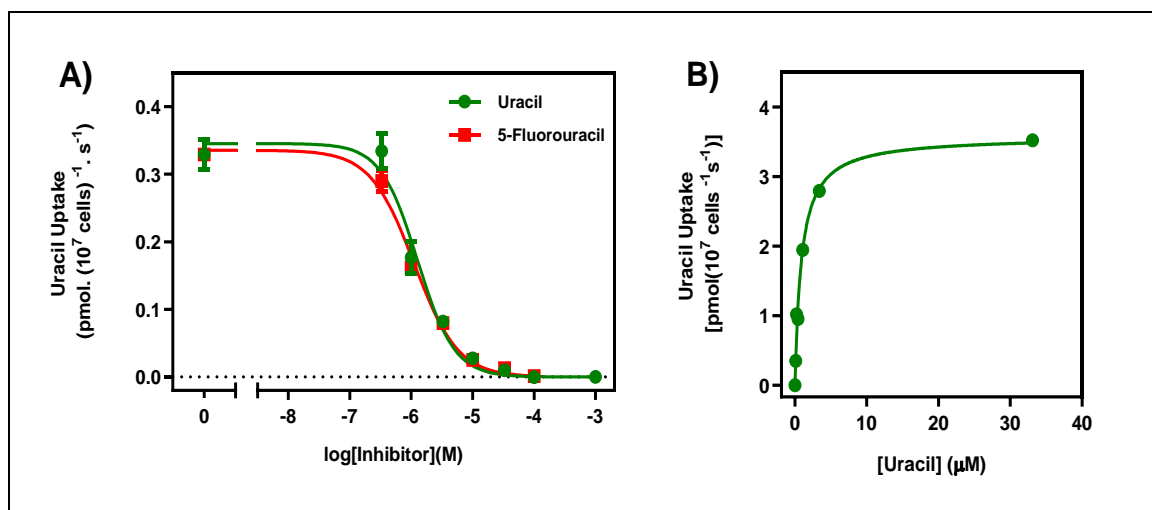


Figure 5.15: Inhibition of 0.1 μM of $[^3\text{H}]$ -uracil over 10 seconds.

A) Inhibition of 0.1 μM of $[^3\text{H}]$ -uracil over 10 seconds by various concentrations of unlabelled uracil (\bullet) and unlabelled 5-fluorouracil (\blacksquare). B) The latter inhibition curve was also converted to a Michaelis-Menten saturation curve. Figure shows a representative out of three independent experiments in triplicates. Symbols represent the average of triplicate determinations in a single representative experiment and error bars represent \pm SEM.

The data from the FurD inhibition profiles is listed in Table 5.2, which highlights that the average K_i value for 5-fluorouracil inhibition of uracil transport was almost identical to the average of K_m value for uracil uptake ($n=3$). Interestingly, the interaction of uracil and 5-fluorouracil with FurD led to a very similar Gibbs free energy (ΔG^0) of association: -34.3 and -35.1 kJ/mol, respectively. Thus, the anticancer drug 5-fluorouracil was as good a substrate as uracil for FurD transporter. These results are consistent with the previous characterisations of this transporter in *A. nidulans*, showing that FurD has very high-affinity for uracil (K_m of 0.45 μM) and 5-fluorouracil (K_i of 0.46 μM) (Amillis et al., 2007).

Table 5.2: Transport of uracil in *Lmex-5FUR*es expressing *Aspergillus nidulans* FurD. V_{max} , K_m and K_i values represent the mean of three independent determination in triplicates \pm SEM. Gibbs free energy of substrate-transporter interactions were calculated from the K_m and K_i .

<i>Lmex-5FUR</i> es expressing <i>Aspergillus nidulans</i> FurD				
Radiolabel $[^3\text{H}]$ -Uracil		ΔG^0	$\delta(\Delta G^0)$	n
K_m (μM)	0.971 ± 0.166	-34.3	--	3
V_{max} pmol. (10^7 cells) $^{-1}$.s $^{-1}$	3.897 ± 0.251	--	--	3
Inhibitors (K_i μM)				
5-Fluorouracil	0.758 ± 0.249	-35.1	-0.8	3

5.2.3 The heterologous expression of *FurD* in *L. mexicana* WT promastigotes

Above, it was confirmed that the heterologous expression of *FurD* gene in *Lmex-5FURes* could not increase the sensitivity of the cells to 5-FU; although, it led to increased transportation of radiolabeled uracil and 5-FU to levels exceeding the wild-type activity (see section 5.2.2). Thus, the purpose of this section was to provide further detailed information on the sensitivity/transport to 5-FU in wild-type *L. mexicana* promastigotes expressing *FurD*.

5.2.3.1 PCR and qRT-PCR confirmation of the existence of *FurD* in *L. mexicana* WT

A plasmid construct used to express *FurD* gene in *L. mexicana* WT, pHDK254 (Figure 5.7) had been used previously for the heterologous expression of *FurD* in *Lmex-5FURes*. Following transfection of this episomal plasmid pHDK254, which was based on the pNUS-HcN plasmid, into the *L. mexicana* WT strain, PCR was applied to verify the existence of pHDK254 in positive clones, using HDK531 as forward primer for the *FurD* gene and HDK340 as reverse primer for the pNUS-HcN plasmid (Figure 5.16). Quantitative real time PCR was performed to quantify the levels of *FurD* gene expression in *L. mexicana* WT cells compared to that in the control. All three clones 1, 2 and 3 of expressing of *FurD* gene in *L. mexicana* wild-type significantly increased the mRNA levels compared to the control *L. mexicana* WT (27-fold, 50-fold and 25-fold; $P < 0.001$, respectively) (Figure 5.17).

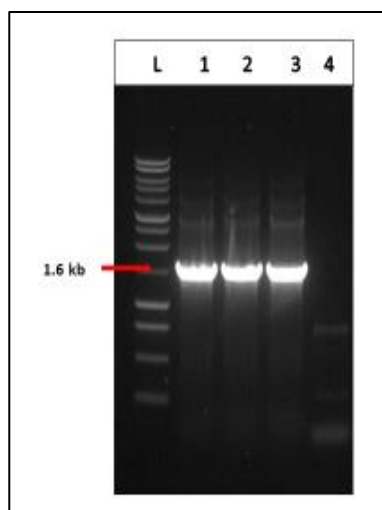


Figure 5.16: Confirmation of the presence of *FurD* gene into *L. mexicana*-WT strain after transfection by using HDK531 as forward primer for *FurD* gene and HDK340 as a reverse primer for pNUS-HcN plasmid.

L: 1kb DNA Ladder (Promega); 1: Clone1; 2: Clone2; 3: Clone3; 4: Non-transfected control (genomic DNA of *L. mexicana*-WT).

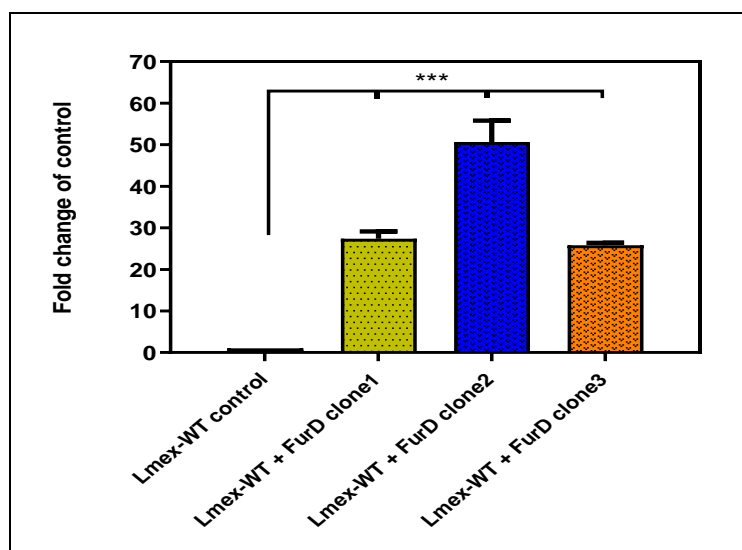


Figure 5.17: The expression levels of *FurD* gene in *L. mexicana*-WT and compared to the control (*L. mexicana*-WT) determined by qRT-PCR.

Levels were corrected against the expression level of the housekeeping gene (*L. mexicana* GPI8). The presented results are the average of 4 replicates \pm SEM. *** $P < 0.001$ by Unpaired Student's T-test.

5.2.3.2 Drug sensitivity assay with 5-FU and 6-AU

The sensitivity of the *L. mexicana* wild-type and the three *FurD* clones in the *L. mexicana*-WT parasites to 5-FU and 6-AU was investigated using the usual Alamar blue assay (Figure 5.18). Expression of *FurD* gene did not lead to increasing or decreasing the sensitivity to 5-FU or 6-AU in *L. mexicana* wild-type expressing *FurD*, as the EC_{50} values of *Lmex-5FURes* and three clones for *Lmex-5FURes* + *FurD* were almost the same ($n=3$; $P > 0.05$). In addition, there were no significant differences in the EC_{50} values of pentamidine between the expressing cell lines and the control ($P > 0.05$).

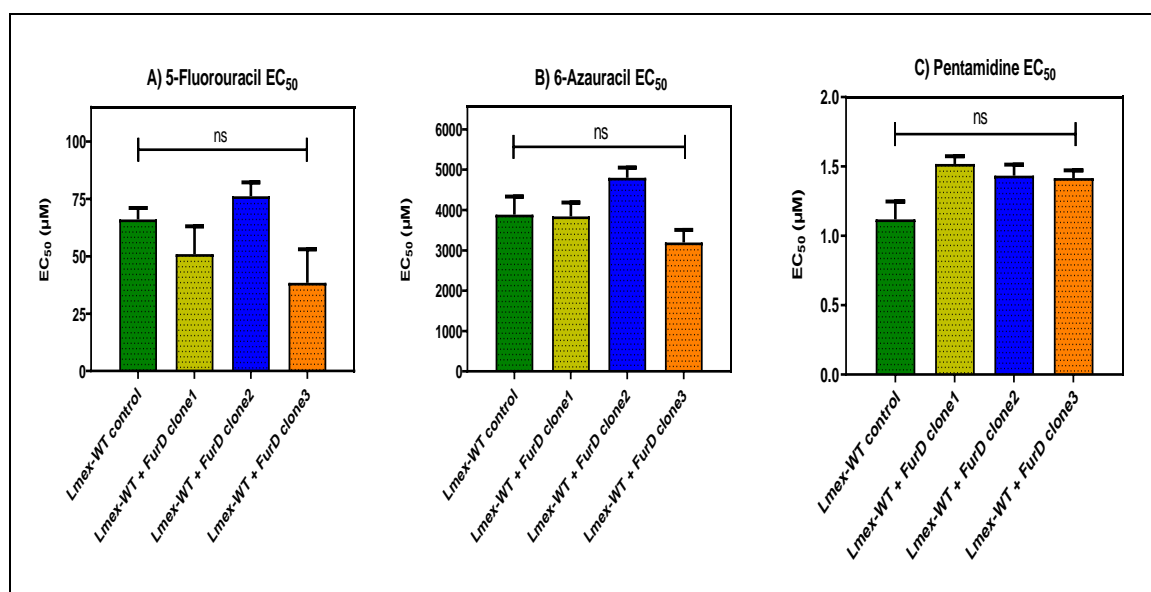


Figure 5.18: Alamar blue drug sensitivity assay of expression of *FurD* gene in *L. mexicana*-WT by using 5-fluorouracil (A), 6-azauracil (B) and pentamidine (C). The mean of three independent determinations is shown \pm SEM.

5.2.3.3 Transport assay with 5-Fluorouracil

The uptake rate of 0.1 μ M of [³H]-5-fluorouracil in *L. mexicana* wild-type expressing FurD was investigated in order to check whether the introduction of FurD could cause increases in the 5-fluorouracil transport (Figure 5.19). This study assessed the uptake of 0.1 μ M of [³H]-5-fluorouracil by promastigotes of *L. mexicana* wild-type and found that the transport was linear for at least 120 seconds with a rate of 0.0024 ± 0.0007 pmol.(10⁷ cells)⁻¹.s⁻¹ (n=2). However, under these conditions, the [³H]-5-fluorouracil in *L. mexicana*-WT + *FurD* was quickly saturated, resulting in a non-linear rate of uptake after 30 seconds (blue dashed line). The linear phase of 30 s displayed a rate of uptake of 0.022 ± 0.004 pmol.(10⁷ cells)⁻¹.s⁻¹ (solid blue line; $r^2=0.99$; n=2). In both strains, [³H]-5-fluorouracil transport was completely inhibited in the presence of 1 mM unlabelled 5-fluorouracil indicating that the uptake was saturable.

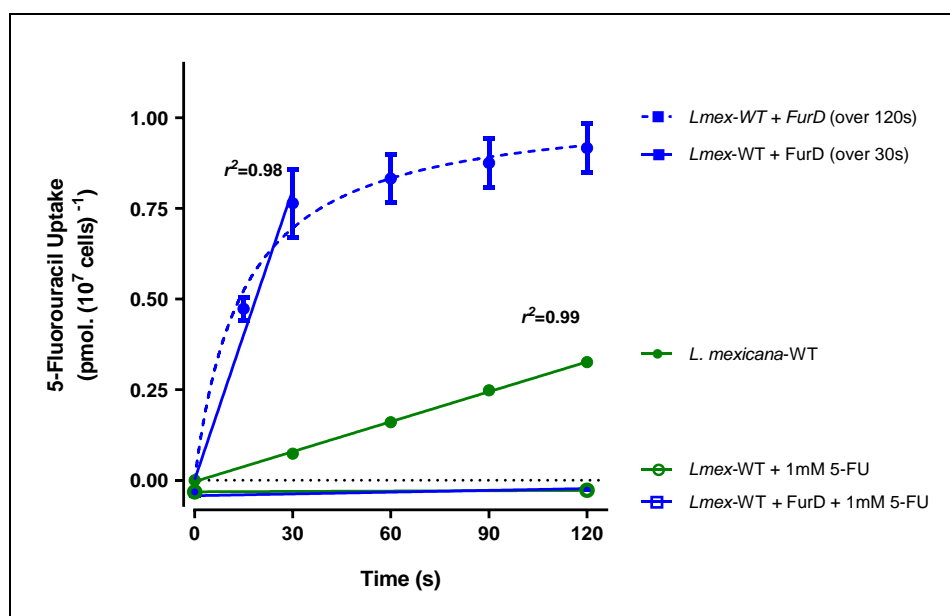


Figure 5.19: [³H]-5-Fluorouracil transport by *L mexicana*-WT and *L mexicana*-WT expressing FurD.

Transport of 0.1 μ M of [³H]- 5-fluorouracil by *Lmex*-WT (●) and *Lmex*-WT + FurD (■) was measured over 120 seconds in the presence or absent of 1 mM unlabelled 5-fluorouracil (○) and (□) respectively. The blue dashed line is showing the rate of uptake using non-linear regression analysis (equation for a saturation curve). Figure shows a representative out of two independent experiments. Symbols represent the average of triplicate determinations in a single representative experiment, and error bars represent \pm SEM.

5.3 Discussion

Uracil transport is recognised as an ubiquitous cellular activity that usually exists in free-living prokaryotes as well as eukaryote cells (de Koning and Dhalluin, 2000). Uracil transporter mutants are known for their resistance to 5-fluorouracil (Palmer et al., 1975; Jund et al., 1977; Andersen et al., 1995; Amillis et al., 2007; Stoffer-Bittner et al., 2018). It was also confirmed earlier that when the *FurD* gene is deleted from *A. nidulans*, the cells gain resistance against 5-fluorouracil and they exhibit a significantly reduced ability to transport radiolabeled uracil (Amillis et al., 2007). *A. nidulans* FurD belongs to the NAT family that works as an active proton-driven transporter with the ability to transport uracil and protons (Gournas et al., 2008; de Koning and Dhalluin, 2000). However, protozoan genomes do not contain any *FurD* homologues and the uracil uptake must be mediated by a transporter from a different gene family (Amillis et al., 2007; De Koning, 2007). Up to this moment, the only known genes involved in encoding transporters for pyrimidines and purines in protozoans are the ENT genes (De Koning et al., 2005; Campagnaro and de Koning, 2020). However, proposals for other families of genes have been

suggested (Bellofatto, 2007; De Koning, 2007; Campagnaro et al., 2018a; Balcazar et al., 2017).

Several close homologues of *FurD* gene have been identified. They include the *Fur4p* gene encoding the *S. cerevisiae* uracil transporter (Jund et al., 1977; JUND et al., 1988), and *UraA* gene encoding *E. coli* uracil permease and *PIUP* gene encoding the *P. larvae* uracil transporter, which show a similarity in amino acids of 46.2%, 37.1% and 54.6% with *FurD*, respectively (Jund et al., 1977; JUND et al., 1988; Andersen et al., 1995; Stoffer-Bittner et al., 2018), see Appendix 7 for a multiple alignment. Known mutants of these transporters include a *Fur4p* mutant in *S. cerevisiae*, a *PIUP* mutant in *P. Larvae*, and a *UraA* mutant in *E. coli*. Notably, these mutants cannot transport radiolabeled uracil and they are resistant to the 5-fluorouracil. Furthermore, their protein families resemble those of other prokaryotic and eukaryotic uracil transporters since *Fur4p* belongs to the NCS1 family, while *P1UP* and *UraA* are proton symporters and prototypical members of the NCS2/NAT family (Jund et al., 1977; Andersen et al., 1995; JUND et al., 1988; Stoffer-Bittner et al., 2018; Kryptou et al., 2015).

Resistance to 5-fluorouracil was generated in both *T. b. brucei* s427-wild type BSF and *L. mexicana* promastigotes, which led to the production of clonal lines *Tbb-5FURes* and *Lmex-5FURes*, respectively (Ali et al., 2013a; Alzahrani et al., 2017). These cell lines exhibit a notably reduced ability to transport uracil and 5-FU, which is virtually abolished in the cell lines of *L. mexicana*. The possibility of restoring sensitivity to 5-FU through the expression of *FurD* in the resistant strains was assessed using the Alamar blue assay. According to the results, there was no significant difference in the EC₅₀ values of 5-FU and 6-AU between the parental cells and those expressing *FurD* in *Tbb-5FURes* and *Lmex-5FURes* cell lines. In addition, the expression of *FurD* did not affect the sensitivity of the *L. mexicana* wild type to 5-FU, and it seems likely that the rate of transport is not limiting 5-FU toxicity, but the rate of incorporation into the nucleotide pool in *L. mexicana* wild-type.

We investigated whether heterologous expression of *FurD* gene in 5-FU resistant cell lines of *T. b. brucei* and *L. mexicana* is indeed able to restore the uptake of uracil/5-fluorouracil. The findings confirmed that the cells expressing *FurD* in

Lmex-5FURes and *L. mexicana*-WT had a much higher uptake of [³H]-uracil/5FU than the wild type activity. As the resistance was induced, stepwise, to a very high concentration of 5-FU in *Lmex-5FURes*, it is possible that the cells developed defects in both the uptake and the metabolism of the 5-FU, making them fully resistant to 5-FU, whether it enters the cells or not. Therefore, a metabolic adaptation appears to have rendered the *Lmex-5FURes* cells insensitive to intracellular 5-FU. It was additionally noted that the transport rate of [³H]-uracil and [³H]-5-fluorouracil is highly concentrated in *Lmex-5FURes* cells expressing FurD, but this saturates in less than 5 minutes and 9 seconds, respectively. Radiolabelled 5-fluorouracil and uracil are taken up for 9 seconds and 5 minutes linearly and then completely flat. The introduction of FurD into *Tbb-5FURes* cells did not significantly increase the rate of transport of [³H]-uracil, although the rate did trend higher. There are two possible reasons for this outcome. First, the transport rate of [³H]-uracil in the *Tbb-5FURes* cells was only partly reduced from the wild-type levels, as it entails the problem of high background generated by transport via TbU3. Second, it could be because FurD was not correctly produced or routed to the *Tbb-5FURes* cells plasma membrane. The latter is however unlikely since the expression of FurD in *Lmex-5FURes* and *L. mexicana*-WT highlighted significantly higher levels of [³H]-uracil/5FU transport.

We further kinetically characterised the transport activity of the *A. nidulans* uracil transporter FurD in *Lmex-5FURes* promastigotes. The findings confirm that FurD has a very high affinity for uracil with (K_m of $0.97 \pm 0.17 \mu\text{M}$) and 5-fluorouracil (K_i of $0.76 \pm 0.25 \mu\text{M}$). This result is almost identical to the previous characterisations of this uracil transporter in *A. nidulans*, which also showed that FurD has very high-affinity for uracil (K_m of $0.45 \mu\text{M}$) and 5-fluorouracil (K_i of $0.46 \mu\text{M}$) (Amillis et al., 2007). Another report by Amillis et al. (2007) found that FurD exhibited high affinity for several 5 substituted analogues of uracil and 6-azauracil (K_i $0.46 \mu\text{M}$ for 5-chlorouracil, K_i $0.86 \mu\text{M}$ for 5-aminouracil, $3.3 \mu\text{M}$ for thymine (5-Methyluracil) and K_i $1.9 \mu\text{M}$ for 6-azauracil), showing remarkable tolerance for 5-position substitutions. However, no affinity was observed in other pyrimidines and purines including thymidine, uridine, hypoxanthine, adenine, cytosine, or guanine ($K_i > 1500 \mu\text{M}$). Thus, FurD is a highly selective and

high-affinity transporter for uracil when expressed in *Lmex-5FURes* promastigotes. The anticancer drug 5-fluorouracil was as good substrate as uracil for FurD transporter in *Lmex-5FURes*. Regarding to the uracil transporter in *Leishmania* and *Trypanosoma spp*, *L. major* promastigotes the LmajU1 (K_m of 0.32 μM) was the only transporter identified with high affinity for uracil (Papageorgiou et al., 2005). The LmajU1 closely resembles the TbU1 transporter found in *T. brucei* procyclic forms (K_m of 0.46 μM) and TbU3 transporter in *T. brucei* BSF (K_m of 0.54 μM). The anti-metabolite 5-fluorouracil was found to be a good inhibitor for LmajU1, TbU1 and TbU3 transporters (de Koning and Jarvis, 1998; Ali et al., 2013a).

The observations described in this chapter clearly show that the 5-FURes cell lines are not solely resistant because of deficiencies in 5-FU uptake and that the resistance phenotype cannot be rescued by restoring 5-FU uptake to wild-type levels and even beyond, by the introduction of a known uracil/5-FU transporter. As the resistance was induced, stepwise *in vitro*, to a very high concentration of 5-FU in the *5FU-Res* cells, it is possible that the cells developed defects in both the uptake and the metabolism of the 5-FU. Thus, it is possible to speculated that the metabolic adaptation appears to have rendered the *5FURes* cells insensitive to intracellular 5-FU. Therefore, we highly recommended to assess the metabolism of 5-FU, using metabolomic assessments of *L. mexicana* clonal lines adapted to high concentrations of 5-FU, the sensitive *L. mexicana*-WT and 5-FU resistant cell lines expressing FurD.

6 Investigation of glucose transporters in *L. mexicana* promastigotes in the sensitivity to 5-FU

6.1 Introduction

There is no doubt that glucose is one of the most basic and significant sources of energy for different organisms. Due to the hydrophilic profile of glucose, however, it cannot enter the cells by itself through the cell membranes, and thus relies on transporters (Pereira and Silber, 2012; Delrot et al., 2000). Considering *Leishmania* spp, the parasite goes through a complex life cycle; this makes the organism pass through different kinds of environments, with varying concentrations and types of sugar available to them. The procyclic promastigotes rely on the catalysis of glucose and amino acids, and at subsequent stages of promastigote development, an increased level of amino acid is used and glucose usage is reduced, likely because the availability of glucose is highly limited after the sandfly has digested its bloodmeal (Inbar et al., 2017; Landfear, 2010; Rodriguez-Contreras et al., 2007). The African trypanosomes that reside in the bloodstream depend entirely on the uptake of glucose to generate energy by glycolysis (Lamour et al., 2005; Landfear, 2010). Conversely, trypanosomes of procyclic form (PCF) use amino acids (mainly proline) as their main source of energy using the Krebs cycle and the respiratory chain (Pereira and Silber, 2012; Tetaud et al., 1997). It is in the cell membranes that the glucose transporters are embedded and exercise the ability to conduct the passive transportation of glucose to the intracellular space (Delrot et al., 2000; Akpunarlieva and Burchmore, 2017; Manolescu et al., 2007; Landfear, 2010). Glucose transporters were proposed as candidate genes with the responsibility for facilitating uracil uptake by following the analyses of the wild-type and 5-FU resistant lines for *T. b. brucei* BSF and *L. mexicana* promastigotes after RNA sequencing of 5-FU resistant cell lines, as well as RIT sequencing analyses of the 2T1 PYR6-5^{-/-} cell line challenged with 5-FU and 6-AU (Alzahrani, 2017).

Tbb-5FURes were found to down-regulated glucose transporters THT2 (Tb927.10.8520) and 2A (Tb927.10.8530) levels of expression with a log₂ fold-change of -0.78 and -1.09 relative to the reference *T. b. brucei* TREU 927 genome ($P \leq 0.01$). In contrast, *Tbb-5FURes* up-regulated glucose transporter 1B (Tb927.10.8440) with a log₂ change of 0.29 ($P < 0.05$). Similarly, Tb927.10.8460 is another glucose transporter gene that was also up-regulated in *Tbb-5FURes*

with \log_2 of 0.29 ($P < 0.05$). The transcription of a glucose transporter D2 (recently named as *LmexGT4*; LmxM.32.0290) was significantly elevated in *Lmex-5FURes* ($\log_2 = 0.52$) in comparison with *L. mexicana* wild-type ($P \leq 0.01$). Moreover, glucose transporter 2A (Tb927.10.8530) was the top hit in RIT sequencing results, contributing to 4058 and 6317 RPKM (Reads Per Kilobase of transcript per Million mapped reads) after analysis was conducted on the pyrimidine-auxotrophic 2T1 cell lines selection with 6-AU and 5-FU respectively (Alzahrani, 2017). The link between uracil transport and glucose transport emerges from the transcriptomic analysis of 5-FU resistant cell lines and RIT-seq analysis of the selected RNAi library (Alzahrani, 2017). There is a possibility that the knockdown or down-regulation of either one or several of these glucose transporter genes such as glucose transporter 2A in 5-FU resistant cell lines can be responsible for causing increased levels of resistance to 5-FU.

A cluster of three glucose transporter genes named as *LmexGT1*, *LmexGT2* and *LmexGT3*, which belong to the encoding permeases of the SLC2 or GLUT transporter family, is contained in the genome of *L. mexicana* (Pereira and Silber, 2012; Augustin, 2010). These three *LmexGTs* exhibit 90% identity in amino acid sequences and are arranged as a *tandem* repeat on chromosome 20 (GeneDB). *L. mexicana*'s glucose transporters *LmexGT1*, *LmexGT2* and *LmexGT3* are characterised by 12 transmembrane domains as the proteins promoting the passive transportation of glucose (Burchmore et al., 2003a; Silber et al., 2009). In order to investigate an link between glucose transporters and 5-FU sensitivity, Glucose Transporter null mutants in *L. mexicana* wild-type promastigotes (*Lmex-GT1-3* KO), from which all three glucose transporter genes had been deleted by targeted gene replacement, and the re-expression of each of these three glucose transporter genes individually into *Lmex-GT1-3* KO cells (Burchmore et al., 2003a), were kindly gifted by Dr Richard Burchmore (University of Glasgow) (Figure 6.1). The *Lmex-GT1-3* KO cells are not able to transport glucose (Burchmore et al., 2003a), but re-expression of the *LmexGT1*, *LmexGT2* and *LmexGT3* individually into *Lmex-GT1-3* KO cells enables the uptake of glucose (Rodriguez-Contreras et al., 2007).

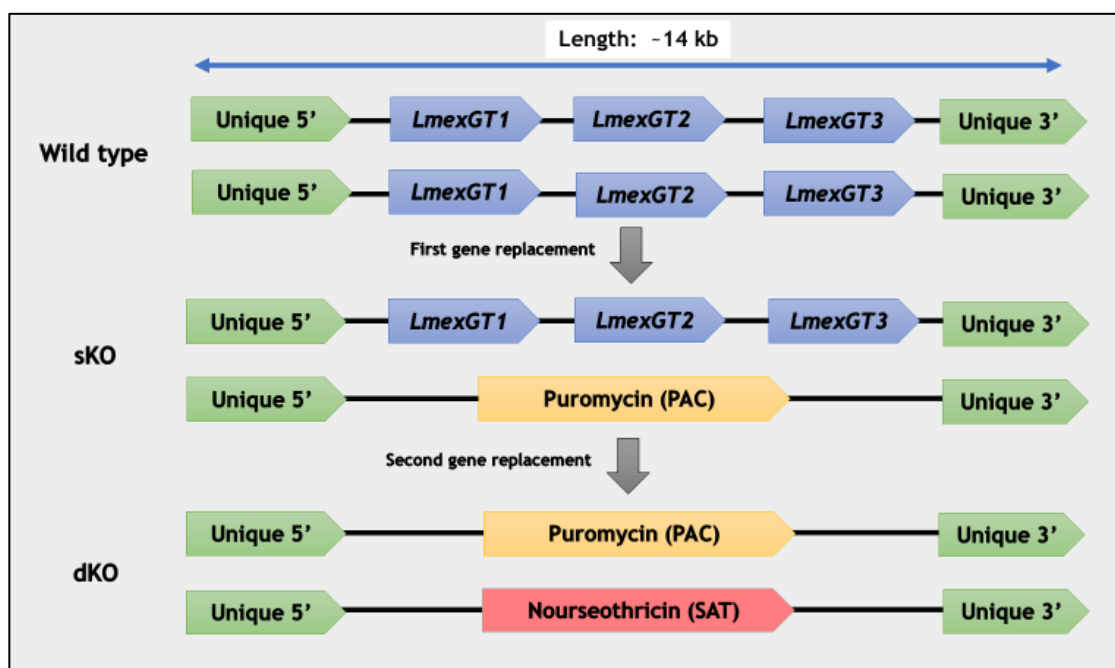


Figure 6.1: Knockout strategy used for the replacement of the genomic *locus* on chromosome 20 containing a *tandem* array of three glucose transporter genes (*LmexGT1-3*). sKO: single knockout; dKO: double knockout. Adapted from (Burchmore et al., 2003a).

The primary aim of this chapter is to determine the sensitivity to and transport of 5-FU after the full knockout of genes responsible for transportation of glucose in *L. mexicana* promastigotes. The chapter also focuses on examining the sensitivity/transport of *Lmex-GT1-3* KO cells that re-express individual glucose transporters to 5-FU/uracil. In addition, an investigation is conducted to ascertain whether, when the FurD uracil transporter is introduced, this is able to restore the sensitivity/transport to 5-FU in *Lmex-GT1-3* KO cells. Moreover, an assessment is carried out to find out the effects of the absence of glucose in the extracellular medium *T. b. brucei* s427 WT procyclic form in the sensitivity to 5-FU and the growth rate.

6.2 Results

6.2.1 The assessment of growth rate of *Lmex-GT1-3* KO in the presence and absence of 5 mM L-proline

To examine the effect of the deletion of glucose transporters locus in *L. mexicana* on the growth rate, the growth of the *L. mexicana* wild-type, *Lmex-5FURes* and *Lmex-GT1-3* KO cell lines was assessed in HOMEM medium supplemented with 10% FBS and incubated at 25 °C (HOMEM media contains 3

g/L glucose); the cell densities were determined every 24 h. The *Lmex-GT1-3* KO cultures had almost the same density as *L. mexicana*-WT and *Lmex-5FURes* (Figure 6.2A). However, to understand the potential impact of an energy source on the glucose transporter knockout cell lines, we prepared a new medium supplemented with 5 mM L-proline. As *T. brucei* and *T. cruzi* will consume much more proline from the medium when in a glucose-limited environment (Lamour et al., 2005; Silber et al., 2009; Tonelli et al., 2004; Drew et al., 2003), it is possible that *Lmex-GT1-3* KO also need proline as energy sources. It was anticipated that adding 5 mM proline to HOMEM medium would cause an increase in the growth rates of the *Lmex-GT1-3* KO cell lines. However, the density of the *Lmex-GT1-3* KO culture (8.6×10^8 cell/mL) was very slightly below that of the *L. mexicana*-WT (1.05×10^9 cell/mL) and *Lmex-5FURes* strains (8.8×10^8 cell/ml) (Figure 6.2B). Although reproducible, this does not constitute a major growth defect in the *LmexGT* knockout of *L. mexicana* promastigotes.

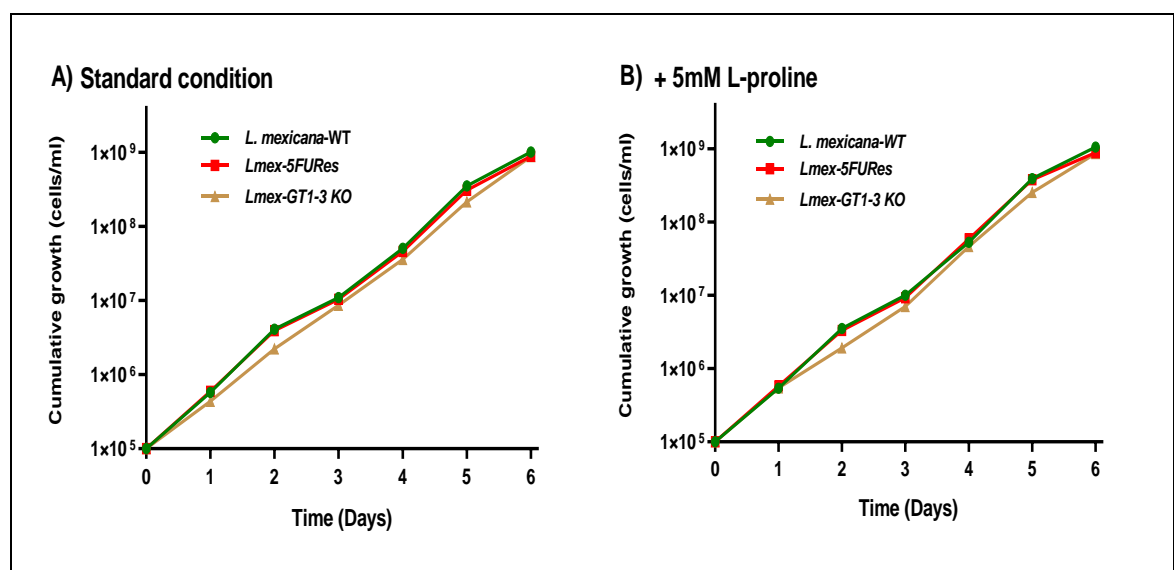


Figure 6.2: The growth curves of *L. mexicana* WT, *Lmex-5FURes* and *Lmex-1-3* KO on HOMEM medium supplemented with 10% FBS and incubated at 25 °C.

A) Standard condition and B) with 5 mM of L-proline. Cells were seeded at a density of 1×10^5 cells/mL, and cell densities were determined every 24 h. Cells were passaged every 48 h once growth had reached between 5 and 8×10^6 cells/mL. Each data point in this result represents the average of three independent repeats.

6.2.2 Drug sensitivity assay with 5-FU in the presence and absence of 5 mM L-proline

By using the Alamar blue assay as a proxy for cell numbers, a close look at the growth inhibition curve of *L. mexicana* promastigotes in the presence of 5-FU

revealed a noticeably biphasic inhibition curve, which is attributed to a leishmanistatic effect at low concentrations and a leishmanicidal effect at higher concentrations (Figure 6.3). As mentioned in the introduction, glucose transporters have been identified as a potential candidate carrier for uracil, or at least a modulator of uracil uptake. Therefore, the viability assay using Alamar blue dye was performed to determine the effect of the deletion of glucose transporter locus in *L. mexicana* on sensitivity to 5-fluorouracil, while pentamidine was used as a positive control (Figure 6.4).

Interestingly, the EC_{50} values of the double knockout of glucose transporter genes in *L. mexicana* to 5-FU significantly increased compared to the *L. mexicana* WT at low concentrations (EC_{50} (1)), with an average $3430 \pm 440 \mu\text{M}$ and $36.6 \pm 3.6 \mu\text{M}$ respectively ($n = 3$; figure 6.4A). The *Lmex-GT1-3* KO cells was found to be 93-fold resistant when comparison was made with the *L. mexicana* WT ($n=3$; $P < 0.001$). The *Lmex-GT1-3* KO cells also exhibited a small but highly significantly increased sensitivity to pentamidine with an EC_{50} value of $0.36 \pm 0.03 \mu\text{M}$ (0.6-fold more sensitive to pentamidine; $n=3$; $P < 0.001$) compared to $0.61 \pm 0.02 \mu\text{M}$ in *L. mexicana* wild-type cells (Figure 6.4B).

In order to determine whether the choice of energy source can influence the sensitivity of the *L. mexicana* glucose transporters KO cell lines to 5-FU, HOMEM media with 5 mM of L-proline were prepared. The results showed that there was no significant difference in the EC_{50} values of 5-FU against *L. mexicana* WT, *Lmex-5FURes* and *Lmex-GT1-3* KO in the presence or absence of 5 mM of L-proline in the extracellular media ($P > 0.05$).

In conclusion, the loss of glucose transporter genes is associated with resistance to 5-FU as the *Lmex-GT1-3* KO leads to decreasing the sensitivity to 5-FU in kinetoplastid parasites. Sensitivity to 5-FU is not different in the presence of high levels of proline.

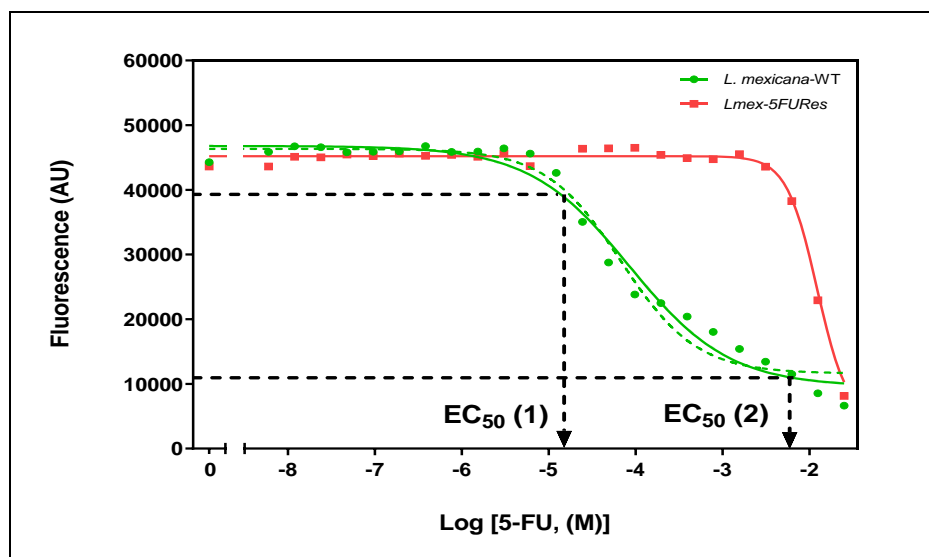


Figure 6.3: The biphasic inhibition curve of *L. mexicana* WT promastigotes against 5-fluorouracil by using the Alamar blue fluorescent dye as a proxy for the cell number. The leishmanistatic effect at low concentrations EC_{50} (1) was $36.6 \pm 3.6 \mu M$ whereas the leishmanicidal effect at higher concentrations (EC_{50})2 was $12221 \pm 1940 \mu M$. The curve shown is representative of several independent repeats.

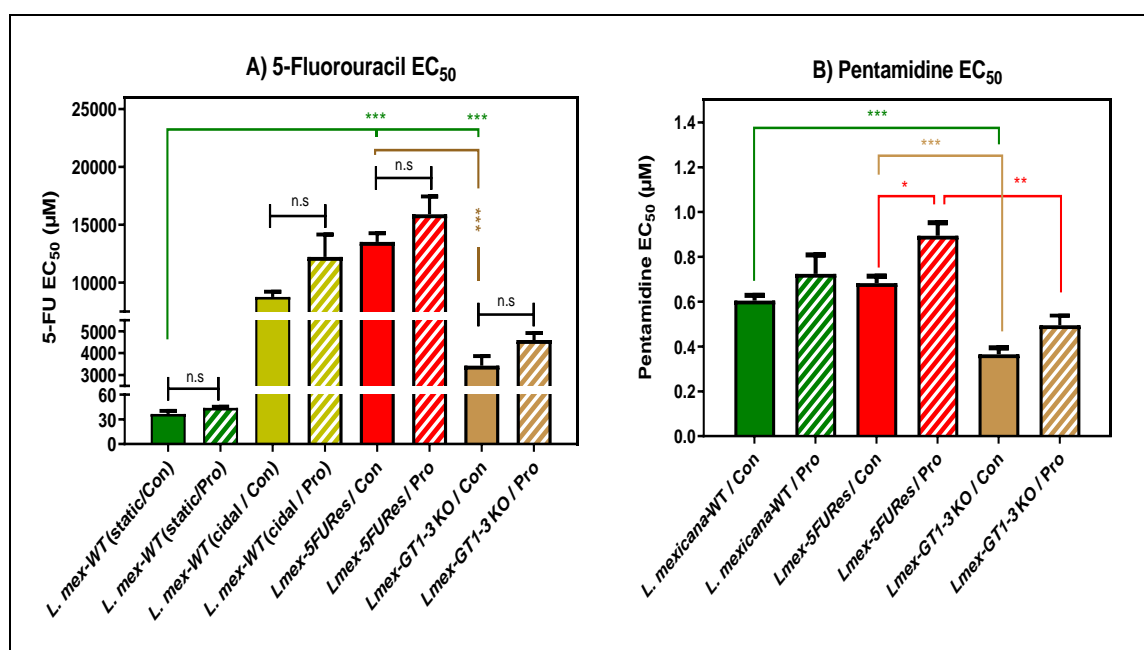


Figure 6.4: The Alamar blue drug sensitivity assay of *L. mexicana* WT, *Lmex-5FURes*, *Lmex-GT1-3* KO using 5-fluorouracil (A) and pentamidine (B).

The mean of three independent determinations is shown \pm SEM. Con: Normal condition; Pro: +5 mM L-proline; Cidal: leishmanicidal effect; Static: leishmanistatic effect. * $P < 0.05$; ** $P < 0.01$; *** $P < 0.001$. P value was determined by unpaired two-tailed Student's T-test.

6.2.3 Transport assays with 5-fluorouracil, uracil, 2-deoxy-D-glucose and pentamidine

The rate of uptake of $[^3H]$ -uracil and $[^3H]$ -5-fluorouracil in *L. mexicana*-WT and *Lmex-GT1-3* KO was investigated in order to check whether the deletion of

glucose transporter locus in *L. mexicana* could cause reduced uracil and 5-fluorouracil transport. The uptake of radiolabelled uracil and 5-fluorouracil by *L. mexicana*-WT and *Lmex-GT1-3* KO was performed in parallel on the same day, using the same solutions (Figure 6.5A and B). The uptake of 0.1 μM [^3H]-uracil (Figure 6.5A) and [^3H]-5-fluorouracil (Figure 6.5B) was linear over the 8 minutes (for uracil and 5-fluorouracil) duration of the experiment in *L. mexicana*-WT with a rate of $0.062 \pm 0.012 \text{ pmol.}(10^7 \text{ cells})^{-1}.\text{s}^{-1}$ and $0.11 \pm 0.03 \text{ pmol.}(10^7 \text{ cells})^{-1}.\text{s}^{-1}$, respectively ($n=3$). In contrast, the transport of 0.1 μM of [^3H]-uracil by *Lmex-GT1-3* KO cells was reduced by 81% compared with wild-type cells ($n=3$; Figure 6.5C). The transport of 0.1 μM of [^3H]-5-fluorouracil by *Lmex-GT1-3* KO was almost completely absent (98%) and became not significantly different from the uptake in the presence of 1 mM unlabelled 5-fluorouracil, with a calculated rate of $0.0013 \pm 0.0005 \text{ pmol. } (10^7 \text{ cells})^{-1}.\text{s}^{-1}$ ($n=3$, linear regression; Figure 6.5D), so that it is believed that the *Lmex-GT1-3* KO cells have lost the uracil transport activity (*Lmex-U1*)(Alzahrani et al., 2017). In conclusion, the full knockout of glucose transporters in *L. mexicana* promastigotes lead to significant decrease in the transport rate of [^3H]-Uracil/5-FU, as the uptake of radiolabelled uracil and 5-fluorouracil in the *Lmex-GT1-3* KO cells was 81% and 98% lower than in wild-type cells, respectively.

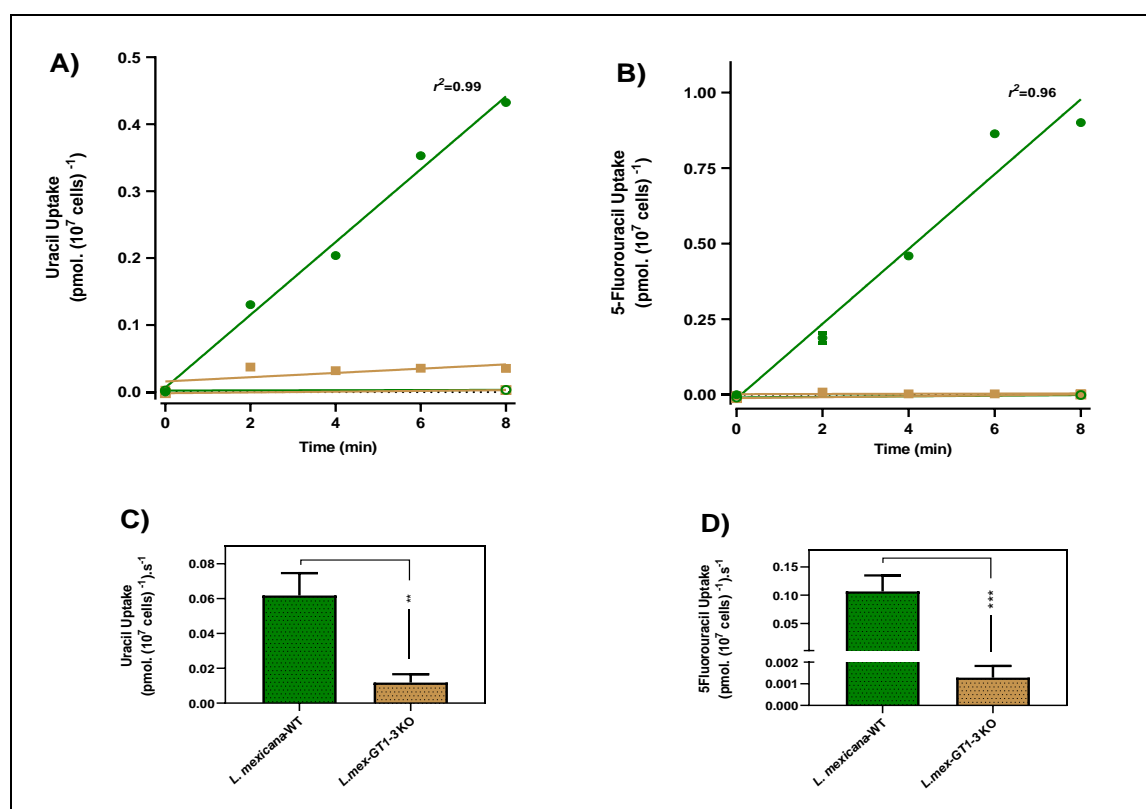


Figure 6.5: [^3H]-Uracil and [^3H]-5-Fluorouracil transport were performed in parallel on the same day by *L. mexicana*-WT and *Lmex-GT1-3* KO.

A) Transport of 0.1 μM of [^3H]-uracil by *L. mexicana*-WT (●) and *Lmex-GT1-3* KO (■) was measured over 8 minutes in the presence or absent of 1mM unlabelled uracil (○) and (□) respectively. B) Transport of 0.1 μM of [^3H]-5-fluorouracil by *L. mexicana*-WT (●) and *Lmex-GT1-3* KO (■) was measured over 8 minutes in the presence or absent of 1mM unlabelled 5-fluorouracil (○) and (□) respectively. Symbols in A and B panels represent the average of triplicate determinations in a single representative experiment and error bars represent \pm SEM. C) and D) Comparison between *L. mexicana*-WT and *Lmex-GT1-3* KO cell lines for the transport rate of [^3H]-uracil and [^3H]-5-fluorouracil. Data in C and D panels represent the average rate of transport of 0.1 μM of [^3H]-uracil and [^3H]-5-fluorouracil as obtained in three independent experiments each performed in triplicate and error bars are \pm SEM. ** $P < 0.001$ and *** $P < 0.001$, Statistical relevance was found by unpaired Student's T-test ($n=3$).

In section 6.2.2, it was observed that the double knockout of glucose transporters in *L. mexicana* promastigotes significantly increased the sensitivity to pentamidine compared with wild-type cells ($n=3$; $P < 0.001$). Thus, the uptake of 25 nM of [^3H]-pentamidine in *Lmex-GT1-3* KO was investigated in order to check whether the deletion of glucose transporters leads to an increase in the rate of pentamidine transport. The results show that there was no significant difference in the transport of 25 nM of [^3H]-pentamidine between the *Lmex-GT1-3* KO and wild-type strain ($P > 0.05$; $n=3$; figure 6.6A). The transport of 25 nM of [^3H]-pentamidine was statistically identical in *L. mexicana*-WT and *Lmex-GT1-3* KO cells, with a rate of 0.083 ± 0.01 pmol. (10^7 cells) $^{-1}$.s $^{-1}$ and 0.057 ± 0.007 pmol. (10^7 cells) $^{-1}$.s $^{-1}$, respectively ($P > 0.05$; $n=3$; Figure 6.6B). Therefore, the results indicate that the *Lmex-GT1-3* KO parasites can up-regulate the other transporter(s) and might conceivably lead to increased pentamidine sensitivity.

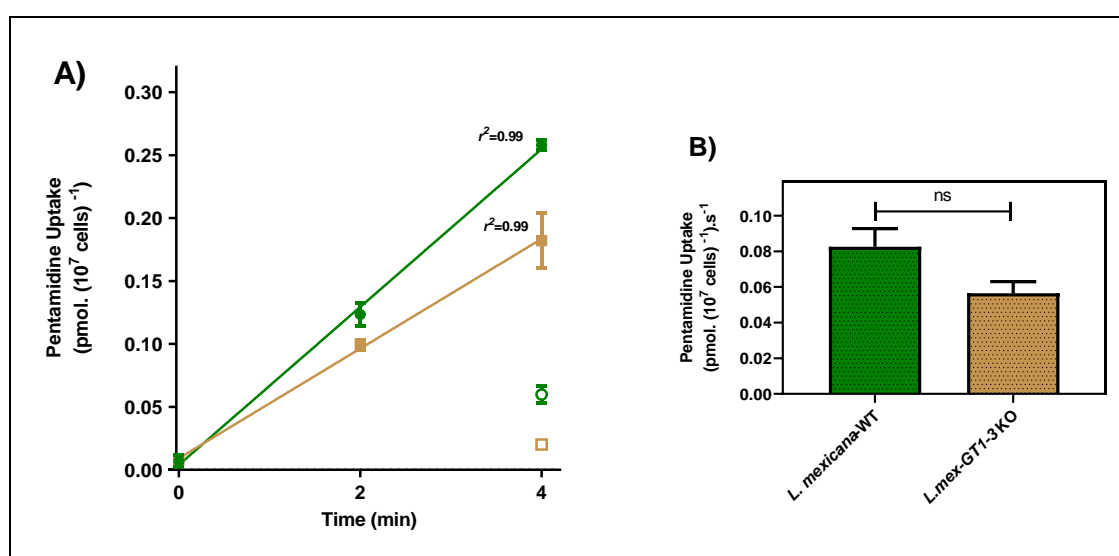


Figure 6.6: [^3H]-Pentamidine transport by *L. mexicana*-WT and *Lmex-GT1-3* KO.

A) Transport of 25 nM of [^3H]-pentamidine by *L. mexicana*-WT (●) and *Lmex-GT1-3* KO (■) was measured over 4 minutes in the presence or absent of 1 mM unlabelled pentamidine (○) and (□) respectively. Symbols represent the average of triplicate determinations in a single

representative experiment and error bars represent \pm SEM. B) Comparison between *L. mexicana*-WT and *Lmex-GT1-3* KO cell lines for the transport rate of 25 nM of [3 H]-pentamidine. Data represent the average rate of transport of 25 nM of [3 H]-pentamidine as obtained in three independent experiments each performed in triplicate and error bars are \pm SEM. No statistical relevance was found by unpaired Student's T-test ($n=3$).

Next, the rate of uptake of [3 H]-2-deoxy-D-glucose in *L. mexicana*-WT, *Lmex-5FURes* and *Lmex-GT1-3* KO investigated in order to check whether *Lmex-5FURes* cells resistance to 5-fluorouracil was linked to changes in the transport of radiolabelled 2-deoxy-D-glucose transport (Figure 6.7). The results showed that the rate of 0.1 μ M of [3 H]-2-deoxy-D-glucose uptake in *Lmex-5FURes* cells was completely identical to the rate in *L. mexicana*-WT, with an average of 0.0079 ± 0.0003 pmol. $(10^7 \text{ cells})^{-1} \cdot \text{s}^{-1}$ and 0.0072 ± 0.00005 pmol. $(10^7 \text{ cells})^{-1} \cdot \text{s}^{-1}$ and a linear phase over 60 seconds, respectively ($P > 0.05$ by F-test; $n=1$). The uptake of 0.1 μ M of [3 H]-2-deoxy-D-glucose in both strains was completely inhibited in the presence of 1 mM unlabelled 2-deoxy-D-glucose. As expected, the transport of 0.1 μ M of [3 H]-2-deoxy-D-glucose by *Lmex-GT1-3* KO was completely abolished and became identical to the uptake in the presence of 1 mM unlabelled 2-deoxy-D-glucose, so that it is believed that the *Lmex-GT1-3* KO cells have lost the glucose transport activity (*Lmex-GT*). It is clear that *Lmex-5FURes* cells are still maintaining the glucose transport activity, but lost uracil/5-fluorouracil transporter. Notwithstanding the observation that *Lmex-5FURes* and *Lmex-GT1-3* KO cells had somewhat similar resistance profiles (see section 6.2.2), these data clarify that glucose and uracil/5-fluorouracil are taken up by different transport proteins.

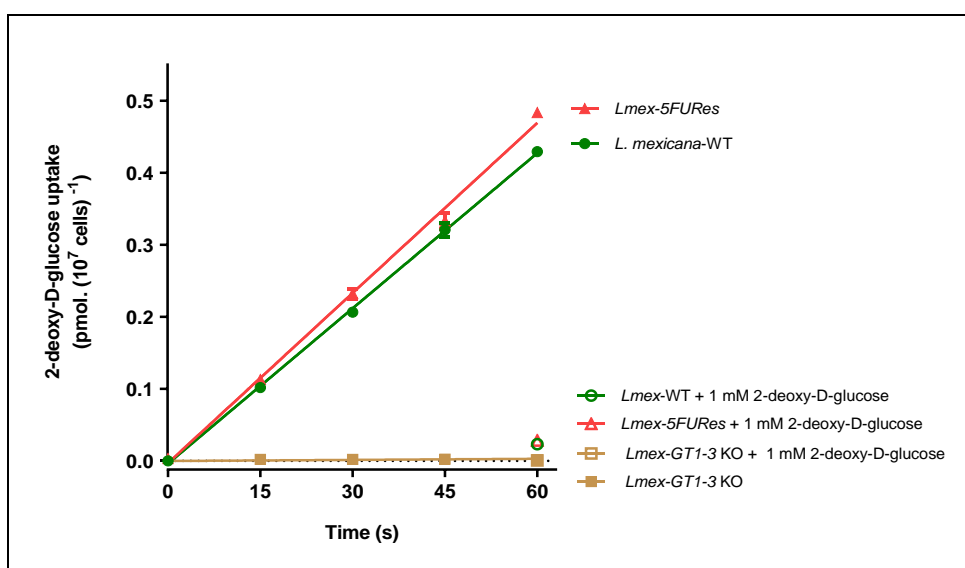


Figure 6.7: [^3H]-2-deoxy-D-glucose transport by *L. mexicana*-WT, *Lmex-5FUR*es and *Lmex-GT1-3* KO.

Transport of 0.1 μM of [^3H]- 2-deoxy-D-glucose by *L. mexicana*-WT, *Lmex-5FUR*es and *Lmex-GT1-3* KO was measured over 60 seconds in the presence or absent of 1 mM unlabelled 2-deoxy-D-glucose. Figure shows a representative experiment in triplicate and error bars represent \pm SEM. $P > 0.05$; F-test was determined by GraphPad Prism 8.

6.2.4 The evaluation of 5-FU EC_{50} of *L. mexicana* in normal and glucose free medium

The Alamar blue assay was used to determine the EC_{50} values for the *L. mexicana*-WT in the standard condition, *L. mexicana*-WT in glucose-free medium and *Lmex-GT1-3* KO, to test whether the absence of glucose in the extracellular medium could potentially decrease the susceptibility of *L. mexicana*-WT to 5-fluorouracil, as the absence of glucose transporters does. The result showed that there was no significant difference against 5-FU between the *L. mexicana*-WT cells in glucose free medium and *L. mexicana*-WT cells in standard condition ($n=4$; $P > 0.05$; Figure 6.8A). The presence or absence of glucose in the medium therefore does not affect the sensitivity of *L. mexicana*-WT parasites to 5-FU. It is clear that the presence of glucose in the medium is not necessary for uracil/5FU transport but the presence of the glucose transporters *is* necessary for uracil/5FU transport.

Throughout the assessment, pentamidine was used as an unrelated control drug. Surprisingly, the *Lmex-GT1-3* KO cells exhibited a small but highly significantly increased sensitivity to pentamidine in standard medium, with an EC_{50} value of $0.36 \pm 0.02 \mu\text{M}$ ($P < 0.0001$) compared to $1.01 \pm 0.03 \mu\text{M}$ in *L. mexicana* wild-type cells (Figure 6.8B). Moreover, the sensitivity of the *Lmex-GT1-3* KO cell lines in glucose free medium to pentamidine was significantly decreased ($\text{RF}=2$; $n=4$; $P < 0.001$) compared to the *Lmex-GT1-3* KO cells in the standard medium. The nature of the association of low glucose levels and glucose transporter knockout with pentamidine efficacy remains unclear at this moment. However, it could be speculated that, since pentamidine accumulates in the parasite's mitochondrion (Baker et al., 2013), a shift in mitochondrial energy pathways, related to the usage of either glucose or amino acids as primary energy source, could contribute to this, with the different pathways being more or less sensitive to inhibition by the drug.

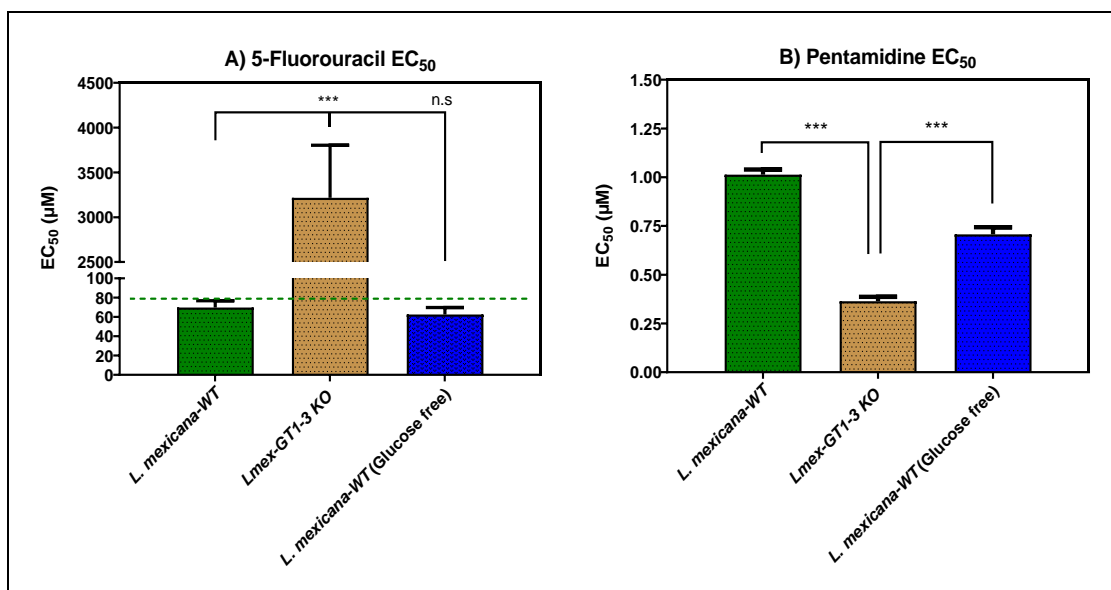


Figure 6.8: The Alamar blue drug sensitivity assay of *L. mexicana*-WT, *Lmex-5FUR*es and *L. mexicana*-WT in glucose free medium using 5-fluorouracil (A) and pentamidine (B). The mean of four independent determinations is shown \pm SEM. *** $P < 0.001$ by unpaired two-tailed Student's T-test.

6.2.5 Re-expression of *LmexGT1*, *LmexGT2* and *LmexGT3* into *Lmex-GT1-3* KO promastigotes

The genome of *L. mexicana* contains three genes that encode glucose transporters, named as *LmexGT1*, *LmexGT2*, and *LmexGT3*. These genes have 12 transmembrane domains and are located on chromosome 20 in a *tandem* array (geneDB). The proteins are similar isoforms but reflect some differences that distinguish them at the C and N terminal domains (Burchmore and Landfear, 1998). The alignment of the amino acid sequences for *L. mexicana* glucose transporters *LmexGT1*, *LmexGT2*, and *LmexGT3* is presented in Appendix 8. The *LmexGT1*, *LmexGT2* and *LmexGT3* genes were expressed episomally in the *Lmex-GT1-3* Knockout cell lines through the use of the pX63NEO plasmid containing the neomycin resistance gene (LeBowitz et al., 1991; Burchmore et al., 2003a). This section aims to conduct an investigation as to whether the sensitivity to 5-FU, or the transport of 5-FU/uracil *in vitro* can be restored through the add-back of *LmexGT1*, *LmexGT2*, and *LmexGT3* individually into *Lmex-GT1-3* KO cells.

6.2.5.1 Drug sensitivity assay with 5-fluorouracil

As previously reported in section 6.2.2, the deletion of the glucose transporter locus in *L. mexicana* promastigotes was found to confer resistance to 5-FU. It

was therefore decided to test the sensitivity of the *Lmex-GT1-3* KO cells re-expressing the individual glucose transporter genes (*LmexGT1*, *LmexGT2* and *LmexGT3*) to 5-FU (Figure 6.9). The re-expression of *LmexGT1*, *LmexGT2* and *LmexGT3* in *Lmex-GT1-3* KO cells caused significant sensitisation to 5-FU, with average EC_{50} values of $98.1 \pm 12.3 \mu\text{M}$, $393 \pm 96 \mu\text{M}$ and $304 \pm 59 \mu\text{M}$, respectively ($n=3$; $P < 0.001$), while *Lmex-GT1-3* KO cells displayed EC_{50} value amounting to $1597 \pm 116 \mu\text{M}$. Surprisingly, *Lmex-GT1-3* KO + *LmexGT1*, *Lmex-GT1-3* KO + *LmexGT2* and *Lmex-GT1-3* KO + *LmexGT3* displayed a significant decrease in pentamidine sensitivity relative to the parental cell line ($n=3$; $P < 0.01$; 2-fold, 3.2-fold and 3.3-fold, respectively). It should be noted that *LmexGT1*, *LmexGT2* and *LmexGT3* transporters encoded by the episomal expression vector are somewhat under-expressed compared to wild-type parasites as shown by (Rodriguez-Contreras et al., 2007). It is clear that the expression of individual *LmexGT* in *Lmex-GT1-3* KO cells significantly increased the sensitivity to 5-FU but not quite back to wild-type cells.

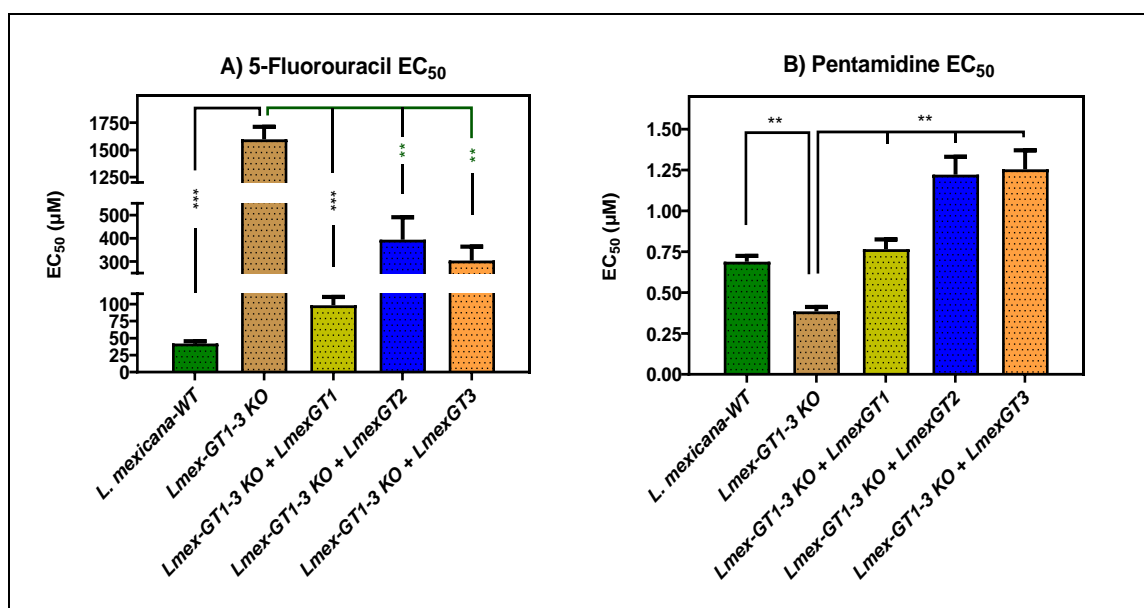


Figure 6.9: Alamar blue drug sensitivity assay of re-expression of glucose transporter genes (*LmexGT1*, *LmexGT2* and *LmexGT3*) in *Lmex-GT1-3* KO by using 5-fluorouracil (A) and pentamidine (B).

The mean of three independent determinations is shown \pm SEM. ** $P < 0.01$ and *** $P < 0.001$ by unpaired two-tailed Student's T-test.

6.2.5.2 Transport assay with 5-fluorouracil and uracil

The transport rate of [^3H]-uracil and [^3H]-5-fluorouracil in *L. mexicana*-WT, *Lmex-GT1-3* KO, *Lmex-GT1-3* KO + *LmexGT1*, *Lmex-GT1-3* KO + *LmexGT2* and

Lmex-GT1-3 KO + *LmexGT3* was investigated in order to check whether the re-expression of individual glucose transporter genes in *Lmex-GT1-3* KO cells could cause changes in the uracil and 5-fluorouracil transport (Figure 6.10). The uptake of 0.1 μM of [^3H]-uracil (Figure 6.10A) and [^3H]-5-fluorouracil (Figure 6.10B) was linear over the 8 minutes (for uracil and 5-fluorouracil) duration of the experiment in *L. mexicana*-WT with a rate of $0.044 \pm 0.008 \text{ pmol. } (10^7 \text{ cells})^{-1} \cdot \text{s}^{-1}$ and $0.051 \pm 0.006 \text{ pmol. } (10^7 \text{ cells})^{-1} \cdot \text{s}^{-1}$, respectively. The uptake of 0.1 μM of [^3H]-uracil in both *Lmex-GT1-3* KO + *LmexGT1*, *Lmex-GT1-3* KO + *LmexGT2* and *Lmex-GT1-3* KO + *LmexGT3* was significantly increased, with a rate of 0.013 ± 0.0002 , 0.011 ± 0.002 and 0.012 ± 0.001 , respectively compared with the parental *Lmex-GT1-3* KO cells ($n=2$; $P < 0.01$ by Paired Student's T-test). Moreover, the re-introduction of *LmexGT1*, *LmexGT2* and *LmexGT3* into *Lmex-GT1-3* KO cells greatly increased the rate of 0.1 μM of [^3H]-5-fluorouracil uptake to 0.03 ± 0.002 , 0.03 ± 0.001 and 0.023 ± 0.0001 , respectively compared with the control *Lmex-GT1-3* KO cells. The expression of individual glucose transporters correlates with increased uptake of radiolabelled uracil and 5-FU (30% and 50%, respectively). All of them appear to be responsible to uracil and 5-FU transport, but indirect effects are likely.

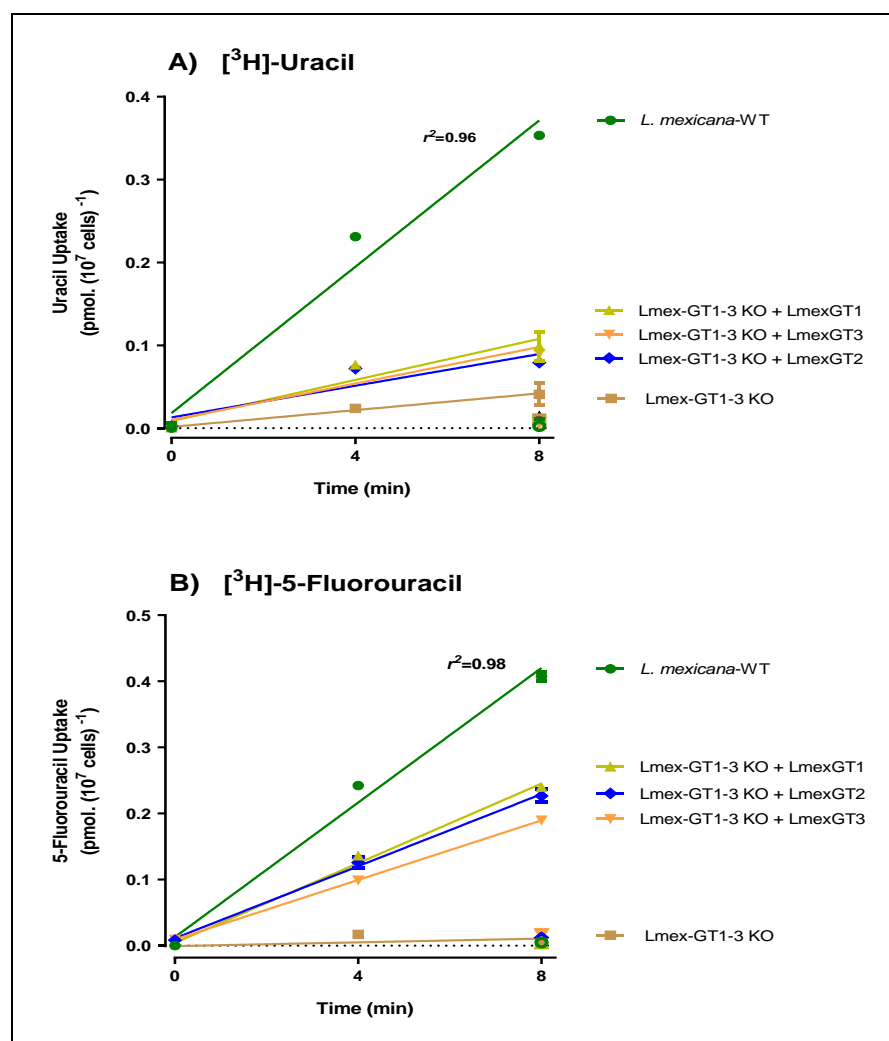


Figure 6.10: [3H]-Uracil and [3H]-5-Fluorouracil transport by *L. mexicana*-WT, *Lmex-GT1-3* KO and re-expression of each glucose transporter genes (*LmexGT1*, *LmexGT2* and *LmexGT3*) in *Lmex-GT1-3* KO.

A) Transport of 0.1 μ M of [3H]-uracil by *L. mexicana*-WT, *Lmex-GT1-3* KO, *Lmex-GT1-3* KO + *LmexGT1*, *Lmex-GT1-3* KO + *LmexGT2* and *Lmex-GT1-3* KO + *LmexGT3* was measured over 8 minutes in the presence or absent of 1 mM unlabelled uracil. B) Transport of 0.1 μ M of [3H]-5-fluorouracil by *L. mexicana*-WT, *Lmex-GT1-3* KO, *Lmex-GT1-3* KO + *LmexGT1*, *Lmex-GT1-3* KO + *LmexGT2* and *Lmex-GT1-3* KO + *LmexGT3* was measured over 8 minutes in the presence or absent of 1 mM unlabelled 5-Fluorouracil. Symbols in A and B figures represent the average of triplicate determinations in a single representative experiment and error bars represent \pm SEM.

6.2.5.3 Affinity of *LmexGT1*, *LmexGT2* and *LmexGT3* in the *Lmex-GT1-3* KO cells for glucose, uracil and 5-fluorouracil

In order to investigate whether the glucose, uracil and 5-fluorouracil shared the same transporter, the inhibition of 0.1 μ M of [3H]-2-deoxy-D-glucose uptake in *Lmex-GT1-3* KO cells re-expressing *LmexGT1*, *LmexGT2* and *LmexGT3* by various concentrations of unlabelled glucose, uracil and 5-fluorouracil - over 30 seconds as our time point - was assessed (Figure 6.11). The affinity of *LmexGT1*, *LmexGT2* and *LmexGT3* for glucose was evaluated by competition with 0.1 μ M of

[³H]-2-deoxy-D-glucose, LmexGT1 had a lower affinity for glucose (K_i of 577 ± 78 μM ; $n=3$), while LmexGT2 and LmexGT3 showed relatively high affinity for glucose (K_i of 59 ± 8 and 123 ± 9 μM , respectively; $n=3$; table 6.1). These results are consistent with the previous characterisations of LmexGT1, LmexGT2 and LmexGT3 for glucose in *L. mexicana* promastigotes, showing that LmexGT1 has a higher K_m for glucose (1.22 ± 0.22 mM) compared to LmexGT2 or LmexGT3 (109 ± 22 μM and 208 ± 40 μM , respectively) (Rodriguez-Contreras et al., 2007). These values were approximately double the K_i values determined by us for the three glucose transporter isoforms.

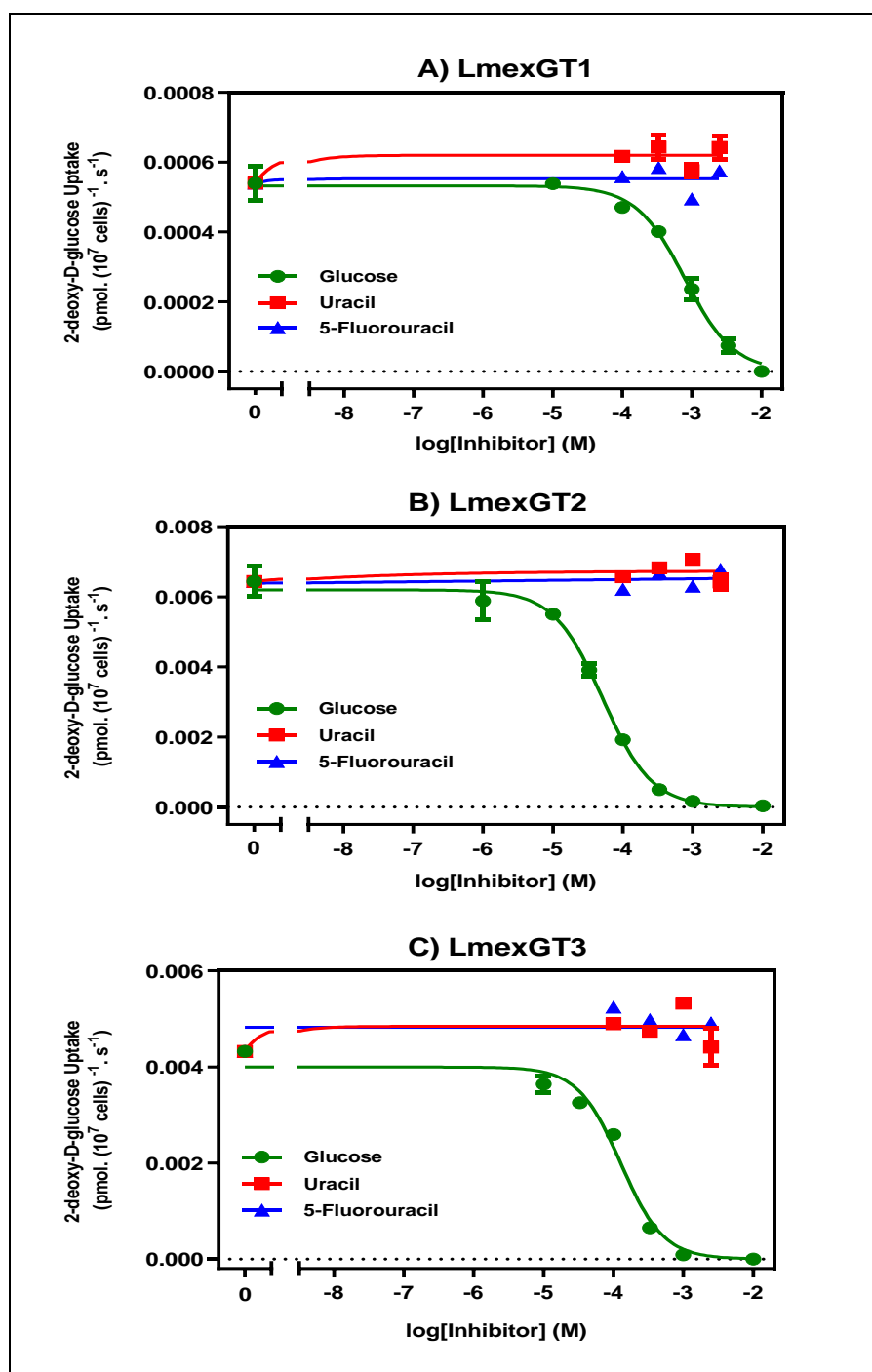


Figure 6.11: Inhibitory effect of various concentrations of unlabelled glucose (●), unlabelled uracil (■) and unlabelled 5-fluorouracil (▲) on the uptake of 0.1 μM of $[^3\text{H}]$ -2-deoxy-D-glucose over 30 seconds by *Lmex-GT1-3 KO + LmexGT1* (A), *Lmex-GT1-3 KO + LmexGT2* (B) and *Lmex-GT1-3 KO + LmexGT3* (C).

Figures show a representative out of three independent experiments in triplicates. Symbols represent the average of triplicate determinations in a single representative experiment and error bars represent \pm SEM.

Moreover, uracil and 5-fluorouracil had no considerable effect on transport mediated by LmexGT1, LmexGT2 and LmexGT3 as none of them inhibited the transport of 0.1 μM of $[^3\text{H}]$ -2-deoxy-D-glucose up to 2.5 mM ($n=2$; Table 6.1). These results clearly confirmed that the effect of D-glucose on 2-deoxy-D-

glucose transport is very different from the effect of uracil and 5-fluorouracil in *L. mexicana* promastigote form (*LmexGT1*, *LmexGT2* and *LmexGT3* as a straightforward glucose transporter).

Table 6.1: K_i for various concentrations of glucose, uracil and 5-fluorouracil on the uptake of 0.1 μM of [^3H]-2-deoxy-D-glucose over 30 seconds by *Lmex-GT1-3 KO* + *LmexGT1*, *Lmex-GT1-3 KO* + *LmexGT2* and *Lmex-GT1-3 KO* + *LmexGT3*. K_i values represent the mean of at least three independent determination in triplicate \pm SEM. N.E: No effect.

Inhibitors	K_i (μM)			n
	<i>LmexGT1</i>	<i>LmexGT2</i>	<i>LmexGT3</i>	
D-glucose	577 \pm 78	58.9 \pm 7.8	123 \pm 9	3
Uracil	N.E (> 2.5 mM)	N.E (> 2.5 mM)	N.E (> 2.5 mM)	2
5-Fluorouracil	N.E (> 2.5 mM)	N.E (> 2.5 mM)	N.E (> 2.5 mM)	2

6.2.5.4 The heterologous expression of the FurD in *Lmex-GT1-3 KO* promastigotes

It has been determined that the introduction of the FurD transporter in the *Lmex-5FURes* and *L. mexicana*-WT does not result in increased sensitivity to 5-FU (Chapter 5). However, high levels of [^3H]-uracil and 5-FU uptake do occur in those cells, and these levels are much higher than those of wild type activity (see sections 5.2.2 and 5.2.3). Thus, the purpose of this section is to examine the effects of expression of FurD in the *Lmex-GT1-3 KO* cell lines on the sensitivity/transport to 5-FU when a confirmed uracil/5-FU transporter is introduced.

6.2.5.5 PCR and qRT-PCR confirmation of the existence of FurD in *Lmex-GT1-3 KO* cells

A plasmid construct used in the expression of *FurD* gene in *Lmex-GT1-3 KO* strain, pHDK254 (Figure 5.7) had been used previously to express of FurD transporter in *Lmex-5FURes* and *L. mexicana*-WT. Following the transfection of episomal pHDK254 plasmid into the *Lmex-GT1-3 KO* strain, PCR was used to verify the presence of pHDK254 vector in several positive clones. The verification process is conducted using HDK340 as reverse primer for the pNUS-

HcN plasmid and HDK531 as forward primer for the *FurD* gene (Figure 6.12). Quantitative real time PCR is performed for the purpose of quantifying the levels of *FurD* gene expression in *Lmex-GT1-3* KO cells in comparison to the control cell lines. All three clones expressing (1, 2 and 3) of *FurD* gene in the *Lmex-GT1-3* KO cells recorded a significant increase in the gene expression signal in comparison to the control *Lmex-GT1-3* KO cells (9.1-fold, 7.6-fold and 6.3-fold; $P < 0.001$, respectively; Figure 6.13).

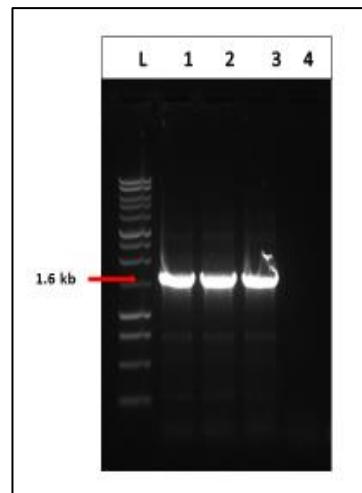


Figure 6.12: Confirmation of the presence of *FurD* gene into *Lmex-GT1-3* KO strain after transfection by using HDK531 as forward primer for *FurD* gene and HDK340 as a reverse primer for pNUS-HcN plasmid.

L: 1kb DNA Ladder (Promega); 1: Clone 1; 2: Clone 2; 3: Clone 3; 4: Non-transfected control (gDNA of *Lmex-GT1-3* KO).

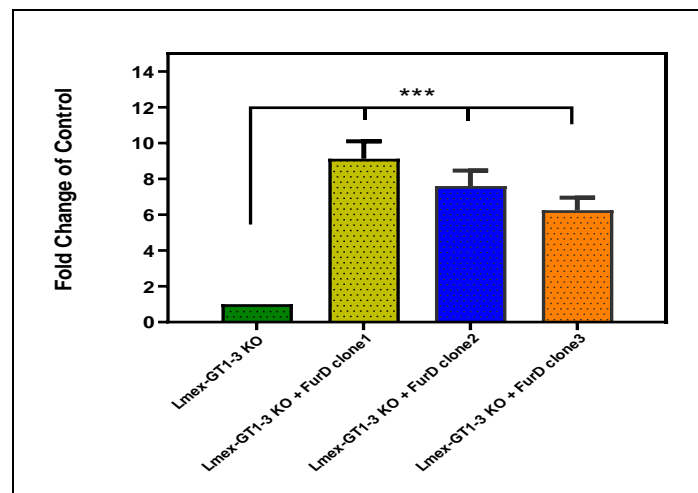


Figure 6.13: The expression levels of *FurD* gene in *Lmex-GT1-3* KO and compared to the control (*Lmex-GT1-3* KO) determined by qRT-PCR.

Levels were corrected against the expression level of the housekeeping gene (*L. mexicana* GPI8). The presented results are the average of 2 cDNA each performed in duplicates, and error bars are \pm SEM. *** $P < 0.001$ by unpaired student's T-test.

6.2.5.6 Drug sensitivity assay with 5-fluorouracil

The sensitivity of the *Lmex-GT1-3* KO cells and the three *FurD* clones in the *Lmex-GT1-3* KO parasites to 5-FU and pentamidine was investigated using the usual Alamar blue assay (Figure 6.14). Results showed a significant increase in the sensitivity of *Lmex-GT1-3* KO + *FurD* clone 1, 2 and 3 to 5-FU (213 ± 48 , 247 ± 54 and 90 ± 9 μ M, respectively) compared with the parental cell lines *Lmex-GT1-3* KO (1460 ± 256 μ M; $n=4$; $P < 0.01$ by unpaired Student's T-test). The susceptibility of clones 1, 2 and 3 to 5-FU was increased 7-fold, 6-fold and 16-fold, respectively. The expression of *FurD* gene did not change the sensitivity to pentamidine in *Lmex-GT1-3* KO cell lines, as the EC_{50} values of *Lmex-GT1-3* KO cells and three clones for *Lmex-GT1-3* KO + *FurD* were almost identical ($n=4$; $P > 0.05$).

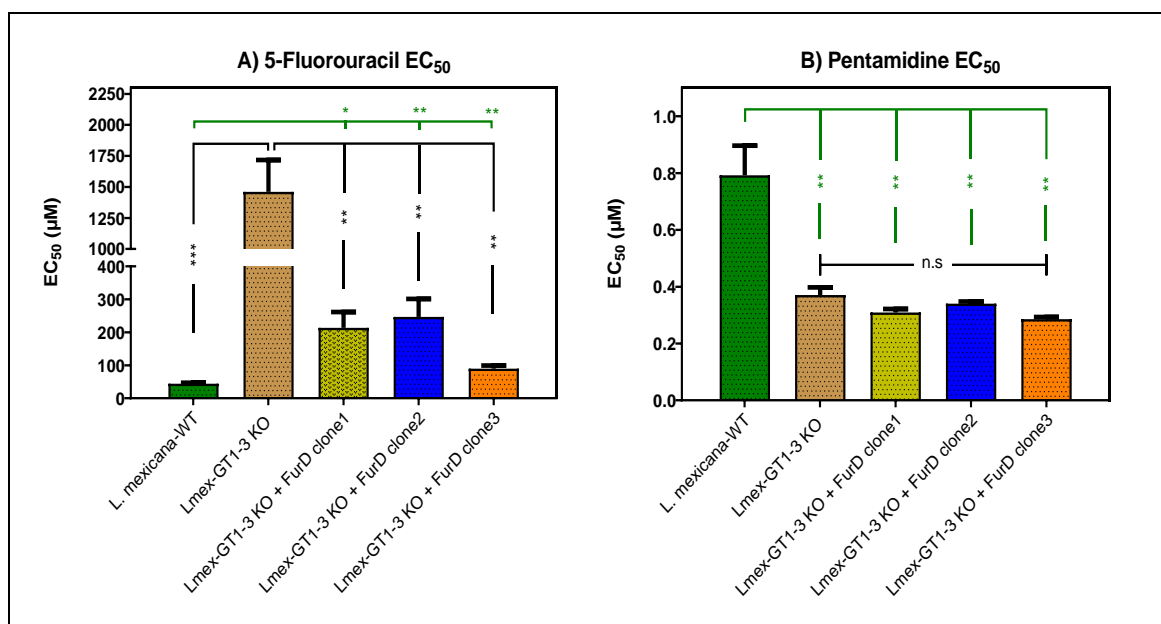


Figure 6.14: Alamar blue drug sensitivity assay of expression of *FurD* gene in *Lmex-GT1-3* KO and *L. mexicana* by using 5-fluorouracil (A) and pentamidine (B).

The mean of four independent determinations is shown \pm SEM. * $P < 0.05$, ** $P < 0.01$ and *** $P < 0.001$ by unpaired Student's T-test.

6.2.5.7 Transport assay with 5-fluorouracil

The transport rate of 0.1 μM of $[^3\text{H}]$ -5-fluorouracil in *Lmex-GT1-3* KO expressing FurD was investigated in order to check whether the introduction of FurD transporter could cause increases in the 5-fluorouracil transport as well (Figure 6.15). This study evaluated the uptake of 0.1 μM of $[^3\text{H}]$ -5-fluorouracil by promastigotes of *L. mexicana* wild-type and found that the transport was linear for at least 120 seconds with a rate of $0.0025 \pm 0.0002 \text{ pmol. (10}^7 \text{ cells)}^{-1} \cdot \text{s}^{-1}$. Indeed, the introduction of FurD in *Lmex-GT1-3* KO cells revealed a very high level of $[^3\text{H}]$ -5-fluorouracil uptake, with a rate of uptake of $0.0056 \pm 0.0004 \text{ pmol. (10}^7 \text{ cells)}^{-1} \cdot \text{s}^{-1}$ and a linear phase over 120 seconds ($P < 0.0001$ by F-test; $n=1$). The uptake of 0.1 μM of $[^3\text{H}]$ -5-fluorouracil by *Lmex-GT1-3* KO parasites was not significantly different from zero ($P > 0.05$, F-test). In both strains, $[^3\text{H}]$ -5-fluorouracil transport was completely inhibited in the presence of 1 mM unlabelled 5-fluorouracil indicating that the uptake was saturable. In conclusion, the effect of expression of FurD in *Lmex-GT1-3* KO increased the rate of transport of $[^3\text{H}]$ -5-FU, even much above the wild type activity, as well as increasing the sensitivity to 5-FU.

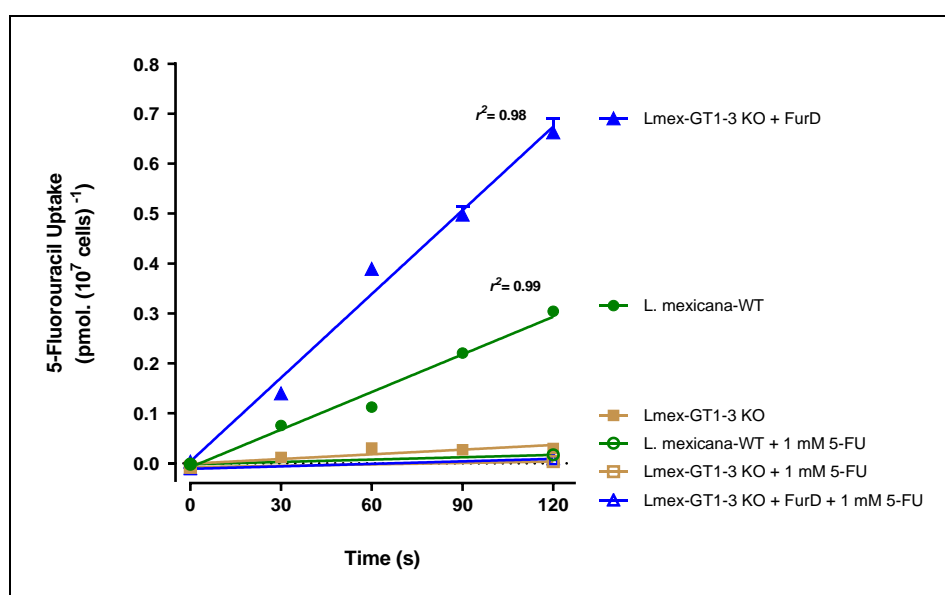


Figure 6.15: [³H]-5-Fluorouracil transport by *L. mexicana*-WT, *Lmex-GT1-3* KO and *Lmex-GT1-3* KO + *FurD*.

Transport of 0.1 μ M of [³H]-5-fluorouracil by *L. mexicana*-WT, *Lmex-GT1-3* KO and *Lmex-GT1-3* KO + *FurD* was measured over 120 seconds in the presence or absent of 1 mM unlabelled 5-fluorouracil. F-test was calculated using Prism 8 GraphPad Software.

6.2.6 Trypanosoma brucei brucei s427-WT procyclic form

The bloodstream forms of *T. b. brucei* is entirely dependent on blood glucose to gain energy by glycolysis (Bayele et al., 2000). For this reason, the procyclic form of *T. b. brucei* is used to determine the growth rate and sensitivity of 5-FU and 6-AU pyrimidine analogues. This section chiefly aims at specifying and characterising the relationship that exists between mechanism of action of 5-FU and glucose metabolism in *T. b. brucei* s427-WT PCF.

6.2.6.1 The assessment of growth rate of *T. b. brucei* s427-WT PCF with and without glucose

In examining how the absence of glucose within the extracellular medium in *T. brucei* Lister s427 PCF affects the growth rate, the growth of *T. b. brucei* procyclic cell lines are assessed in SDM-79 medium supplemented with 10% FBS and 0.6 g/L proline. There was the testing of three different D-glucose concentrations in SDM-79 medium: 1 g/L D-glucose (standard condition), 0.2 g/L of D-glucose and D-glucose-free incubated at 27 °C. After every 24 h, the cell densities were determined, and the cells were passaged every 24 h into fresh medium. Despite the reduction or absence of D-glucose in *T. b. brucei*-s427 WT PCF, there was no difference in the growth rate of the three conditions (Figure 6.16). The conclusion arrived at was that the decreased concentration of D-glucose did not cause any changes in the rate of growth for *T. b. brucei*-s427 wild type PCF *in vitro*.

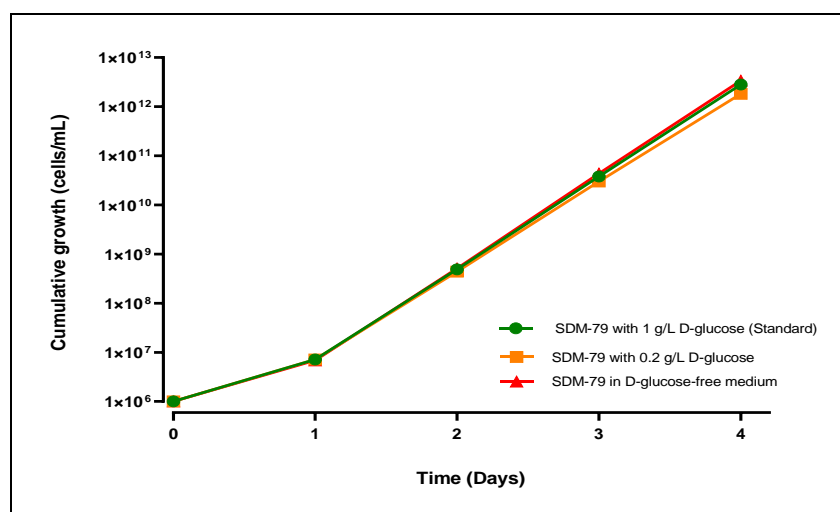


Figure 6.16: The growth rate of *T. b. brucei*-s427 wild type PCF on SDM-79 medium supplemented with 10% FBS, 0.6 g/L proline, and 1 g/L glucose 'standard condition' (●), 0.2 g/L D-glucose (●) and D-glucose free (●), and incubated at 27°C, and cell densities were determined every 24h.

Cells were passaged every 24 hours into a fresh medium. Each data point in this result represents the average of three similar independent determinations.

6.2.6.2 The evaluation of 5-FU and 6-AU EC_{50} of *T. b. brucei* s427 PCF in normal medium, low glucose and glucose-free medium

6-AU is considered to be an inhibitor of pyrimidine *de novo* biosynthesis pathway, specifically an inhibitor of orotidylate decarboxylase in trypanosomes (Jaffe, 1961). For this reason, we test the sensitivity of 6-AU against the *T. b. brucei* s427 PCF cell lines in normal medium, low glucose and glucose-free medium. In Figure 6.17, a biphasic inhibition curve of 6-azauracil shows a depiction that is not typical of a drug sensitivity curve. The situation thus depicts the potential presence of two EC_{50} values for 6-AU. According to the property of 6-AU, the presentation of the first EC_{50} value shows how the cell growth is inhibited by the drug (trypanostatic effect) and the second EC_{50} shows how the cells are killed by drug (trypanocidal effect). In the sensitive test of 6-AU, the three different conditions of growth provide the same results and biphasic inhibition curves. The viability assay with using Alamar blue dye was performed to determine the effects of the presence or absence of D-glucose in SDM-79 medium on sensitivity of the *T. b. brucei* s427 PCF cells to 5-FU and 6-AU, while pentamidine was used as an unrelated control drug (Figure 6.18). The results of the study showed that, in all the three different conditions of growth, no significant difference existed on the sensitivity (normal conditions, 0.2 g/L D-glucose and D-glucose-free) in *T. b. brucei* s427 PCF cells to 5-FU, with an EC_{50}

values of $13 \pm 2.8 \mu\text{M}$, $11 \pm 1.5 \mu\text{M}$ and $6 \pm 0.8 \mu\text{M}$, respectively ($n=4$; $P > 0.05$ by unpaired Student's T-test). There is no significant different in the sensitivity of three different growth conditions of D-glucose to 6-AU ($n=4$; $P > 0.05$ by unpaired Student's T-test). There was no significant difference in the sensitivity to pentamidine for all the three different growth conditions of the *T. b. brucei* s427 PCF cells. It was concluded that, in the extracellular media, neither the absence nor presence of glucose has any effect on the sensitivity of procyclic form of *T. b. brucei* to 5-FU, 6-AU and pentamidine.

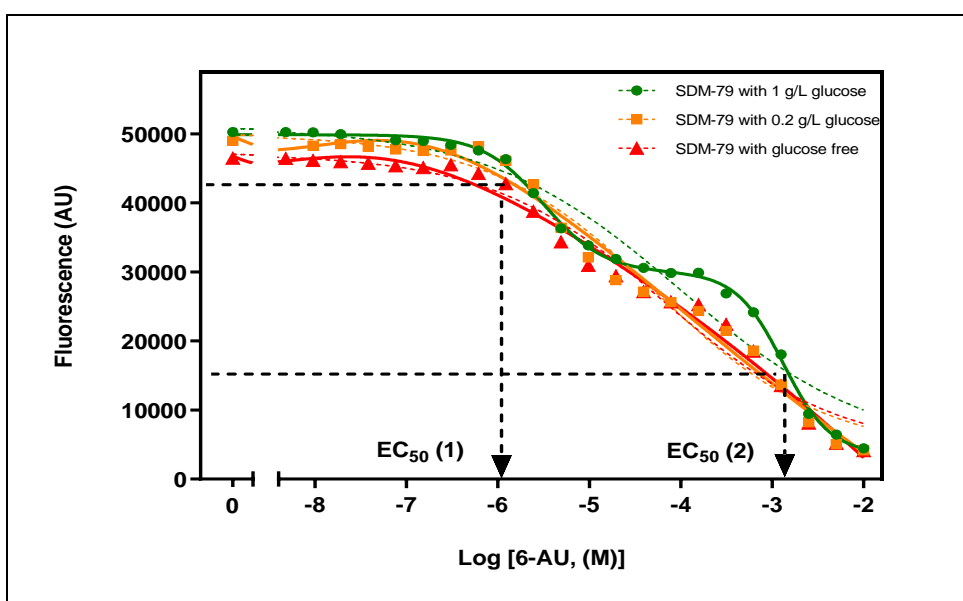


Figure 6.17: The biphasic inhibition curve of *T. b. brucei*-s427 wild type PCF against 6-azauracil by using the Alamar blue fluorescent dye as a representative for the cell number. The trypanostatic effect at low concentrations $\text{EC}_{50} (1)$ was $1218 \pm 83.8 \mu\text{M}$ and the trypanocidal effect at higher concentrations $\text{EC}_{50} (2)$ was $3.50 \pm 1.04 \mu\text{M}$.

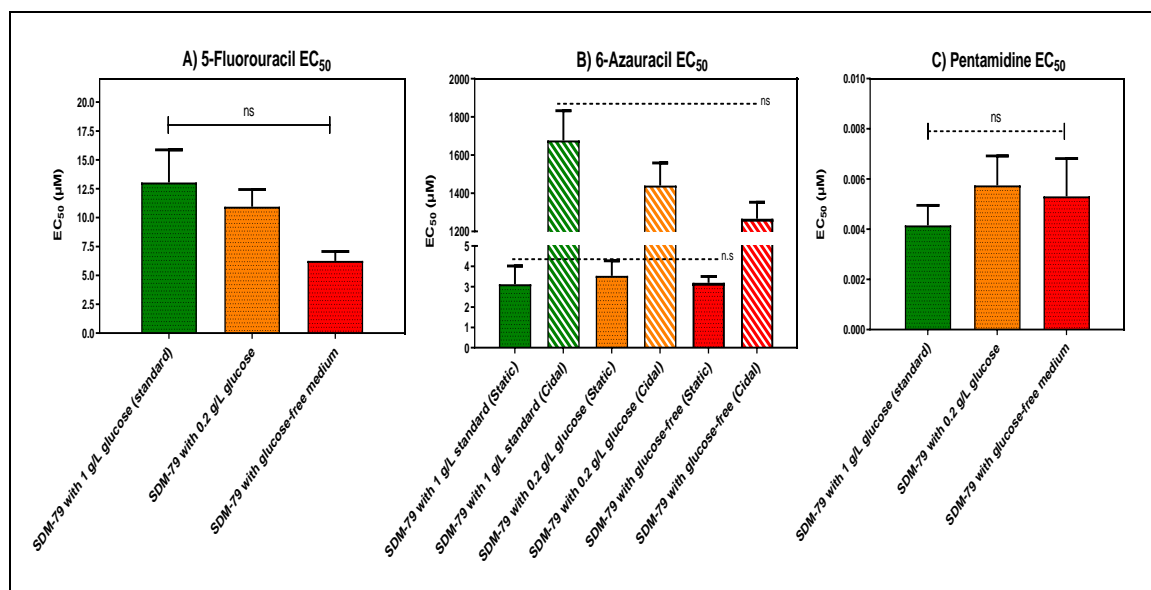


Figure 6.18: The Alamar blue drug sensitivity assay of *T. b. brucei*-s427 wild type PCF on SDM-79 medium supplemented with 10% FBS, 0.6 g/L of proline and three different growth conditions for glucose (1 g/L glucose 'standard condition', 0.2 g/L glucose and glucose free medium) using 5-fluorouracil (A), 6-azauracil (B) and pentamidine (C). The mean of four independent determinations is shown \pm SEM. *P* value was determined by unpaired two-tailed Student's T-test.

6.3 Discussion

Promastigotes and amastigotes of *L. mexicana* are supplied with energy by glucose as a primary nutrient and building blocks enhancing the synthesis process of different biomolecules. Glucose and amino acid catabolism are relied upon by the procyclic promastigotes, while the utilisation of amino acids is increased in the later stages of promastigote development (Inbar et al., 2017; Landfear, 2010). It is through the pentose phosphate pathway and glycolysis that glucose is metabolised (Barrett, 1997; Landfear, 2011). Glycolysis is a pathway responsible for converting one glucose molecule to two pyruvate molecules following the generation of two ATP molecules (Saunders et al., 2011; Drew et al., 2003). It is both through the three high-affinity glucose transporters, LmexGT1-3, and the low-affinity glucose transporter LmexGT4 that *L. mexicana* promastigotes take up exogenous glucose. However, the major sources of glucose are LmexGT1-3, but the situation is not exclusive for the *L. mexicana* promastigotes since *Lmex-GT1-3* Knockout cell lines are still grown in culture (Burchmore et al., 2003a; Feng et al., 2013; Feng et al., 2009). The situation indicates that *Lmex-GT1-3* KO cells have the potential to up-regulate the alternative lower affinity glucose

transporter LmexGT4 as an alternative source of carbon and energy, as well as use amino acids for their energy needs (Feng et al., 2013; Landfear, 2011).

There is a close relationship between the three glucose transporters LmexGT1-3, but they each display distinct biological and functional properties, including differential localisation, substrate specificity, and developmental stage expression (Burchmore and Landfear, 1998; Akpunarlieva and Burchmore, 2017). It was confirmed through multiple alignments that the three LmexGT transporters represented up to 90% identity in the sequence of amino acids due to their differences at the C and N terminal domains (Burchmore et al., 2003a). The separate and independent re-expression of the LmexGT1, LmexGT2, and LmexGT3 into *Lmex-GT1-3* KO cells enables the uptake of glucose, fructose, galactose and mannose. LmexGT1 is a low-affinity glucose transporter while LmexGT2 and LmexGT3 are high-affinity glucose transporters. Fluorescent microscopy showed that LmexGT1 is localised mainly in the flagellum whereas LmexGT2 and LmexGT3 are predominantly localized on the plasma membranes (Burchmore et al., 2003a; Rodriguez-Contreras et al., 2007).

Previous work in our laboratory's RNA-seq and RIT-seq analyses of the 5-FU resistant cell lines have identified candidate genes for uracil transporter including glucose transporter 2A and glucose transporter THT2 in *T. b. brucei* BSF. The most striking results that emerged from the RIT-seq and RNA-seq data is the presence of glucose transporter 2A in both the RNA-sequencing data and the genome-wide RNA-interference screen. Therefore, there is the possibility that the knockdown or down-regulation of either one or some of these glucose transporter genes in 5-FU resistant cell lines can be responsible for causing increased levels of resistance to 5-FU. Several genes encoding for glucose transporters were identified up-regulated in *Tbb-5FURes* and *Lmex-5FURes* using RNA-sequencing. The conclusion made was that there is a high probability that *Lmex-5FURes* and *Tbb-5FURes* up-regulated some glucose transporter genes to help in compensating for the glucose transporter genes that had been down-regulated. The purpose of this compensation is to create a balance in the provision of sufficient amounts of glucose to the cells. A glucose transporter *null* mutant line, *Lmex-GT1-3* KO cells, was created by Burchmore et al. (2003a)

through the deletion of the glucose transporters locus which including *LmexGT1*, *LmexGT2*, and *LmexGT3* genes in *L. mexicana* promastigotes.

Thus, we decided to determine the sensitivity of the full knockout of glucose transporter genes in *L. mexicana* against 5-fluorouracil. The result revealed a significant reduction in the sensitivity of the double knockout of *LmexGT1-3* genes in *L. mexicana* to 5-FU when compared to the wild type cell lines. Using radiolabelled 5-FU and uracil, transport assays were performed in *L. mexicana*-WT and *Lmex-GT1-3* KO strain. The results showed that the *Lmex-GT1-3* KO cells no longer accumulate uracil and 5-FU. The situation is evidence showing that the uptake of pyrimidine in *L. mexicana* promastigotes is either mediated or regulated by the glucose transporters. The Alamar blue assay results from the *L. mexicana*-WT in glucose free medium have demonstrated that the presence or absence of glucose in the medium does not influence the sensitivity to 5-FU. Similarly, the presence or absence of glucose in the extracellular medium does not affect the sensitivity of *T. b. brucei* procyclic form to 5-FU and 6-AU. The results of our study show that the *Lmex-5FURes* cell lines are still maintaining the glucose transport activity, but lost uracil/5-FU transporter. Thus, it is not the uptake of glucose that is important for the uptake of uracil, but the presence of the transporters, occupied or not.

There was a significant increase of the sensitivity to 5-FU in the re-expression of individual *LmexGT* in *Lmex-GT1-3* KO cells but not quite back to wild-type cells. After the introduction of the glucose transporter genes, all the three genes did appear to have a very similar ability of functioning with regards to the (regulation of) uptake of 5-fluorouracil and uracil (restoring uptake to ~50% of 5-FU and ~30% of uracil uptake of wild type, respectively). There were no measurable effects of 5-fluorouracil and uracil on glucose transport by *LmexGT1*, *LmexGT2* and *LmexGT3*, showing that none of them caused any inhibition to the transport of 0.1 μ M of [3 H]-2-deoxy-D-glucose up to 2.5 mM. Therefore, these results clearly confirmed that the effect of D-glucose on 2-deoxy-D-glucose transport is very different from the effect of uracil and 5-FU on the same process in *L. mexicana* promastigotes and that *LmexGT1*, *LmexGT2* and *LmexGT3* are straightforward glucose transporters.

An evaluation of the affinity of LmexGT1, LmexGT2 and LmexGT3 for glucose was conducted by competition with 0.1 μM of [^3H]-2-deoxy-D-glucose. The result showed that LmexGT1 has a lower affinity for glucose (K_i of $577 \pm 78 \mu\text{M}$), while LmexGT2 and LmexGT3 showed higher affinity for glucose (K_i of 59 ± 8 and $123 \pm 9 \mu\text{M}$, respectively). These results are consistent with the previous characterisations of LmexGT1, LmexGT2 and LmexGT3 for glucose in *Lmex-GT1-3* KO parasites, showing that LmexGT1 has a higher K_m for glucose compared to LmexGT2 or LmexGT3 (Rodriguez-Contreras et al., 2007). These K_m values were within 2-fold of the K_i values determined by us. The sequence of the *L. donovani* LdGT4 is orthologous to *L. mexicana* LmexGT4, and shares 66.5% of the nucleotide identity. LdGT4 expressed in *Xenopus oocytes* was estimated to have a K_m of $\sim 150 \text{ mM}$, which was an indication that LmexGT4 is a very lower-affinity substrate for D-glucose (Feng et al., 2009; Langford et al., 1995) and that its primary function may in fact not be the uptake of glucose, especially considering that the promastigotes of GT1-3-KO strain appear to be truly *null* for glucose uptake, at least at the assay conditions and label concentration used. In *L. mexicana* wild type, the amastigote and promastigote glucose transporter have a high affinity for glucose, with a K_m value of $24 \pm 8 \mu\text{M}$ and $29 \pm 3 \mu\text{M}$ respectively. However, the V_{max} of amastigote for glucose uptake was $0.132 \text{ pmol} \cdot (10^7 \text{ cells})^{-1} \cdot \text{s}^{-1}$ and ~ 20 -fold lower than the V_{max} of promastigote ($2.21 \text{ pmol} \cdot (10^7 \text{ cells})^{-1} \cdot \text{s}^{-1}$). In amastigote and promastigote forms, the similar values of K_m for glucose transport is a likely suggestion of the expression of the same transporter in both of these developmental stages (Burchmore and Hart, 1995).

The findings show that the uptake of uracil and glucose by separate transporters in *L. mexicana* promastigotes is an indication that LmexGT1, LmexGT2 and LmexGT3 are straightforward glucose transporting genes and not the 5-FU transporter. Considering that both 5-FU and uracil are pyrimidines, it could be speculated that the metabolism of glucose regulates the uptake of uracil and 5-FU, as the pathways overlap in the process of glycosylation (e.g. UDP-glucose, UDP-galactose, UDP-N-acetylglucosamine) and lipid biosynthesis (CDP-ethanolamine, CDP-choline). The effect of introduction of FurD transporter in *Lmex-GT1-3* KO cells increased the rate of transport of [^3H]-5FU and reversed 5-FU resistance in the *Lmex-GT1-3* KO cells. It therefore appears that the effect of

the LmexGT knockout is to severely restrict 5-FU uptake, because they are still sensitive to the drug when FurD transporter is introduced. Also, the activity of the FurD transporter, unlike the *Leishmania* uracil transporter, is not regulated by the presence or absence of the glucose transporters. The study by Ortiz et al. (2010) indicated that the deletion of the purine nucleobase transporter 3 (NT3) or both NT3 and the nucleoside transporter 2 (NT2) in *L. major* parasites resulted in strong up-regulation of uridine and adenosine uptake mediated by the nucleoside transporter 1 (NT1) and also induced up to a 200-fold increase in the level of the NT1 protein but not mRNA. Another study by Seyfang and Landfear (1999) showed that a strong up-regulation of glucose (5-fold), adenosine (11-fold) or myo-inositol (25-fold) uptake was found when *Leishmania* species were depleted of the respective substrates during culture. When *T. brucei* PCF for tubercidin resistance were subjected to RNAi library screening, it was reported that silencing of glucose transporters conferred resistance to the toxic levels of tubercidin (Drew et al., 2003). The study from Drew et al. (2003) with functionally expressed THT1 and THT2 in *Xenopus oocytes* showed that the uptake of [³H]-tubercidin and [³H]-adenosine was not significantly increased, while there was a significant increase of [³H]-glucose. Tubercidin (7-deazaadenosine), as a substrate for adenosine kinase in mammalian cells, is reported to be incorporated into DNA and RNA. However, the inhibition of tubercidin to phosphoglycerate kinase specifically targets the glycolysis pathway and kills procyclic trypanosomes (Drew et al., 2003; Hulpia et al., 2019). However, RNAi silencing of the glucose transporters occurs over several days. The lengthy duration consequently gives time to tubercidin resistant cell lines to increase their reliance on such amino acids as proline, which serves both as energy source and carbon (Drew et al., 2003), and thus reduces the need for glycolysis. Ali et al. (2013a) found that the level of 5F-UDP-glucose and of 5F-UDP-N-acetylglucosamine in *Tbb-5FUR* cells treated with 5-FU was 6.5-fold reduced relative to *T. b. brucei* s427-WT cells treated with 5-FU. The situation is an indicated that changes in the glycosylation pathway could make substantial contributions to 5-FU resistance. The most important conclusion from this investigation is that glucose transporters are required for the expression of functioning of uracil/5-FU transporters in *L. mexicana* promastigotes.

7 Cloning and functional expression of *T. cruzi* ENT in *L. mexicana*-Cas9^{ΔNT1} promastigotes

7.1 Introduction

Chagas' disease, also known as American trypanosomiasis, is an illness that threatens the life of many people in the endemic regions. Chagas' disease is caused by the protozoan *Trypanosoma cruzi*. The condition is named after a Brazilian physician, Carlos Chagas, who discovered the disease in 1909. Chagas' disease is transmitted to animals as well as human beings by an arthropod vector (triatomine bugs) (Rassi Jr et al., 2010; Pérez-Molina and Molina, 2018). The disease is named as one of the 13 most neglected tropical diseases (NTD) by the World Health Organisation (WHO). Approximately 9 million individuals are affected by American trypanosomiasis. Regarding this, people from Mexico, Central America, and South America are most affected, but the infection is also increasingly prevalent in the southern United States. However, most of the people remain unaware of the infection. If Chagas' disease is left untreated, it may result in disabilities and conditions that are life-long, resulting in the poor quality of life and, in complicated cases, death (Souto et al., 2019). Currently, there are no vaccines for the treatment of Chagas' disease. However, nifurtimox and benznidazole are the only drugs possessing a proven efficacy against the infections of *T. cruzi* (Bern, 2015; Pérez-Molina and Molina, 2018). Concerning this, nifurtimox and benznidazole are not effective in infections that are recognised as chronic. Therefore, they are only useful for the acute phases of the infection. Some strains of *T. cruzi* have natural resistance to these drugs, thus, novel drugs with better efficacy for the protozoa with minimal side effects for the host are needed (Filardi and Brener, 1987).

.In kinetoplastid parasites such as *T. cruzi*, *Leishmania* spp and African trypanosomes, only members of the ENT family have been found to be involved in nucleoside and nucleobase uptake (Campagnaro and de Koning, 2020; De Koning et al., 2005). Apart from their role in nucleoside salvage, the ENT transporters have been shown to play a vital role in the pharmacology of protozoan chemotherapy, particularly of African trypanosomes, but also of *Leishmania* (Carter et al., 1999; Geiser et al., 2005; Al-Salabi and de Koning, 2005; Rodenko et al., 2007; Kazibwe et al., 2009; Stewart et al., 2010; Vodnala

et al., 2013; Munday et al., 2015; Ranjbarian et al., 2017). These chemotherapeutic compounds include purine and pyrimidine nucleoside analogues (5-fluoro-2'-deoxyuridine, idoxuridine, cordycepin, aristeromycin and neplanocin), as well as purine (allopurinol) and pyrimidine (5-fluorouracil) nucleobases.

Through the comparison of genomic of *T. cruzi* ENT gene sequences with sequences of other trypanosomatids, Campagnaro et al. (2018b) indicated the presence of four ENT genes in *T. cruzi*; for instance, TcrNB1, TcrNB2, TcrNT1, and TcrNT2 genes. Three of the four genes, TcrNB1, TcrNT1 and TcrNT2 were cloned and characterised in *T. brucei* procyclic TbNBT-KO cells. However, TcrNB2 did not show any detectable activity with all substrates that were tested. Campagnaro et al. (2018b) reported that TcrNB1 has a high affinity for hypoxanthine and guanine. TcrNT1 is a high affinity inosine and guanosine transporter, whereas TcrNT2 has an affinity for 2'-deoxypyrimidines with K_m of 0.223 μ M for thymidine. Notably, the 4 ENT genes in *T. cruzi* do not transport adenosine or adenine (Campagnaro and de Koning, 2020). Thus, two issues remain outstanding: the identity of the *T. cruzi* adenosine transporter and the substrate of TcrNB2. It should be noted that adenosine uptake would be hard to detect in the *T. brucei* expression system, due to the very active P1 transport system.

In *L. mexicana* promastigotes, nucleoside transporter 1 (LmexNT1) mediates the uptake of adenosine as well as pyrimidine nucleosides (Alzahrani et al., 2017). More importantly, the locus of the NT1 comprises two similar genes. These genes are *NT1.1* and *NT1.2* (Table 7.1). According to Alzahrani et al. (2017) posits the sensitivity of NT1.1 from *L. major* and *L. mexicana* to inhibition by uracil, which was then named uridine-uracil transporter 1 (UUT1). In these species, NT1.2 will carry the NT1's title.

Thus, the research that is linked with the previous study by (Campagnaro et al., 2018b), cloned TcrNT2 and TcrNB2 in *L. mexicana*-Cas9 nucleoside transporter 1 knockout cell lines (*L. mexicana*-Cas9 ^{Δ NT1}) hence, assessing its transport activity.

Another objective of this study is to continue working on the characterisation of TcrNT2 and TcrNB2 transporters to establish if they can be used in the drug delivery system. The *T. cruzi* being a very pathogenic parasite poses a great challenge in working with its cellular culture. Additionally, it was not possible to culture the *T. cruzi* parasites in the research laboratory at University of Glasgow. Given that almost the entirety of nucleoside transport studies in trypanosomatids has been performed on *Leishmania* and *T. brucei* spp., we decided to rationally characterise the TcrNT2 and TcrNB2 from *T. cruzi*.

Table 7.1: Annotation of the nucleoside transporter 1 (LmexNT1) in the genome of *L. mexicana* M379 promastigote form.

Gene ID	Annotation	Chromosome	TM domains	Transcript length	Name	Identity
LmxM.15.1230	Nucleoside transporter 1, putative	15	11	1476 bp	NT1.1	98.9%
LmxM.15.1240	Nucleoside transporter 1, putative			1476 bp	NT1.2	

7.2 Results

7.2.1 PCR and qRT-PCR confirmation of knockout of NT1 in *L. mexicana*-Cas9 by using CRISPR technique

In order to eliminate the transport of adenosine and pyrimidine nucleoside mediated by LmexNT1, we knocked out the cluster of two *tandem* arrayed NT1.1 and NT1.2 genes encoding for LmexNT1 transporter on chromosome 15 in *L. mexicana*-Cas9^{ΔNT1} cells by using the CRISPR-Cas9 system (Beneke et al., 2017; Beneke and Gluenz, 2019) (Figure 7.1). The nucleotide sequence alignment results of the NT1.1 and NT1.2 genes in *L. mexicana* promastigotes, showed a high level of identity, 98.98%, as presented in Appendix 9. In this study, we used the genome editing CRISPR-Cas9 system in *L. mexicana* promastigotes following the protocols designed by (Beneke et al., 2017). Briefly, the deletion of the NT1 locus requires the amplification of 5' sgRNA-NT1 and 3' sgRNA-NT1 by using HDK1508 and HDK1510 as forward primers, respectively; and HDK1502 as reverse

primer that serves as template. 5' sgRNA-NT1 and 3' sgRNA-NT1 were amplified to direct *Cas9* to cut immediately upstream (5') or downstream (3') of the target locus of *NT1*. The presence of the expected product (~120 bp for both 5' sgRNA-NT1 and 3' sgRNA-NT1) was verified by running on 2% of agarose gel to be observed visually (Figure 7.2A). To create CRISPR plasmids specific to the target locus of *NT1*, pTBlast-NT1 and pTPuro-NT1 were amplified using HDK1507 as forward primer and HDK1509 as reverse primer; and pTBlast and pTPuro plasmids served as template to amplify the blasticidin and puromycin resistance markers for the *NT1* region. The presence of the expected product (~1.7 kb for pTBlast-NT1 and ~1.8 kb for pTPuro-NT1) was verified by running The PCR products on 1% of agarose gel to be seen visually under UV light (Figure 7.2B).

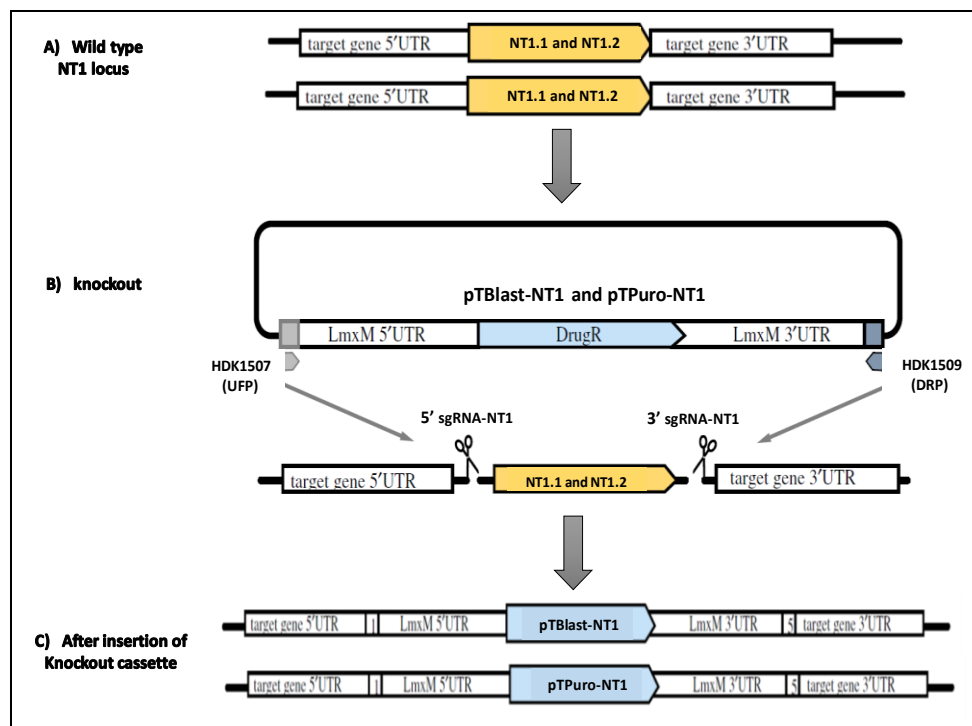


Figure 7.1: Workflow of CRISPR-Cas9 rapid gene knockout used for the replacement of the *NT1* locus on chromosome 15 containing a *tandem* array of two nucleoside transporter 1 genes (*NT1.1* and *NT1.2*) in *L. mexicana*-*Cas9*. Abbreviations are described in the text. Adapted from Beneke et al. (2017).

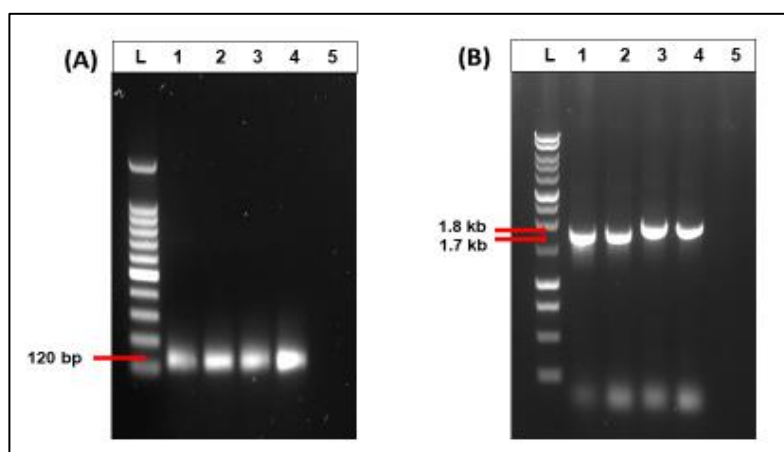


Figure 7.2: PCR amplification of 5' sgRNA-NT1 and 3' sgRNA-NT1 templates for knockout of *NT1* locus in *L. mexicana*-Cas9; and PCR amplification of blasticidin and puromycin resistance markers.

A) PCR amplification of 5' sgRNA-NT1 and 3' sgRNA-NT1 templates for knockout of *NT1* region (*NT1.1* and *NT1.2* genes) in *L. mexicana*-Cas9. L: 100 bp DNA ladder (Promega); 1 and 2: 5' sgRNA-NT1 (~120 bp); 3 and 4: 3' sgRNA-NT1 (~120 bp); Negative control (No sgRNA scaffold). **B)** PCR amplification of blasticidin and puromycin resistance markers. L: 1 kb DNA ladder (Promega); 1 and 2: Blasticidine-NT1 (~1.7 kb); 3 and 4: Puromycin-NT1 (~1.8 kb); Negative control (No genomic DNA).

To verify the loss of *NT1* locus in drug-resistant transfectants diagnostic PCR was performed to amplify PCR products within the open reading frame of the *NT1* locus, using primers that are unique to the *NT1* locus. A region of the *NT1* amplicon was amplified with genomic DNA-specific primers, using HDK1523 as forward primer and HDK1524 as reverse primer, and PCR products were run on 1% of agarose gel to be observed visually. PCR diagnostics of the *L. mexicana*-cas9 and *L. mexicana*-Cas9^{ΔNT1} cells showing the approximate expected presence and absence of the *NT1*-specific bands (~1 kb) (Figure 7.3).

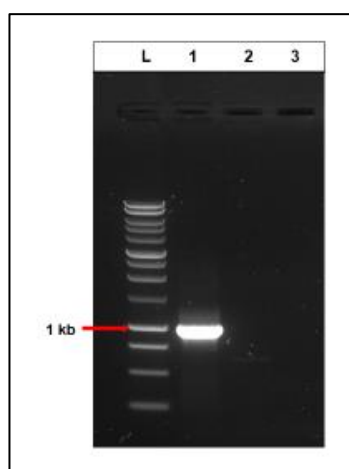


Figure 7.3: PCR validation of knockout of *NT1* region in *L. mexicana*-Cas9 by using CRISPR-Cas9 system.

L: 1kb DNA Ladder (Promega); 1: *L. mexicana*-Cas9; 2: *L. mexicana*-Cas9^{ΔNT1} 3: Negative control (No genomic DNA).

Confirmation of fold decreases of gene mRNA level due to the deletion of a double *NT1* region was assessed using qRT-PCR and gene expression was normalised to GPI-8 expression in *L. mexicana*. From the below Figure 7.4, we can see the mRNA levels of the *L. mexicana*-Cas9 cell lines are 1 as the endogenous double alleles are still existence. However, in *L. mexicana*-Cas9^{ΔNT1}, the gene expression of the *NT1* locus could not be detected by qRT-PCR confirming the complete loss of the *NT1* region in *L. mexicana*-Cas9^{ΔNT1} and thus the transcription into mRNA.

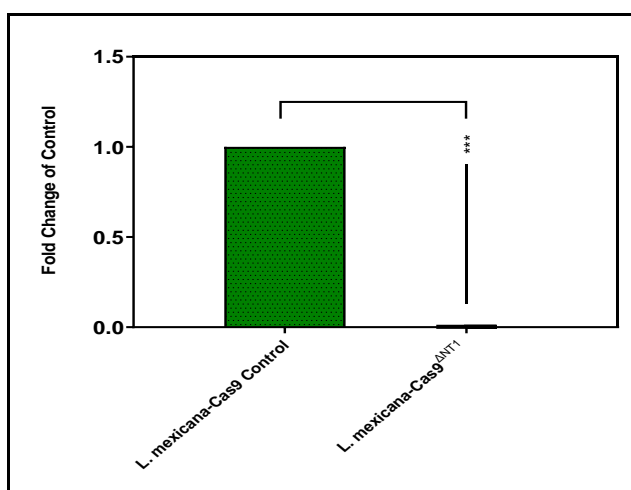


Figure 7.4: The expression levels of *NT1* in *L. mexicana*-Cas9^{ΔNT1} compared to the control (*L. mexicana*-Cas9) determined by qRT-PCR. Levels were corrected against the expression level of the housekeeping gene (*L. mexicana* GPI8).

The presented results are the average of 2 cDNA preparations, each performed in duplicate, and error bars are \pm SEM. ***, $P < 0.001$ by unpaired student's T-test.

7.2.2 Confirmation of tubercidin resistance phenotype in *L. mexicana*-Cas9^{ΔNT1}

As a cytotoxic adenosine analogue for *Leishmania*, tubercidin is transported by the NT1 transporter (Scott, 2008). In the determination of EC₅₀ of the tubercidin resistant cells (*L. mexicana*-Cas9^{ΔNT1}), the Alamar blue assay was applied to verify if the clone is resistant to tubercidin before performing the transport assays; the assay was performed in parallel with the *L. mexicana*-Cas9 cells. Throughout the assessment, pentamidine was used as the specific control.

Tubercidin showed anti-leishmanial activity against *L. mexicana*-Cas9 promastigotes, with an average EC₅₀ value of $0.43 \pm 0.15 \mu\text{M}$ (n=4) (Figure 7.5). On the other hand, *L. mexicana*-Cas9^{ΔNT1} cells were becoming highly resistant to tubercidin and displayed an average EC₅₀ value of $25.9 \pm 1.9 \mu\text{M}$ (n=4). When comparing *L. mexicana*-Cas9^{ΔNT1} to the parental cell lines, *L. mexicana*-Cas9^{ΔNT1} was thus 60-fold more resistant to tubercidin ($P < 0.0001$). In contrast, the sensitivity of *L. mexicana*-Cas9 and *L. mexicana*-Cas9^{ΔNT1} to pentamidine was not significant different ($P > 0.05$). These results clearly confirmed that *L. mexicana*-Cas9^{ΔNT1} had lost NT1 transport activity, with NT1 null mutants becoming resistant to very high concentrations of tubercidin *in vitro*.

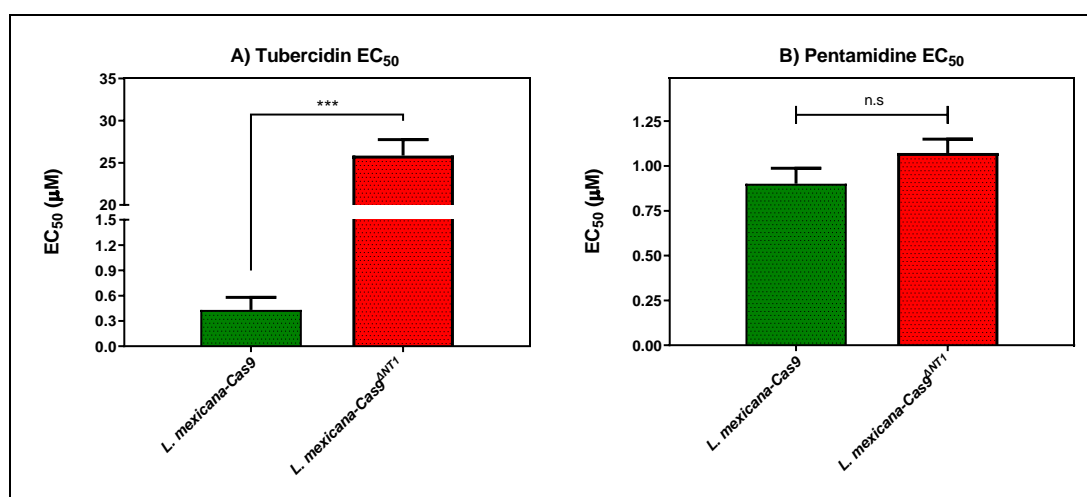


Figure 7.5: Alamar blue drug sensitivity assay of the deletion of LmexNT1 in *L. mexicana*-cas9 by using tubercidin (A) and pentamidine (B) as positive control. The mean of four independent determinations is shown \pm SEM. *** $P < 0.001$ by unpaired Student's T-test.

7.2.3 Confirmation of the abolition of adenosine and thymidine uptake in *L. mexicana*-Cas9^{ΔNT1}

We assessed adenosine and thymidine transport in the *L. mexicana*-Cas9 and *L. mexicana*-Cas9^{ΔNT1} cell lines. Figure 7.6A shows that the uptake of $0.1 \mu\text{M}$ of [³H]-adenosine by *L. mexicana*-Cas9 cells had a high rate of adenosine uptake and thus became non-linear within a second, with metabolism apparently limiting the rate of uptake. In contrast, the transport of $0.1 \mu\text{M}$ of [³H]-adenosine by *L. mexicana*-Cas9^{ΔNT1} promastigotes was virtually abolished (~98%) and became statistically identical to the uptake in the presence of 1 mM

unlabelled adenosine ($P > 0.05$), so it is clear that the *L. mexicana*-Cas9^{ΔNT} cells have lost at least the high affinity adenosine transport activity (LmexNT1) (if *Leishmania* expresses any low affinity adenosine transporter it has not been reported and we found no evidence for it). We similarly found that the transport of 0.05 μM of [³H]-thymidine was greatly reduced in *L. mexicana*-Cas9^{ΔNT1} cells compared with *L. mexicana*-Cas9, with a rate of uptake 0.00004 ± 0.000006 pmol. (10⁷ cells)⁻¹.s⁻¹ (Figure 7.6B). Thymidine transport by *L. mexicana*-Cas9^{ΔNT1} cells were reduced by ~85% but still significantly different from zero (F-test, $P = 0.026$), meaning the little transport seen by the *L. mexicana*-Cas9^{ΔNT1} strain is not negligible, and it was higher than the saturation control with 1 mM unlabelled thymidine. This could be taken as preliminary evidence of a low affinity secondary transporter for thymidine, but this would need further investigation. Knockout of LmexNT1 in *L. mexicana*-Cas9 promastigote form completely abolished the uptake of adenosine and greatly reduced thymidine uptake. These findings agree with the Alamar Blue data (Figure 7.5, above) which showed that *L. mexicana*-Cas9^{ΔNT1} cell lines became highly resistant to tubercidin.

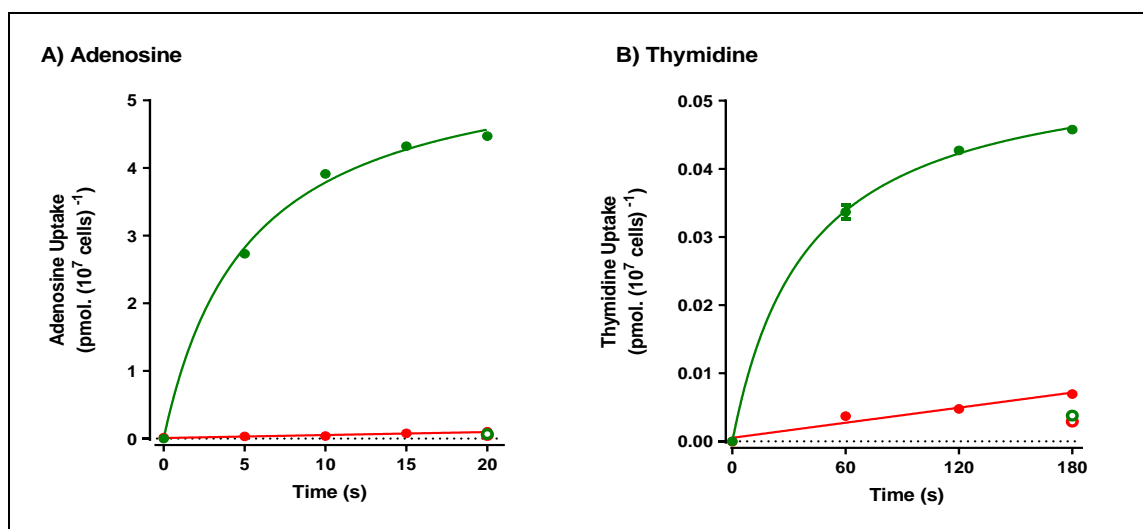


Figure 7.6: [^3H]-Adenosine and [^3H]-Thymidine transport by *L. mexicana-cas9* and *L. mexicana-Cas9^{ΔNT1}*.

A) Transport of 0.1 μM of [^3H]-adenosine by *L. mexicana-cas9* (●) and *L. mexicana-Cas9^{ΔNT1}* (●) was measured over 20 s in the presence or absence of 1 mM unlabelled adenosine (○) and (○) respectively. B) Transport of 0.05 μM of [^3H]-thymidine by *L. mexicana-cas9* (●) and *L. mexicana-Cas9^{ΔNT1}* (●) was measured over 180 seconds in the presence or absence of 1 mM unlabelled thymidine (○) and (○) respectively. Symbols represent the average of triplicate determinations in a single representative experiment and error bars represent \pm SEM. F-test was determined by GraphPad Prism 8.

7.2.4 The heterologous expression of TcrNT2 in *L. mexicana-Cas9^{ΔNT1}*

In a phylogenetic analysis of *T. cruzi* ENT transporters with other trypanosomatids (*Leishmania* spp., *T. brucei* and *T. congolense*), TcrNT2 is grouped close to the *Leishmania* NT1 transporter, which transports pyrimidine nucleosides and adenosine. Furthermore, it possesses a structural similarity to the *Leishmania* NT1 transporters which supports that the TcrNT2 transporter would take part in the transportation of pyrimidine nucleosides and adenosine (Campagnaro et al., 2018b). Using this information, TcrNT2 transporter was expressed in a model cell line, *L. mexicana-Cas9^{ΔNT1}*, to continue the characterisation of its transporter activity, and in testing the susceptibility of the TcrNT2 expressing cells to adenosine and pyrimidine analogues. We also test the possibility of using *L. mexicana-Cas9^{ΔNT1}* promastigotes as a surrogate system for the expression of TcrNT2 transporters of *T. cruzi*, particularly transportation of thymidine through *L. mexicana-Cas9^{ΔNT1}* cells indicated a strong reduction of approximately ~85%.

7.2.4.1 PCR confirmation of the presence and growth rate of TcrNT2 in *L. mexicana-Cas9^{ΔNT1}*

Using HDK1551 as forward primer while HDK1552 as reverse primer, the *TcrNT2* gene was amplified from plasmid pHDK222 using PCR. The pNUS-HcN plasmid was used to express the *TcrNT2* gene in the *L. mexicana-Cas9^{ΔNT1}* (Tetaud et al., 2002). The pNUS-HcN plasmid as well as *TcrNT2* gene were digested using *Bgl*II and *Xho*I restriction enzymes; the digested *TcrNT2* gene was ligated, using T4 DNA ligase, into the digested pNUS-HcN plasmid to generated plasmid pHDK270 (Figure 7.7). The integration of *TcrNT2* gene into pHDK270 vector was verified by

diagnostic digest with *Bgl*II and *Xho*I, which resulted in a band of ~6.2 kb for the plasmid and *TcrNT2* gene band at ~1.4 kb (Figure 7.8A). After transfection of the pHDK270 plasmid into *L. mexicana-Cas9^{ΔNT1}*, PCR was applied to verify the existence of the pHDK270 plasmid in positive clones, using forward primer HDK1551 for *TcrNT2* gene and HDK340 as reverse primer for the pNUS-HcN plasmid sequence (Figure 7.8B).

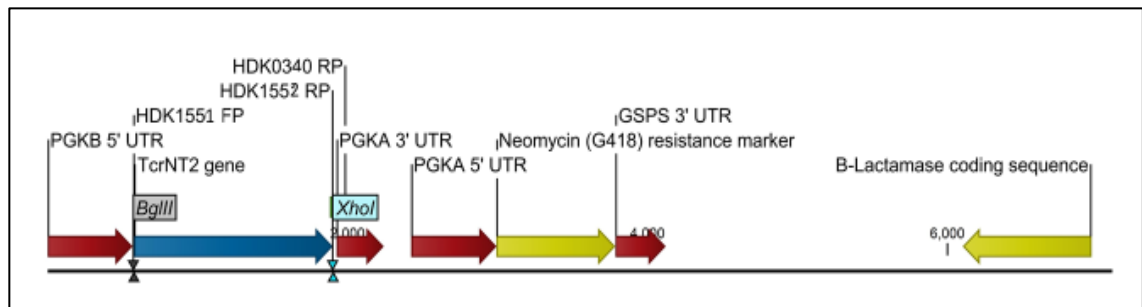


Figure 7.7: Plasmid map of pHDK270 vector for the heterologous expression of *T. cruzi* high-affinity thymidine transporter (*TcrNT2*) in *L. mexicana-Cas9^{ΔNT1}* cells.

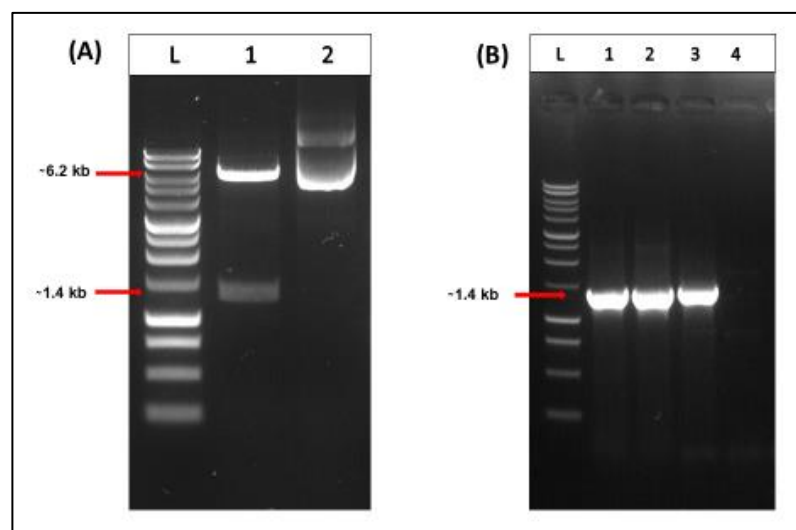


Figure 7.8: Restriction digest products for pHDK270 plasmid and confirmation of the presence of *TcrNT2* gene into *L. mexicana-Cas9^{ΔNT1}* cells after transfection.

A) Restriction digest products for plasmid pHDK270 with *Bgl*II and *Xho*I to release the *TcrNT2* gene. L: 1 kb DNA ladder (Promega); 1: Digested plasmid by *Bgl*II and *Xho*I to release *TcrNT2* (1323 bp) from pHDK270 (~6.2 kb); 2: Undigested plasmid for pHDK270. **B)** Confirmation of the presence of *TcrNT2* gene into *L. mexicana-Cas9^{ΔNT1}* strain after transfection by using HDK1551 as forward primer for *TcrNT2* and HDK340 as a reverse primer for pNUS-HcN. L: 1kb DNA Ladder (Promega); 1: Clone 1; 2: Clone 2; 3: Clone 3; 4: Non-transfected control (gDNA from *L. mexicana-Cas9^{ΔNT1}*).

The growth rate of *L. mexicana-Cas9*, *L. mexicana-Cas9^{ΔNT1}* and *L. mexicana-Cas9^{ΔNT1}+TcrNT2* strains were plotted after measuring the growth of the cell cultures

for 6 days at 24 h intervals (Figure 7.9). The growth rates of these cell lines, although the rate of difference is small (*L. mexicana-Cas9^{ΔNT1+TcrNT2}*: 1.53×10^7 cell/mL, *L. mexicana-Cas9*: 1.42×10^7 cell/mL and *L. mexicana-Cas9^{ΔNT1}*: 1.14×10^7 cell/mL). All the three cell lines displayed very good growth, almost at the same rate over 6 days, just reaching the stationary phase after day 3. Similar to what was observed earlier, the doubling time of all the cell lines was ~6.5 hours (Beneke et al., 2017).

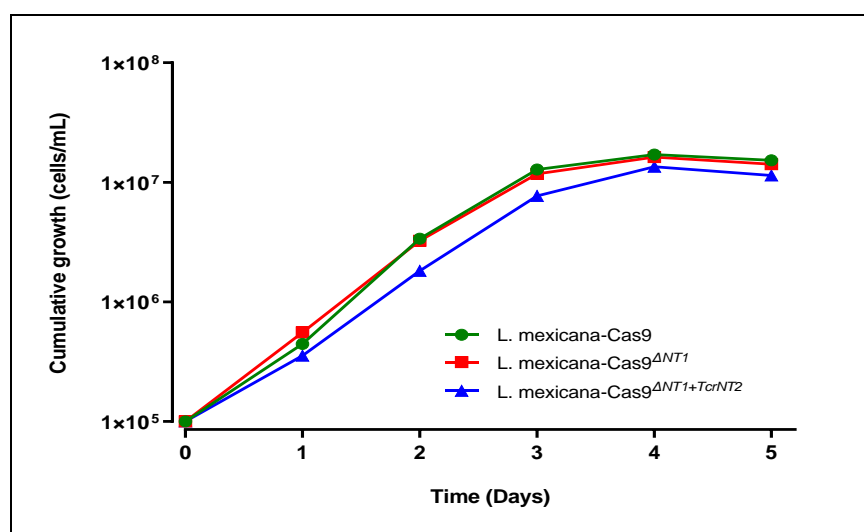


Figure 7.9: The growth rate of *L. mexicana-Cas9* and *L. mexicana-Cas9^{ΔNT1}* and *L. mexicana-Cas9^{ΔNT1}* expressing *TcrNT2* on HOMEM medium supplemented with 10% FBS at 25°C. The cells were seeded at the density of 1×10^5 cells/mL, and cell densities were determined every 24 h. Each data point in this result represents the mean of two similar independent repeats.

The Alamar blue assay was used to assess the effects of deleting *LmexNT1* from the *L. mexicana-Cas9* cell line and of the expression of *TcrNT2* in *L. mexicana-Cas9^{ΔNT1}* cells with respect to sensitivity to analogues of 5-fluoro-2'-deoxyuridine, tubercidin, and other adenosine analogues (Table 7.2). The main interest is checking whether the drugs are effective only when it is taken up by the *TcrNT2* transporter. Thus, *L. mexicana-Cas9^{ΔNT1+TcrNT2}* acts as the main cell line while the remaining two cell types are used as controls, although the experiment also gives information about the ability of *LmexNT1* to transport these analogues.

7.2.4.2 Drug sensitivity assay with adenosine and pyrimidine analogues

Table 7.2: The EC₅₀ of different adenosine analogues and 5-fluoro-2'-deoxyuridine (pyrimidine analogue) on *L. mexicana*-Cas9, *L. mexicana*-Cas9^{ΔNT1} and *L. mexicana*-Cas9^{ΔNT1+TcrNT2} promastigotes, obtained from drug sensitivity assay.

Adenosine analogues/ 5-F-2'dU	<i>L. mexicana</i> -Cas9	<i>L. mexicana</i> -Cas9 ^{ΔNT1}			<i>L. mexicana</i> -Cas9 ^{ΔNT1+TcrNT2}		
	EC ₅₀ ± SEM (μM)	EC ₅₀ ± SEM (μM)	RF vs Cas9	P value vs Cas9	EC ₅₀ ± SEM (μM)	RF vs ΔNT1	P value vs ΔNT1
FH3141	1.08 ± 0.202	14.5 ± 1.77	13.4	<i>P</i> < 0.01	1.86 ± 0.21	7.83	<i>P</i> < 0.01
FH3143	0.12 ± 0.021	0.93 ± 0.18	7.74	<i>P</i> < 0.05	0.30 ± 0.01	3.11	<i>P</i> < 0.05
FH3147	8.41 ± 1.613	> 100 ± 0.00	> 11.8	<i>P</i> < 0.001	13.7 ± 1.25	7.28	<i>P</i> < 0.01
FH3167	0.22 ± 0.091	8.95 ± 1.59	40.7	<i>P</i> < 0.01	0.21 ± 0.02	41.9	<i>P</i> < 0.01
FH3169	0.24 ± 0.055	2.00 ± 0.19	8.43	<i>P</i> < 0.01	0.32 ± 0.05	6.26	<i>P</i> < 0.01
FH8517	3.18 ± 0.775	12.5 ± 1.47	3.93	<i>P</i> < 0.01	9.77 ± 0.67	1.28	<i>P</i> > 0.05
JB588	0.51 ± 0.093	8.82 ± 1.12	17.3	<i>P</i> < 0.01	4.10 ± 0.19	2.15	<i>P</i> < 0.05
TH1003	0.16 ± 0.018	2.90 ± 0.57	18.4	<i>P</i> < 0.01	0.38 ± 0.02	7.68	<i>P</i> < 0.05
FH8505	47.2 ± 1.47	53.27 ± 5.29	1.13	<i>P</i> > 0.05	36.2 ± 1.34	1.47	<i>P</i> < 0.05
FH6367	1.42 ± 0.177	2.05 ± 0.42	1.44	<i>P</i> > 0.05	1.07 ± 0.09	1.91	<i>P</i> > 0.05
FH7429-UP	8.0 ± 0.825	9.37 ± 1.15	1.17	<i>P</i> > 0.05	4.12 ± 0.88	2.27	<i>P</i> < 0.05
Tubercidin	1.02 ± 0.160	25.7 ± 0.94	25.2	<i>P</i> < 0.001	0.82 ± 0.13	31.2	<i>P</i> < 0.001
5-F-2'dU	2.19 ± 0.111	58.4 ± 8.66	26.6	<i>P</i> < 0.01	3.94 ± 0.36	14.8	<i>P</i> < 0.01
Pentamidine	0.87 ± 0.104	1.25 ± 0.22	1.43	<i>P</i> > 0.05	1.12 ± 0.17	1.11	<i>P</i> > 0.05

The EC₅₀ are shown as averages in μM (± SEM) of at least 3 independent determinations. Pentamidine is a standard drug used as control in this assay. The *P* values show the level of significance of the sensitivity of the analogues have on the cell lines. The drugs in bold have a significantly different level of sensitivity on the cells. *P* values were determined by unpaired Student's T-test: Not significant *P* > 0.05; * *P* < 0.05; ** *P* < 0.01; *** *P* < 0.001. RF: resistance factor in comparison to Cas9 (*L. mexicana*-cas9) and ΔNT1 (*L. mexicana*-Cas9^{ΔNT1}); SEM: standard error of mean. 5-F-2'dU: 5-fluoro-2'-deoxyuridine.

Generally, most of the tested tubercidin analogues indicated EC_{50} values in the low micro molar or sub micromolar range and with comparable or superior activity compared to pentamidine. *L. mexicana-Cas9^{ΔNT1+TcrNT2}* displayed increased sensitivity to 5-fluoro-2'-deoxyuridine (14.8-fold more sensitive to 5-fluoro-2'-deoxyuridine; $P < 0.01$) as compared to the strain of *L. mexicana-Cas9^{ΔNT1}*. However, its inhibition to 5-fluoro-2'-deoxyuridine, a pyrimidine analogue, was as expected. The sensitivity of *L. mexicana-Cas9^{ΔNT1}* cells to 5-fluoro-2'-deoxyuridine was decreased (RF = 26.6; $P < 0.001$) compared to the *L. mexicana-Cas9* cells. 5-Fluoro-2'-deoxyuridine was used as control for the proper knockout of the LmexNT1 in *L. mexicana-Cas9^{ΔNT1}* cell line.

Interestingly, the sensitivity to tubercidin was increased due to addition of TcrNT2 in *L. mexicana-Cas9^{ΔNT1}* cells compared to *L. mexicana-Cas9^{ΔNT1}* ($25.7 \pm 0.94 \mu\text{M}$), with an average EC_{50} of $0.82 \pm 0.13 \mu\text{M}$ ($P < 0.001$). It was found that the *L. mexicana-Cas9^{ΔNT1+TcrNT2}* strain has a 7.8, 41.9, 6.3 and 7.7-fold higher sensitivity to FH3141, FH3167, FH3169 and TH1003, respectively, relative to *L. mexicana-Cas9^{ΔNT1}*. These analogues are all analogues of tubercidin, following a halogen addition at the C7 position (Hulpia et al., 2020a). For all the three cell lines, TH1003 showed the best performance, thus, the bromo group at C7 presence increased the sensitivity of these cell lines to this analogue. Notably, the *L. mexicana-Cas9^{ΔNT1+TcrNT2}* cell line restored the sensitivity to tubercidin and most of tubercidin analogues with substitutions on C7. Therefore, transport assays were conducted next to check the rate of uptake of the interesting adenosine and thymidine analogues.

7.2.4.3 Transport studies and kinetic characterisation

As it was noted that the cells containing the *T. cruzi* NT2 transporter are more sensitive to some of the tubercidin and adenosine analogues, it was decided to check the transport rate of 50 nM of [^3H]-adenosine by the same transporter (Figure 7.10). The *L. mexicana-Cas9* cell lines showed very high levels of uptake when incubated with 50 nM of [^3H]-adenosine, with a linear phase of at least 15 seconds and a rate of $0.104 \pm 0.012 \text{ pmol. (10}^7 \text{ cells)}^{-1}.\text{s}^{-1}$. However, the

expression of TcrNT2 in *L. mexicana*-Cas9^{ΔNT1} did not change the rate of adenosine uptake in comparison to the parental cell lines *L. mexicana*-Cas9^{ΔNT1} ($P > 0.05$ by F-test). The addition of 1 mM unlabelled adenosine completely inhibited the uptake of [³H]-adenosine in all three cell lines, showing it is saturable. From Figure 7.10, it is clear that the TcrNT2 did not recognise adenosine as a substrate, at least not at the low adenosine concentration used. As a result, other sets of experiments were conducted, applying 50 nM of [³H]-thymidine as a substrate and its uptake rate was measured, as observed from the figure 7.11.

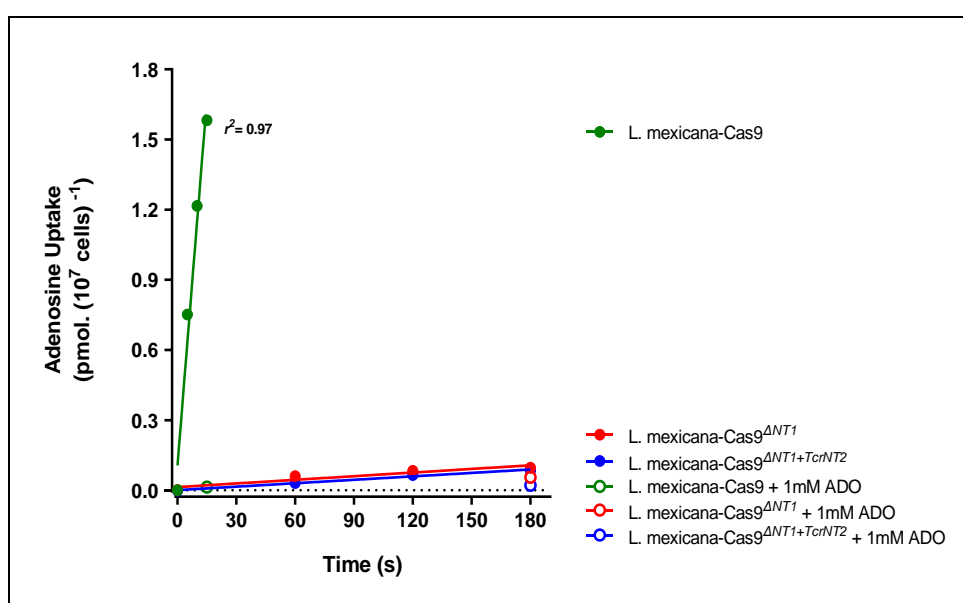


Figure 7.10: [³H]-Adenosine transport was by *L. mexicana*-Cas9, *L. mexicana*-Cas9^{ΔNT1} and *L. mexicana*-Cas9^{ΔNT1+TcrNT2}.

Transport of 50 nM of [³H]-adenosine by *L. mexicana*-cas9 (●), *L. mexicana*-Cas9^{ΔNT1} (●) and *L. mexicana*-Cas9^{ΔNT1+TcrNT2} (●) was measured over 180 seconds in the presence or absent of 1 mM unlabelled adenosine (○), (○) and (○) respectively. Figure shows a representative experiment in triplicate, and error bars represent \pm SEM. F-test was determined by GraphPad Prism 8.

First, uptake was measured applying 50 nM of [³H]-thymidine over 3 minutes, but this incubation time was not sufficient (Figure 7.11A), as a result of the low amount of radiolabel accumulated. Thus, we conducted the thymidine time course using an incubation time of 10 minutes. This showed that [³H]-thymidine at 50 nM was transported by *L. mexicana*-Cas9^{ΔNT1+TcrNT2} in a linear manner over a period of 10 minutes with an uptake rate of 0.0048 ± 0.0002 pmol. (10⁷ cells)⁻¹.s⁻¹ (Figure 7.11B), indicating that the transporter has not yet saturated at 50 nM

for 10 minutes. When compared to the parental cell lines *L. mexicana*-Cas9^{ΔNT1}, the rate of transport of the *L. mexicana*-Cas9^{ΔNT1} expressing TcrNT2 over 3 min and 10 min were significantly increased (~ 6.5- and 6.2-fold; $P < 0.001$ by F-test, respectively). The uptake of 50 nM of [³H]-thymidine by promastigotes of *L. mexicana*-Cas9 was linear for at least 30 seconds, but with a rate of only 0.00042 ± 0.000003 pmol.(10⁷ cells)⁻¹.s⁻¹ (Figure 7.11A). The rate of 50 nM of [³H]-thymidine uptake for 3 minutes and 10 minutes incubation by the three cell lines was not completely inhibited by addition of 1 mM unlabelled thymidine (Figure 7.11A and B). The *L. mexicana*-Cas9^{ΔNT1} transport rate was observed, albeit, the points of saturation overlap the ΔNT1 uptake rate, this means that the little uptake observed by the strain of ΔNT1 could be considered negligible. As the linear uptake was expressed for a long period, checking the affinity of the nucleosides' transporter would be the next step, as done in the next section.

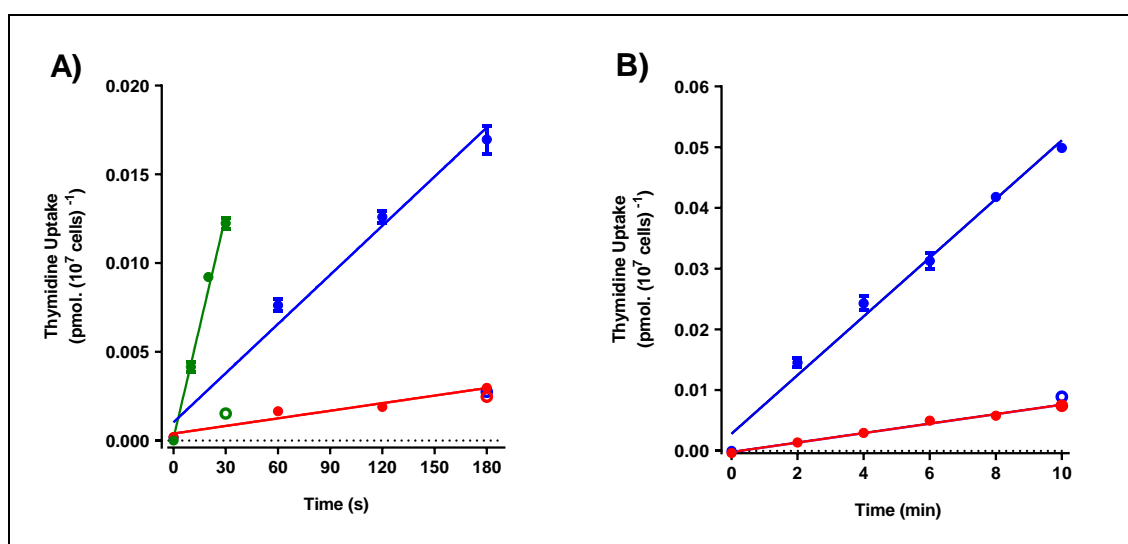


Figure 7.11: [³H]-Thymidine transport was by *L. mexicana*-cas9, *L. mexicana*-Cas9^{ΔNT1} and *L. mexicana*-Cas9^{ΔNT1+TcrNT2} over 3 and 10 minutes.

A) Transport of 50 nM of [³H]-thymidine by *L. mexicana*-cas9 (●), *L. mexicana*-Cas9^{ΔNT1} (●) and *L. mexicana*-Cas9^{ΔNT1+TcrNT2} (●) was measured over 180 seconds in the presence or absent of 1mM unlabelled thymidine (○, (○) and (◐) respectively. **B)** Transport of 50 nM of [³H]-thymidine by *L. mexicana*-Cas9^{ΔNT1} (●) and *L. mexicana*-Cas9^{ΔNT1+TcrNT2} (●) was measured over 10 minutes in the presence or absent of 1 mM unlabelled thymidine (○) and (◐) respectively. Symbols represent the average of triplicate determinations in a single representative experiment and error bars represent \pm SEM. $P < 0.001$ by F-test.

The application of 25 nM of [³H]-thymidine and an incubation time of 6 minutes within the linear phase permitted characterisation of the uptake of the thymidine in *L. mexicana*-Cas9^{ΔNT1} expressing TcrNT2. Figure 7.12 shows

representative inhibition curves for the competition of 25 nM of [^3H]-thymidine transport by unlabelled thymidine. Thymidine was a strong inhibitor. Based on the Michaelis-Menten saturation plots (Figure 7.12), the value of K_m was $0.156 \pm 0.017 \mu\text{M}$ and V_{max} was $0.023 \pm 0.002 \text{ pmol. (10}^7 \text{ cells)}^{-1} \cdot \text{s}^{-1}$ for thymidine (n=4). The Hill slope was consistently very close to -1, indicating that it was likely performed by a single transporting mechanism in *L. mexicana-Cas9 ΔNT1 + TcrNT2* cells. Therefore, TcrNT2 is a high-affinity thymidine transporter when expressed in *L. mexicana-Cas9 ΔNT1* cells. This result is identical to the previous characterisations of this TcrNT2 in a different cell line, the *T. brucei* Lister 427 procyclic form, which also indicated that TcrNT2 has very high-affinity for thymidine ($K_m = 0.223 \mu\text{M}$)(Campagnaro et al., 2018b).

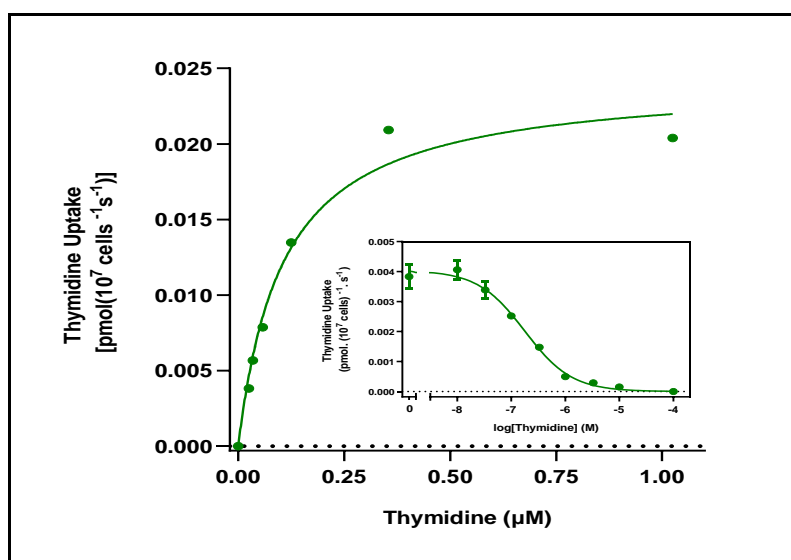


Figure 7.12: K_m and V_{max} measurement for *TcrNT2* upon expression by *L. mexicana-Cas9 ΔNT1* cell lines.

L. mexicana-Cas9 ΔNT1 cells expressing *TcrNT2* were incubated with 25 nM of [^3H]-thymidine in the presence of increasing concentrations of unlabelled thymidine and a dose-dependent inhibition curve with Hillslope near -1 (inset) was observed. Conversion of the data into a Michaelis-Menten plot yielded a K_m of $0.156 \pm 0.017 \mu\text{M}$ and V_{max} of $0.023 \pm 0.002 \text{ pmol. (10}^7 \text{ cells)}^{-1} \cdot \text{s}^{-1}$ (n=4). The figure shows one representative out of four independent experiments and error bars represent \pm SEM.

In section 7.2.4.2 it was shown that the *L. mexicana-Cas9 $\Delta\text{NT1+TcrNT2}$* cells are more sensitive to some adenosine analogues. Thus, it is important to test the rate of uptake of [^3H]-thymidine in the presence of these inhibitors. The data showed low affinity of the *T. cruzi* NT2 transporter for the adenosine analogues (K_i of $804 \pm 2 \mu\text{M}$ for tubercidin and K_i of $740 \pm 39 \mu\text{M}$ for TH1003 in competition

with just 25 nM of [^3H]-thymidine), as compared to the high affinity for thymidine (K_m of $0.156 \pm 0.017 \mu\text{M}$) (Figure 7.13A). The study of Finley et al. (1988) indicated that the decreased ability of laboratory-generated tubercidin-resistant clones of *T. cruzi* to transport radiolabelled tubercidin was associated with a decrease in the transport of thymidine and uridine. Although our results showed that tubercidin possesses only a low-affinity for the TcrNT2 transporter, the expression of this transporter did significantly increase sensitivity to tubercidin and its analogues. The incubation of *L. mexicana*-Cas9^{ΔNT1} + TcrNT2 cells with 25 nM of [^3H]-thymidine in presence of increasing concentrations of other thymidine analogues (Figure 7.13B), revealed that TcrNT2 has a high affinity for 2-thiothymidine and 4-thiothymidine (K_i of $3.21 \pm 0.25 \mu\text{M}$ and K_i of 2.83 ± 0.14 , respectively), whereas it has a much lower affinity for 3'-deoxythymidine with a K_i value of 385.7 ± 42.8 (Table 7.3). 2-thiothymidine and 4-thiothymidine displayed almost similar K_i values to thymidine. The conversion of K_i values of 2-thiothymidine and 4-thiothymidine to the Gibbs free binding energy (ΔG^0), shows that the difference in binding energy ($\delta(\Delta G^0)$) between these analogues is 0.4 kJ/mol (ΔG^0 of -31.3 KJ/mol for 2-thiothymidine and -31.7 KJ/mol for 4-thiothymidine). However, both analogues were found to have lost more than 7 kJ/mL in Gibbs free energy of binding relative to thymidine, showing that the two keto group are involved in medium-strength interactions with the transporter (Table 7.3). Moreover, the 3'-hydroxygroup seems to engage in an even stronger interaction, judging by the $\delta(\Delta G^0)$ of 19.4 kJ/mol of 3'-deoxythymidine with thymidine.

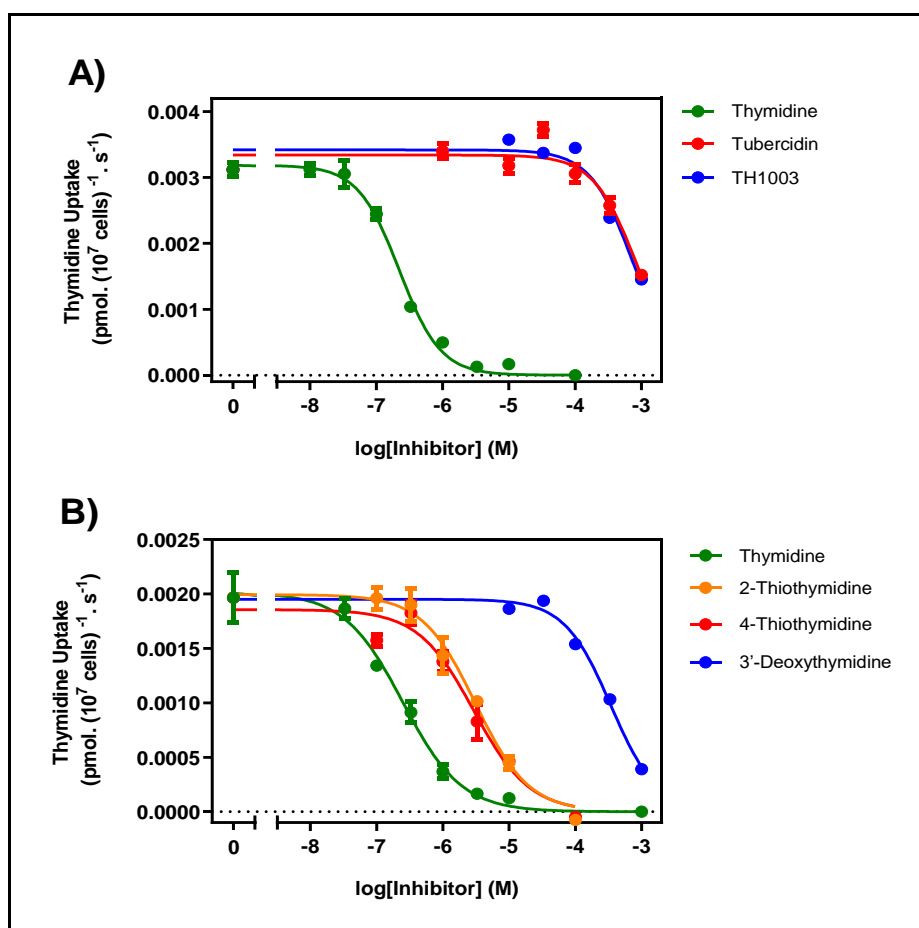


Figure 7.13: Affinity of *TcrNT2* for thymidine and adenosine analogues.

A) and B) 1×10^7 *L. mexicana*-Cas9^{ΔNT1+TcrNT2} cells were incubated with 25 nM of [³H]-thymidine in presence of increasing concentrations of thymidine, 2-thiothymidine, 4-thiothymidine, 3'-deoxythymidine, tubercidin and TH1003. 2 mM ice-cold unlabelled thymidine was used as a stop solution. Figure shows a representative out of 2-3 independent experiments and error bars represent \pm SEM.

To find out more about the specificity of *TcrNT2*, the assessment of the effects of uridine analogues was performed for inhibition of the uptake of 25 nM of [³H]-thymidine. From table 7.3 it is clear that *TcrNT2* has high affinity towards 5-fluoro-2'-deoxyuridine and 5-iodo-2'-deoxyuridine (K_i of 1.42 ± 0.12 μ M and K_i of 0.180 ± 0.036 , respectively), with ~ 7.8 -fold difference. When comparing uridine with these, the transporter has negligible affinity towards uridine (K_i of 162.5 ± 7.6), with 114.4-fold difference for 5-fluoro-2'-deoxyuridine and 903-fold for 5-iodo-2'-deoxyuridine. Substitutions at position 5 of the pyrimidine ring (Fluoro and Iodo) appear to be slightly favoured by the *TcrNT2* transporter, yet 5-bromouridine displayed quite low affinity ($K_i = 30.9$ μ M). The latter observation

clearly shows that the 2'-hydroxy group is detrimental to high affinity binding by TcrNT2, hence the large differential between thymidine and uridine.

From table 7.3, due to the comparison of the K_i values obtained for 5'-deoxyuridine (964.5 μM) and uridine (162.5 μM), it was found that the transporter favours a hydroxyl group at the 5'-position of the ribose ring of the pyrimidine analogues ($\delta(\Delta G^0 = 4.2)$ uridine *versus* 5'-deoxyUrd). In conclusion, *L. mexicana-Cas9^{ANT1}* promastigotes express a TcrNT2 with a broad specificity for 2'-deoxypyrimidines over other pyrimidines, which was not observed for LdNT1 (Aronow et al., 1987; Vasudevan et al., 1998). Binding involves interactions with the pyrimidine keto groups, and with the 3' and 5' hydroxy groups; the sum of the individual interactions adds up to $-7.2 + -7.5 + -19.5 + -4.2 = -38.4$ kJ/mol, which is an extremely close match for the experimental ΔG^0 of thymidine, -38.8 kJ/mol. This occurs under the standard *in vitro* laboratory conditions.

Table 7.3: K_i for pyrimidine nucleosides and adenosine analogues on the transport of [^3H]-thymidine by TcrNT2 into *L. mexicana-Cas9^{ANT1}*.

IC_{50} values obtained were converted to K_i based on the K_m of TcrNT2. ΔG^0 represents the change in Gibbs free energy and $\delta(\Delta G^0)$ represents the change in ΔG^0 of the respective analogues with respect to ΔG^0 of thymidine. All the averages and standard deviations are based on at least three independent experiments in triplicate \pm SEM.

Inhibitor	K_m or K_i (μM)	ΔG^0 (kJ/mol)	$\delta(\Delta G^0)$ (kJ/mol)	n
Thymidine	0.156 ± 0.017	-38.8	--	4
3'-deoxythymidine	385.7 ± 42.8	-19.5	-19.4	3
2-thiothymidine	3.21 ± 0.25	-31.3	-7.5	3
4-thiothymidine	2.83 ± 0.14	-31.7	-7.2	3
Uridine	162.5 ± 7.6	-21.6	-17.2	3
5-fluoro-2'-deoxyUridine	1.42 ± 0.12	-33.4	-5.5	3
5-iodo-2'-deoxyUridine	0.180 ± 0.036	-38.5	-0.3	3
2-thioUridine	186.7 ± 24.0	-21.3	-17.6	3
5-bromoUridine	30.9 ± 3.2	-25.7	-13.1	3
4-thioUridine	165.9 ± 10.6	-21.6	-17.3	3

5'-deoxyUridine	964.5 ± 53.9	-17.2	-21.6	3
Adenosine ¹	1560 ± 60	-15.75	-22.2	3
Tubercidin	804.2 ± 1.9	-17.7	-21.2	2
TH1003	740.2 ± 39.1	-17.9	-21.0	2

Value highlighted in bold represents the K_m for thymidine. ΔG^0 was calculated at 37°C.

¹. From Campagnaro *et al.* Biochim Biophys Acta 2018.

7.2.5 The heterologous expression of TcrNB2 in *L. mexicana-Cas9^{ΔNT1}*

The study by (Campagnaro *et al.*, 2018b) showed that four ENT genes TcrNB1, TcrNB2, TcrNT1 as well as TcrNT2 are encoded by *T. cruzi*. Despite getting the evidence of successfully cloning and characterising most of *T. cruzi* ENT transporters, the research reveals the failure in characterising the TcrNB2 transporter's activity. However, the research suggested, but based on phylogenetic analysis only, that TcrNB2 may function as a low affinity purine nucleobase transporter, given its sequence and predicted structural similarities to *Leishmania* NT4 transporters. Thus, this study, which is a follow-on of the previous work by (Campagnaro *et al.*, 2018b), through cloning and functionally expressing TcrNB2 in *L. mexicana-Cas9^{ΔNT1}* cell lines and assesses its transporter activity.

7.2.5.1 PCR confirmation of the existence of TcrNB2 in *L. mexicana-Cas9^{ΔNT1}*

The *T. cruzi* putative nucleobase transporter TcrNB2 TcCLB.506773.50 was amplified by PCR from pHDK223 using HDK1537 as forward and HDK1538 reverse primers. The pNUS-HcN plasmid was used to express the TcrNB2 gene in *L. mexicana-Cas9^{ΔNT1}*. *Bgl*III and *Xho*I restriction enzymes were used to digest the pNUS-HcN plasmid and the *TcrNB2* gene and T4 DNA Ligase was used to perform the ligation, generating plasmid pHDK271 (Figure 7.14). The *TcrNB2* gene integration into the pHDK271 was verified by a diagnostic restriction digest with restriction enzymes *Bgl*III and *Xho*I. As shown in figure 7.15A, *TcrNB2* is represented by a band of ~1.4 kb, while ~6.2 kb represents the empty pHDK271

vector. Following the transfection of the episomal plasmid pHDK271 into *L. mexicana-Cas9^{ΔNT1}*, PCR was applied in the verification of the presence of pHDK271 in positive clones, using HDK1537 as a forward primer for the *TcrNB2* gene and HDK340 as a reverse primer for the pNUS-HcN plasmid (Figure 7.15B).

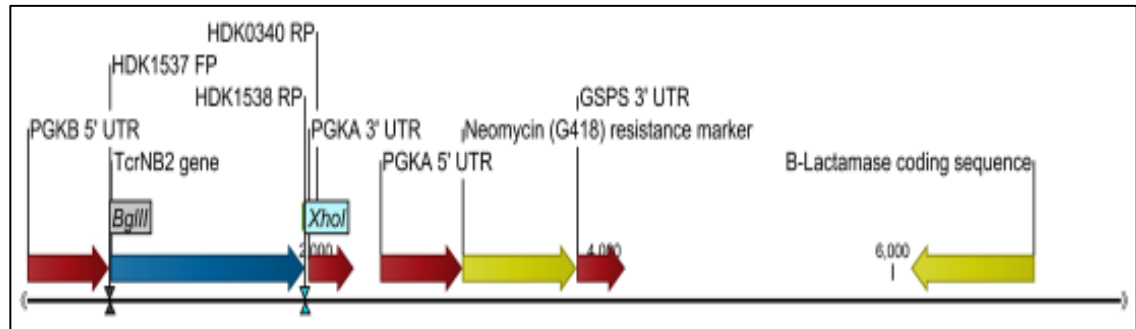


Figure 7.14: Plasmid map of pHDK271 vector for the expression of *T. cruzi* NB2 transporter (*TcrNB2*) in *L. mexicana-Cas9^{ΔNT1}* cell lines.

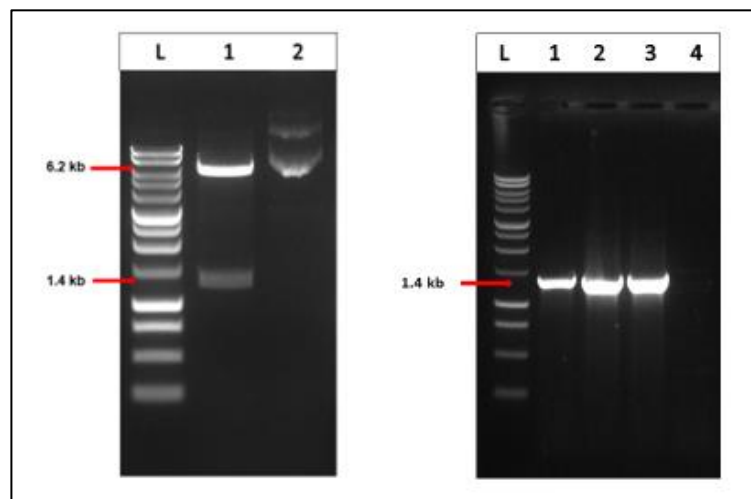


Figure 7.15: Restriction digest products for pHDK271 plasmid and confirmation of the presence of *TcrNB2* gene into *L. mexicana-Cas9^{ΔNT1}* cells after transfection.

A) Restriction digest products for pHDK271 plasmid with *BglII* and *XhoI* to release *TcrNB2* gene. L: 1 kb DNA ladder (Promega); 1: Digested plasmid by *BglII* and *XhoI* to release *TcrNB2* (1347 bp); 2: Undigested plasmid for pHDK271. B) Confirmation of the existence of *TcrNB2* gene into *L. mexicana-Cas9^{ΔNT1}* strain after transfection by using HDK1537 as forward primer for *TcrNB2* gene and HDK340 as a reverse primer for pNUS-HcN plasmid. L: 1kb DNA Ladder (Promega); 1: Clone 1; 2: Clone 2; 3: Clone 3; 4: Non-transfected control (gDNA of *L. mexicana-Cas9^{ΔNT1}*).

7.2.5.2 qRT-PCR and growth rate of *TcrNB2* in *L. mexicana-Cas9^{ΔNT1}*

Three clones of the *L. mexicana-Cas9^{ΔNT1+TcrNB2}* and *L. mexicana-Cas9^{ΔNT1}*, and its parental cell line (*L. mexicana-Cas9*), were assessed on their growth in HOMEM medium supplemented with 10% FBS and incubated at 25 °C. The cell densities

were determined every 24 h (Figure 7.16). The study indicated that the knocking out of *LmexNT1* in *L. mexicana-Cas9* and the knocking in of *TcrNB2* into *L. mexicana-Cas9^{ΔNT1}* did not impact on the rate of growth of these cultures.

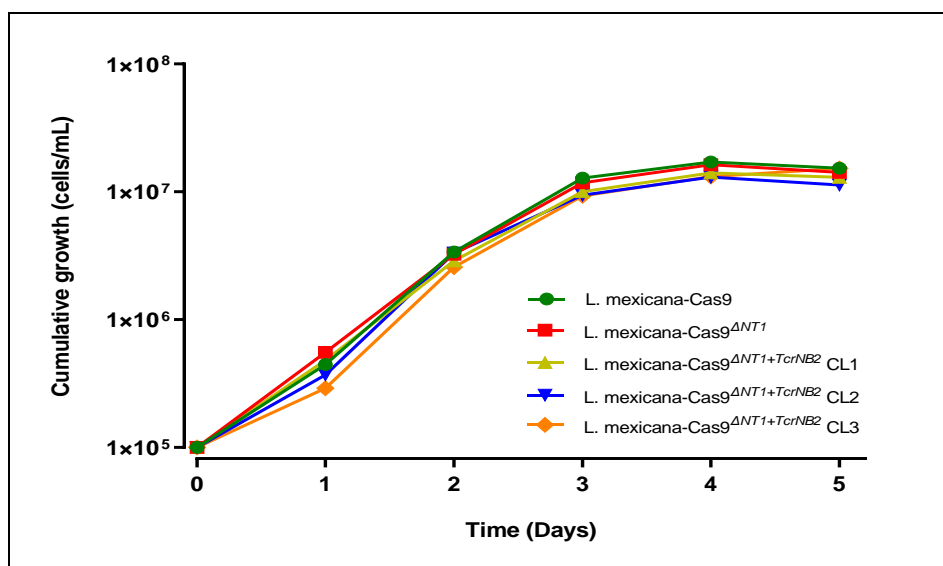


Figure 7.16: The growth rates of *L. mexicana-Cas9*, *L. mexicana-Cas9^{ΔNT1}* and three clones of *L. mexicana-Cas9^{ΔNT1}* expressing *TcrNB2* on HOMEM medium supplemented with 10% FBS. The cells were seeded at a density of 1×10⁵ cells/mL, and cell densities were determined every 24 h. Each data point in this result represents the mean of two similar independent repeats from separate cultures.

To quantify the levels of expression of *TcrNB2* gene in *L. mexicana-Cas9^{ΔNT1}* cells, qRT-PCR was undertaken compared to that in the control cells. All three clones expressing *TcrNB2* in *L. mexicana-Cas9^{ΔNT1}* promastigotes increased the mRNA levels compared to the control *L. mexicana-Cas9^{ΔNT1}* (15-fold, 21.9-fold and 18.9-fold; $P < 0.001$, respectively) (Figure 7.17).

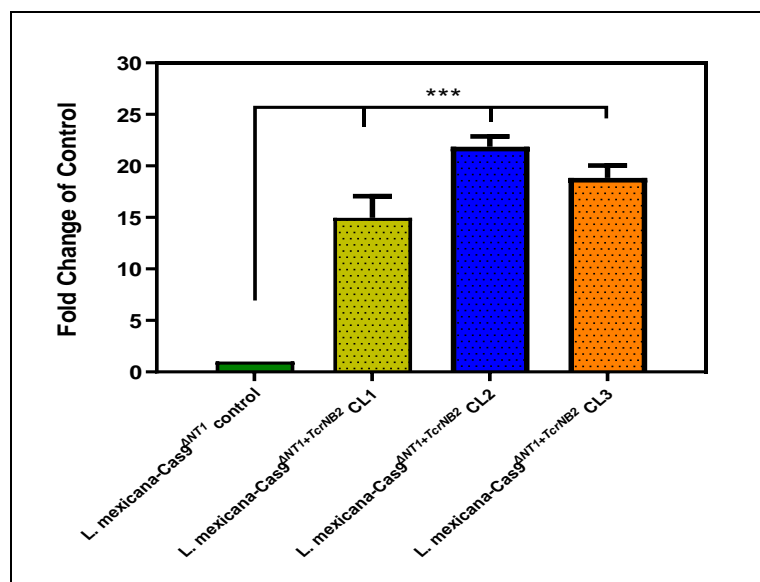


Figure 7.17: The expression levels of *TcrNB2* gene in *L. mexicana-Cas9^{ΔNT1}* compared to the control (*L. mexicana-Cas9^{ΔNT1}*) determined by qRT-PCR. Levels were corrected against the expression level of the housekeeping gene (*L. mexicana* GPI8). The presented results are the average of 3 cDNA each performed in triplicates and error bars are \pm SEM. *** $P < 0.001$. P values were measured by unpaired Student's T-test.

Through applying the Alamar blue drug sensitivity assay, the EC_{50} values of synthesised tubercidin analogues were determined by screening for their inhibitory action against the *L. mexicana-Cas9*, *L. mexicana-Cas9^{ΔNT1}* and *L. mexicana-Cas9^{ΔNT1}+TcrNB2*. Pentamidine and tubercidin were used as controls. The results are presented in the table below.

7.2.5.3 Drug sensitivity assay with adenosine analogues and 5-FU

Table 7.4: The EC₅₀ sensitivity values of *L. mexicana-cas9*, *L. mexicana-Cas9^{ΔNT1}* and *L. mexicana-Cas9^{ΔNT1+TcrNB2}* promastigotes to various adenosine analogues, obtained from drug sensitivity assay. EC₅₀ are shown as averages in μM (± SEM) of at least 3 independent determinations. Pentamidine is a standard drug used as control in this assay.

Adenosine analogues	<i>L. mexicana-Cas9</i>	<i>L. mexicana-Cas9^{ΔNT1}</i>			<i>L. mexicana-Cas9^{ΔNT1+TcrNB2}</i>		
	EC ₅₀ ± SEM (μM)	EC ₅₀ ± SEM (μM)	RF vs <i>Cas9</i>	<i>P</i> value vs <i>Cas9</i>	EC ₅₀ ± SEM (μM)	RF vs <i>ΔNT1</i>	<i>P</i> value vs <i>ΔNT1</i>
FH3141	0.834 ± 0.128	16.1 ± 0.70	19.3	<i>P</i> < 0.001	14.4 ± 3.36	1.12	<i>P</i> > 0.05
FH3143	0.098 ± 0.015	1.07 ± 0.16	10.9	<i>P</i> < 0.01	1.18 ± 0.21	0.91	<i>P</i> > 0.05
FH3147	9.30 ± 1.53	>100 ± 0.00	10.8	<i>P</i> < 0.001	>100 ± 0.00	1.00	<i>P</i> > 0.05
FH3167	0.227 ± 0.094	9.95 ± 1.78	43.8	<i>P</i> < 0.01	10.1 ± 1.15	0.98	<i>P</i> > 0.05
FH3169	0.345 ± 0.108	2.98 ± 1.02	8.64	<i>P</i> > 0.05	2.86 ± 0.47	1.04	<i>P</i> > 0.05
FH8517	3.23 ± 0.679	10.6 ± 1.72	3.27	<i>P</i> < 0.05	13.3 ± 2.75	0.80	<i>P</i> > 0.05
JB588	0.570 ± 0.07	9.24 ± 0.34	16.2	<i>P</i> < 0.001	8.41 ± 0.37	1.10	<i>P</i> > 0.05
TH1003	0.166 ± 0.012	3.37 ± 0.13	20.3	<i>P</i> < 0.001	3.90 ± 0.48	0.86	<i>P</i> > 0.05
FH8505	44.3 ± 1.5	51.8 ± 5.82	1.17	<i>P</i> > 0.05	38.1 ± 3.83	1.36	<i>P</i> > 0.05
FH6367	1.27 ± 0.3	1.93 ± 0.32	1.52	<i>P</i> > 0.05	1.99 ± 0.82	0.97	<i>P</i> > 0.05
FH7429-UP	9.31 ± 0.483	10.6 ± 0.41	1.14	<i>P</i> > 0.05	4.61 ± 0.89	2.30	<i>P</i> < 0.01
Tubercidin	0.811 ± 0.295	37.7 ± 7.52	46.5	<i>P</i> < 0.01	27.6 ± 4.9	1.36	<i>P</i> > 0.05
Pentamidine	0.861 ± 0.109	1.28 ± 0.18	1.49	<i>P</i> > 0.05	0.39 ± 0.0487	3.32	<i>P</i> < 0.01

The *P* values show the level of significance of the sensitivity of the analogues have on the cell lines. The drugs in bold have a significantly different level of sensitivity on the cells. *P* values were determined by unpaired Student's T-test: Not significant *P* > 0.05; * *P* < 0.05; ** *P* < 0.01; *** *P* < 0.001. RF: resistance factor in comparison to *Cas9* (*L. mexicana-cas9*) and *ΔNT1* (*L. mexicana-Cas9^{ΔNT1}*); SEM: standard error of mean.

In general, apart from FH7429-UP, the *L. mexicana*-Cas9^{ΔNT1+TcrNB2} cell lines did not indicate any difference in the EC₅₀ values when compared to *L. mexicana*-Cas9^{ΔNT1} cells ($P > 0.05$) (Table 7.4). In contrast, significant differences in the EC₅₀ values of 5-FU and pentamidine were obtained in the assessment of *L. mexicana*-Cas9^{ΔNT1+TcrNB2} clonal derivatives when compared to the parental cells *L. mexicana*-Cas9^{ΔNT1} (Figure 7.18). The sensitivity of *L. mexicana*-Cas9^{ΔNT1+TcrNB2} clone 2 and 3 to 5-FU significantly increased with mean an EC₅₀ values of $9.96 \pm 0.36 \mu\text{M}$ and $12.8 \pm 3.3 \mu\text{M}$, respectively. However, there was no significant difference in the sensitivity of *L. mexicana*-Cas9^{ΔNT1+TcrNB2} clone 1 to 5-FU with mean an EC₅₀ value of $17.7 \pm 3.0 \mu\text{M}$ when compared to *L. mexicana*-Cas9^{ΔNT1}, which displayed an EC₅₀ value of $29.4 \pm 3.5 \mu\text{M}$. All clonal derivatives of *L. mexicana*-Cas9^{ΔNT1+TcrNB2} (clones 1-3) were significantly sensitised to pentamidine, compared with the parental cell lines. The link between TcrNB2 heterologous expression and the LmexNT1 deletion impacts 5-FU and pentamidine efficacy against *L. mexicana*-WT is still unclear. However, NT1 is the main pyrimidine salvage transporter in *L. mexicana*, taking up uridine, thymidine and cytidine (Vasudevan et al., 1998) and its deletion could well lead to an increase in the expression other elements of pyrimidine salvage and/or biosynthesis. The data suggest that TcrNB2 might be able to mediate the uptake of 5-FU and pentamidine but if so, only small amounts, considering the very small sensitisations to each drug.

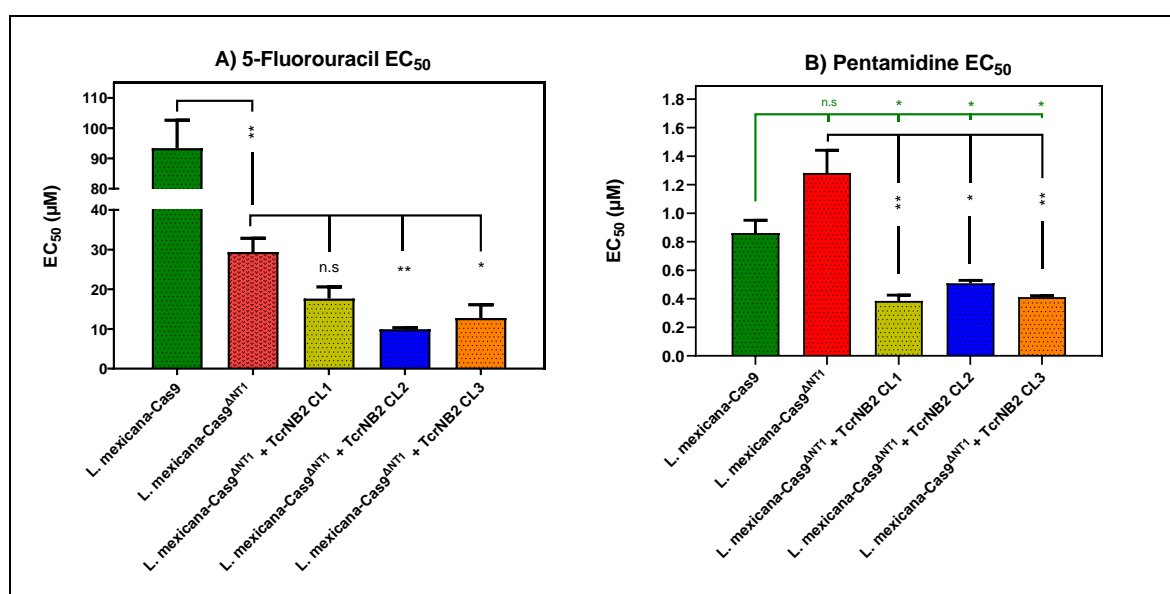


Figure 7.18: Alamar blue drug sensitivity assay of expression of *TcrNB2* in *L. mexicana-Cas9^{ΔNT1}* clones 1-3 using 5-fluorouracil (A) and pentamidine (B).

The mean of three independent repeats is shown \pm SEM in μM . * $P < 0.05$ and ** $P < 0.01$ were determined by unpaired Student's T-test.

7.2.5.4 Transport studies with various substrates

The transport assay of each substrate by *L. mexicana-Cas9^{ΔNT1+TcrNB2}* was investigated in order to determine which substrate TcrNB2 transports. The expression of TcrNB2 in *L. mexicana-Cas9^{ΔNT1}* did not change the rate of 50 nM of [³H]-adenosine transport in comparison to the parental cell lines *L. mexicana-Cas9^{ΔNT1}* ($P > 0.05$ by F-test; $n=1$; Figure 7.19A). The addition of 1 mM unlabelled adenosine completely inhibited the uptake of [³H]-adenosine in all three cell lines, showing it is saturable. The uptake of 100 nM of [³H]-adenine by *L. mexicana-Cas9^{ΔNT1+TcrNB2}* cells was investigated to establish whether adenine is a substrate for the TcrNB2 transporter. [³H]-Adenine uptake was linear for 15 seconds in *L. mexicana-Cas9* promastigotes, with a rate of 0.082 ± 0.005 pmol.(10^7 cells)⁻¹.s⁻¹ ($r^2=0.99$; $n=1$; Figure 7.19B). The results show that there was no significant difference in the transport of 100 nM of [³H]-adenine between the *L. mexicana-Cas9^{ΔNT1+TcrNB2}* and *L. mexicana-Cas9^{ΔNT1}* strain ($P > 0.05$ by F-test), with a rate of 0.062 ± 0.003 and 0.089 ± 0.007 pmol.(10^7 cells)⁻¹.s⁻¹, respectively; ($n=1$); in both strains [³H]-adenine transport was completely inhibited in the presence of 250 μM unlabelled adenine.

In section 7.2.5.3, it was clear that introducing TcrNB2 transporter in *L. mexicana-Cas9^{ΔNT1}* promastigotes sensitised the cells to 5-FU when comparing it with the parental cells ($n=3$; $P < 0.01$). Therefore, to find out if introducing TcrNB2 can cause an increase in uracil transport, we investigated the uptake of 0.1 μM of [³H]-uracil in *L. mexicana-Cas9^{ΔNT1+TcrNB2}*. However, no difference was observed regarding the transport of 0.1 μM of [³H]-uracil between the *L. mexicana-Cas9^{ΔNT1+TcrNB2}* and *L. mexicana-Cas9^{ΔNT1}* cells ($P > 0.05$ by t-test; $n=2$; Figure 7.19C). The transport of 0.1 μM of [³H]-uracil was almost identical in *L. mexicana-Cas9^{ΔNT1+TcrNB2}* and *L. mexicana-Cas9^{ΔNT1}* cells, with a rate of 0.0011 ± 0.00030 and 0.00099 ± 0.00026 pmol. (10^7 cells)⁻¹.s⁻¹ ($n=2$), respectively.

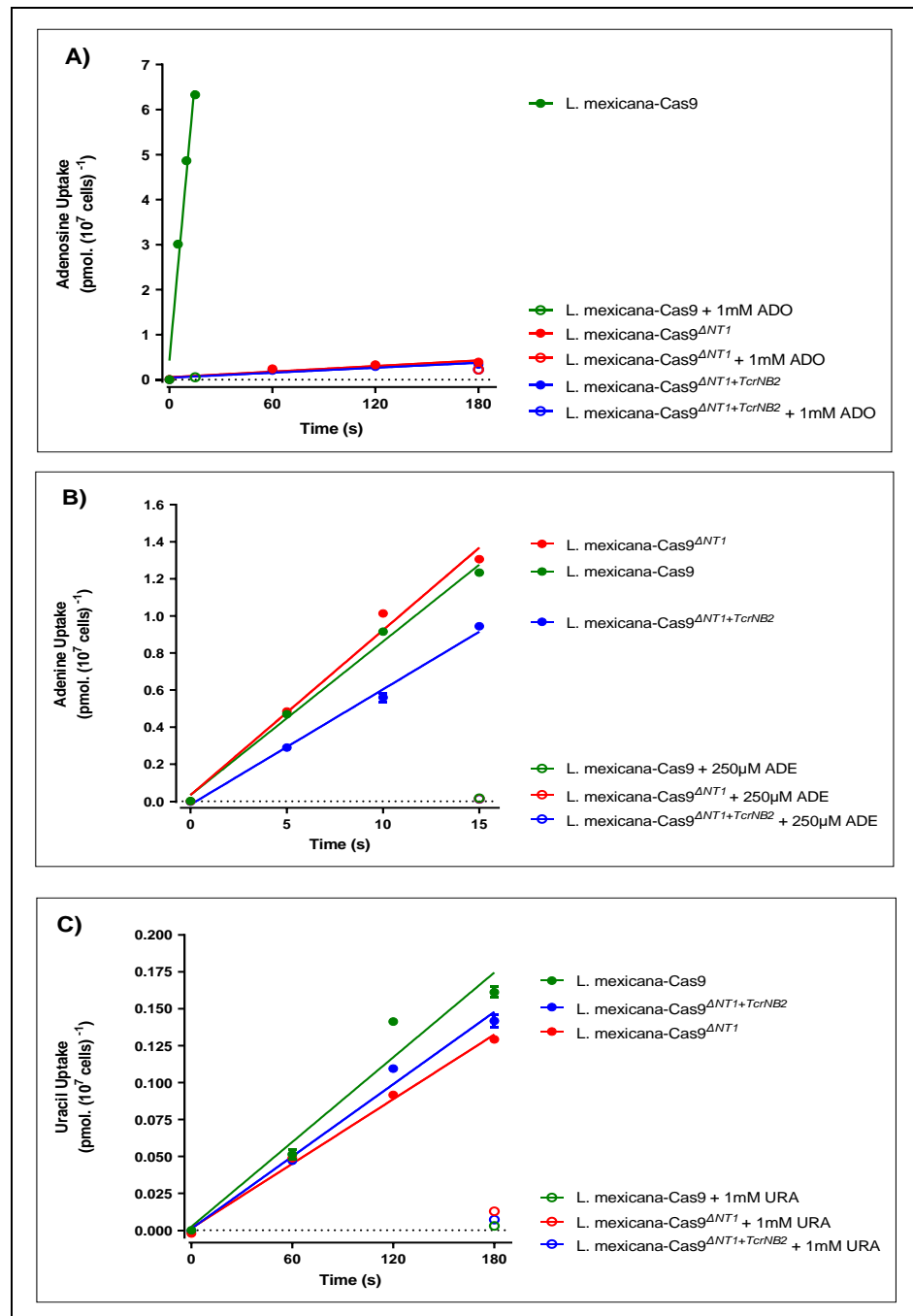


Figure 7.19: [³H]-Adenosine, [³H]-Adenine and [³H]-Uracil transport by *L. mexicana*-Cas9, *L. mexicana*-Cas9^{ΔANT1} and *L. mexicana*-Cas9^{ΔANT1+TcrNB2}.

A) Transport of 0.05 μM of [³H]-adenosine by *L. mexicana*-cas9 (●), *L. mexicana*-Cas9^{ΔANT1} (●) and *L. mexicana*-Cas9^{ΔANT1+TcrNB2} (●) was measured over 180 seconds in the presence or absent of 1 mM unlabelled adenosine (○), (○) and (○) respectively. B) Transport of 0.1 μM of [³H]-adenine by *L. mexicana*-cas9 (●), *L. mexicana*-Cas9^{ΔANT1} (●) and *L. mexicana*-Cas9^{ΔANT1} + *TcrNB2* (●) was measured over 15 seconds in the presence or absent of 250 μM unlabelled adenine (○), (○) and (○) respectively. C) Transport of 0.1 μM of [³H]-uracil by *L. mexicana*-cas9 (●), *L. mexicana*-Cas9^{ΔANT1} (●) and *L. mexicana*-Cas9^{ΔANT1} + *TcrNB2* (●) was measured over 180 seconds in the presence or absent of 1 mM unlabelled uracil (○), (○) and (○) respectively. Symbols represent the average of triplicate determinations in a single representative experiment and error bars represent ± SEM. F-test was determined by GraphPad Prism 8.

7.2.6 The introduction of the *T. cruzi* NB2 in *Lmex-5FURes* promastigotes

In section 7.2.5.3, it was observed that introduction of TcrNB2 transporter in *L. mexicana-Cas9^{ANT1}* strain significantly increased the sensitisation to 5-fluorouracil compared with the parental cells. It was therefore decided to transfect TcrNB2 transporter into 5-FU resistant cell lines of the *L. mexicana* promastigotes as well as determine the sensitivity of *Lmex-5FURes* cell lines expressing of TcrNB2 to 5-FU *in vitro*.

7.2.6.1 PCR and qPCR confirmation of the presence of *TcrNB2* in in *Lmex-5FURes* promastigotes

A plasmid construct used to express the *TcrNB2* gene in *Lmex-5FURes*, pHDK271 (Figure 7.14) had been used previously for the expression of TcrNB2 in *L. mexicana-Cas9^{ANT1}*. Following transfection of this episomal plasmid pHDK271, which was based on the pNUS-HcN plasmid, into the *Lmex-5FURes* strain, PCR was applied to verify the existence of pHDK271 in positive clones, using HDK1537 as forward primer for the *TcrNB2* gene and HDK340 as reverse primer for the pNUS-HcN plasmid (Figure 7.20).

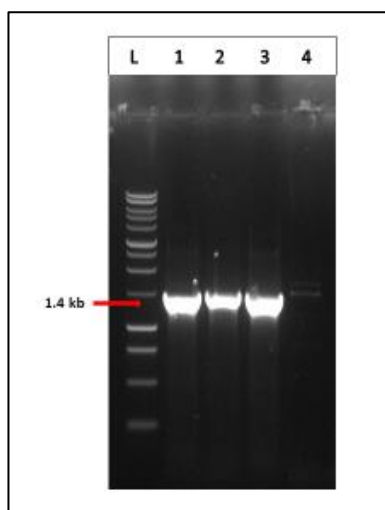


Figure 7.20: Confirmation of the presence of *TcrNB2* gene into *Lmex-5FURes* strain after transfection by using HDK1537 as forward primer for *TcrNB2* gene and HDK340 as reverse primer for pNUS-HcN plasmid.

L: 1kb DNA Ladder (Promega); 1: Clone 1; 2: Clone 2; 3: Clone 3; 4: Non-transfected control (gDNA of *Lmex-5FURes*).

Quantitative RT-PCR was performed to quantify the levels of *TcrNB2* gene expression in *Lmex-5FURes* cells compared to that in the control cell lines. All three clones 1, 2 and 3 of expressing of *TcrNB2* gene in *Lmex-5FURes* significantly increased the expression levels compared to the control *Lmex-5FURes* (23-fold, 28-fold and 24-fold; $P < 0.001$, respectively) (Figure 7.21).

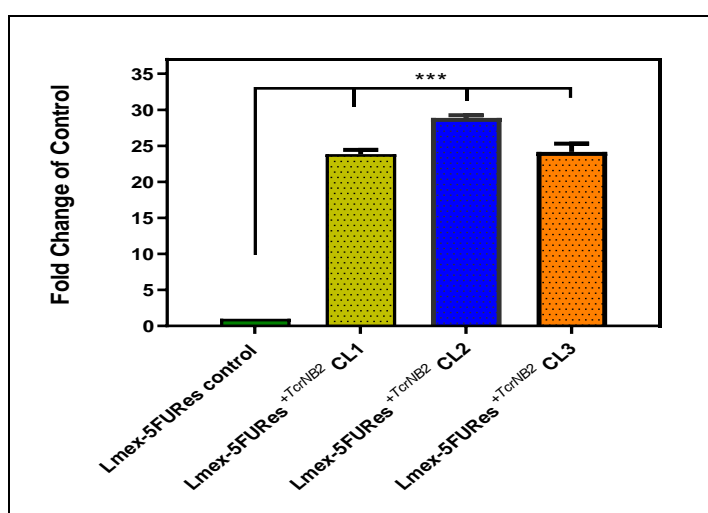


Figure 7.21: The expression levels of *TcrNB2* gene in *Lmex-5FURes* and compared to the control (*Lmex-5FURes*) determined by qRT-PCR.

Levels were corrected against the expression level of the housekeeping gene (*L. mexicana* GPI8). The presented results are the average of 2 cDNA each performed in triplicates, and error bars are \pm SEM. *** $P < 0.001$ by unpaired student's T-test.

7.2.6.2 Drug sensitivity assay with 5-FU, pentamidine and diminazene

The sensitivity of the *Lmex-5FURes* and the three *TcrNB2* clones in the *Lmex-5FURes* parasites to 5-fluorouracil, pentamidine and diminazene aceturate was investigated using the usual Alamar blue assay (Figure 7.22). Pentamidine and diminazene were included as an unrelated control drug that does not act on the purine and pyrimidine system. Expression of *TcrNB2* gene did not lead to increasing the sensitivity to 5-FU in the *Lmex-5FURes*^{+TcrNB2} clones 1-3 ($n = 4$; $P > 0.05$). In contrast, the results a significant increase was observed in the sensitivity of *Lmex-5FURes*^{+TcrNB2} clones 1-3 to pentamidine in comparison with the *Lmex-5FURes* (by 2.3-fold, 2-fold and 2.2-fold, respectively; $n = 4$). The expression of *TcrNB2* in the three *Tbb-5FURes* clones also significantly increased

sensitivity to diminazene compared to *Tbb-5FURes* ($6.8 \pm 0.3 \mu\text{M}$), with an average $4.2 \pm 0.2 \mu\text{M}$, $2.3 \pm 0.2 \mu\text{M}$ and $3.2 \pm 0.4 \mu\text{M}$; respectively.

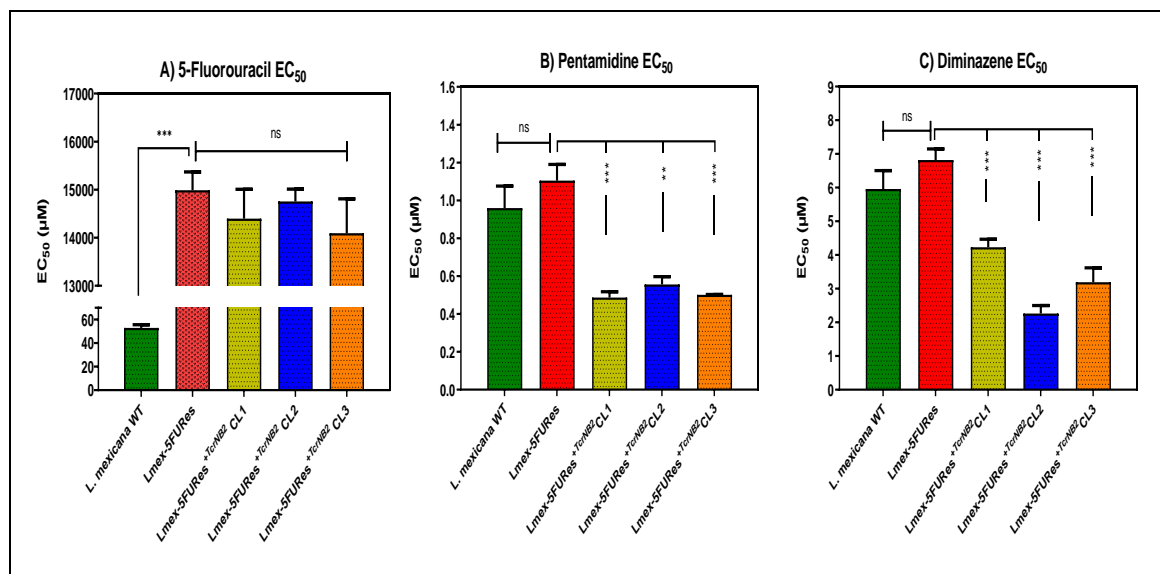


Figure 7.22: Alamar blue drug sensitivity assay of expression of *TcrNB2* gene in *Lmex-5FURes* clones 1-3 by using 5-fluorouracil (A), pentamidine (B) and diminazene acetate (C).

The mean of four independent repeats is shown \pm SEM in μM . ** $P < 0.01$ and *** $P < 0.001$ by unpaired student's T-test.

7.2.7 The introduction of *TcrNB2* transporter in the *T. b. brucei* B48 strain

It has been previously shown that the introduction of *TcrNB2* transporter in the *L. mexicana-Cas9^{ΔNT1}* and *Lmex-5FURes* lead to increasing the sensitisation to pentamidine (see section 7.2.5.3 and 7.2.6.2). Thus, the purpose of this section was to examine the effect of expression of *TcrNB2* in *T. b. brucei* clone B48 parasites, a multi-drug resistant B48 cell lines, could cause changes to the sensitivity to pentamidine by the introduction of the *TcrNB2* transporter.

7.2.7.1 PCR confirmation of the linearity of plasmid and integration of *TcrNB2* in *T. b. brucei* B48 strain

A plasmid construct used to express *TcrNB2* genes in the *T. b. brucei* B48 strain, pHDK223 (Figure 7.23) had previously been generated by Dr. Gustavo Campagnaro (Prof Harry de Koning Lab, University of Glasgow). Following transfection of the *NotI*-linearised pHDK223 plasmid, based on pH1336 plasmid (Biebinger et al., 1997), into the *T. b. brucei* B48 strain, PCR was applied to verify the linearisation of the circular pHDK223 vector and the integration of the

TcrNB2 gene in positive clones. The presence of the expected products, ~1.4 kb for the integration, and lack of band for the linearity of the circular pHDK223 plasmid was confirmed by running the PCR products on 1% of agarose gel to be seen visually under UV light (Figure 7.24).

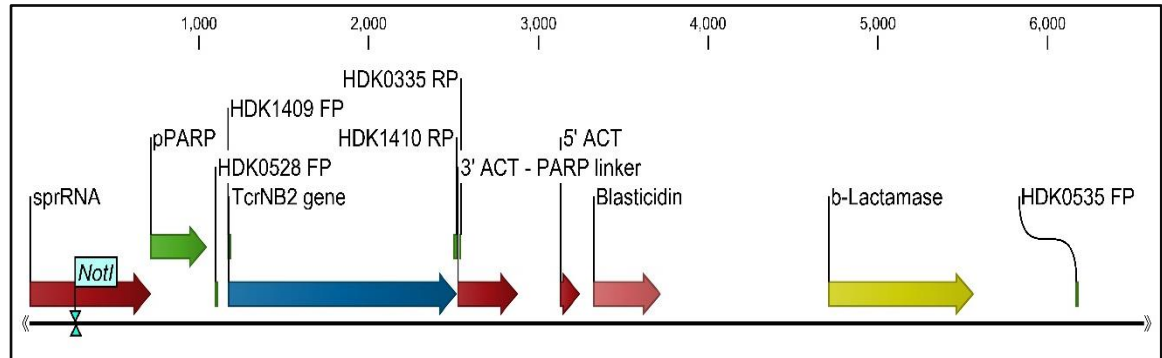


Figure 7.23: Plasmid map of pHDK223 vector for the heterologous expression of *TcrNB2* gene in *B48*.

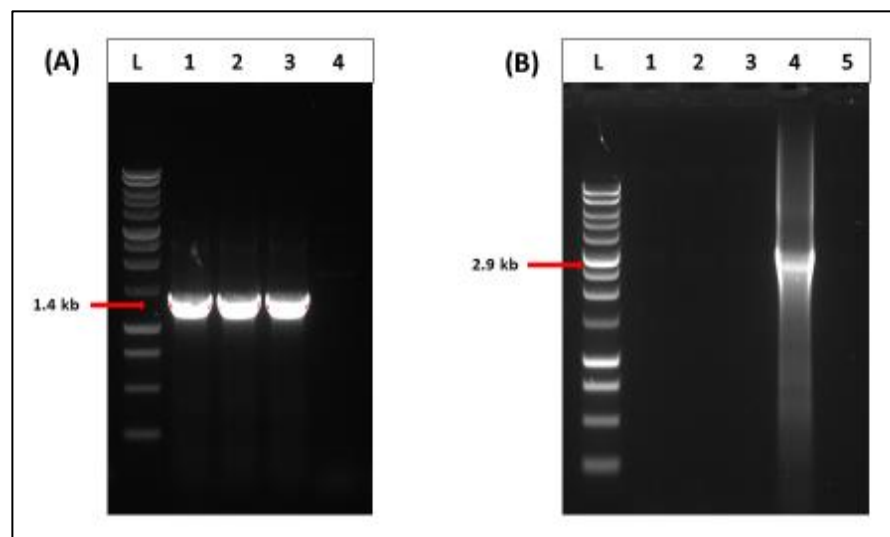


Figure 7.24: PCR conformation for the linearisation of the circular pHDK223 plasmid and the integration of *TcrNB2* gene into *B48* strain after transfection.

A) Confirmation of the integration of *TcrNB2* gene into *B48* strain after transfection by using HDK1409 as forward primer for *TcrNB2* gene and HDK335 as reverse primer for pHD1336 plasmid. L: 1kb DNA Ladder (Promega); 1: Clone 1; 2: Clone 2; 3: Clone 3; 4: Non-transfected control (gDNA from *B48* strain). **B)** Confirmation of the linearization of pHDK223 vector into *B48* strain after transfection by using HDK535 as forward primer for pHD1336 plasmid and HDK1410 as reverse primer for *TcrNB2* gene. L: 1kb DNA Ladder (Promega); 1: Clone 1; 2: Clone 2; 3: Clone 3; 4: Undigested PHDK223; 5: negative control (No gDNA).

7.2.7.2 qRT-PCR confirmation and growth rate of *TcrNB2* in *B48* strain

The level of gene expression for *B48*^{*TcrNB2*} clones 1-3 was analysed and compared to the control cell line by qRT-PCR (Figure 7.25). The results showed that *TcrNB2* expression in *B48*^{*TcrNB2*} clone 2 was at 239-fold ($P < 0.001$), while the results in

B48^{+TcrNB2} clone 3 increased to 139-fold ($P < 0.001$) in relation to the control cell lines, but *B48^{+TcrNB2}* clone 1 recorded the highest expression level, amounting to a 280-fold increase ($P < 0.001$) compared to the parental cells.

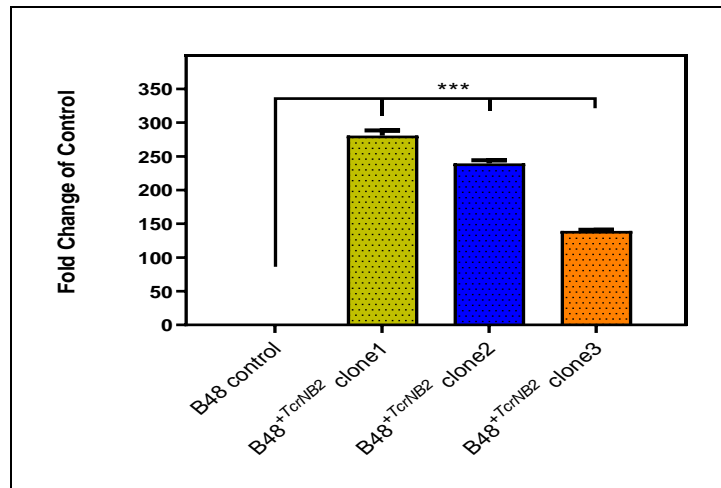


Figure 7.25: The expression levels of *TcrNB2* gene in *B48* cells and compared to the control (*B48*) determined by qRT-PCR.

Levels were corrected against the expression level of the housekeeping gene (*T. b. brucei* GPI8). The presented results are the average of 2 cDNA each performed in triplicates, and error bars are \pm SEM. *** $P < 0.001$ by unpaired student's T-test.

Figure 7.26 shows the analysis of the growth of *B48* parasites and *B48^{+TcrNB2}* clones 1-3 was assessed in HMI-9 medium complemented with 10% FBS and cell densities were determined every 24 h. The result show that there was no effect on the growth of *B48^{+TcrNB2}* clones 1-3 when *TcrNB2* genes was introduced in comparison with the control *B48* strain.

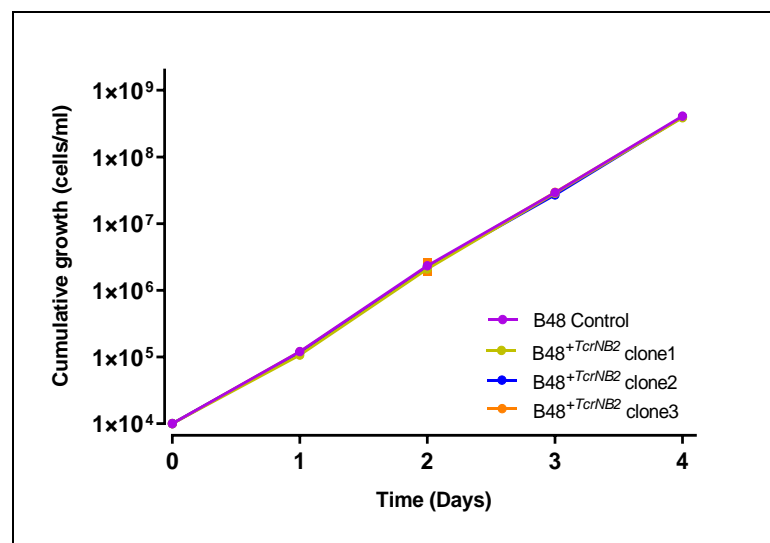


Figure 7.26: The growth curve of *B48* cell lines and *B48* expressing *TcrNB2* clones 1-3 on HMI-9 medium supplemented with 10% FBS.

The cells were seeded at the density of 1×10^4 cells/mL, and cell densities were determined every 24 h. Cells were passaged every 48 h, when the growth had reached between 1.5 and 2×10^6 cells/mL. Each data point in this result represents the mean of two similar independent repeats. Error bars are Standard Deviation; when not shown the bar falls within the symbol.

7.2.7.3 Drug sensitivity assay with pentamidine and diminazene

As shown in Figure 7.27, the Alamar blue assay was used to assess the susceptibility of the *B48* resistant cell lines expressing *TcrNB2*. As expected and well-documented (Bridges et al., 2007), the sensitivity of *B48* parasites to pentamidine was strongly decreased (Resistance Factor (RF) = 104; $n=4$; $P < 0.0001$) compared to the *Tbb-s427* wild-type. Results showed a small but significant increase in the sensitivity of *B48*^{*TcrNB2*} clones 1, 2 and 3 to pentamidine (0.47 ± 0.04 , 0.44 ± 0.03 and 0.50 ± 0.009 μM ; respectively) compared with the parental cells (0.60 ± 0.02 μM ; $n=4$; $P < 0.001$ by unpaired Student's T-test). The susceptibility of clone 1, 2 and 3 to pentamidine was increased 1.25-fold, 1.35-fold and 1.18-fold, respectively. Bloodstream *B48* trypanosomes that expressed *TcrNB2* exhibited a significant increase in the sensitivity to diminazene when compared to the parental cells. The *B48*^{*TcrNB2*} clones 1-3 displayed increased sensitivity to diminazene (2.2-fold, 3.1-fold and 2.3-fold more sensitive to diminazene aceturate, respectively; $n=4$; $P < 0.001$) when compared to the control cells.

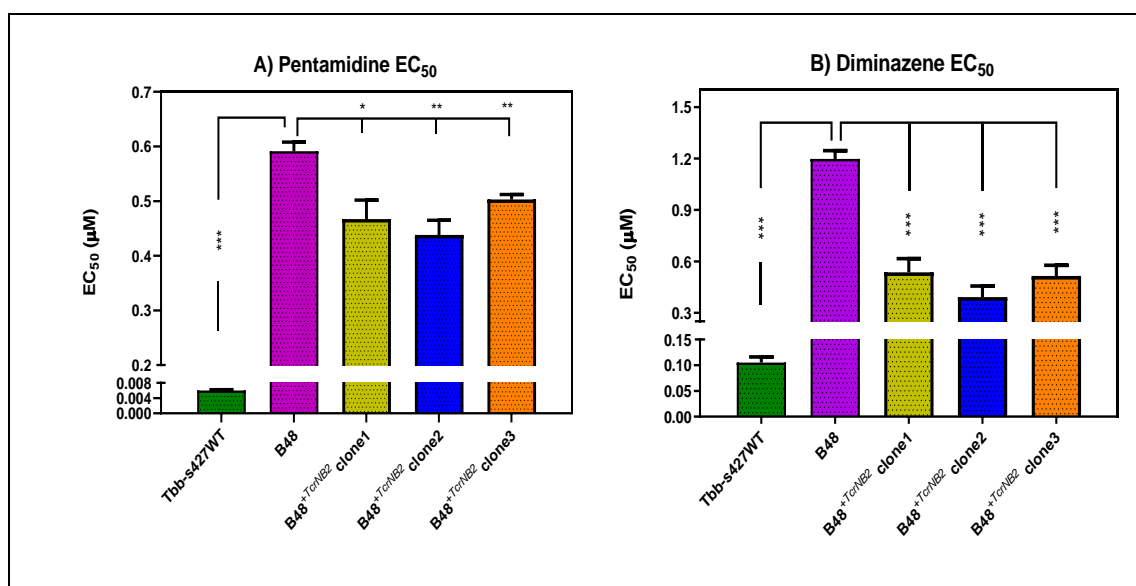


Figure 7.27: Alamar blue drug sensitivity assay of expression of *TcrNB2* gene in *B48* clones 1-3, *B48* strain and *Tbb-s427WT* by using pentamidine (A) and diminazene aceturate (B). The mean of four independent determinations is shown \pm SEM. * $P < 0.05$; ** $P < 0.01$; *** $P < 0.001$ by unpaired student's T-test.

7.3 Discussion

The activities of purine and pyrimidine transport have been characterised in detail, and the main observation is that all purine and pyrimidine transporters identified, to date, in protozoa are members of the ENT family, which has orthologues in many species ranging from prokaryotes to metazoa (De Koning, 2007; Bellofatto, 2007; Acimovic and Coe, 2002; Baldwin et al., 2004; de Koning and Diallinas, 2000; De Koning et al., 2005; Ali et al., 2013a). However, the presence of other gene families has been suggested (De Koning, 2007; Campagnaro et al., 2018a; Balcazar et al., 2017; Bellofatto, 2007). For understanding the efficacy of anti-parasite chemotherapy the cloning and characterising of purine and pyrimidine transporters has been very important (de Koning and Jarvis, 1999; Alzahrani et al., 2017). The research carried out by Campagnaro et al. (2018b), involved characterising the four ENT family of *T. cruzi*. *T. cruzi* cannot synthesise its own purines and, hence, relies on the salvage from its hosts (Campagnaro and de Koning, 2020). This research study cloned four *T. cruzi* ENT genes: TcrNB1, TcrNB2, TcrNT1 and TcrNT2 in order to investigate the functionality of these transporters. The research showed that TcrNB1 had a high affinity for hypoxanthine and guanine (K_m 0.093 μ M and K_i 0.122 μ M, respectively). TcrNT1 displayed a high affinity in the transport of inosine and guanosine (K_m 1.0 μ M and K_i is 0.92 μ M, respectively). Additionally, a high affinity for thymidine (K_m of 0.223 μ M) was exhibited by TcrNT2. *T. cruzi* NT2 transporter is the only known dedicated thymidine transporter in protozoa described to date. TcrNB2 remained an as yet uncharacterised transporter, as no substrate was identified. Notably, this was the first study to report the cloning of any *T. cruzi* purine and pyrimidine transporters (Campagnaro et al., 2018b).

The five genes involved in the transport of purines and pyrimidines in *Leishmania* include, NT1.1, NT1.2, NT2, NT3 and NT4 (Campagnaro and de Koning, 2020). The function of Nucleoside transporter 1 (NT1) is to mediate the adenosine and pyrimidine nucleosides (uridine, thymidine and cytidine) uptake. Nucleoside

Transporter 2 (NT2) is involved in transporting the 6-oxopurine nucleosides inosine, guanosine and xanthosine (Boitz et al., 2012; Carter et al., 2001). More importantly, of the two *L. major* and *L. mexicana* NT1 sequences that are similar, NT1.1 and NT1.2, NT1.1 was recently shown by Alzahrani et al. (2017) to be more sensitive to inhibition by uracil. As a result, it was renamed uridine-uracil transporter 1 (UUT1); it was proposed that NT1.2 would carry the title of NT1 in the species. NT1 and NT2 transporters also serve as the main transporters for the transport of the adenosine analogue tubercidin and the inosine analogue formycin B, respectively (Landfear, 2013; Ortiz et al., 2007). Nucleobase transporter 3 (NT3) and nucleobase transporter 4 (NT4) transporters are purine nucleobase transporters (Landfear, 2011). NT3 is the main carrier for purine nucleobases at physiological pH and, consequently, displays high rates of adenine, guanine, xanthine and hypoxanthine transport (Ortiz et al., 2007; Ortiz et al., 2009a). Apart from NT4 being the main purine nucleobase transporter in intracellular amastigotes, it is also able to transport adenine, albeit with low affinity (Ortiz et al., 2007; Ortiz et al., 2009a).

The technology of genome editing, particularly, by clustered regularly interspaced short palindromic repeats (CRISPR), has been developed for use in parasites such as *L. mexicana* (Beneke et al., 2017), *L. donovani* (Zhang and Matlashewski, 2015), *L. major* (Sollelis et al., 2015), *T. brucei* (Rico et al., 2018), *T. cruzi* (Peng et al., 2015; Lander et al., 2015), *T. gondii* (Sidik et al., 2016), *Plasmodium* spp. (Ghorbal et al., 2014; Zhang et al., 2014) and *C. parvum* (Vinayak et al., 2015). CRISPR-Cas9 is a system of new technology for precise cleavage of double stranded DNA (dsDNA) by a Cas9 nuclease with sequence-specificity determined by a single-guide RNA (sgRNA) (Beneke et al., 2017; Beneke and Gluenz, 2019). In our study, we applied the system of CRISPR-Cas9 that was successfully developed by Beneke et al. (2017) in *L. mexicana* promastigotes, to help in generating a double knockout of *LmexNT1*. The pNUS-HcN plasmid was used to heterologously express TcrNT2 and TcrNB2 transporters in *L. mexicana-Cas9* promastigotes and maintained episomally in the presence of G418 (neomycin) (Tetaud et al., 2002). We show that deletion of the *LmexNT1* locus in *L. mexicana-Cas9* promastigotes by using CRISPR-Cas9 system completely

abolished adenosine and thymidine uptake. Moreover, it became highly resistant to tubercidin (and its analogues) and to 5-fluoro-2'-deoxyuridine.

In a phylogenetic tree of *T. cruzi* ENT transporters with other trypanosomatids, TcrNT2 transporter was grouped close to the *Leishmania* NT1 transporter. As such, it would be most likely to transport pyrimidine nucleosides as well as adenosine due to possessing structural similarity to the *Leishmania* NT1 (Campagnaro et al., 2018b). The uptake of thymidine in *T. brucei* BSF is mediated by P1-type transporters with moderate affinity ($K_i = 44 \mu\text{M}$) (de Koning and Jarvis, 1999; Ali et al., 2013a), while LmexNT1 transporter mediates the uptake of thymidine in *L. mexicana* and its more efficient to transport thymidine than the P1 carrier in *T. brucei* BSF (K_m value of $\sim 11 \mu\text{M}$) (Alzahrani et al., 2017). We functionally characterised the transport activity of TcrNT2 in *L. mexicana-Cas9 Δ NT1* promastigotes. The findings confirm that TcrNT2 has a very high affinity for thymidine with (K_m of $0.156 \pm 0.017 \mu\text{M}$) and are almost identical to the previous characterisations of this TcrNT2 transporter in *T. brucei* procyclic TbNBT-KO cells, which likewise found that TcrNT2 possess a high-affinity for thymidine (K_m of $0.223 \pm 0.007 \mu\text{M}$) (Campagnaro et al., 2018b). The *T. cruzi* parasites might need a very high affinity 2'-deoxypyrimidines transporter with K_m of $0.156 \mu\text{M}$ for thymidine in *L. mexicana-Cas9 Δ NT1* cells and K_m of $0.223 \mu\text{M}$ for thymidine in *T. brucei* procyclic TbNBT-KO cells (Campagnaro et al., 2018b). Moreover, Caradonna et al. (2013) observe that *T. cruzi* may require salvage pyrimidines originating from the host. A decline in production of pyrimidine within the host cells disturbs the intracellular development of *T. cruzi* amastigotes challenges the overall idea of the inessentiality of pyrimidine salvage via the trypanosomatids (Ali et al., 2013b; Liu et al., 2006). Further, we kinetically identified the characteristics of the transport activity of the *T. cruzi* NT2 transporter in *L. mexicana-Cas9 Δ NT1* promastigotes. The outcomes show that 2-thiothymidine and 4-thiothymidine displays almost similar K_i values (K_i of $3.21 \mu\text{M}$ for 2-thiothymidine and K_i of $2.83 \mu\text{M}$ for 4-thiothymidine) to thymidine (Table 7.3).

The Alamar Blue assay enabled the identification of a few nucleoside analogues with potent antiprotozoal activity. *L. mexicana-Cas9 Δ NT1* expressing TcrNT2 cells

was more sensitive to tubercidin (and its analogues) and 5-fluoro-2'-deoxyuridine (pyrimidine analogue). Transport assay with radiolabelled thymidine and adenosine showed that the introduction of TcrNT2 in *L. mexicana-Cas9^{ΔNT1}* restored [³H]-thymidine transport, whereas the uptake rate of [³H]-adenosine did not change when compared to the parental cells (*L. mexicana-Cas9^{ΔNT1}*). Nevertheless, the cells were sensitive to the analogues of adenosine as well as tubercidin although the TcrNT2 transporter displayed only low affinity for them, with high K_i values (K_i 804 ± 2 μ M for tubercidin and K_i 740 ± 39 μ M for TH1003). At the C7 position, TcrNT2 transporter could not recognise any additional group of the purine since the low-affinity for tubercidin and TH1003 were nearly identical. As a result, we conclude that the addition of halogens to the C7 position does not change the transporter interaction process, but the presence of a larger additional group may make it more unfit for transport owing to its size. Although previously it was thought that a thymidine transporter (TcrNT2) mediated the uptake of tubercidin (Finley et al., 1988), the low affinity of TcrNT2 for tubercidin analogues seems to make this unlikely. However, the expression of the TcrNT2 transporter did influence the sensitivity to tubercidin as well as its analogues *in vitro*. A previous report indicated the presence of at least three mechanisms of nucleoside transportation in *T. cruzi*: one for pyrimidines and tubercidin, one for thymidine with no affinity for tubercidin, and one for adenosine and inosine. Notably, the tubercidin-resistant *T. cruzi* strains used in that study were created by exposure of parasites to ionising radiation, which may have resulted in the mutations in other mechanisms of transportation as well (Finley et al., 1988; Nozaki and Dvorak, 1993).

In addition to TcrNT2, the TcrNB2 transporter (TcCLB.506773.50) was cloned from *T. cruzi* and was studied through expression of the gene in *L. mexicana-Cas9^{ΔNT1}* promastigotes. The advantage of using *L. mexicana-Cas9^{ΔNT1}* cells over the previous work in *T. brucei* PCF TbNBT-KO cells by Campagnaro et al. (2018b); *L. mexicana-Cas9^{ΔNT1}* cells has completely lost the adenosine transport activity by about ~98% while *T. brucei* PCF TbNBT-KO cells has still maintaining the adenosine transport activity especially via P1-type transporters. Transport assays with the TcrNB2-expressing cells used [³H]-adenosine, [³H]-adenine and [³H]-uracil. Unfortunately, we are not able to determine the substrate for

TcrNB2 as there was no significant uptake of any of the three substrates. PCR and qRT-PCR techniques were used to confirm the presence as well as expression of TcrNB2 in the *L. mexicana-Cas9^{ΔNT1}* cell lines. There are four possible reasons for this outcome; firstly, TcrNB2 is an intracellular transporter. As a result, it transports substrates within the cell, and this cannot be measured by offering substrate to intact cells. Secondly, TcrNB2 is not a functional transporter. Next, it may be because of TcrNB2 is not correctly routed to the *L. mexicana-Cas9* cells plasma membrane, or unstable. Lastly, TcrNB2 does not transport purine or pyrimidine. According to Campagnaro et al. (2018b), they suggest that the similarities in sequence and structure of TcrNB2 and LmjNT4 indicates that TcrNB2 should be expected to have a medium-to-low affinity for purine nucleobases. Moreover, the high level of adenine transport in *L. mexicana-Cas9^{ΔNT1}* cells could easily mask any adenine uptake mediated by the TcrNB2 transporter, especially if TcrNB2 presents low affinity for its substrates. Therefore, we highly recommended the heterologous expression of TcrNB2 in the *L. mexicana-Cas9^{ΔNT3}* cell lines in order to determine whether adenine is a substrate for TcrNB2. The expression of a tagged version of TcrNB2 and its immunolocalization could show whether it is present in the cellular membrane or not and help to explain why we have been unable to identify its substrate.

Nitroimidazole benznidazole and nitrofurane nifurtimox, the drugs that treat the Chagas' disease, have been approved by the FDA to be the first-line drugs to suppress the parasite (Seebeck et al., 2011; Bern, 2015). The expression of TcrNT2 in *L. mexicana-Cas9^{ΔNT1}* significantly sensitised the cells to 5-fluoro-2'-deoxyuridine (pyrimidine analogue), therefore, it indicates to be a good substrate. This indicates that the application of anticancer and antiviral thymidine analogues against *T. cruzi* should be explored. Moreover, if researchers can understand the nutritional requirements of *T. cruzi*, and the mechanisms that are applied to meet this requirement, this will assist in the discovery as well as the advancement of novel chemotherapeutics against Chagas' disease (Campagnaro et al., 2018b). As a result, individuals will lead a healthy life and there will be a reduction in mortality rate.

8 General discussion

Kinetoplastida is a widespread order of flagellated protozoans with the primary feature that defines it as a group of parasites being the presence of large regions of mitochondrial DNA referred to as the kinetoplast (Stuart et al., 2008). In this order, the respective members have been reported to have the potential of parasitising several groups of plants and every group of animal (Maslov et al., 2001). Some of these kinetoplastida include *Leishmania* spp, which causes leishmaniasis; *T. brucei*, which causes sleeping sickness, or HAT (Human African trypanosomiasis); and *T. cruzi*, which causes Chagas' disease, or American trypanosomiasis. The WHO has designated these insect-transmitted infections as neglected parasitic diseases (Maslov et al., 2001; Barrett and Croft, 2012; Field et al., 2017). Parasitic trypanosomatids cause diseases that range from mild and self-curing, to fatal if untreated. The WHO has channeled numerous efforts towards addressing this problem, but these diseases still pose a severe threat to public health and present economic burdens to the poorest areas globally (Field et al., 2017; Krishna et al., 2020).

There are limited options available for treatment. These options are also quite far from ideal because of their ineffectiveness to different stages of the disease or strains/subspecies of the parasites, high cost, and inconvenient drug administration routes (Field et al., 2017; Barrett and Croft, 2012; Ranjbarian et al., 2017; Kalel et al., 2017; P De Koning, 2020). Currently, besides the toxicity that has been associated with the difficulty in administering antiparasitic drugs, both the emergence and spread of parasites that are resistant to the drugs have been reported. For instance, resistance to eflornitine in *T. b. rhodesiense* infections (Vincent et al., 2010) and melarsoprol (Delespaulx and de Koning, 2007; Graf et al., 2013) for late stage HAT, and pentavalent antimonials for leishmaniasis (Sundar et al., 2008) have been reported, further limiting treatment options. Regarding the recent approval of fexinidazole, the cross-resistance between fexinidazole and nifurtimox is of potential concern as any strains that survive fexinidazole monotherapy will also likely cause NECT failure (P De Koning, 2020). With the pathogens increasingly becoming resistant to most of the drugs being used currently, there is an urgent need for new therapeutic strategies. The development of vaccines, proven as a powerful approach to the management of disease, continues to be challenging and ineffective when it

comes to the trypanosomatid diseases since these parasites have been found to suppress and evade the host's immune mechanisms. Examples are antigenic variation in African trypanosomes (Horn, 2014), and the intracellular locations of *T. cruzi* and *Leishmania* spp in the human host (Cardoso et al., 2016). The primary control strategy recommended is vector control, which is performed through screens and traps in combinations with insecticides and pesticides; early detection and treatment are also important, particularly in Chagas disease and sleeping sickness (Lidani et al., 2019; Legros et al., 2002).

Drug combinations have been used for the treatment of a number of infectious diseases (such as tuberculosis, HIV and malaria) and are now being considered for treatment of neglected diseases like leishmaniasis and HAT. There exist two critical reasons for the need to establish combination therapies, delaying the possibility of resistance emergence for the protection of the few molecules available, and reducing the treatment length for compliance improvement (for instance, the miltefosine regimen requires the intake of drugs for 4 weeks two times a day) (Leprohon et al., 2015; Chakravarty and Sundar, 2010; Croft et al., 2006). A combination therapy serves to improve drug efficacy and consequently result in a shortened course of treatment and reduced resistance. When sodium stibogluconate is administered along with paromomycin, it reported as safe and effective (Cobo, 2014; Croft and Coombs, 2003).

Purines and pyrimidines are nucleotides that are intracellularly phosphorylated and are specifically significant for the functioning of all cells (De Koning et al., 2005; Carter et al., 2008). Their significance ranges from the synthesis of nucleic acids such as DNA and RNA kinetoplastid parasites to metabolic processes of eukaryotic and prokaryotic cells (Carter et al., 2008). In contrast to the majority of mammalian cells in, protozoan parasites cannot synthesise the purine rings and are dependent on salvage mechanisms for the acquisition of these essential nutrients. Conversely, most protozoan pathogens have the ability to synthesise the pyrimidine ring, apart from the amitochondriate parasites *T. vaginalis*, *T. foetus*, and *G. lamblia*. Apart from *Plasmodium*, most protozoa can salvage pyrimidines (De Koning et al., 2005; Carter et al., 2008; Campagnaro and de Koning, 2020; Hulpia et al., 2020a). Since purine and pyrimidine nucleobases

and/or nucleosides have a hydrophilic profile, their movement into the cell relies on the transportation through transmembrane proteins (Molina-Arcas et al., 2009; Carter et al., 2008).

Membrane transport proteins are vital for moving most drugs in and out of cells, meaning that they are special intermediaries in both therapy and drug resistance. Therefore, generating and characterising drug resistant lines offers valuable information on resistance mechanisms and could possibly be used for identifying new drug transporters. For instance, multi-drug resistant *T. b. brucei* line B48 was generated *in vitro* by exposure to stepwise increasing concentrations of pentamidine until these cells lost the transport activity associated with high affinity pentamidine transport (HAPT1) (Matovu et al., 2003; Bridges et al., 2007). Recently, the HAPT1 activity was found to be encoded by the gene *TbAQP2* (Baker et al., 2012; Munday et al., 2014). Moreover, the identification of the genes encoding for adenosine/pyrimidine transporter (NT1) and inosine and guanosine transporter (NT2) were discovered in the promastigote form of *L. donovani*, using the TUBA5 and FBD5 resistant cell lines that were generated *in vitro* by adaptation to 20 μM tubercidin and 1 μM formycin B, respectively. The gene believed to encode TgAT1 (*Toxoplasma gondii* adenosine transporter 1) was identified from an adenine arabinoside (AraA) resistant cell line and characterized by expression in *Xenopus oocytes*, confirming it as a low-affinity high-capacity adenosine transporter (Iovannisci et al., 1984; Aronow et al., 1987; Vasudevan et al., 1998; Chiang et al., 1999). Up to this moment, only ENT genes are identified as encoding purine and pyrimidine transporters in protozoans (De Koning et al., 2005; Campagnaro and de Koning, 2020), however, the involvement of other gene families has been proposed (Bellofatto, 2007; De Koning, 2007; Campagnaro et al., 2018a; Balcazar et al., 2017).

The analogues of pyrimidine and purine are used as drugs in the treatment of different infections and diseases. There is the use of some of these analogues against protozoa (pyrimethamine, allopurinol), viruses (penciclovir, acyclovir, brivudin, ganciclovir and many others), and malignant cells (e.g. thioguanine, 6-mercaptopurine, 5-fluorouracil) (de Koning and Dhalluin, 2000; Razonable, 2011;

Momeni et al., 2002; Kolb, 1997). 5-fluorouracil (5-FU) is a fluoropyrimidine that is classified as an antimetabolite. It works by inhibiting biosynthetic processes and through incorporating itself to macromolecules such as DNA and RNA and disrupting their normal function (Longley et al., 2003). Because of its functionality and aromatic structure, which is heterocyclic in nature, 5-FU was used as a chemotherapeutic drug for cancer. The F atom found on C5 instead of an H atom, makes it a toxic analogue of uracil and thymine (Zhang et al., 2008a; Longley et al., 2003; Yssel et al., 2017). Fluorinated pyrimidines such as 5-FU, 5-fluoroorotic acid, 5-fluoro-2'deoxy- (uridine or cytidine) and 5-chloro-2'deoxyuridine displayed anti-trypanosomal activity in the micromolar range (Ali, 2013). Fluorinated pyrimidines have recently been reported as an innovative series of 5'-norcarbocyclic uridine analogues against *L. mexicana* and *T. b. brucei*, with some their compounds exhibiting similar activities against *Leishmania* and *Trypanosoma*, which consequently make them ideal leads for structure optimization (Alzahrani et al., 2017).

While 5-FU is widely used to treat a wide array of cancers which include colorectal cancer and breast cancer (Longley et al., 2003), there is still need for a deeper understanding of how 5-FU induces cytotoxicity and cell death; not just in cancer cells but in protozoa such as *T. b. brucei* as well as *L. mexicana* species. Munday et al. (2015) noted that drug resistance in protozoa such as *T. b. brucei* is a result of changes to the 'transportome' of the parasites. 5-FU uses the same mechanism to enter cells as the uracil transport mechanism, and once in the cells, there is conversion of 5-FU to several active metabolites such as 5-fluorodeoxyuridine monophosphate (5F-dUMP), 5-fluorodeoxyuridine triphosphate (5F-dUTP) and fluorouridine triphosphate (5F-UTP). 5F-dUTP and 5F-UTP are incorporated into DNA and RNA and causes an impairment in their function and maturation. F-dUTP triggers DNA mutations considering that there is the pairing of 5-FU with guanine at the expense of adenine, and the cell's attempts at repairs result in double or single breaks in the strand. 5F-dUMP is an inhibitor of thymidylate synthase that cannot be reversed; this causes a deprivation of thymidine monophosphate (TMP) deprivation that subsequently disrupts DNA synthesising. This means that the drugs bind to the protein

inhibiting irreversibly (Longley et al., 2003; Galmarini et al., 2002; Yssel et al., 2017).

5-FU was found to be an excellent substrate for all the kinetoplastid uracil transporters; LmexU1 in *L. mexicana* and LmajU1 in *L. major* (Papageorgiou et al., 2005; Alzahrani et al., 2017) as well as TbU1 in *T. b. brucei* PCF and TbU3 in *T. b. brucei* BSF (de Koning and Jarvis, 1998; Ali et al., 2013a; Campagnaro and de Koning, 2020). Therefore, it may be possible to develop a new chemotherapy for kinetoplastid parasites based on the efficiency of 5-FU against *Leishmania* and *Trypanosoma* species *in vitro* (Gudin et al., 2006; Papageorgiou et al., 2005), although host toxicity of this antimetabolite might be a limiting factor. Unlike the transporters for the therapeutically active nucleoside analogues and allopurinol, the transporter for 5-FU has not been identified. However, by the method of exclusion, it can be concluded that the 5-FU transporter in *Trypanosoma* and *Leishmania* species is not an ENT transporter, as all their ENT transporters have been cloned and at least partially characterised (De Koning, 2007; Ali et al., 2013a; Campagnaro and de Koning, 2020).

As such, we are highly interested in identifying the pyrimidine transporter gene family of kinetoplastids using the antimetabolite 5-FU as a probe, which we anticipate will not be of a gene family previously associated with this activity (Domin et al., 1993; de Koning and Diallinas, 2000; De Koning, 2007; Bellofatto, 2007). For that reason, resistance to 5-FU was generated in both *T. b. brucei* s427-WT BSF and *L. mexicana* promastigotes, producing clonal lines *Tbb-5FURes* and *Lmex-5FURes*, respectively (Ali et al., 2013a; Alzahrani et al., 2017). Uracil/5-FU transport rates in these cell lines are strongly reduced, particularly in the *L. mexicana* cell line.

The fast identification of transporters and new pathways is facilitated by the current genomic technologies, particularly in the protozoan parasites for which these techniques are most advanced. Multiple lines of investigation have been followed to date to try to identify the gene(s) coding for kinetoplastid pyrimidine transporters. The BLAST searches for pyrimidine transporter genes using fungal, yeast and prokaryote sequences have, until this day, not produced a single candidate gene from any of the available protozoan genomes, leading us

to conclude that no genes can be identified by homology to known pyrimidine transporter genes. Therefore, previous work in our laboratory undertook whole genome sequencing, RNA-seq and RIT-seq as a way of finding the pyrimidine transporter genes of *T. b. brucei* and *L. mexicana* promastigotes (Ali, 2013; Alzahrani, 2017).

RNA sequencing (RNA-seq) is considered to be a powerful technique, utilising deep-sequencing technologies in sequencing RNA for the determination of differential gene expression under different environmental and physiological conditions (Wang et al., 2009; Kukurba and Montgomery, 2015). Siegel et al. (2010) showed that there was differential expression of 6% of genes in *T. b. brucei* between the two stages of life cycle (BSF and PCF) using RNA-seq. Therefore, comparative sequencing of the resistant and parental strains through the use of RNA-seq in the analysis of the differences in transcription within resistant and sensitive parasites was carried out with the aim of identifying the pyrimidine transporter genes. From RNA-seq data, the aim was to find the down-regulated genes both in the resistant lines of *L. mexicana* and *T. b. brucei* that constituted of at least three trans-membrane domains. Such candidate transporters were subsequently overexpressed in the resistant strain to allow a fast confirmation by resistance reversal.

A very strong technique for genetic screens for genes to be linked to function and precise phenotypes, where knockdown confers resistant populations, is the genome-wide RNA interference (RNAi) library screen. The first organism utilised in the application of this technique is *T. b. brucei* PCF (Alsford et al., 2012; Mohr and Perrimon, 2012; Chou et al., 2015; Morris et al., 2002). The utilisation of RNAi library screening helped to identify novel trypanosomal drug transporters in the last few years, including TbAQP2 as a determinant of pentamidine sensitivity (Baker et al., 2012; Munday et al., 2014), the aminopurine transporter TbAT1 as the carrier for melarsoprol (Burkard et al., 2011) and amino acid transporter TbAAT6 as the carrier for eflornithine (Baker et al., 2011; Burkard et al., 2011).

RNA-seq results show that three CAT transporters were significantly down-regulated in the *Tbb-5FURes* strain (Alzahrani, 2017). However, in chapter 3 of this thesis it is shown that there was no significant difference in the

sensitivity to 5-FU and 6-AU pyrimidine analogues and uracil transport through a single knockout of the *Tbb CAT1-4* genes in *T. b. brucei* BSF s427-WT, although mRNA levels in some sKO clones was halved. We also showed that the transport rate of [³H]-uracil in *Tbb-5FURes* was only partly reduced from the wild-type levels, as it entails the problem of high background generated by transport via TbU3. However, this outcome does not mean that *Tbb-CAT1-4* genes are not involved in the 5-FU sensitivity or transport, for the reason that the first allele of these genes was deleted while the second allele still exists in the genome of hemizygous knockout cells. Unfortunately, we were unable to make a full double knockout for the *Tbb-CAT1-4* genes, as this led to the death of the cells, showing that their function is essential for the growth of the *T. b. brucei*. Also, Alzahrani (2017) proved that the genes encoding CATs are essential for the viability of *T. b. brucei* BSF cells, as RNAi-mediated the downregulation of Tbb-Cation1-4 genes showed that the genes are essential for the survival of *T. b. brucei* BSF, a severe growth defect noticed after inducing expression of the RNAi construct with tetracycline. The potential utility of this system is the investigation of the connection between the uptake of uracil/5-FU and Tbb-CAT1-4 proteins within the *T. brucei*. According to a Pfam analysis (<https://pfam.xfam.org>) Tbb-CAT1-4 protein can be part of the Zip Zinc transporter family (PF02535). Thus, it is possible that the double knockout effect of the *Tbb-CAT1-4* genes would disrupt intracellular ion distribution in *T. brucei*. Consequently, it is possible that these CATs are belong to Zip zinc transporter family, and iron ions are very important in mitochondrial metabolism, as they are essential to the function of cytochromes and of Trypanosome Alternative Oxidase (TAO) (Saimoto et al., 2013; Shiba et al., 2013). However, this appears to rule out the possible involvement of CAT transporters in uracil uptake as we have reason to believe that the uracil/5-FU transporters are not essential when it comes to *T. b. brucei* and *L. mexicana* parasites although they are important when it comes to 5-FU anti-protozoal activity (Alzahrani et al., 2017). We firmly believed that the pyrimidine transporter gene is not likely to be essential in *T. b. brucei* BSF because of the following two reasons. 1) The ability of pyrimidine prototrophic *T. b. brucei* cells to grow in pyrimidine-free HMI-9 media (Ali et al., 2013b). 2) There was a reduction of [³H]-5-FU uptake rate by greater than 65% when *T. b. brucei* WT adapted to high levels of 5-FU (*Tbb-5FURes*) (Ali et al., 2013a).

Additionally, a similar experiment was done using *L. mexicana* promastigotes almost completely eliminated (94.5%) [³H]-5-FU transport in the *Lmex-5FURes* (Alzahrani et al., 2017), demonstrating that the uracil/5-FU transporters are non-essential in this organism.

Another class of genes highlighted in the 5-FU resistance analyses leading up to the work reported in this thesis are the fatty acid desaturases (FADs). FADs are categorized into three classes observed in Kinetoplastid parasites. The first class is Delta 'Δ' desaturases, which introduces the double-bond x-carbons from the carboxyl end. The second class is Omega 'ω,' which comprises of enzymes that introduce double-bond x-carbons from the methyl end. The third class is Chi and nu 'ν + x' desaturases, which add double-bond x-carbons from the existing double bond (Alloatti and Uttaro, 2011; Petrini et al., 2004). *L. mexicana* and *T. brucei* cells have the ability of taking up lipids from the host environments through the receptor-mediated endocytosis of lipoproteins or transportation of protein-bound fatty acid. In addition they have the ability to synthesize their own fatty acids *de novo* via mitochondrial type II (prokaryotic-type) pathways (Smith and Bütikofer, 2010; Zhang and Beverley, 2010).

RNA-seq and RIT-seq data revealed FAD as one of the most prominent hits to be linked to 5-FU resistance in *T. b. brucei* BSF. *Tbb-FAD* gene showed significant decreases in the transcription in *Tbb-5FURes* with a log₂ fold-change of -0.68 ($P \leq 0.01$) (Ali, 2013; Alzahrani, 2017). Moreover, RNA-seq also showed that FAD is an interesting hit also connected to 5-FU resistance in *L. mexicana* promastigotes. *Lmex-FAD* gene was downregulated in the *Lmex-5FURes* with a Log₂ fold-change of -0.32 ($P \leq 0.01$) (Alzahrani, 2017). The results in chapter 4 show that overexpression of the *Tbb-FAD* gene in *Tbb-5FURes* and *Lmex-FAD* gene in *Lmex-5FURes* do not cause an increase in the sensitivity to 5-FU *in vitro* as well as did not change the transport rate of [³H]-uracil. Therefore, it is still not clear how FAD determines sensitivity to pyrimidine nucleobases or transport in *L. mexicana* and *T. b. brucei*. However, while it is clear that the regular expression of the FAD gene is not limiting the sensitivity to 5-FU, it appears that a strong reduction in expression may cause resistance, hence the observation that overexpression did not change susceptibility to 5-FU, but RNAi-mediated

downregulation (RITseq) did. If time had allowed, we recommend functional characterisation of *Tbb-FAD* gene in *T. brucei* using RNAi technique to study FAD knockdown phenotypes. We also recommend tagging *Tbb-FAD* gene with GFP and transfecting the tagged gene in *T. brucei*. Then, immunofluorescence assay could be performed to determine the localization of the protein.

It has been determined that uracil transporter mutants are resistant to 5-FU in several instances (Palmer et al., 1975; Jund et al., 1977; Andersen et al., 1995; Amillis et al., 2007; Stoffer-Bittner et al., 2018). For instance, it has been identified by previous studies that deleting the uracil transporter *FurD* from *A. nidulans* is responsible for contributing to full resistance to 5-FU and a reduced uptake rate of [³H]-uracil (Amillis et al., 2007). However, protozoan genomes do not contain any *FurD* homologues and the uptake of uracil is required to be mediated by a transporter from different gene families. For that reason, we functionally expressed *FurD* in the 5-FU resistant cell lines (*Tbb-5FURes* and *Lmex-5FURes*) in order to investigate whether the sensitivity to 5-FU *in vitro* resistant strains could be restored by the introduction of a confirmed uracil/5-FU transporter. This would allow a functional screening of potential transporter genes.

We found no significant differences in the EC₅₀ values of 5-FU of resistant and expressing cell lines. It was, however, revealed that the expression of *FurD* in *Lmex-5FURes* caused high levels of [³H]-5FU/uracil uptake, to a level that is considerably above the wild type activity. We characterised the transport activity of *FurD* in *Lmex-5FURes* promastigotes and found *FurD* to be a highly selective and high-affinity transporter for uracil, as originally reported in *Aspergillus nidulans* (Amillis et al., 2007), and confirmed that 5-FU was also a good substrate for *FurD*. As the resistance was induced, stepwise, to a very high concentration of 5-FU in *Lmex-5FURes*, it is possible that the cells developed defects in both the uptake and the metabolism of the 5-FU, making them fully resistant to 5-FU, whether it enters the cells or not. Therefore, a metabolic adaptation appears to have rendered the *Lmex-5FURes* cells insensitive to intracellular 5-FU. Therefore, we highly recommended to assess the metabolism of 5-FU, using metabolomic assessments of *L. mexicana* clonal lines adapted to

high concentrations of 5-FU, the sensitive *L. mexicana*-WT and 5-FU resistant cell lines expressing FurD.

Many *Trypanosoma* and *Leishmania* protists including *L. mexicana* and *T. brucei* species, possess hexose transporters that are related in sequence to the mammalian GLUT1, an equilibrative glucose transporter and is a member of the major facilitator superfamily (MFS) (Dean et al., 2014; Deng et al., 2014). In *L. mexicana*, three transport proteins are designated to transport hexoses such as glucose, ribose, and amino sugars. These permeases are LmexGT1, LmexGT2 and LmexGT3 and while they close related, they differ in functionality and biological properties, including aspects such as differential localisation, substrate specificity, and developmental stage expression (Burchmore et al., 2003a; Rodriguez-Contreras et al., 2007).

In comparison to LmexGT2 and LmexGT3, LmexGT1 displays a lower affinity towards hexoses and serves only as a signal transducer and glucose sensor. LmexGT1 functions by promoting the transition from the exponential phase of growth to the stationary phase when there is low glucose level, and is thus is needed in the survival and adaptation of the promastigote (Akpunarlieva and Burchmore, 2017). In contrast, LmexGT2 and LmexGT3 are high affinity hexose permeases specifically localized on the plasma membrane (Akpunarlieva and Burchmore, 2017). *LmexGT1*, *LmexGT2* and *LmexGT3* belong to the SLC2 or GLUT transporter family (Pereira and Silber, 2012; Augustin, 2010).

One of the most striking results to emerge from our data is that glucose transporter genes showed up in both our RNA-seq and RIT-seq data. Determination of sensitivity of glucose transporter genes to 5-FU was achieved by a full knockout of these genes in *L. mexicana* (Burchmore et al., 2003a). This revealed a significant reduction in the sensitivity of the *LmexGT1-3* double knockout to 5-FU when compared to the wild type cell lines. The result also showed that there is no longer any accumulation of 5-FU and uracil by the *LmexGT1-3* KO cells. Yet, there were no measurable effects of uracil and 5-FU on the transportation of glucose by LmexGT1, LmexGT2, and LmexGT3.

Although, there was a significant increase in the sensitivity to 5-FU from the re-expression of individual LmexGT transporters in *Lmex-GT1-3* KO cells, ultimately the results of our study indicate that uracil/5-FU and glucose do not share the same transporters. Considering that both 5-FU and uracil are pyrimidines, it could be speculated that the metabolism of glucose regulates the uptake of uracil and 5-FU, as the pathways overlap in the process of glycosylation (e.g. UDP-glucose, UDP-galactose and UDP-N-acetylglucosamine) and/or lipid biosynthesis (CDP-ethanolamine, CDP-choline). However, the presence of glucose in the medium did not affect the uptake rate of uracil or 5-FU, or sensitivity to 5-FU, so we are left with the conclusion that although the presence of glucose transporters is essential for uracil uptake in *Leishmania*, the uptake of glucose is not. The mechanism for this is currently unclear but could conceivably be related to a complexing of different membrane proteins including LmexGTs, necessary to enable uracil transport.

The possibility of the use of *L. mexicana-Cas9^{ΔNT1}* promastigotes as surrogate systems for expressing TcrNB2 and TcrNT2 transporters of *T. cruzi* was also tested. We found TcrNT2 to be a high-affinity thymidine transporter, confirming and elaborating on the results obtained by former PhD student Gustavo Campagnaro (Campagnaro et al., 2018b). TcrNT2 transporter is the only known dedicated thymidine transporter in protozoa described to date. It was not possible to perform the biochemical characterization of TcrNB2, however, although it had structural and sequence similarities to the *Leishmania* NT4 transporters, indicating that it might possibly be a low-affinity purine transporter (Ortiz et al., 2009a; Campagnaro et al., 2018b). The high level of adenine transport in *L. mexicana-Cas9^{ΔNT1}* cells could easily have masked any adenine uptake mediated by the TcrNB2 transporter, especially if TcrNB2 presents low affinity for its substrates. Thus, we highly recommend the heterologous expression of TcrNB2 in *L. mexicana-Cas9^{ΔNT3}* cell lines in order to determine whether adenine is a substrate for TcrNB2. The expression of a tagged version of TcrNB2 and its immunolocalization could show whether it is present in the cellular membrane or not and help to explain why we have been unable to identify its substrate.

To date, the gene family responsible for the encoding of pyrimidine transporters in kinetoplast parasites has not been discovered. In the dataset of RNA-seq and RIT-seq experiments, the reverse genetic validation of top hits has not yet resulted in the identification of the protozoan pyrimidine transporter genes (PPTs) in *Trypanosoma* and *Leishmania* species. Though there is still need for much to be done, good progress has been achieved when it comes to identifying the PPTs. The identification of these genes will serve to improve the understanding of nutrient and drug transporters as well as increase the insights into nucleotide metabolism and pyrimidine salvage processes of kinetoplast parasites. Finally, the knowledge obtained herein will be of importance in providing a foundation for conducting further studies on the developing and complex universe that pertains to the nutrient transporters of protozoa.

Appendices

Appendix 1: Preparation of culture medium.

A) Standard HMI-9 Media

1 tub HMI-9 powder

15 g NaHCO_3

4.5 L ddH₂O (+ more to 5 L)

71.5 μL 13.4M β -mercaptoethanol

HCl / NaOH

1. Put tub of HMI-9 powder into 5 L flask, add 15 g NaHCO_3 .
2. Add 4.5 L of ddH₂O, rinsing out tub with some of the water.
3. Add 71.5 μL 13.4 M β -mercaptoethanol
4. Stir flask overnight in coldroom.
5. Add 1 bottle of 500 mL of Heat Inactivated Fetal Bovine Serum(FBS)
6. Adjust the pH to 7.4
7. Filter sterilise through 0.22 μm filter units, into sterile bottles
8. Store in cold room 4°C.

B) SDM 79 without glucose media

Compounds	For 1 Liter
NaH_2PO_4	157 mg
NaCl	6.8 g
MgSO_4	100 mg
KCl	400 mg
CaCl_2	200 mg
L-Arginine	100 mg
L-Methionine	70 mg
L-Phenylalanine	80 mg
L-Threonine	350 mg
L-proline	600 mg
L-Tyrosine	100 mg
Taurine	160 mg
L-Alanine	200 mg

L-Asparagine	13,2 mg
L-Aspartate	13.3 mg
L-Glutamate	14.7 mg
L-Glutamine	200 mg
Glycine	7.5 mg
L.Serine	60 mg
HEPES	8 g
MOPS	5 g
NaHCO ₃	2.2 g
Pyruvate	220 mg
Mercatoethanol 0.1 M	2 mL
Hypoxanthine	14 mg
Thymidine	4 mg
Vitamins 100 X	10 mL
Essential amino acids 50 X	20 mL
Phenol Red	4 mL
Hemin (2.5 mg/mL)	2mL

Add 50 mL of Heat Inactivated Fetal Bovine Serum (FBS). Make up to 1 Liter. Adjust the pH to 7.4. Filter sterilise through 0.22 µm filter units, into sterile bottles. Store in cold room 4°C.

C) HOMEM without glucose media

Compounds	For 5 Liter
SOD DIHYD PHOS 2H ₂ O EP	7.9 g
MAG SULPHATE 7H ₂ O EP	1 g
SODIUM CHLORIDE EP	34 g
POTASSIUM CHLORIDE EP	2 g
SODIUM PYRUVATE	0.55 g
MEM A/A (x50)	150 mL
200mM L-GLUTAMINE (x100)	50 mL
MEM NEAA (x100)	50 mL
MEM VIT (x100)	50 mL
D-BIOTIN EP	0.0005 g

P-AMINOBENZOIC ACID	0.005 g
PHENOL RED NA SALT	0.05 g
HEPES	29.7875 g
SODIUM BICARBONATE EP	1.5 g

Add 500 mL of Heat Inactivated Fetal Bovine Serum (FBS). Make up to 5 Liter. Adjust the pH to 7.4. Filter sterilise through 0.22 μ m filter units, into sterile bottles. Store in cold room 4°C.

Appendix 2: Prepration of general buffers and solutions.

A) Luria Bertani (LB) broth (pH 7)

LB powder (Sigma-Aldrich)	12.5 g
Distilled water	500 mL

B) LB Agar

Luria Agar (Sigma-Aldrich)	17.5 g
Distilled water	500 mL

C) Cytomex buffer (pH 7.6)

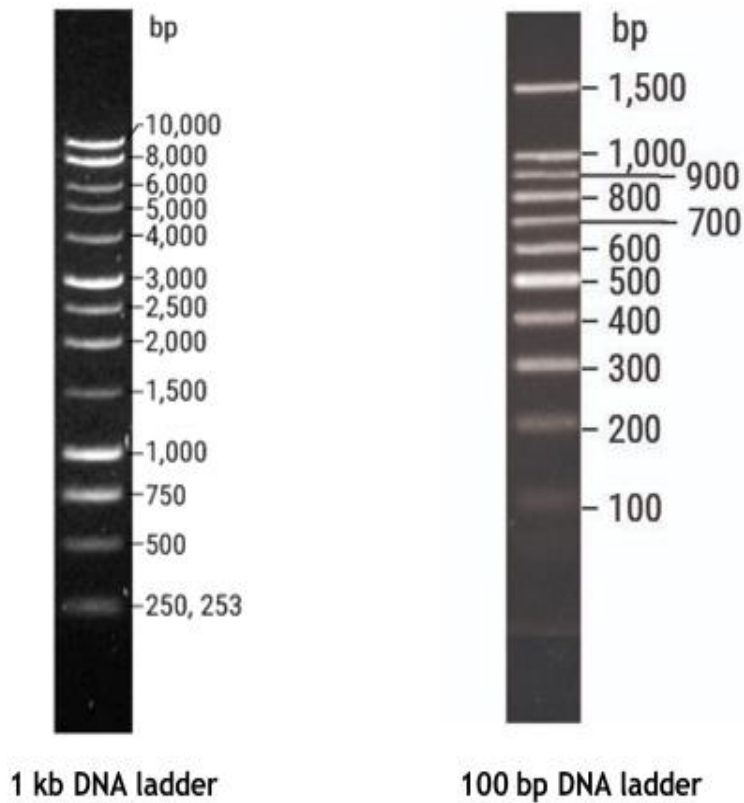
KCl	120 mM
HEPES pH 7.6	25 mM
MgCl ₂ .6H ₂ O	5 mM
K ₂ HPO ₄ /KH ₂ PO ₄ pH 7.6	10 mM
EGTA pH 7.6	2 mM
CaCl ₂	150 μ M
Glucose	0.5%
Albumin, bovine serum	100 μ g/mL
Hypoxanthine	1 mM

Appendix 3: Transformation of XL1 blue *E. coli* cells with plasmid DNA

1. Defrost aliquot of XL1 blue cells on ice.
2. Put 5 μ L of ligation into Eppendorf tube.
3. Add 50 μ L of XL1 blue cells.
4. Incubate on ice for 30 min.

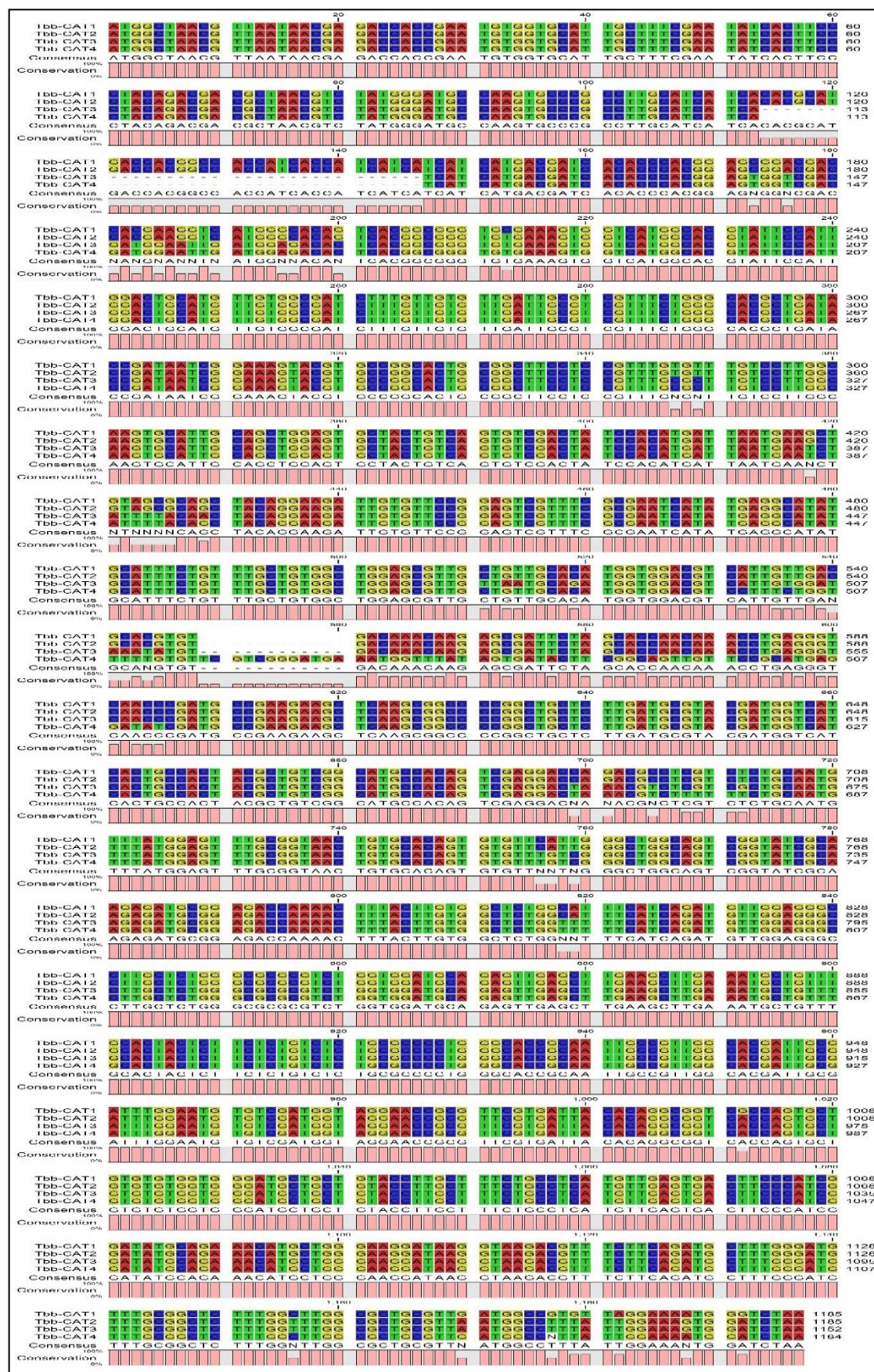
5. Heat shock at 42°C for 45 s.
6. Incubate on ice for 2 min.
7. Add 100 µL SOC media or LB broth.
8. Incubate at 37°C for one hour with shaking.
9. Spread cells on LB agar containing ampicillin (100 µg/mL).
10. Incubate at 37°C overnight.

Appendix 4: Ladders



Source: www.promega.com

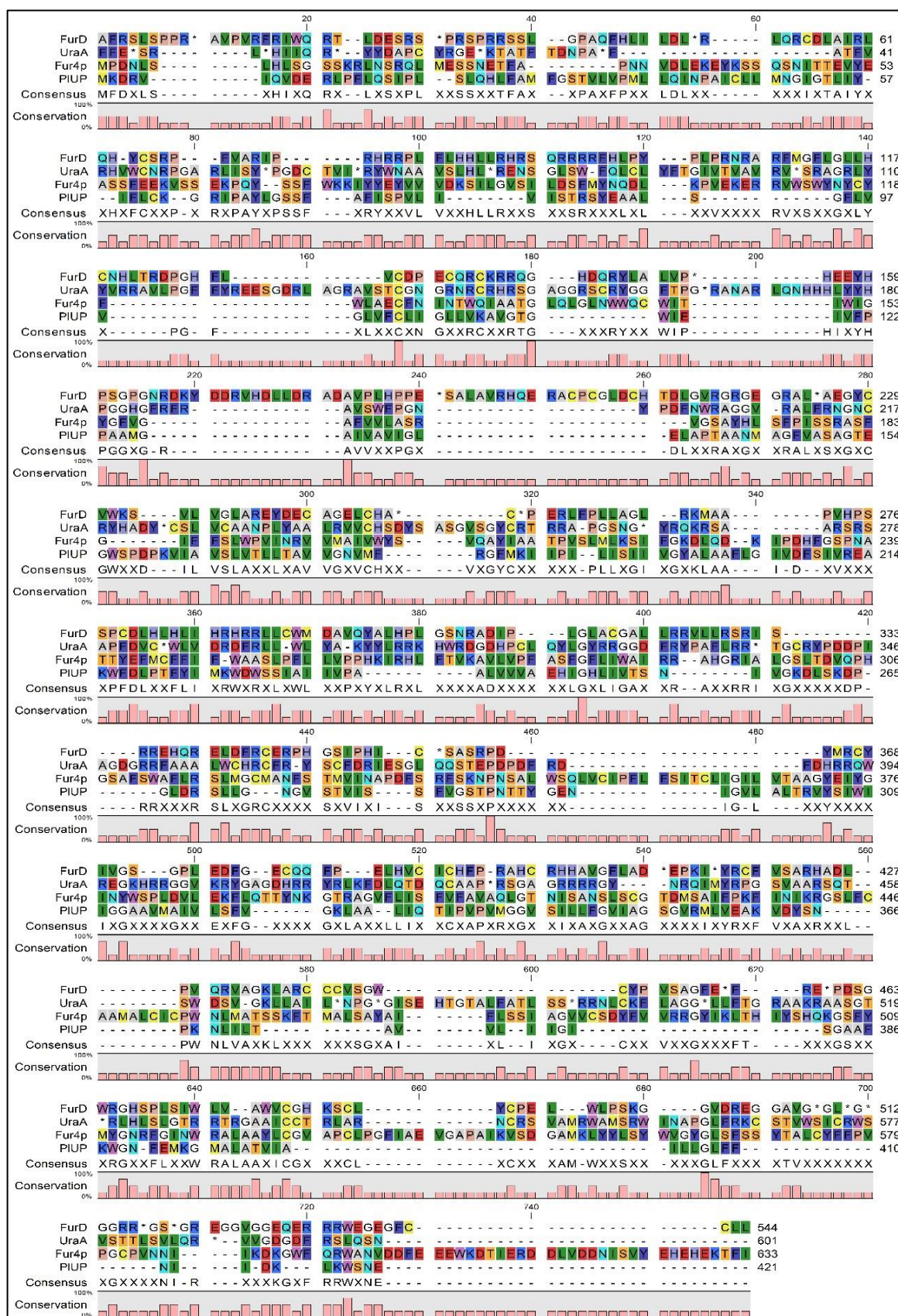
Appendix 5: The multiple sequence alignment result of the Tbb-CAT1, Tbb-CAT2, Tbb-CAT3 and Tbb-CAT4. Alignments were performed using CLC Genomics Workbench version 7.0 software package.



Appendix 6: Kinetoplastid *Tbb-FAD* and *Lmex-FAD* genes sequence alignment. Alignments were performed using CLC Genomics Workbench version 7.0 software package.



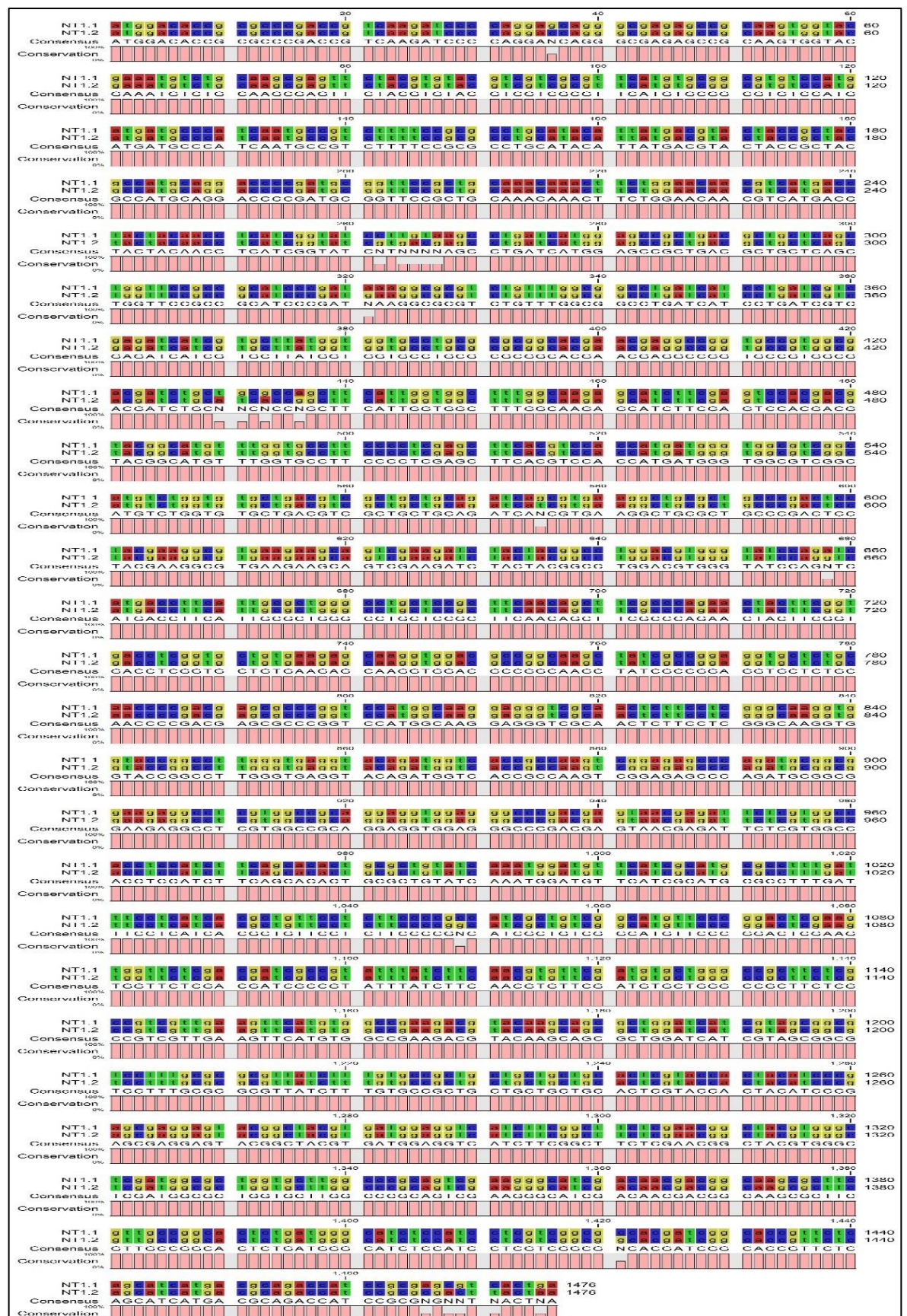
Appendix 7: Amino acid sequence alignment of the four different uracil transporters in *A. nidulans*, *S. cerevisiae*, *E. coli* and *P. larvae* organisms. Alignments were performed using CLC Genomics Workbench version 7.0 software package.



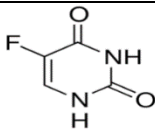
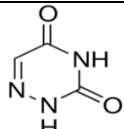
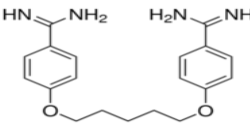
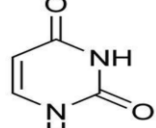
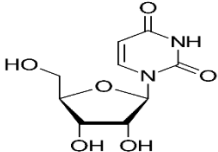
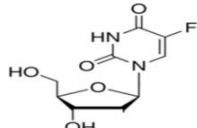
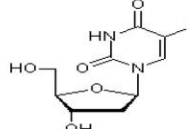
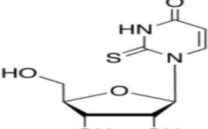
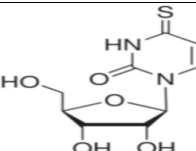
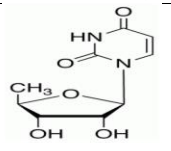
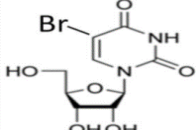
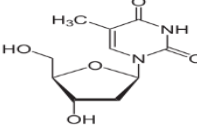
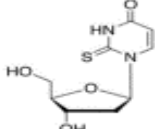
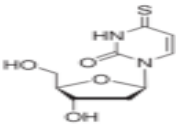
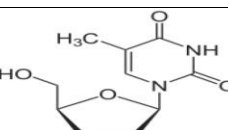
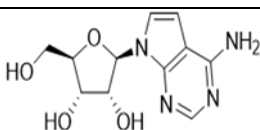
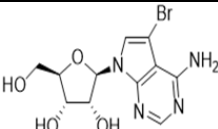
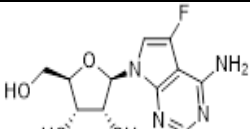
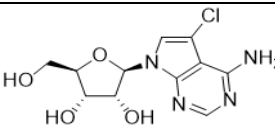
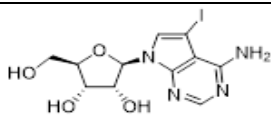
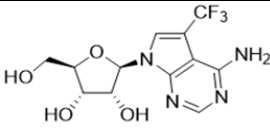
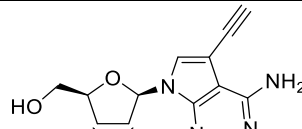
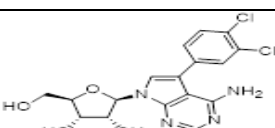
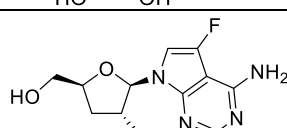
Appendix 8: The amino acid sequences alignment of three glucose transporter genes (*LmexGT1*, *LmexGT2* and *LmexGT3*) in *L. mexicana* promastigotes. Alignments were performed using CLC Genomics Workbench version 7.0 software package.

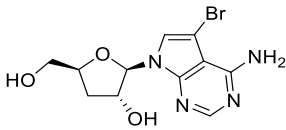
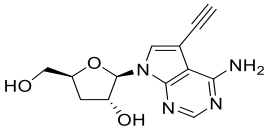
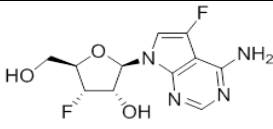


Appendix 9: The multiple sequence alignment result of the *NT1.1* and *NT1.2* genes in *L. mexicana* promastigotes. Alignments were performed using CLC Genomics Workbench version 7.0 software package.



Appendix 10: Structures of pyrimidine and adenosine analogues used.

5-Fluorouracil		6-Azauracil	
Pentamidine		Uracil	
Uridine		5-fluoro-2'-deoxyUridine	
5-iodo-2'-deoxyUridine		2-thioUridine	
4-thioUridine		5'-deoxyUridine	
5'-bromoUridine		Thymidine	
2-thiothymidine		4-thiothymidine	
3'-deoxythymidine		Tubercidin	
TH1003		FH3167	
FH3169		FH3141	
FH6367		FH3143	
FH3147		FH8517	

FH7429-up		FH8505	
JB588			

References

- ACESTOR, N., PANIGRAHI, A. K., OGATA, Y., ANUPAMA, A. & STUART, K. D. 2009. Protein composition of *Trypanosoma brucei* mitochondrial membranes. *Proteomics*, 9, 5497-5508.
- ACIMOVIC, Y. & COE, I. R. 2002. Molecular evolution of the equilibrative nucleoside transporter family: identification of novel family members in prokaryotes and eukaryotes. *Molecular biology and evolution*, 19, 2199-2210.
- AKPUNARLIEVA, S. & BURCHMORE, R. 2017. The role of membrane transporters in *Leishmania* virulence. *Emerging Topics in Life Sciences*, 1, 601-611.
- AKSOY, S., BUSCHER, P., LEHANE, M., SOLANO, P. & VAN DEN ABEELE, J. 2017. Human African trypanosomiasis control: achievements and challenges. *PLoS neglected tropical diseases*, 11.
- AL-SALABI, M. I. & DE KONING, H. P. 2005. Purine nucleobase transport in amastigotes of *Leishmania mexicana*: involvement in allopurinol uptake. *Antimicrobial agents and chemotherapy*, 49, 3682-3689.
- AL-SALABI, M. I., WALLACE, L. J. & DE KONING, H. P. 2003. A *Leishmania* major Nucleobase Transporter Responsible for Allopurinol Uptake Is a Functional Homolog of the *Trypanosoma brucei* H2 Transporter. *Molecular pharmacology*, 63, 814-820.
- AL-SALABI, M. I., WALLACE, L. J., LÜSCHER, A., MÄSER, P., CANDLISH, D., RODENKO, B., GOULD, M. K., JABEEN, I., AJITH, S. N. & DE KONING, H. P. 2007. Molecular interactions underlying the unusually high adenosine affinity of a novel *Trypanosoma brucei* nucleoside transporter. *Molecular pharmacology*, 71, 921-929.
- ALGHAMDI, A., MUNDAY, J. C., CAMPAGNARO, G. D., GURVIC, D., SVENSSON, F., OKPARA, C. E., KUMAR, A., ABRIL, M. E. M., WATSON, L. & PAAPE, D. 2020. Positively selected modifications in the pore of TbAQP2 allow pentamidine to enter *Trypanosoma brucei*. *BioRxiv*.
- ALI, J. A., CREEK, D. J., BURGESS, K., ALLISON, H. C., FIELD, M. C., MASER, P. & DE KONING, H. P. 2013a. Pyrimidine salvage in *Trypanosoma brucei* bloodstream forms and the trypanocidal action of halogenated pyrimidines. *Mol Pharmacol*, 83, 439-53.
- ALI, J. A., TAGOE, D. N., MUNDAY, J. C., DONACHIE, A., MORRISON, L. J. & DE KONING, H. P. 2013b. Pyrimidine biosynthesis is not an essential function for *Trypanosoma brucei* bloodstream forms. *PLoS One*, 8.
- ALI, J. A. M. 2013. *PYRIMIDINE SALVAGE AND METABOLISM IN KINETOPLASTID PARASITES*. PhD, University of Glasgow.
- ALLOATTI, A., GUPTA, S., GUALDRÓN-LÓPEZ, M., IGOILLO-ESTEVE, M., NGUEWA, P. A., DEUMER, G., WALLEMACQ, P., ALTABE, S. G., MICHELS, P. A. & UTTARO, A. D. 2010. Genetic and chemical evaluation of *Trypanosoma brucei* oleate desaturase as a candidate drug target. *PloS one*, 5.

- ALLOATTI, A. & UTTARO, A. D. 2011. Highly specific methyl-end fatty-acid desaturases of trypanosomatids. *Molecular and biochemical parasitology*, 175, 126-132.
- ALSFORD, S., ECKERT, S., BAKER, N., GLOVER, L., SANCHEZ-FLORES, A., LEUNG, K. F., TURNER, D. J., FIELD, M. C., BERRIMAN, M. & HORN, D. 2012. High-throughput decoding of antitrypanosomal drug efficacy and resistance. *Nature*, 482, 232-6.
- ALSFORD, S., KAWAHARA, T., GLOVER, L. & HORN, D. 2005. Tagging a *T. brucei* RRNA locus improves stable transfection efficiency and circumvents inducible expression position effects. *Molecular and biochemical parasitology*, 144, 142-148.
- ALSFORD, S., TURNER, D. J., OBADO, S. O., SANCHEZ-FLORES, A., GLOVER, L., BERRIMAN, M., HERTZ-FOWLER, C. & HORN, D. 2011. High-throughput phenotyping using parallel sequencing of RNA interference targets in the African trypanosome. *Genome research*, 21, 915-924.
- ALTAMURA, F., RAJESH, R., CATTAPRETA, C. M., MORETTI, N. S. & CESTARI, I. 2020. The current drug discovery landscape for trypanosomiasis and leishmaniasis: Challenges and strategies to identify drug targets. *Drug Development Research*.
- ALZHRANI, K. J. 2017. *Strategies for the identification and cloning of genes encoding pyrimidine transporters of Leishmania and Trypanosoma species*. PhD Thesis, University of Glasgow.
- ALZHRANI, K. J., ALI, J. A., EZE, A. A., LOOI, W. L., TAGOE, D. N., CREEK, D. J., BARRETT, M. P. & DE KONING, H. P. 2017. Functional and genetic evidence that nucleoside transport is highly conserved in *Leishmania* species: Implications for pyrimidine-based chemotherapy. *International Journal for Parasitology: Drugs and Drug Resistance*, 7, 206-226.
- AMBIT, A., WOODS, K. L., CULL, B., COOMBS, G. H. & MOTTRAM, J. C. 2011. Morphological events during the cell cycle of *Leishmania major*. *Eukaryotic cell*, 10, 1429-1438.
- AMILLIS, S., HAMARI, Z., AMILLIS, S., HAMARI, Z., ROUMELIOTI, K., SCAZZOCCHIO, C. & DIALLINAS, G. 2007. Regulation of expression and kinetic modeling of substrate interactions of a uracil transporter in *Aspergillus nidulans*. *Molecular membrane biology*, 24, 206-214.
- ANDERSEN, P. S., FREES, D., FAST, R. & MYGIND, B. 1995. Uracil uptake in *Escherichia coli* K-12: isolation of *uraA* mutants and cloning of the gene. *Journal of Bacteriology*, 177, 2008-2013.
- ANNOURA, T., NARA, T., MAKIUCHI, T., HASHIMOTO, T. & AOKI, T. 2005. The origin of dihydroorotate dehydrogenase genes of kinetoplastids, with special reference to their biological significance and adaptation to anaerobic, parasitic conditions. *Journal of molecular evolution*, 60, 113-127.

- ARONOW, B., KAUR, K., MCCARTAN, K. & ULLMAN, B. 1987. Two high affinity nucleoside transporters in *Leishmania donovani*. *Molecular and biochemical parasitology*, 22, 29-37.
- ARRÚA, E. C., SEREMETA, K. P., BEDOGNI, G. R., OKULIK, N. B. & SALOMON, C. J. 2019. Nanocarriers for effective delivery of benznidazole and nifurtimox in the treatment of chagas disease: A review. *Acta tropica*, 105080.
- AUGUSTIN, R. 2010. The protein family of glucose transport facilitators: It's not only about glucose after all. *IUBMB life*, 62, 315-333.
- BAKER, N., ALSFORD, S. & HORN, D. 2011. Genome-wide RNAi screens in African trypanosomes identify the nifurtimox activator NTR and the eflornithine transporter AAT6. *Molecular and biochemical parasitology*, 176, 55-57.
- BAKER, N., DE KONING, H. P., MÄSER, P. & HORN, D. 2013. Drug resistance in African trypanosomiasis: the melarsoprol and pentamidine story. *Trends in parasitology*, 29, 110-118.
- BAKER, N., GLOVER, L., MUNDAY, J. C., ANDRÉS, D. A., BARRETT, M. P., DE KONING, H. P. & HORN, D. 2012. Aquaglyceroporin 2 controls susceptibility to melarsoprol and pentamidine in African trypanosomes. *Proceedings of the National Academy of Sciences*, 109, 10996-11001.
- BALAÑA-FOUCE, R., REGUERA, R., CUBRIA, J. & ORDÓÑEZ, D. 1998. The pharmacology of leishmaniasis. *General Pharmacology: The Vascular System*, 30, 435-443.
- BALCAZAR, D. E., VANRELL, M. C., ROMANO, P. S., PEREIRA, C. A., GOLDBAUM, F. A., BONOMI, H. R. & CARRILLO, C. 2017. The superfamily keeps growing: Identification in trypanosomatids of RibJ, the first riboflavin transporter family in protists. *PLoS neglected tropical diseases*, 11, e0005513.
- BALDWIN, S. A., BEAL, P. R., YAO, S. Y., KING, A. E., CASS, C. E. & YOUNG, J. D. 2004. The equilibrative nucleoside transporter family, SLC29. *Pflügers Archiv*, 447, 735-743.
- BALDWIN, S. A., MACKEY, J. R., CASS, C. E. & YOUNG, J. D. 1999. Nucleoside transporters: molecular biology and implications for therapeutic development. *Molecular medicine today*, 5, 216-224.
- BARNES, K., DOBRZYNSKI, H., FOPPOLO, S., BEAL, P. R., ISMAT, F., SCULLION, E. R., SUN, L., TELLEZ, J., RITZEL, M. & CLAYCOMB, W. C. 2006. Distribution and functional characterisation of ENT4, a novel cardiac adenosine transporter activated at acidic pH.
- BARRETT, M. 1997. The pentose phosphate pathway and parasitic protozoa. *Parasitology Today*, 13, 11-16.
- BARRETT, M. P. & CROFT, S. L. 2012. Management of trypanosomiasis and leishmaniasis. *British medical bulletin*, 104, 175-196.

- BARRETT, M. P., TETAUD, E., SEYFANG, A., BRINGAUD, F. & BALTZ, T. 1995. Functional expression and characterization of the *Trypanosoma brucei* procyclic glucose transporter, THT2. *Biochemical Journal*, 312, 687-691.
- BARRETT, M. P., VINCENT, I. M., BURCHMORE, R. J., KAZIBWE, A. J. & MATOVU, E. 2011. Drug resistance in human African trypanosomiasis. *Future microbiology*, 6, 1037-1047.
- BASU, R., BHAUMIK, S., BASU, J. M., NASKAR, K., DE, T. & ROY, S. 2005. Kinetoplastid membrane protein-11 DNA vaccination induces complete protection against both pentavalent antimonial-sensitive and-resistant strains of *Leishmania donovani* that correlates with inducible nitric oxide synthase activity and IL-4 generation: evidence for mixed Th1-and Th2-like responses in visceral leishmaniasis. *The Journal of Immunology*, 174, 7160-7171.
- BATES, P. A. 2007. Transmission of *Leishmania* metacyclic promastigotes by phlebotomine sand flies. *International journal for parasitology*, 37, 1097-1106.
- BAYELE, H. K., EISENTHAL, R. S. & TOWNER, P. 2000. Complementation of a Glucose Transporter Mutant of *Schizosaccharomyces pombe* by a Novel *Trypanosoma brucei* Gene. *Journal of Biological Chemistry*, 275, 14217-14222.
- BELLOFATTO, V. 2007. Pyrimidine transport activities in trypanosomes. *Trends in parasitology*, 23, 187-189.
- BENEKE, T. & GLUENZ, E. 2019. LeishGEdit: A Method for Rapid Gene Knockout and Tagging Using CRISPR-Cas9. *Leishmania*. Springer.
- BENEKE, T., MADDEN, R., MAKIN, L., VALLI, J., SUNTER, J. & GLUENZ, E. 2017. A CRISPR Cas9 high-throughput genome editing toolkit for kinetoplastids. *Royal Society open science*, 4, 170095.
- BERENS, R. L., KRUG, E. C. & MARR, J. J. 1995. Purine and pyrimidine metabolism. *Biochemistry and molecular biology of parasites*. Elsevier.
- BERN, C. 2015. Chagas' disease. *New England Journal of Medicine*, 373, 456-466.
- BERN, C., MESSENGER, L. A., WHITMAN, J. D. & MAGUIRE, J. H. 2019. Chagas disease in the United States: a public health approach. *Clinical microbiology reviews*, 33.
- BERRIMAN, M., GHEDIN, E., HERTZ-FOWLER, C., BLANDIN, G., RENAULD, H., BARTHOLOMEU, D. C., LENNARD, N. J., CALER, E., HAMLIN, N. E. & HAAS, B. 2005. The genome of the African trypanosome *Trypanosoma brucei*. *science*, 309, 416-422.
- BESTEIRO, S., WILLIAMS, R. A., COOMBS, G. H. & MOTTRAM, J. C. 2007. Protein turnover and differentiation in *Leishmania*. *International journal for parasitology*, 37, 1063-1075.
- BHATTACHARYA, A., LEPROHON, P., BIGOT, S., PADMANABHAN, P. K., MUKHERJEE, A., ROY, G., GINGRAS, H., MESTDAGH, A., PAPADOPOULOU, B. & OUELLETTE, M. 2019. Coupling chemical mutagenesis to next

- generation sequencing for the identification of drug resistance mutations in *Leishmania*. *Nature communications*, 10, 1-14.
- BIEBINGER, S., WIRTZ, L. E., LORENZ, P. & CLAYTON, C. 1997. Vectors for inducible expression of toxic gene products in bloodstream and procyclic *Trypanosoma brucei*. *Molecular and biochemical parasitology*, 85, 99-112.
- BOELAERT, M. & SUNDAR, S. 2014. Leishmaniasis.
- BOITZ, J. M., ULLMAN, B., JARDIM, A. & CARTER, N. S. 2012. Purine salvage in *Leishmania*: complex or simple by design? *Trends in parasitology*, 28, 345-352.
- BONNET, J., BOUDOT, C. & COURTILOUX, B. 2015. Overview of the diagnostic methods used in the field for human African trypanosomiasis: what could change in the next years? *BioMed research international*, 2015.
- BORST, P. & FAIRLAMB, A. 1998. Surface receptors and transporters of *Trypanosoma brucei*. *Annual review of microbiology*, 52, 745-778.
- BOSWELL-CASTEEL, R. C. & HAYS, F. A. 2017. Equilibrative nucleoside transporters—A review. *Nucleosides, Nucleotides and Nucleic Acids*, 36, 7-30.
- BOWERS, K. & SRAI, S. K. 2018. The trafficking of metal ion transporters of the Zrt-and Irt-like protein family. *Traffic*, 19, 813-822.
- BRAY, P. G., BARRETT, M. P., WARD, S. A. & DE KONING, H. P. 2003. Pentamidine uptake and resistance in pathogenic protozoa: past, present and future. *Trends in parasitology*, 19, 232-239.
- BRIDGES, D. J., GOULD, M. K., NERIMA, B., MASER, P., BURCHMORE, R. J. & DE KONING, H. P. 2007. Loss of the high-affinity pentamidine transporter is responsible for high levels of cross-resistance between arsenical and diamidine drugs in African trypanosomes. *Mol Pharmacol*, 71, 1098-108.
- BRINGAUD, F. & BALTZ, T. 1993. Differential regulation of two distinct families of glucose transporter genes in *Trypanosoma brucei*. *Molecular and cellular biology*, 13, 1146-1154.
- BRUN, R., BLUM, J., CHAPPUIS, F. & BURRI, C. 2010. Human african trypanosomiasis. *The Lancet*, 375, 148-159.
- BRUN, R., SCHUMACHER, R., SCHMID, C., KUNZ, C. & BURRI, C. 2001. The phenomenon of treatment failures in human African trypanosomiasis. *Tropical Medicine & International Health*, 6, 906-914.
- BURCHMORE, R. J. & HART, D. T. 1995. Glucose transport in amastigotes and promastigotes of *Leishmania mexicana mexicana*. *Molecular and biochemical parasitology*, 74, 77-86.
- BURCHMORE, R. J. & LANDFEAR, S. M. 1998. Differential regulation of multiple glucose transporter genes in *Leishmania mexicana*. *Journal of Biological Chemistry*, 273, 29118-29126.

- BURCHMORE, R. J., RODRIGUEZ-CONTRERAS, D., MCBRIDE, K., BARRETT, M. P., MODI, G., SACKS, D. & LANDFEAR, S. M. 2003a. Genetic characterization of glucose transporter function in *Leishmania mexicana*. *Proceedings of the National Academy of Sciences*, 100, 3901-3906.
- BURCHMORE, R. J., WALLACE, L. J., CANDLISH, D., AL-SALABI, M. I., BEAL, P. R., BARRETT, M. P., BALDWIN, S. A. & DE KONING, H. P. 2003b. Cloning, heterologous expression, and in situ characterization of the first high affinity nucleobase transporter from a protozoan. *Journal of Biological Chemistry*, 278, 23502-23507.
- BURKARD, G. S., JUTZI, P. & RODITI, I. 2011. Genome-wide RNAi screens in bloodstream form trypanosomes identify drug transporters. *Molecular and biochemical parasitology*, 175, 91-94.
- BURRI, C. & BLUM, J. 2017. Human African trypanosomiasis.
- BÜSCHER, P., CECCHI, G., JAMONNEAU, V. & PRIOTTO, G. 2017. Human african trypanosomiasis. *The Lancet*, 390, 2397-2409.
- BÜSCHER, P., GILLEMANN, Q. & LEJON, V. 2013. Rapid diagnostic test for sleeping sickness. *New England Journal of Medicine*, 368, 1069-1070.
- BÜSCHER, P., GONZATTI, M. I., HÉBERT, L., INOUE, N., PASCUCCHI, I., SCHNAUFER, A., SUGANUMA, K., TOURATIER, L. & VAN REET, N. 2019. Equine trypanosomosis: enigmas and diagnostic challenges. *Parasites & vectors*, 12, 234.
- BYRNE, B., ALGUEL, Y., SCULL, N., CRAVEN, G., ARMSTRONG, A., IWATA, S., DIALLINAS, G., AMILLIS, S., CAPALDI, S. & CAMERON, A. 2016. Structure of eukaryotic purine/Hp symporter UapA suggests a role for homodimerization in transport activity.
- CALDAS, I. S., SANTOS, E. G. & NOVAES, R. D. 2019. An evaluation of benznidazole as a Chagas disease therapeutic. *Expert opinion on pharmacotherapy*, 20, 1797-1807.
- CAMPAGNARO, G. D., ALZAHIRANI, K. J., MUNDAY, J. C. & DE KONING, H. P. 2018a. Trypanosoma brucei bloodstream forms express highly specific and separate transporters for adenine and hypoxanthine; evidence for a new protozoan purine transporter family? *Molecular and biochemical parasitology*, 220, 46-56.
- CAMPAGNARO, G. D., DE FREITAS NASCIMENTO, J., GIRARD, R. B., SILBER, A. M. & DE KONING, H. P. 2018b. Cloning and characterisation of the equilibrative nucleoside transporter family of Trypanosoma cruzi: ultra-high affinity and selectivity to survive in the intracellular niche. *Biochimica et Biophysica Acta (BBA)-General Subjects*, 1862, 2750-2763.
- CAMPAGNARO, G. D. & DE KONING, H. P. 2020. Purine and pyrimidine transporters of pathogenic protozoa-conduits for therapeutic agents. *Medicinal Research Reviews*.
- CANUTO, G. A., CASTILHO-MARTINS, E. A., TAVARES, M. F., RIVAS, L., BARBAS, C. & LÓPEZ-GONZÁLEZ, Á. 2014. Multi-analytical platform metabolomic

- approach to study miltefosine mechanism of action and resistance in Leishmania. *Analytical and bioanalytical chemistry*, 406, 3459-3476.
- CARADONNA, K. L., ENGEL, J. C., JACOBI, D., LEE, C.-H. & BURLEIGH, B. A. 2013. Host metabolism regulates intracellular growth of *Trypanosoma cruzi*. *Cell host & microbe*, 13, 108-117.
- CARDOSO, M. S., REIS-CUNHA, J. L. & BARTHOLOMEU, D. C. 2016. Evasion of the immune response by *Trypanosoma cruzi* during acute infection. *Frontiers in Immunology*, 6, 659.
- CARTER, N. S., BARRETT, M. P. & DE KONING, H. P. 1999. A drug resistance determinant in *Trypanosoma brucei*. *Trends in microbiology*, 7, 469-471.
- CARTER, N. S., DREW, M. E., SANCHEZ, M., VASUDEVAN, G., LANDFEAR, S. M. & ULLMAN, B. 2000. Cloning of a Novel Inosine-Guanosine Transporter Gene from *Leishmania donovani* by Functional Rescue of a Transport-deficient Mutant. *Journal of Biological Chemistry*, 275, 20935-20941.
- CARTER, N. S. & FAIRLAMB, A. H. 1993. Erratum: Arsenical-resistant trypanosomes lack an unusual adenosine transporter. *Nature*, 361, 374-374.
- CARTER, N. S., LANDFEAR, S. M. & ULLMAN, B. 2001. Nucleoside transporters of parasitic protozoa. *Trends in parasitology*, 17, 142-145.
- CARTER, N. S., RAGER, N. & ULLMAN, B. 2002. Purine and pyrimidine transport and metabolism. *Molecular Medical Parasitology*. Academic Press London, UK.
- CARTER, N. S., YATES, P., ARENDT, C. S., BOITZ, J. M. & ULLMAN, B. 2008. Purine and pyrimidine metabolism in *Leishmania*. *Drug targets in kinetoplastid parasites*. Springer.
- CASPARY, W. F. 1992. Physiology and pathophysiology of intestinal absorption. Oxford University Press.
- CHAKRAVARTY, J. & SUNDAR, S. 2010. Drug resistance in leishmaniasis. *Journal of global infectious diseases*, 2, 167.
- CHAPPUIS, F., SUNDAR, S., HAILU, A., GHALIB, H., RIJAL, S., PEELING, R. W., ALVAR, J. & BOELAERT, M. 2007. Visceral leishmaniasis: what are the needs for diagnosis, treatment and control? *Nature Reviews Microbiology*, 5.
- CHAPPUIS, F., UDAYRAJ, N., STIETENROTH, K., MEUSSEN, A. & BOVIER, P. A. 2005. Eflornithine is safer than melarsoprol for the treatment of second-stage *Trypanosoma brucei* gambiense human African trypanosomiasis. *Clinical Infectious Diseases*, 41, 748-751.
- CHAWLA, B., JHINGRAN, A., PANIGRAHI, A., STUART, K. D. & MADHUBALA, R. 2011. Paromomycin affects translation and vesicle-mediated trafficking as revealed by proteomics of paromomycin-susceptible-resistant *Leishmania donovani*. *PloS one*, 6.

- CHECKLEY, A., PEPIN, J., GIBSON, W., TAYLOR, M., JÄGER, H. & MABEY, D. 2007. Human African trypanosomiasis: diagnosis, relapse and survival after severe melarsoprol-induced encephalopathy. *Transactions of the Royal Society of Tropical Medicine and Hygiene*, 101, 523-526.
- CHENG, Y.-C. & PRUSOFF, W. H. 1973. Relationship between the inhibition constant (K_i) and the concentration of inhibitor which causes 50 per cent inhibition (I_{50}) of an enzymatic reaction. *Biochemical pharmacology*, 22, 3099-3108.
- CHIANG, C. W., CARTER, N., SULLIVAN, W., DONALD, R. G., ROOS, D. S., NAGUIB, F. N., EL KOUNI, M. H., ULLMAN, B. & WILSON, C. M. 1999. The adenosine transporter of *Toxoplasma gondii*. Identification by insertional mutagenesis, cloning, and recombinant expression. *Journal of Biological Chemistry*, 274, 35255-35261.
- CHOU, Y.-C., LAI, M. M., WU, Y.-C., HSU, N.-C., JENG, K.-S. & SU, W.-C. 2015. Variations in genome-wide RNAi screens: lessons from influenza research. *Journal of clinical bioinformatics*, 5, 2.
- CHOUDHURI, S. & CHANDERBHAN, R. F. 2016. The Biology of Nutrients: Genetic and Molecular Principles. *Nutraceuticals*. Elsevier.
- CLAYTON, C. 1999. Genetic manipulation of kinetoplastida. *Parasitology today*, 15, 372-378.
- COBO, F. 2014. Treatment. Leishmaniasis, in *Tropical Infectious Diseases*.
- COUPPIE, P., CLYTI, E., SOBESKY, M., BISSUEL, F., DEL GIUDICE, P., SAINTE-MARIE, D., DEDET, J., CARME, B. & PRADINAUD, R. 2004. Comparative study of cutaneous leishmaniasis in human immunodeficiency virus (HIV)-infected patients and non-HIV-infected patients in French Guiana. *British Journal of Dermatology*, 151, 1165-1171.
- COURA, J. R. & DE CASTRO, S. L. 2002. A critical review on Chagas disease chemotherapy. *Memórias do Instituto Oswaldo Cruz*, 97, 3-24.
- CROFT, S. & COOMBS, G. 2003. Leishmaniasis-current chemotherapy and recent advances in the search for novel drugs. *Trends in parasitology*, 19, 502-8.
- CROFT, S. L., SUNDAR, S. & FAIRLAMB, A. H. 2006. Drug resistance in leishmaniasis. *Clinical microbiology reviews*, 19, 111-126.
- CROVETTO-MARTÍNEZ, R., AGUIRRE-URIZAR, J., ORTE-ALDEA, C., ARALUCE-ITURBE, I., WHYTE-OROZCO, J. & CROVETTO-DE LA TORRE, M. 2015. Mucocutaneous leishmaniasis must be included in the differential diagnosis of midline destructive disease: two case reports. *Oral surgery, oral medicine, oral pathology and oral radiology*, 119, e20-e26.
- DE CARVALHO, L. P. & DE MELO, E. J. T. 2017. Life and death of *Trypanosoma cruzi* in presence of metals. *Biometals*, 30, 955-974.
- DE KONING, H. & DIALLINAS, G. 2000. Nucleobase transporters. *Molecular membrane biology*, 17, 75-94.

- DE KONING, H. P. 2007. Pyrimidine transporters of trypanosomes-a class apart? *Trends in Parasitology*, 23, 190.
- DE KONING, H. P. 2008. Ever-increasing complexities of diamidine and arsenical crossresistance in African trypanosomes. *Trends in parasitology*, 24, 345-349.
- DE KONING, H. P., ANDERSON, L. F., STEWART, M., BURCHMORE, R. J., WALLACE, L. J. & BARRETT, M. P. 2004. The trypanocide diminazene aceturate is accumulated predominantly through the TbAT1 purine transporter: additional insights on diamidine resistance in African trypanosomes. *Antimicrobial Agents and Chemotherapy*, 48, 1515-1519.
- DE KONING, H. P., BRIDGES, D. J. & BURCHMORE, R. J. 2005. Purine and pyrimidine transport in pathogenic protozoa: from biology to therapy. *FEMS microbiology reviews*, 29, 987-1020.
- DE KONING, H. P. & JARVIS, S. M. 1997a. Hypoxanthine Uptake through a Purine-Selective Nucleobase Transporter in Trypano Soma Brucei Brucei Procyclic Cells is Driven by Protonmotive Force. *European journal of biochemistry*, 247, 1102-1110.
- DE KONING, H. P. & JARVIS, S. M. 1997b. Purine nucleobase transport in bloodstream forms of Trypanosoma brucei brucei is mediated by two novel transporters. *Molecular and biochemical parasitology*, 89, 245-258.
- DE KONING, H. P. & JARVIS, S. M. 1998. A highly selective, high-affinity transporter for uracil in Trypanosoma brucei brucei: evidence for proton-dependent transport. *Biochemistry and Cell Biology*, 76, 853-858.
- DE KONING, H. P. & JARVIS, S. M. 1999. Adenosine transporters in bloodstream forms of Trypanosoma brucei brucei: substrate recognition motifs and affinity for trypanocidal drugs. *Molecular pharmacology*, 56, 1162-1170.
- DE KONING, H. P. & JARVIS, S. M. 2001. Uptake of pentamidine in Trypanosoma brucei brucei is mediated by the P2 adenosine transporter and at least one novel, unrelated transporter. *Acta tropica*, 80, 245-250.
- DE KONING, H. P., MACLEOD, A., BARRETT, M. P., COVER, B. & JARVIS, S. M. 2000. Further evidence for a link between melarsoprol resistance and P2 transporter function in African trypanosomes. *Molecular and biochemical parasitology*, 106, 181-185.
- DE PABLOS, L., FERREIRA, T. & WALRAD, P. 2016. Developmental differentiation in Leishmania lifecycle progression: post-transcriptional control conducts the orchestra. *Current opinion in microbiology*, 34, 82-89.
- DEAN, P., MAJOR, P., NAKJANG, S., HIRT, R. P. & EMBLEY, T. M. 2014. Transport proteins of parasitic protists and their role in nutrient salvage. *Frontiers in plant science*, 5, 153.
- DELESPAUX, V. & DE KONING, H. P. 2007. Drugs and drug resistance in African trypanosomiasis. *Drug resistance updates*, 10, 30-50.

- DELROT, S., ATANASSOVA, R. & MAUROSSET, L. 2000. Regulation of sugar, amino acid and peptide plant membrane transporters. *Biochimica et Biophysica Acta (BBA)-Biomembranes*, 1465, 281-306.
- DEMIRBILEK, H., GALCHEVA, S., VURALLI, D., AL-KHAWAGA, S. & HUSSAIN, K. 2019. Ion transporters, channelopathies, and glucose disorders. *International Journal of Molecular Sciences*, 20, 2590.
- DENG, D., XU, C., SUN, P., WU, J., YAN, C., HU, M. & YAN, N. 2014. Crystal structure of the human glucose transporter GLUT1. *Nature*, 510, 121-125.
- DENISE, H. & BARRETT, M. P. 2001. Uptake and mode of action of drugs used against sleeping sickness. *Biochemical pharmacology*, 61, 1-5.
- DESJEUX, P. 1996. Leishmaniasis: public health aspects and control. *Clinics in dermatology*, 14, 417-423.
- DESJEUX, P. 2004. Leishmaniasis: current situation and new perspectives. *Comparative immunology, microbiology and infectious diseases*, 27, 305-318.
- DESQUESNES, M., HOLZMULLER, P., LAI, D.-H., DARGANTES, A., LUN, Z.-R. & JITTAPLAPONG, S. 2013. Trypanosoma evansi and surra: a review and perspectives on origin, history, distribution, taxonomy, morphology, hosts, and pathogenic effects. *BioMed research international*, 2013.
- DICKIE, E. A., GIORDANI, F., GOULD, M. K., MÄSER, P., BURRI, C., MOTTRAM, J. C., RAO, S. P. & BARRETT, M. P. 2020. New Drugs for Human African Trypanosomiasis: A Twenty First Century Success Story. *Tropical Medicine and Infectious Disease*, 5, 29.
- DOCAMPO, R. & MORENO, S. N. 2003. Current chemotherapy of human African trypanosomiasis. *Parasitology research*, 90, S10-S13.
- DOLEZEL, D., JIRKŮ, M., MASLOV, D. A. & LUKES, J. 2000. Phylogeny of the bodonid flagellates (Kinetoplastida) based on small-subunit rRNA gene sequences. *International journal of systematic and evolutionary microbiology*, 50, 1943-1951.
- DOMIN, B. A., MAHONY, W. B. & ZIMMERMAN, T. P. 1993. Transport of 5-fluorouracil and uracil into human erythrocytes. *Biochemical pharmacology*, 46, 503-510.
- DONELSON, J. E. 2002. The genome of the African trypanosome. *The African Trypanosomes*. Springer.
- DONELSON, J. E. 2003. Antigenic variation and the African trypanosome genome. *Acta tropica*, 85, 391-404.
- DORLO, T. P. & KAGER, P. A. 2008. Pentamidine dosage: a base/salt confusion. *PLoS neglected tropical diseases*, 2.
- DOWLATI, Y. 1996. Cutaneous leishmaniasis: clinical aspect. *Clinics in dermatology*, 14, 425-431.

- DOWNING, T., IMAMURA, H., DECUYPERE, S., CLARK, T. G., COOMBS, G. H., COTTON, J. A., HILLEY, J. D., DE DONCKER, S., MAES, I. & MOTTRAM, J. C. 2011. Whole genome sequencing of multiple *Leishmania donovani* clinical isolates provides insights into population structure and mechanisms of drug resistance. *Genome research*, 21, 2143-2156.
- DREW, M. E., MORRIS, J. C., WANG, Z., WELLS, L., SANCHEZ, M., LANDFEAR, S. M. & ENGLUND, P. T. 2003. The adenosine analog tubercidin inhibits glycolysis in *Trypanosoma brucei* as revealed by an RNA interference library. *Journal of Biological Chemistry*, 278, 46596-46600.
- EHRLICH, P. 1907. Chemotherapeutische trypanosomen-studien. *Berliner Munch Tierarztl Wochenschr*, 11, 233-238.
- EIDE, D. J. 2004. The SLC39 family of metal ion transporters. *Pflügers Archiv*, 447, 796-800.
- ELARABI, A. S., SAAD, Z. A., SAADAWI, W. K., ALDOBEA, N. M. & SAGHER, F. A. 2020. A rare encounter in nonsuspecting circumstances: First congenital visceral leishmaniasis (kala-azar) in Libya. *Ibnosina Journal of Medicine and Biomedical Sciences*, 12, 44.
- ELIAS, M. C., DA CUNHA, J. P., DE FARIA, F. P., MORTARA, R. A., FREYMÜLLER, E. & SCHENKMAN, S. 2007. Morphological events during the *Trypanosoma cruzi* cell cycle. *Protist*, 158, 147-157.
- EREN, E. & ARGÜELLO, J. M. 2004. Arabidopsis HMA2, a divalent heavy metal-transporting PIB-type ATPase, is involved in cytoplasmic Zn²⁺ homeostasis. *Plant Physiology*, 136, 3712-3723.
- FAIRLAMB, A. H. 2003. Chemotherapy of human African trypanosomiasis: current and future prospects. *Trends in parasitology*, 19, 488-494.
- FEISTEL, T., HODSON, C. A., PEYTON, D. H. & LANDFEAR, S. M. 2008. An expression system to screen for inhibitors of parasite glucose transporters. *Molecular and biochemical parasitology*, 162, 71-76.
- FENG, X., RODRIGUEZ-CONTRERAS, D., BUFFALO, C., BOUWER, H. A., KRUVAND, E., BEVERLEY, S. M. & LANDFEAR, S. M. 2009. Amplification of an alternate transporter gene suppresses the avirulent phenotype of glucose transporter null mutants in *Leishmania mexicana*. *Molecular microbiology*, 71, 369-381.
- FENG, X., RODRIGUEZ-CONTRERAS, D., POLLEY, T., LYE, L. F., SCOTT, D., BURCHMORE, R. J., BEVERLEY, S. M. & LANDFEAR, S. M. 2013. 'Transient' genetic suppression facilitates generation of hexose transporter null mutants in *Leishmania mexicana*. *Molecular microbiology*, 87, 412-429.
- FERNÁNDEZ, M. M., MALCHIODI, E. L. & ALGRANATI, I. D. 2011. Differential effects of paromomycin on ribosomes of *Leishmania mexicana* and mammalian cells. *Antimicrobial agents and chemotherapy*, 55, 86-93.

- FIEBIG, M., KELLY, S. & GLUENZ, E. 2015. Comparative life cycle transcriptomics revises *Leishmania mexicana* genome annotation and links a chromosome duplication with parasitism of vertebrates. *PLoS pathogens*, 11.
- FIELD, M. C., HORN, D., FAIRLAMB, A. H., FERGUSON, M. A., GRAY, D. W., READ, K. D., DE RYCKER, M., TORRIE, L. S., WYATT, P. G. & WYLLIE, S. 2017. Anti-trypanosomatid drug discovery: an ongoing challenge and a continuing need. *Nature Reviews Microbiology*, 15, 217-231.
- FIJOLEK, A., HOFER, A. & THELANDER, L. 2007. Expression, purification, characterization, and in vivo targeting of trypanosome CTP synthetase for treatment of African sleeping sickness. *Journal of biological chemistry*, 282, 11858-11865.
- FILARDI, L. & BRENER, Z. 1987. Susceptibility and natural resistance of *Trypanosoma cruzi* strains to drugs used clinically in Chagas disease. *Transactions of the Royal Society of Tropical Medicine and Hygiene*, 81, 755-759.
- FINLEY, R. W., COONEY, D. A. & DVORAK, J. A. 1988. Nucleoside uptake in *Trypanosoma cruzi*: analysis of a mutant resistant to tubercidin. *Molecular and biochemical parasitology*, 31, 133-140.
- FIRE, A., XU, S., MONTGOMERY, M. K., KOSTAS, S. A., DRIVER, S. E. & MELLO, C. C. 1998. Potent and specific genetic interference by double-stranded RNA in *Caenorhabditis elegans*. *nature*, 391, 806-811.
- FLANNERY, A. R., HUYNH, C., MITTRA, B., MORTARA, R. A. & ANDREWS, N. W. 2011. LFR1 ferric iron reductase of *Leishmania amazonensis* is essential for the generation of infective parasite forms. *Journal of Biological Chemistry*, 286, 23266-23279.
- FRANCO, J. R., SIMARRO, P. P., DIARRA, A. & JANNIN, J. G. 2014. Epidemiology of human African trypanosomiasis. *Clinical epidemiology*, 6, 257.
- FRANCO, J. R., SIMARRO, P. P., DIARRA, A., RUIZ-POSTIGO, J. A., SAMO, M. & JANNIN, J. G. 2012. Monitoring the use of nifurtimox-eflornithine combination therapy (NECT) in the treatment of second stage gambiense human African trypanosomiasis. *Research and Reports in Tropical Medicine*, 3, 93.
- FREITAS-JUNIOR, L. H., CHATELAIN, E., KIM, H. A. & SIQUEIRA-NETO, J. L. 2012. Visceral leishmaniasis treatment: what do we have, what do we need and how to deliver it? *International Journal for Parasitology: Drugs and Drug Resistance*, 2, 11-19.
- FRENCH, J. B., YATES, P. A., SOYSA, D. R., BOITZ, J. M., CARTER, N. S., CHANG, B., ULLMAN, B. & EALICK, S. E. 2011. The *Leishmania donovani* UMP synthase is essential for promastigote viability and has an unusual tetrameric structure that exhibits substrate-controlled oligomerization. *Journal of Biological Chemistry*, 286, 20930-20941.
- FRÉZARD, F. & DEMICHELI, C. 2010. New delivery strategies for the old pentavalent antimonial drugs. *Expert opinion on drug delivery*, 7, 1343-1358.

- GALMARINI, C. M., MACKEY, J. R. & DUMONTET, C. 2002. Nucleoside analogues and nucleobases in cancer treatment. *The lancet oncology*, 3, 415-424.
- GEE, K. R., ZHOU, Z.-L., TON-THAT, D., SENSI, S. & WEISS, J. 2002. Measuring zinc in living cells.: A new generation of sensitive and selective fluorescent probes. *Cell calcium*, 31, 245-251.
- GEHRIG, S. & EFFERTH, T. 2008. Development of drug resistance in *Trypanosoma brucei rhodesiense* and *Trypanosoma brucei gambiense*. Treatment of human African trypanosomiasis with natural products. *International journal of molecular medicine*, 22, 411-419.
- GEISER, F., LÜSCHER, A., DE KONING, H. P., SEEBECK, T. & MÄSER, P. 2005. Molecular pharmacology of adenosine transport in *Trypanosoma brucei*: P1/P2 revisited. *Molecular pharmacology*, 68, 589-595.
- GHORBAL, M., GORMAN, M., MACPHERSON, C. R., MARTINS, R. M., SCHERF, A. & LOPEZ-RUBIO, J.-J. 2014. Genome editing in the human malaria parasite *Plasmodium falciparum* using the CRISPR-Cas9 system. *Nature biotechnology*, 32, 819.
- GHORBANI, M. & FARHOUDI, R. 2018. Leishmaniasis in humans: drug or vaccine therapy? *Drug design, development and therapy*, 12, 25.
- GLOVER, L., ALSFORD, S., BAKER, N., TURNER, D. J., SANCHEZ-FLORES, A., HUTCHINSON, S., HERTZ-FOWLER, C., BERRIMAN, M. & HORN, D. 2015. Genome-scale RNAi screens for high-throughput phenotyping in bloodstream-form African trypanosomes. *nature protocols*, 10, 106-133.
- GOULD, M. K., VU, X. L., SEEBECK, T. & DE KONING, H. P. 2008. Propidium iodide-based methods for monitoring drug action in the kinetoplastidae: comparison with the Alamar Blue assay. *Analytical biochemistry*, 382, 87-93.
- GOURNAS, C., PAPAGEORGIOU, I. & DIALLINAS, G. 2008. The nucleobase-ascorbate transporter (NAT) family: genomics, evolution, structure-function relationships and physiological role. *Molecular Biosystems*, 4, 404-416.
- GRAF, F. E., LUDIN, P., WENZLER, T., KAISER, M., BRUN, R., PYANA, P. P., BÜSCHER, P., DE KONING, H. P., HORN, D. & MÄSER, P. 2013. Aquaporin 2 mutations in *Trypanosoma brucei gambiense* field isolates correlate with decreased susceptibility to pentamidine and melarsoprol. *PLoS Negl Trop Dis*, 7, e2475.
- GRAY, J. H., OWEN, R. P. & GIACOMINI, K. M. 2004. The concentrative nucleoside transporter family, SLC28. *Pflügers Archiv*, 447, 728-734.
- GREGUS, Z. & GYURASICS, Á. 2000. Role of glutathione in the biliary excretion of the arsenical drugs trimelarsan and melarsoprol. *Biochemical pharmacology*, 59, 1375-1385.
- GRUNFELDER, C. G., ENGSTLER, M., WEISE, F., SCHWARZ, H., STIERHOF, Y.-D., MORGAN, G. W., FIELD, M. C. & OVERATH, P. 2003. Endocytosis of a glycosylphosphatidylinositol-anchored protein via clathrin-coated vesicles,

sorting by default in endosomes, and exocytosis via RAB11-positive carriers. *Molecular biology of the cell*, 14, 2029-2040.

- GUALDRÓN-LÓPEZ, M., MICHELS, P. A., QUIÑONES, W., CÁCERES, A. J., AVILÁN, L. & CONCEPCIÓN, J. L. 2013. Function of glycosomes in the metabolism of trypanosomatid parasites and the promise of glycosomal proteins as drug targets. *Trypanosomatid diseases: molecular routes to drug discovery*, 121-151.
- GUDIN, S., QUASHIE, N. B., CANDLISH, D., AL-SALABI, M. I., JARVIS, S. M., RANFORD-CARTWRIGHT, L. C. & DE KONING, H. P. 2006. Trypanosoma brucei: a survey of pyrimidine transport activities. *Experimental parasitology*, 114, 118-125.
- HAANSTRA, J. R., KERKHOVEN, E. J., VAN TUIJL, A., BLITS, M., WURST, M., VAN NULAND, R., ALBERT, M. A., MICHELS, P. A., BOUWMAN, J. & CLAYTON, C. 2011. A domino effect in drug action: from metabolic assault towards parasite differentiation. *Molecular microbiology*, 79, 94-108.
- HAMARI, Z., AMILLIS, S., DREVET, C., APOSTOLAKI, A., VÁGVÖLGYI, C., DIALLINAS, G. & SCAZZOCCHIO, C. 2009. Convergent evolution and orphan genes in the Fur4p-like family and characterization of a general nucleoside transporter in Aspergillus nidulans. *Molecular microbiology*, 73, 43-57.
- HAMMOND, D. J. & GUTTERIDGE, W. E. 1982. UMP synthesis in the kinetoplastida. *Biochimica et Biophysica Acta (BBA)-General Subjects*, 718, 1-10.
- HAMMOND, D. J. & GUTTERIDGE, W. E. 1984. Purine and pyrimidine metabolism in the Trypanosomatidae. *Molecular and biochemical parasitology*, 13, 243-261.
- HANDLER, M. Z., PATEL, P. A., KAPILA, R., AL-QUBATI, Y. & SCHWARTZ, R. A. 2015. Cutaneous and mucocutaneous leishmaniasis: differential diagnosis, diagnosis, histopathology, and management. *Journal of the American Academy of Dermatology*, 73, 911-926.
- HANNAERT, V. 2011. Sleeping sickness pathogen (Trypanosoma brucei) and natural products: therapeutic targets and screening systems. *Planta medica*, 77, 586-597.
- HART, D. T. & OPPERDOES, F. R. 1984. The occurrence of glycosomes (microbodies) in the promastigote stage of four major Leishmania species. *Molecular and biochemical parasitology*, 13, 159-172.
- HASSAN, H. F. & COOMBS, G. H. 1988. Purine and pyrimidine metabolism in parasitic protozoa. *FEMS microbiology letters*, 54, 47-83.
- HELLIER, I., DEREURE, O., TOURNILLAC, I., PRATLONG, F., GUILLOT, B., DEDET, J.-P. & GUILHOU, J.-J. 2000. Treatment of Old World cutaneous leishmaniasis by pentamidine isethionate. *Dermatology*, 200, 120-123.

- HIRUMI, H. & HIRUMI, K. 1989. Continuous cultivation of *Trypanosoma brucei* blood stream forms in a medium containing a low concentration of serum protein without feeder cell layers. *The Journal of parasitology*, 985-989.
- HOFER, A., STEVERDING, D., CHABES, A., BRUN, R. & THELANDER, L. 2001. *Trypanosoma brucei* CTP synthetase: a target for the treatment of African sleeping sickness. *Proceedings of the National Academy of Sciences*, 98, 6412-6416.
- HORN, D. 2014. Antigenic variation in African trypanosomes. *Molecular and biochemical parasitology*, 195, 123-129.
- HULPIA, F., BOUTON, J., CAMPAGNARO, G. D., ALFAYEZ, I. A., MABILLE, D., MAES, L., DE KONING, H. P., CALJON, G. & VAN CALENBERGH, S. 2020a. C6-O-alkylated 7-deazainosine nucleoside analogues: Discovery of potent and selective anti-sleeping sickness agents. *European Journal of Medicinal Chemistry*, 188, 112018.
- HULPIA, F., CAMPAGNARO, G. D., ALZHRANI, K. J., ALFAYEZ, I. A., UNGOGO, M. A., MABILLE, D., MAES, L., DE KONING, H. P., CALJON, G. & VAN CALENBERGH, S. 2020b. Structure-activity relationship exploration of 3'-deoxy-7-deazapurine nucleoside analogues as anti-*Trypanosoma brucei* agents. *ACS Infectious Diseases*.
- HULPIA, F., MABILLE, D., CAMPAGNARO, G. D., SCHUMANN, G., MAES, L., RODITI, I., HOFER, A., DE KONING, H. P., CALJON, G. & VAN CALENBERGH, S. 2019. Combining tubercidin and cordycepin scaffolds results in highly active candidates to treat late-stage sleeping sickness. *Nature communications*, 10, 1-11.
- HUYNH, C., YUAN, X., MIGUEL, D. C., RENBERG, R. L., PROTCHENKO, O., PHILPOTT, C. C., HAMZA, I. & ANDREWS, N. W. 2012. Heme uptake by *Leishmania amazonensis* is mediated by the transmembrane protein LHR1. *PLoS Pathog*, 8, e1002795.
- INBAR, E., HUGHITT, V. K., DILLON, L. A., GHOSH, K., EL-SAYED, N. M. & SACKS, D. L. 2017. The transcriptome of *Leishmania* major developmental stages in their natural sand fly vector. *MBio*, 8, e00029-17.
- IOVANNISCI, D. M., KAUR, K., YOUNG, L. & ULLMAN, B. 1984. Genetic analysis of nucleoside transport in *Leishmania donovani*. *Molecular and cellular biology*, 4, 1013-1019.
- JACKSON, A. P., SANDERS, M., BERRY, A., MCQUILLAN, J., ASLETT, M. A., QUAIL, M. A., CHUKUALIM, B., CAPEWELL, P., MACLEOD, A. & MELVILLE, S. E. 2010. The genome sequence of *Trypanosoma brucei gambiense*, causative agent of chronic human african trypanosomiasis. *PLoS Neglected Tropical Diseases*, 4.
- JAFFE, J. 1961. The effect of 6-azauracil upon *Trypanosoma equiperdum*. *Biochemical pharmacology*, 8, 216-223.
- JEACOCK, L., BAKER, N., WIEDEMAR, N., MÄSER, P. & HORN, D. 2017. Aquaglyceroporin-null trypanosomes display glycerol transport defects and respiratory-inhibitor sensitivity. *PLoS pathogens*, 13, e1006307.

- JEONG, J. & EIDE, D. J. 2013. The SLC39 family of zinc transporters. *Molecular aspects of medicine*, 34, 612-619.
- JUND, R., CHEVALLIER, M. & LACROUTE, F. 1977. Uracil transport in *Saccharomyces cerevisiae*. *The Journal of membrane biology*, 36, 233-251.
- JUND, R., WEBER, E. & CHEVALLIER, M. R. 1988. Primary structure of the uracil transport protein of *Saccharomyces cerevisiae*. *European journal of biochemistry*, 171, 417-424.
- KALEL, V. C., EMMANOUILIDIS, L., DAWIDOWSKI, M., SCHLIEBS, W., SATTTLER, M., POPOWICZ, G. M. & ERDMANN, R. 2017. Inhibitors of glycosomal protein import provide new leads against trypanosomiasis. *Microbial Cell*, 4, 229.
- KALLI, A. C., SANSOM, M. S. & REITHMEIER, R. A. 2015. Molecular dynamics simulations of the bacterial UraA H⁺-uracil symporter in lipid bilayers reveal a closed state and a selective interaction with cardiolipin. *PLoS computational biology*, 11.
- KANG, X., SZALLIES, A., RAWER, M., ECHNER, H. & DUSZENKO, M. 2002. GPI anchor transamidase of *Trypanosoma brucei*: in vitro assay of the recombinant protein and VSG anchor exchange. *Journal of cell science*, 115, 2529-2539.
- KAZIBWE, A. J., NERIMA, B., DE KONING, H. P., MÄSER, P., BARRETT, M. P. & MATOVU, E. 2009. Genotypic status of the TbAT1/P2 adenosine transporter of *Trypanosoma brucei* gambiense isolates from Northwestern Uganda following melarsoprol withdrawal. *PLoS neglected tropical diseases*, 3.
- KENNEDY, P. G. 2004. Human African trypanosomiasis of the CNS: current issues and challenges. *The Journal of clinical investigation*, 113, 496-504.
- KENNEDY, P. G. 2013. Clinical features, diagnosis, and treatment of human African trypanosomiasis (sleeping sickness). *The Lancet Neurology*, 12, 186-194.
- KENNEDY, P. G. & RODGERS, J. 2019. Clinical and neuropathogenetic aspects of human African trypanosomiasis. *Frontiers in immunology*, 10, 39.
- KHARE, S., NAGLE, A. S., BIGGART, A., LAI, Y. H., LIANG, F., DAVIS, L. C., BARNES, S. W., MATHISON, C. J., MYBURGH, E. & GAO, M.-Y. 2016. Proteasome inhibition for treatment of leishmaniasis, Chagas disease and sleeping sickness. *Nature*, 537, 229-233.
- KING, A. E., ACKLEY, M. A., CASS, C. E., YOUNG, J. D. & BALDWIN, S. A. 2006. Nucleoside transporters: from scavengers to novel therapeutic targets. *Trends in pharmacological sciences*, 27, 416-425.
- KIRK, K. & SALIBA, K. J. 2007. Targeting nutrient uptake mechanisms in *Plasmodium*. *Current drug targets*, 8, 75-88.
- KOBETS, T., GREKOV, I. & LIPOLDOVA, M. 2012. Leishmaniasis: prevention, parasite detection and treatment. *Current medicinal chemistry*, 19, 1443-1474.

- KOHL, L., ROBINSON, D. & BASTIN, P. 2003. Novel roles for the flagellum in cell morphogenesis and cytokinesis of trypanosomes. *The EMBO journal*, 22, 5336-5346.
- KOLB, V. M. 1997. Novel and unusual nucleosides as drugs. *Progress in Drug Research/Fortschritte der Arzneimittelforschung/Progrès des recherches pharmaceutiques*. Springer.
- KOURKOULOU, A., PITTIS, A. A. & DIALLINAS, G. 2018. Evolution of substrate specificity in the Nucleobase-Ascorbate Transporter (NAT) protein family. *Microbial Cell*, 5, 280.
- KOVACIC, P. & COOKSY, A. 2012. Novel, unifying mechanism for amphotericin B and other polyene drugs: electron affinity, radicals, electron transfer, autoxidation, toxicity, and antifungal action. *MedChemComm*, 3, 274-280.
- KRISHNA, S., KLEINE, C. & STICH, A. 2020. African trypanosomiasis. *Hunter's Tropical Medicine and Emerging Infectious Diseases*. Elsevier.
- KRYPOTOU, E., EVANGELIDIS, T., BOBONIS, J., PITTIS, A. A., GABALDÓN, T., SCAZZOCCHIO, C., MIKROS, E. & DIALLINAS, G. 2015. Origin, diversification and substrate specificity in the family of NCS 1/FUR transporters. *Molecular microbiology*, 96, 927-950.
- KUEMMERLE, A., SCHMID, C., KANDE, V., MUTOMBO, W., ILUNGA, M., LUMPUNGU, I., MUTANDA, S., NGANZOBO, P., NGOLO, D. & KISALA, M. 2020. Prescription of concomitant medications in patients treated with Nifurtimox Eflornithine Combination Therapy (NECT) for Tb gambiense second stage sleeping sickness in the Democratic Republic of the Congo. *PLoS neglected tropical diseases*, 14, e0008028.
- KUKURBA, K. R. & MONTGOMERY, S. B. 2015. RNA sequencing and analysis. *Cold Spring Harbor Protocols*, 2015, pdb. top084970.
- LAFFITTE, M.-C. N., LEPROHON, P., LÉGARÉ, D. & OUELLETTE, M. 2016. Deep-sequencing revealing mutation dynamics in the miltefosine transporter gene in *Leishmania infantum* selected for miltefosine resistance. *Parasitology research*, 115, 3699-3703.
- LAFON, S. W., NELSON, D. J., BERENS, R. L. & MARR, J. J. 1982. Purine and pyrimidine salvage pathways in *Leishmania donovani*. *Biochemical pharmacology*, 31, 231-238.
- LAI A FAT, E. J., VREDE, M. A., SOETOSENOJO, R. M. & LAI A FAT, R. F. 2002. Pentamidine, the drug of choice for the treatment of cutaneous leishmaniasis in Surinam. *International journal of dermatology*, 41, 796-800.
- LAMOUR, N., RIVIÈRE, L., COUSTOU, V., COOMBS, G. H., BARRETT, M. P. & BRINGAUD, F. 2005. Proline metabolism in procyclic *Trypanosoma brucei* is down-regulated in the presence of glucose. *Journal of Biological Chemistry*, 280, 11902-11910.

- LANDER, N., LI, Z.-H., NIYOGI, S. & DOCAMPO, R. 2015. CRISPR/Cas9-induced disruption of paraflagellar rod protein 1 and 2 genes in *Trypanosoma cruzi* reveals their role in flagellar attachment. *MBio*, 6, e01012-15.
- LANDFEAR, S. M. 2010. Glucose transporters in parasitic protozoa. *Membrane Transporters in Drug Discovery and Development*. Springer.
- LANDFEAR, S. M. 2011. Nutrient transport and pathogenesis in selected parasitic protozoa. *Eukaryotic cell*, 10, 483-493.
- LANDFEAR, S. M. 2013. Functional Analysis of Leishmania Membrane (Non-ABC) Transporters Involved in Drug Resistance. *Drug Resistance in Leishmania Parasites*. Springer.
- LANDFEAR, S. M., ULLMAN, B., CARTER, N. S. & SANCHEZ, M. A. 2004. Nucleoside and nucleobase transporters in parasitic protozoa. *Eukaryotic cell*, 3, 245-254.
- LANGFORD, C. K., KAVANAUGH, M. P., STENBERG, P. E., DREW, M. E., ZHANG, W. & LANDFEAR, S. M. 1995. Functional expression and subcellular localization of a high-Km hexose transporter from *Leishmania donovani*. *Biochemistry*, 34, 11814-11821.
- LAWN, S., YARDLEY, V., VEGA-LOPEZ, F., WATSON, J. & LOCKWOOD, D. 2003. New World cutaneous leishmaniasis in returned travellers: treatment failures using intravenous sodium stibogluconate. *Transactions of the Royal Society of Tropical Medicine and Hygiene*, 97, 443-445.
- LEBOWITZ, J. H., COBURN, C. M. & BEVERLEY, S. M. 1991. Simultaneous transient expression assays of the trypanosomatid parasite *Leishmania* using b-galactosidase and b-glucuronidase as reporter enzymes. *Gene*, 103, 119-23.
- LEGROS, D., OLLIVIER, G., GASTELLU-ETCHEGORRY, M., PAQUET, C., BURRI, C., JANNIN, J. & BÜSCHER, P. 2002. Treatment of human African trypanosomiasis—present situation and needs for research and development. *The Lancet infectious diseases*, 2, 437-440.
- LEPROHON, P., FERNANDEZ-PRADA, C., GAZANION, É., MONTE-NETO, R. & OUELLETTE, M. 2015. Drug resistance analysis by next generation sequencing in *Leishmania*. *International Journal for Parasitology: Drugs and Drug Resistance*, 5, 26-35.
- LIDANI, K. C. F., ANDRADE, F. A., BAVIA, L., DAMASCENO, F. S., BELTRAME, M. H., MESSIAS-REASON, I. J. & SANDRI, T. L. 2019. Chagas disease: from discovery to a worldwide health problem. *Frontiers in public health*, 7.
- LINDNER, A. K., LEJON, V., CHAPPUIS, F., SEIXAS, J., KAZUMBA, L., BARRETT, M. P., MWAMBA, E., ERPHAS, O., AKL, E. A. & VILLANUEVA, G. 2019. New WHO guidelines for treatment of gambiense human African trypanosomiasis including fexinidazole: substantial changes for clinical practice. *The Lancet Infectious Diseases*.
- LINDNER, A. K., LEJON, V., CHAPPUIS, F., SEIXAS, J., KAZUMBA, L., BARRETT, M. P., MWAMBA, E., ERPHAS, O., AKL, E. A. & VILLANUEVA, G. 2020. New

- WHO guidelines for treatment of gambiense human African trypanosomiasis including fexinidazole: Substantial changes for clinical practice. *The Lancet Infectious Diseases*, 20, e38-e46.
- LIPA, J. J. 2012. Infections caused by protozoa other than sporozoa. *Insect pathology*, 2, 335.
- LIU, W., BOITZ, J. M., GALAZKA, J., ARENDT, C. S., CARTER, N. S. & ULLMAN, B. 2006. Functional characterization of nucleoside transporter gene replacements in *Leishmania donovani*. *Molecular and biochemical parasitology*, 150, 300-307.
- LLANES, A., RESTREPO, C. M., DEL VECCHIO, G., ANGUIZOLA, F. J. & LLEONART, R. 2015. The genome of *Leishmania panamensis*: insights into genomics of the *L. (Viannia)* subgenus. *Scientific reports*, 5, 8550.
- LONGLEY, D. B., HARKIN, D. P. & JOHNSTON, P. G. 2003. 5-fluorouracil: mechanisms of action and clinical strategies. *Nature reviews cancer*, 3, 330-338.
- LÓPEZ-VÉLEZ, R., NORMAN, F. F. & BERN, C. 2020. American Trypanosomiasis (Chagas Disease). *Hunter's Tropical Medicine and Emerging Infectious Diseases*. Elsevier.
- LOS, D. A. & MURATA, N. 1998. Structure and expression of fatty acid desaturases. *Biochimica et Biophysica Acta (BBA)-Lipids and Lipid Metabolism*, 1394, 3-15.
- LU, F., LI, S., JIANG, Y., JIANG, J., FAN, H., LU, G., DENG, D., DANG, S., ZHANG, X. & WANG, J. 2011. Structure and mechanism of the uracil transporter UraA. *Nature*, 472, 243-246.
- LUKEŠ, J., SKALICKÝ, T., TÝČ, J., VOTÝPKA, J. & YURCHENKO, V. 2014. Evolution of parasitism in kinetoplastid flagellates. *Molecular and biochemical parasitology*, 195, 115-122.
- LYPACZEWSKI, P., HOSHIZAKI, J., ZHANG, W.-W., MCCALL, L.-I., TORCIVIA-RODRIGUEZ, J., SIMONYAN, V., KAUR, A., DEWAR, K. & MATLASHEWSKI, G. 2018. A complete *Leishmania donovani* reference genome identifies novel genetic variations associated with virulence. *Scientific reports*, 8, 1-14.
- MAGILL, A. J. 2005. Cutaneous leishmaniasis in the returning traveler. *Infectious Disease Clinics*, 19, 241-266.
- MAJUMDER, H. K. 2008. *Drug targets in kinetoplastid parasites*, Springer Science & Business Media.
- MALTEZOU, H. C. 2009. Drug resistance in visceral leishmaniasis. *BioMed Research International*, 2010.
- MALVY, D. & CHAPPUIS, F. 2011. Sleeping sickness. *Clinical Microbiology and Infection*, 17, 986-995.
- MANOLESCU, A. R., WITKOWSKA, K., KINNAIRD, A., CESSFORD, T. & CHEESEMAN, C. 2007. Facilitated hexose transporters: new perspectives on form and function. *Physiology*, 22, 234-240.

- MARFURT, J., NIEDERWIESER, I., MAKIA, N. D., BECK, H.-P. & FELGER, I. 2003. Diagnostic genotyping of Old and New World Leishmania species by PCR-RFLP. *Diagnostic microbiology and infectious disease*, 46, 115-124.
- MARR, J. J., BERENS, R. L. & NELSON, D. J. 1978. Antitrypanosomal effect of allopurinol: conversion in vivo to aminopyrazolopyrimidine nucleotides by *Trypanosoma curzi*. *Science*, 201, 1018-1020.
- MASELENO, A. & HASAN, M. 2012. African Trypanosomiasis Detection using Dempster-Shafer Theory. *arXiv preprint arXiv:1205.0831*.
- MASLOV, D. A., PODLIPAEV, S. A. & LUKES, J. 2001. Phylogeny of the kinetoplastida: taxonomic problems and insights into the evolution of parasitism. *Memórias do Instituto Oswaldo Cruz*, 96, 397-402.
- MASLOV, D. A., VOTÝPKA, J., YURCHENKO, V. & LUKEŠ, J. 2013. Diversity and phylogeny of insect trypanosomatids: all that is hidden shall be revealed. *Trends in parasitology*, 29, 43-52.
- MATOVU, E., STEWART, M. L., GEISER, F., BRUN, R., MASER, P., WALLACE, L. J., BURCHMORE, R. J., ENYARU, J. C., BARRETT, M. P., KAMINSKY, R., SEEBECK, T. & DE KONING, H. P. 2003. Mechanisms of arsenical and diamidine uptake and resistance in *Trypanosoma brucei*. *Eukaryot Cell*, 2, 1003-8.
- MCCARTHY, J. S., WORTMANN, G. W. & KIRCHHOFF, L. V. 2015. Drugs for Protozoal Infections Other Than Malaria. *Mandell, Douglas, and Bennett's Principles and Practice of Infectious Diseases. Updated 8th ed. Philadelphia: Elsevier*, 510-518.
- MCCONVILLE, M. J. & RALPH, S. A. 2013. Chronic arsenic exposure and microbial drug resistance. *Proceedings of the National Academy of Sciences*, 110, 19666-19667.
- MIGCHELSEN, S. J., BÜSCHER, P., HOEPELMAN, A. I., SCHALLIG, H. D. & ADAMS, E. R. 2011. Human African trypanosomiasis: a review of non-endemic cases in the past 20 years. *International journal of infectious diseases*, 15, e517-e524.
- MITASHI, P., HASKER, E., LEJON, V., KANDE, V., MUYEMBE, J.-J., LUTUMBA, P. & BOELAERT, M. 2012. Human African trypanosomiasis diagnosis in first-line health services of endemic countries, a systematic review. *PLoS neglected tropical diseases*, 6.
- MOHR, S. E. & PERRIMON, N. 2012. RNAi screening: new approaches, understandings, and organisms. *Wiley Interdisciplinary Reviews: RNA*, 3, 145-158.
- MOLINA-ARCAS, M., CASADO, F. J. & PASTOR-ANGLADA, M. 2009. Nucleoside transporter proteins. *Current vascular pharmacology*, 7, 426-434.
- MOMENI, A. Z., REISZADAE, M. R. & AMINJAVAHERI, M. 2002. Treatment of cutaneous leishmaniasis with a combination of allopurinol and low-dose meglumine antimoniate. *International journal of dermatology*, 41, 441-443.

- MORRIS, J. C., WANG, Z., DREW, M. E. & ENGLUND, P. T. 2002. Glycolysis modulates trypanosome glycoprotein expression as revealed by an RNAi library. *The EMBO journal*, 21, 4429-4438.
- MORRISON, L. J., VEZZA, L., ROWAN, T. & HOPE, J. C. 2016. Animal African trypanosomiasis: time to increase focus on clinically relevant parasite and host species. *Trends in parasitology*, 32, 599-607.
- MORTARA, R. A., ANDREOLI, W. K., FERNANDES, M. C. D., DA SILVA, C. V., FERNANDES, A. B., L'ABBATE, C. & DA SILVA, S. 2008. Host cell actin remodeling in response to *Trypanosoma cruzi*: trypomastigote versus amastigote entry. *Molecular Mechanisms of Parasite Invasion*. Springer.
- MUKHERJEE, A., PADMANABHAN, P. K., SAHANI, M. H., BARRETT, M. P. & MADHUBALA, R. 2006. Roles for mitochondria in pentamidine susceptibility and resistance in *Leishmania donovani*. *Molecular and biochemical parasitology*, 145, 1-10.
- MULENGA, P., CHENGE, F., BOELAERT, M., MUKALAY, A., LUTUMBA, P., LUMBALA, C., LUBOYA, O. & COPPIETERS, Y. 2019. Integration of human African trypanosomiasis control activities into primary healthcare services: A scoping review. *The American journal of tropical medicine and hygiene*, 101, 1114-1125.
- MÜLLER KRATZ, J., GARCIA BOURNISSEN, F., FORSYTH, C. J. & SOSA-ESTANI, S. 2018. Clinical and pharmacological profile of benznidazole for treatment of Chagas disease. *Expert Review of Clinical Pharmacology*, 11, 943-957.
- MUNDAY, J. C., EZE, A. A., BAKER, N., GLOVER, L., CLUCAS, C., AGUINAGA ANDRÉS, D., NATTO, M. J., TEKA, I. A., MCDONALD, J. & LEE, R. S. 2014. *Trypanosoma brucei* aquaglyceroporin 2 is a high-affinity transporter for pentamidine and melaminophenyl arsenic drugs and the main genetic determinant of resistance to these drugs. *Journal of Antimicrobial Chemotherapy*, 69, 651-663.
- MUNDAY, J. C., LÓPEZ, K. E. R., EZE, A. A., DELESPAUX, V., VAN DEN ABEELE, J., ROWAN, T., BARRETT, M. P., MORRISON, L. J. & DE KONING, H. P. 2013. Functional expression of TcoAT1 reveals it to be a P1-type nucleoside transporter with no capacity for diminazene uptake. *International Journal for Parasitology: Drugs and Drug Resistance*, 3, 69-76.
- MUNDAY, J. C., TAGOE, D. N., EZE, A. A., KREZDORN, J. A., ROJAS LÓPEZ, K. E., ALKHALDI, A. A., MCDONALD, F., STILL, J., ALZHRANI, K. J. & SETTIMO, L. 2015. Functional analysis of drug resistance-associated mutations in the *Trypanosoma brucei* adenosine transporter 1 (TbAT 1) and the proposal of a structural model for the protein. *Molecular microbiology*, 96, 887-900.
- MWENECHANYA, R., KOVÁŘOVÁ, J., DICKENS, N. J., MUDALIAR, M., HERZYK, P., VINCENT, I. M., WEIDT, S. K., BURGESS, K. E., BURCHMORE, R. J. & POUNTAIN, A. W. 2017. Sterol 14 α -demethylase mutation leads to amphotericin B resistance in *Leishmania mexicana*. *PLoS neglected tropical diseases*, 11, e0005649.

- NAGALAKSHMI, U., WAERN, K. & SNYDER, M. 2010. RNA-Seq: a method for comprehensive transcriptome analysis. *Current protocols in molecular biology*, 89, 4.11. 1-4.11. 13.
- NELSON, N. 1999. Metal ion transporters and homeostasis. *The EMBO Journal*, 18, 4361-4371.
- NETO, R. L. M., SOUSA, L. M., DIAS, C. S., BARBOSA FILHO, J. M., OLIVEIRA, M. R. & FIGUEIREDO, R. C. 2011. Morphological and physiological changes in *Leishmania promastigotes* induced by yangambin, a lignan obtained from *Ocotea duckei*. *Experimental parasitology*, 127, 215-221.
- NEVERISKY, D. L. & ABBOTT, G. W. 2016. Ion channel-transporter interactions. *Critical reviews in biochemistry and molecular biology*, 51, 257-267.
- NOK, A. J. 2003. Arsenicals (melarsoprol), pentamidine and suramin in the treatment of human African trypanosomiasis. *Parasitology research*, 90, 71-79.
- NOZAKI, T. & DVORAK, J. A. 1993. Molecular biology studies of tubercidin resistance in *Trypanosoma cruzi*. *Parasitology research*, 79, 451-455.
- NYARKO, E., HARA, T., GRAB, D. J., TABATA, M. & FUKUMA, T. 2002. Toxic effects of mercury (II), cadmium (II) and lead (II) porphyrins on *Trypanosoma brucei brucei* growth. *Chemico-biological interactions*, 139, 177-185.
- OBERHOLZER, M., MARTI, G., BAREŠIĆ, M., KUNZ, S., HEMPHILL, A. & SEEBECK, T. 2007. The *Trypanosoma brucei* cAMP phosphodiesterases TbrPDEB1 and TbrPDEB2: flagellar enzymes that are essential for parasite virulence. *The FASEB Journal*, 21, 720-731.
- OLIVEIRA, R. A., LIMA, C. G., MOTA, R. M., MC MARTINS, A., SANCHES, T. R., SEGURO, A. C., ANDRADE, L. C., JUNIOR, G. B. S., LIBÓRIO, A. B. & DAHER, E. F. 2012. Renal function evaluation in patients with American Cutaneous Leishmaniasis after specific treatment with pentavalent antimonial. *BMC nephrology*, 13, 44.
- OOI, C.-P. & BASTIN, P. 2013. More than meets the eye: understanding *Trypanosoma brucei* morphology in the tsetse. *Frontiers in cellular and infection microbiology*, 3, 71.
- OPPERDOES, F. R. 1987. Compartmentation of carbohydrate metabolism in trypanosomes. *Annual Reviews in Microbiology*, 41, 127-151.
- ORTIZ, D., SANCHEZ, M. A., KOCH, H. P., LARSSON, H. P. & LANDFEAR, S. M. 2009a. An acid-activated nucleobase transporter from *Leishmania major*. *Journal of Biological Chemistry*, 284, 16164-16169.
- ORTIZ, D., SANCHEZ, M. A., PIERCE, S., HERRMANN, T., KIMBLIN, N., ARCHIE BOUWER, H. & LANDFEAR, S. M. 2007. Molecular genetic analysis of purine nucleobase transport in *Leishmania major*. *Molecular microbiology*, 64, 1228-1243.

- ORTIZ, D., SANCHEZ, M. A., QUECKE, P. & LANDFEAR, S. M. 2009b. Two novel nucleobase/pentamidine transporters from *Trypanosoma brucei*. *Molecular and biochemical parasitology*, 163, 67-76.
- ORTIZ, D., VALDÉS, R., SANCHEZ, M. A., HAYENGA, J., ELYA, C., DETKE, S. & LANDFEAR, S. M. 2010. Purine restriction induces pronounced translational upregulation of the NT1 adenosine/pyrimidine nucleoside transporter in *Leishmania major*. *Molecular microbiology*, 78, 108-118.
- OTRANTO, D. & DANTAS-TORRES, F. 2013. The prevention of canine leishmaniasis and its impact on public health. *Trends in parasitology*, 29, 339-345.
- P DE KONING, H. 2020. The drugs of sleeping sickness: their mechanisms of action and resistance, and a brief history. *Tropical Medicine and Infectious Disease*, 5, 14.
- PALMER, L., SCAZZOCCHIO, C. & COVE, D. 1975. Pyrimidine biosynthesis in *Aspergillus nidulans*. Isolation and characterisation of mutants resistant to fluoropyrimidines. *Molecular & general genetics: MGG*, 140, 165-173.
- PAPADOPOULOU, B., KÜNDIG, C., SINGH, A. & OUELLETTE, M. 1998. Drug resistance in *Leishmania*: similarities and differences to other organisms. *Drug Resistance Updates*, 1, 266-278.
- PAPAGEORGIOU, I., YAKOB, L., AL SALABI, M., DIALLINAS, G., SOTERIADOU, K. & DE KONING, H. 2005. Identification of the first pyrimidine nucleobase transporter in *Leishmania*: similarities with the *Trypanosoma brucei* U1 transporter and antileishmanial activity of uracil analogues. *Parasitology*, 130, 275-283.
- PASTOR-ANGLADA, M. & PÉREZ-TORRAS, S. 2018. Emerging roles of nucleoside transporters. *Frontiers in pharmacology*, 9, 606.
- PEACOCK, C. S., SEEGER, K., HARRIS, D., MURPHY, L., RUIZ, J. C., QUAIL, M. A., PETERS, N., ADLEM, E., TIVEY, A. & ASLETT, M. 2007. Comparative genomic analysis of three *Leishmania* species that cause diverse human disease. *Nature genetics*, 39, 839-847.
- PEETERS, Z., BOTTA, O., CHARNLEY, S., KISIEL, Z., KUAN, Y.-J. & EHRENFREUND, P. 2005. Formation and photostability of N-heterocycles in space-I. The effect of nitrogen on the photostability of small aromatic molecules. *Astronomy & Astrophysics*, 433, 583-590.
- PENG, D., KURUP, S. P., YAO, P. Y., MINNING, T. A. & TARLETON, R. L. 2015. CRISPR-Cas9-mediated single-gene and gene family disruption in *Trypanosoma cruzi*. *MBio*, 6, e02097-14.
- PEREIRA, C. A. & SILBER, A. M. 2012. On the evolution of hexose transporters in kinetoplastid Protozoans [corrected]. *PloS one*, 7, e36303-e36303.
- PÉREZ-MOLINA, J. A. & MOLINA, I. 2018. Chagas disease. *The Lancet*, 391, 82-94.
- PERRY, M. R., WYLLIE, S., RAAB, A., FELDMANN, J. & FAIRLAMB, A. H. 2013. Chronic exposure to arsenic in drinking water can lead to resistance to

- antimonial drugs in a mouse model of visceral leishmaniasis. *Proceedings of the National Academy of Sciences*, 110, 19932-19937.
- PETERSON, A. T. & SHAW, J. 2003. Lutzomyia vectors for cutaneous leishmaniasis in Southern Brazil: ecological niche models, predicted geographic distributions, and climate change effects. *International journal for parasitology*, 33, 919-931.
- PETRINI, G. A., ALTABE, S. G. & UTTARO, A. D. 2004. Trypanosoma brucei oleate desaturase may use a cytochrome b5-like domain in another desaturase as an electron donor. *European journal of biochemistry*, 271, 1079-1086.
- PFAFFL, M. W. 2001. A new mathematical model for relative quantification in real-time RT-PCR. *Nucleic acids research*, 29, e45-e45.
- PLOURDE, M., UBEDA, J.-M., MANDAL, G., DO MONTE-NETO, R. L., MUKHOPADHYAY, R. & OUELLETTE, M. 2015. Generation of an aquaglyceroporin AQP1 null mutant in Leishmania major. *Molecular and biochemical parasitology*, 201, 108-111.
- POHLIG, G., BERNHARD, S. C., BLUM, J., BURRI, C., MPANYA, A., LUBAKI, J.-P. F., MPOTO, A. M., MUNUNGU, B. F., N'TOMBE, P. M. & DEO, G. K. M. 2016. Efficacy and safety of pafuramidine versus pentamidine maleate for treatment of first stage sleeping sickness in a randomized, comparator-controlled, international phase 3 clinical trial. *PLoS neglected tropical diseases*, 10.
- PRATA, A. 2001. Clinical and epidemiological aspects of Chagas disease. *The Lancet infectious diseases*, 1, 92-100.
- PRATLONG, F., DEREURE, J., RAVEL, C., LAMI, P., BALARD, Y., SERRES, G., LANOTTE, G., RIOUX, J. A. & DEDET, J. P. 2009. Geographical distribution and epidemiological features of Old World cutaneous leishmaniasis foci, based on the isoenzyme analysis of 1048 strains. *Tropical Medicine & International Health*, 14, 1071-1085.
- PRELICH, G. 2012. Gene overexpression: uses, mechanisms, and interpretation. *Genetics*, 190, 841-854.
- PRIOTTO, G., KASPARIAN, S., MUTOMBO, W., NGOUAMA, D., GHORASHIAN, S., ARNOLD, U., GHABRI, S., BAUDIN, E., BUARD, V. & KAZADI-KYANZA, S. 2009. Nifurtimox-eflornithine combination therapy for second-stage African Trypanosoma brucei gambiense trypanosomiasis: a multicentre, randomised, phase III, non-inferiority trial. *The Lancet*, 374, 56-64.
- PRIOTTO, G., KASPARIAN, S., NGOUAMA, D., GHORASHIAN, S., ARNOLD, U., GHABRI, S. & KARUNAKARA, U. 2007. Nifurtimox-eflornithine combination therapy for second-stage Trypanosoma brucei gambiense sleeping sickness: a randomized clinical trial in Congo. *Clinical infectious diseases*, 45, 1435-1442.
- PURKAIT, B., KUMAR, A., NANDI, N., SARDAR, A. H., DAS, S., KUMAR, S., PANDEY, K., RAVIDAS, V., KUMAR, M. & DE, T. 2012. Mechanism of amphotericin B resistance in clinical isolates of Leishmania donovani. *Antimicrobial agents and chemotherapy*, 56, 1031-1041.

- RANJBARIAN, F., VODNALA, M., ALZHRANI, K. J., EBILOMA, G. U., DE KONING, H. P. & HOFER, A. 2017. 9-(2'-Deoxy-2'-Fluoro- β -d-Arabinofuranosyl) Adenine is a potent antitrypanosomal adenosine analogue that circumvents transport-related drug resistance. *Antimicrobial agents and chemotherapy*, 61, e02719-16.
- RASSI JR, A., RASSI, A. & LITTLE, W. C. 2000. Chagas' heart disease. *Clinical cardiology*, 23, 883-889.
- RASSI JR, A., RASSI, A. & MARIN-NETO, J. A. 2010. Chagas disease. *The Lancet*, 375, 1388-1402.
- RÄZ, B., ITEN, M., GREYER-BÜHLER, Y., KAMINSKY, R. & BRUN, R. 1997. The Alamar Blue® assay to determine drug sensitivity of African trypanosomes (Tb rhodesiense and Tb gambiense) in vitro. *Acta tropica*, 68, 139-147.
- RAZONABLE, R. R. Antiviral drugs for viruses other than human immunodeficiency virus. Mayo Clinic Proceedings, 2011. Elsevier, 1009-1026.
- REAL, F., VIDAL, R. O., CARAZZOLLE, M. F., MONDEGO, J. M. C., COSTA, G. G. L., HERAI, R. H., WÜRTELE, M., DE CARVALHO, L. M., E FERREIRA, R. C. & MORTARA, R. A. 2013. The genome sequence of Leishmania (Leishmania) amazonensis: functional annotation and extended analysis of gene models. *DNA research*, 20, 567-581.
- REITHINGER, R., DUJARDIN, J.-C., LOUZIR, H., PIRMEZ, C., ALEXANDER, B. & BROOKER, S. 2007. Cutaneous leishmaniasis. *The Lancet infectious diseases*, 7, 581-596.
- RICHARD, D., KÜNDIG, C. & OUELLETTE, M. 2002. A new type of high affinity folic acid transporter in the protozoan parasite Leishmania and deletion of its gene in methotrexate-resistant cells. *Journal of Biological Chemistry*, 277, 29460-29467.
- RICO, E., JEACOCK, L., KOVÁŘOVÁ, J. & HORN, D. 2018. Inducible high-efficiency CRISPR-Cas9-targeted gene editing and precision base editing in African trypanosomes. *Scientific reports*, 8, 1-10.
- RODENKO, B., VAN DER BURG, A. M., WANNER, M. J., KAISER, M., BRUN, R., GOULD, M., DE KONING, H. P. & KOOMEN, G.-J. 2007. 2, N6-disubstituted adenosine analogs with antitrypanosomal and antimalarial activities. *Antimicrobial agents and chemotherapy*, 51, 3796-3802.
- RODGERS, J., STEINER, I. & KENNEDY, P. G. 2019. Generation of neuroinflammation in human African trypanosomiasis. *Neurology-Neuroimmunology Neuroinflammation*, 6, e610.
- RODRIGUEZ-CONTRERAS, D., FENG, X., KEENEY, K. M., BOUWER, H. A. & LANDFEAR, S. M. 2007. Phenotypic characterization of a glucose transporter null mutant in Leishmania mexicana. *Molecular and biochemical parasitology*, 153, 9-18.

- RODRIGUEZ, A. E., ESTÉVEZ, J. O., NEVOT, M. C., BARRIOS, A. & FLORIN-CHRISTENSEN, M. 2018. *Leishmania. Parasitic protozoa of farm animals and pets*. Springer.
- ROGERS, M. B., HILLEY, J. D., DICKENS, N. J., WILKES, J., BATES, P. A., DEPLEDGE, D. P., HARRIS, D., HER, Y., HERZYK, P. & IMAMURA, H. 2011. Chromosome and gene copy number variation allow major structural change between species and strains of *Leishmania*. *Genome research*, 21, 2129-2142.
- ROLFS, A. & HEDIGER, M. A. 1999. Metal ion transporters in mammals: structure, function and pathological implications. *The Journal of Physiology*, 518, 1-12.
- ROMERO-MEZA, G. & MUGNIER, M. R. 2019. *Trypanosoma brucei*. *Trends in parasitology*.
- ROMERO, G. A. S., ORGE, M. D. L. G. O., DE FARIAS GUERRA, M. V., PAES, M. G., DE OLIVEIRA MACÊDO, V. & DE CARVALHO, E. M. 2005. Antibody response in patients with cutaneous leishmaniasis infected by *Leishmania* (*Viannia*) *braziliensis* or *Leishmania* (*Viannia*) *guyanensis* in Brazil. *Acta tropica*, 93, 49-56.
- SAIMOTO, H., KIDO, Y., HAGA, Y., SAKAMOTO, K. & KITA, K. 2013. Pharmacophore identification of ascofuranone, potent inhibitor of cyanide-insensitive alternative oxidase of *Trypanosoma brucei*. *The Journal of Biochemistry*, 153, 267-273.
- SANCHEZ, M. A., DRUTMAN, S., VAN AMPTING, M., MATTHEWS, K. & LANDFEAR, S. M. 2004. A novel purine nucleoside transporter whose expression is up-regulated in the short stumpy form of the *Trypanosoma brucei* life cycle. *Molecular and biochemical parasitology*, 136, 265-272.
- SANCHEZ, M. A., TRYON, R., GREEN, J., BOOR, I. & LANDFEAR, S. M. 2002. Six Related Nucleoside/Nucleobase Transporters from *Trypanosoma brucei* Exhibit Distinct Biochemical Functions. *Journal of Biological Chemistry*, 277, 21499-21504.
- SANDERSON, L., DOGRUEL, M., RODGERS, J., DE KONING, H. P. & THOMAS, S. A. 2009. Pentamidine movement across the murine blood-brain and blood-cerebrospinal fluid barriers: effect of trypanosome infection, combination therapy, P-glycoprotein, and multidrug resistance-associated protein. *Journal of Pharmacology and Experimental Therapeutics*, 329, 967-977.
- SANDERSON, L., KHAN, A. & THOMAS, S. 2007. Distribution of suramin, an antitrypanosomal drug, across the blood-brain and blood-cerebrospinal fluid interfaces in wild-type and P-glycoprotein transporter-deficient mice. *Antimicrobial agents and chemotherapy*, 51, 3136-3146.
- SAUNDERS, E. C., NG, W. W., CHAMBERS, J. M., NG, M., NADERER, T., KRÖMER, J. O., LIKIĆ, V. A. & MCCONVILLE, M. J. 2011. Isotopomer profiling of *Leishmania mexicana* promastigotes reveals important roles for succinate fermentation and aspartate uptake in tricarboxylic acid cycle (TCA)

- anaplerosis, glutamate synthesis, and growth. *Journal of Biological Chemistry*, 286, 27706-27717.
- SCOTT, M. 2008. Drugs and transporters in kinetoplastid protozoa. *Drug Targets in Kinetoplastid Parasites*. Springer.
- SEEBECK, T., STERK, G. J. & KE, H. 2011. Phosphodiesterase inhibitors as a new generation of antiprotozoan drugs: exploiting the benefit of enzymes that are highly conserved between host and parasite. *Future medicinal chemistry*, 3, 1289-1306.
- SEKHAR, G. N., GEORGIAN, A. R., SANDERSON, L., VIZCAY-BARRENA, G., BROWN, R. C., MURESAN, P., FLECK, R. A. & THOMAS, S. A. 2017. Organic cation transporter 1 (OCT1) is involved in pentamidine transport at the human and mouse blood-brain barrier (BBB). *PLoS One*, 12, e0173474.
- SERENO, D., HARRAT, Z. & EDDAIKRA, N. 2019. Meta-analysis and discussion on challenges to translate Leishmania drug resistance phenotyping into the clinic. *Acta tropica*, 191, 204-211.
- SEYFANG, A. & DUSZENKO, M. 1993. Functional reconstitution of the Trypanosoma brucei plasma-membrane D-glucose transporter. *European journal of biochemistry*, 214, 593-597.
- SEYFANG, A. & LANDFEAR, S. M. 1999. Substrate depletion upregulates uptake of myo-inositol, glucose and adenosine in Leishmania. *Molecular and biochemical parasitology*, 104, 121-130.
- SEYFANG, A. & LANDFEAR, S. M. 2000. Four Conserved Cytoplasmic Sequence Motifs Are Important for Transport Function of the Leishmanialinositol/H⁺ Symporter. *Journal of Biological Chemistry*, 275, 5687-5693.
- SHIBA, T., KIDO, Y., SAKAMOTO, K., INAOKA, D. K., TSUGE, C., TATSUMI, R., TAKAHASHI, G., BALOGUN, E. O., NARA, T. & AOKI, T. 2013. Structure of the trypanosome cyanide-insensitive alternative oxidase. *Proceedings of the National Academy of Sciences*, 110, 4580-4585.
- SIDIK, S. M., HUET, D., GANESAN, S. M., HUYNH, M.-H., WANG, T., NASAMU, A. S., THIRU, P., SAEIJ, J. P., CARRUTHERS, V. B. & NILES, J. C. 2016. A genome-wide CRISPR screen in Toxoplasma identifies essential apicomplexan genes. *Cell*, 166, 1423-1435. e12.
- SIEGEL, T. N., HEKSTRA, D. R., WANG, X., DEWELL, S. & CROSS, G. A. 2010. Genome-wide analysis of mRNA abundance in two life-cycle stages of Trypanosoma brucei and identification of splicing and polyadenylation sites. *Nucleic acids research*, 38, 4946-4957.
- SILBER, A. M., TONELLI, R. R., LOPES, C. G., CUNHA-E-SILVA, N., TORRECILHAS, A. C. T., SCHUMACHER, R. I., COLLI, W. & ALVES, M. J. M. 2009. Glucose uptake in the mammalian stages of Trypanosoma cruzi. *Molecular and biochemical parasitology*, 168, 102-108.
- SIMARRO, P., FRANCO, J., DIARRA, A., POSTIGO, J. R. & JANNIN, J. 2012. Update on field use of the available drugs for the chemotherapy of human African trypanosomiasis. *Parasitology*, 139, 842-846.

- SINGH, N. 2006. Drug resistance mechanisms in clinical isolates of *Leishmania donovani*. *Indian Journal of Medical Research*, 123, 411.
- SINGH, S. 2014. Changing trends in the epidemiology, clinical presentation, and diagnosis of *Leishmania*-HIV co-infection in India. *International Journal of Infectious Diseases*, 29, 103-112.
- SINGH, S. & SIVAKUMAR, R. 2004. Challenges and new discoveries in the treatment of leishmaniasis. *Journal of infection and chemotherapy*, 10, 307-315.
- SINGH, V., BRECIK, M., MUKHERJEE, R., EVANS, J. C., SVETLÍKOVÁ, Z., BLAŠKO, J., SURADE, S., BLACKBURN, J., WARNER, D. F. & MIKUŠOVÁ, K. 2015. The complex mechanism of antimycobacterial action of 5-fluorouracil. *Chemistry & biology*, 22, 63-75.
- SMITH, T. K. & BÜTIKOFER, P. 2010. Lipid metabolism in *Trypanosoma brucei*. *Molecular and biochemical parasitology*, 172, 66-79.
- SOLLELIS, L., GHORBAL, M., MACPHERSON, C. R., MARTINS, R. M., KUK, N., CROBU, L., BASTIEN, P., SCHERF, A., LOPEZ-RUBIO, J. J. & STERKERS, Y. 2015. First efficient CRISPR-Cas9-mediated genome editing in *Leishmania* parasites. *Cellular microbiology*, 17, 1405-1412.
- SOUTO, E. B., DIAS-FERREIRA, J., CRAVEIRO, S. A., SEVERINO, P., SANCHEZ-LOPEZ, E., GARCIA, M. L., SILVA, A. M., SOUTO, S. B. & MAHANT, S. 2019. Therapeutic Interventions for Countering Leishmaniasis and Chagas's Disease: From Traditional Sources to Nanotechnological Systems. *Pathogens*, 8, 119.
- SRIVASTAVA, S., MISHRA, J., GUPTA, A. K., SINGH, A., SHANKAR, P. & SINGH, S. 2017. Laboratory confirmed miltefosine resistant cases of visceral leishmaniasis from India. *Parasites & vectors*, 10, 49.
- STEINMANN, M. E., GONZÁLEZ-SALGADO, A., BÜTIKOFER, P., MÄSER, P. & SIGEL, E. 2015. A heteromeric potassium channel involved in the modulation of the plasma membrane potential is essential for the survival of African trypanosomes. *The FASEB journal*, 29, 3228-3237.
- STEPHENSON, F. H. 2016. *Calculations for molecular biology and biotechnology*, Academic press.
- STEVERDING, D. 2010. The development of drugs for treatment of sleeping sickness: a historical review. *Parasites & vectors*, 3, 15.
- STEWART, M. L., BURCHMORE, R. J., CLUCAS, C., HERTZ-FOWLER, C., BROOKS, K., TAIT, A., MACLEOD, A., TURNER, C. M. R., DE KONING, H. P. & WONG, P. E. 2010. Multiple genetic mechanisms lead to loss of functional TbAT1 expression in drug-resistant trypanosomes. *Eukaryotic cell*, 9, 336-343.
- STOFFER-BITTNER, A. J., ALEXANDER, C. R., DINGMAN, D. W., MOURAD, G. S. & SCHULTES, N. P. 2018. Functional characterization of the uracil transporter from honeybee pathogen *Paenibacillus larvae*. *Microbial pathogenesis*, 124, 305-310.

- STUART, K., BRUN, R., CROFT, S., FAIRLAMB, A., GÜRTLER, R. E., MCKERROW, J., REED, S. & TARLETON, R. 2008. Kinetoplastids: related protozoan pathogens, different diseases. *The Journal of clinical investigation*, 118, 1301-1310.
- SUNDAR, S. & CHAKRAVARTY, J. 2013. Leishmaniasis: an update of current pharmacotherapy. *Expert opinion on pharmacotherapy*, 14, 53-63.
- SUNDAR, S. & RAI, M. 2002. Laboratory diagnosis of visceral leishmaniasis. *Clin. Diagn. Lab. Immunol.*, 9, 951-958.
- SUNDAR, S., RAI, M., CHAKRAVARTY, J., AGARWAL, D., AGRAWAL, N., VAILLANT, M., OLLIARO, P. & MURRAY, H. W. 2008. New treatment approach in Indian visceral leishmaniasis: single-dose liposomal amphotericin B followed by short-course oral miltefosine. *Clinical Infectious Diseases*, 47, 1000-1006.
- TAKAGISHI, T., HARA, T. & FUKADA, T. 2017. Recent advances in the role of SLC39A/ZIP zinc transporters in vivo. *International Journal of Molecular Sciences*, 18, 2708.
- TEIXEIRA, D. E., BENCHIMOL, M., RODRIGUES, J. C., CREPALDI, P. H., PIMENTA, P. F. & DE SOUZA, W. 2013. The cell biology of Leishmania: how to teach using animations. *PLoS pathogens*, 9.
- TETAUD, E., BARRETT, M. P., BRINGAUD, F. & BALTZ, T. 1997. Kinetoplastid glucose transporters. *Biochemical Journal*, 325, 569-580.
- TETAUD, E., LECUIX, I., SHELDRAKE, T., BALTZ, T. & FAIRLAMB, A. H. 2002. A new expression vector for Crithidia fasciculata and Leishmania. *Molecular and biochemical parasitology*, 120, 195-204.
- THUITA, J. K., KAGIRA, J. M., MWANGANGI, D., MATOVU, E., TURNER, C. & MASIGA, D. 2008. Trypanosoma brucei rhodesiense transmitted by a single tsetse fly bite in vervet monkeys as a model of human African trypanosomiasis. *PLoS neglected tropical diseases*, 2.
- TIUMAN, T. S., SANTOS, A. O., UEDA-NAKAMURA, T., DIAS FILHO, B. P. & NAKAMURA, C. V. 2011. Recent advances in leishmaniasis treatment. *International Journal of Infectious Diseases*, 15, e525-e532.
- TONELLI, R. R., SILBER, A. M., ALMEIDA-DE-FARIA, M., HIRATA, I. Y., COLLI, W. & ALVES, M. J. M. 2004. L-proline is essential for the intracellular differentiation of Trypanosoma cruzi. *Cellular microbiology*, 6, 733-741.
- TROCHINE, A., CREEK, D. J., FARAL-TELLO, P., BARRETT, M. P. & ROBELLO, C. 2014. Benznidazole biotransformation and multiple targets in Trypanosoma cruzi revealed by metabolomics. *PLoS neglected tropical diseases*, 8.
- TRYPTAG. 2020. TrypTag.org [Online]. Available: <http://tryptag.org/> [Accessed 10/04/2020 2020].
- TYLER, K. & ENGMAN, D. 2001. The life cycle of Trypanosoma cruzi revisited. *International journal for parasitology*, 31, 472-481.

- UZCATEGUI, N. L., SZALLIES, A., PAVLOVIC-DJURANOVIC, S., PALMADA, M., FIGARELLA, K., BOEHMER, C., LANG, F., BEITZ, E. & DUSZENKO, M. 2004. Cloning, heterologous expression, and characterization of three aquaglyceroporins from *Trypanosoma brucei*. *Journal of Biological Chemistry*, 279, 42669-42676.
- VAN DER AUWERA, G. & DUJARDIN, J.-C. 2015. Species typing in dermal leishmaniasis. *Clinical microbiology reviews*, 28, 265-294.
- VAN HELLEMOND, J. J., OPPERDOES, F. R. & TIELENS, A. 2005. The extraordinary mitochondrion and unusual citric acid cycle in *Trypanosoma brucei*. Portland Press Ltd.
- VANNIER-SANTOS, M., MARTINY, A. & SOUZA, W. D. 2002. Cell biology of *Leishmania* spp.: invading and evading. *Current pharmaceutical design*, 8, 297-318.
- VASUDEVAN, G., CARTER, N. S., DREW, M. E., BEVERLEY, S. M., SANCHEZ, M. A., SEYFANG, A., ULLMAN, B. & LANDFEAR, S. M. 1998. Cloning of *Leishmania* nucleoside transporter genes by rescue of a transport-deficient mutant. *Proceedings of the National Academy of Sciences*, 95, 9873-9878.
- VÉLEZ, I., LÓPEZ, L., SÁNCHEZ, X., MESTRA, L., ROJAS, C. & RODRÍGUEZ, E. 2010. Efficacy of miltefosine for the treatment of American cutaneous leishmaniasis. *The American journal of tropical medicine and hygiene*, 83, 351-356.
- VINAYAK, S., PAWLOWIC, M. C., SATERIALE, A., BROOKS, C. F., STUDSTILL, C. J., BAR-PELED, Y., CIPRIANO, M. J. & STRIEPEN, B. 2015. Genetic modification of the diarrhoeal pathogen *Cryptosporidium parvum*. *Nature*, 523, 477-480.
- VINCENT, I. M., CREEK, D., WATSON, D. G., KAMLEH, M. A., WOODS, D. J., WONG, P. E., BURCHMORE, R. J. & BARRETT, M. P. 2010. A molecular mechanism for eflornithine resistance in African trypanosomes. *PLoS pathogens*, 6.
- VODNALA, S. K., LUNDBÄCK, T., YEHESKIELI, E., SJOBERG, B., GUSTAVSSON, A.-L., SVENSSON, R., OLIVERA, G. C., EZE, A. A., DE KONING, H. P. & HAMMARSTRÖM, L. G. 2013. Structure-activity relationships of synthetic cordycepin analogues as experimental therapeutics for African trypanosomiasis. *Journal of medicinal chemistry*, 56, 9861-9873.
- VOULDOUKIS, I., ROUGIER, S., DUGAS, B., PINO, P., MAZIER, D. & WOEHLÉ, F. 2006. Canine visceral leishmaniasis: comparison of in vitro leishmanicidal activity of marbofloxacin, meglumine antimoniate and sodium stibogluconate. *Veterinary parasitology*, 135, 137-146.
- W.H.O. 2020a. *Chagas disease (American trypanosomiasis)* [Online]. Available: https://www.who.int/health-topics/chagas-disease#tab=tab_1 [Accessed 19 May 2020].
- W.H.O. 2020b. *Epidemiological Situation, Leishmaniasis* [Online]. Available: <https://www.who.int/leishmaniasis/burden/en/> [Accessed 6 March 2020].

- W.H.O. 2020c. *Leishmaniasis* [Online]. Available: <https://www.who.int/news-room/fact-sheets/detail/leishmaniasis> [Accessed 17 March 2020].
- W.H.O. 2020d. *Trypanosomiasis, African* [Online]. Available: <https://www.afro.who.int/health-topics/trypanosomiasis-african> [Accessed 9 May 2020].
- WAJIHULLAH, K. & ZAKAI, H. A. 2014. Epidemiology, pathology and treatment of cutaneous leishmaniasis in Taif region of Saudi Arabia. *Iranian journal of parasitology*, 9, 365.
- WALKER, J. & SARAIVA, N. G. 2004. Inhibition of *Leishmania donovani* promastigote DNA topoisomerase I and human monocyte DNA topoisomerases I and II by antimonial drugs and classical antitopoisomerase agents. *The Journal of parasitology*, 90, 1155-1162.
- WALLACE, L. J., CANDLISH, D. & DE KONING, H. P. 2002. Different substrate recognition motifs of human and trypanosome nucleobase transporters selective uptake of purine antimetabolites. *Journal of Biological Chemistry*, 277, 26149-26156.
- WAMWIRI, F. N. & CHANGASI, R. E. 2016. Tsetse flies (*Glossina*) as vectors of human African trypanosomiasis: a review. *BioMed research international*, 2016.
- WANG, Z., GERSTEIN, M. & SNYDER, M. 2009. RNA-Seq: a revolutionary tool for transcriptomics. *Nature reviews genetics*, 10, 57-63.
- WHEELER, R. J., GULL, K. & SUNTER, J. D. 2019. Coordination of the Cell Cycle in Trypanosomes. *Annual review of microbiology*, 73, 133-154.
- WIEDEMAR, N., GRAF, F. E., ZWYER, M., NDOMBA, E., KUNZ RENGGLI, C., CAL, M., SCHMIDT, R. S., WENZLER, T. & MÄSER, P. 2018. Beyond immune escape: a variant surface glycoprotein causes suramin resistance in *Trypanosoma brucei*. *Molecular microbiology*, 107, 57-67.
- WIEDEMAR, N., HAUSER, D. A. & MÄSER, P. 2020. 100 years of suramin. *Antimicrobial Agents and Chemotherapy*, 64.
- WILKINSON, S. R., TAYLOR, M. C., HORN, D., KELLY, J. M. & CHEESEMAN, I. 2008. A mechanism for cross-resistance to nifurtimox and benznidazole in trypanosomes. *Proceedings of the National Academy of Sciences*, 105, 5022-5027.
- WILLERT, E. & PHILLIPS, M. A. 2012. Regulation and function of polyamines in African trypanosomes. *Trends in parasitology*, 28, 66-72.
- WRIGHT, N. J. & LEE, S.-Y. 2019. Structures of human ENT1 in complex with adenosine reuptake inhibitors. *Nature structural & molecular biology*, 26, 599-606.
- YOUNG, J., YAO, S., SUN, L., CASS, C. & BALDWIN, S. 2008. Human equilibrative nucleoside transporter (ENT) family of nucleoside and nucleobase transporter proteins. *Xenobiotica*, 38, 995-1021.

- YOUNG, J. D., YAO, S. Y., BALDWIN, J. M., CASS, C. E. & BALDWIN, S. A. 2013. The human concentrative and equilibrative nucleoside transporter families, SLC28 and SLC29. *Molecular aspects of medicine*, 34, 529-547.
- YSSEL, A., VANDERLEYDEN, J. & STEENACKERS, H. 2017. Repurposing of nucleoside-and nucleobase-derivative drugs as antibiotics and biofilm inhibitors. *Journal of Antimicrobial Chemotherapy*, 72, 2156-2170.
- YU, X., YANG, G., YAN, C., BAYLON, J. L., JIANG, J., FAN, H., LU, G., HASEGAWA, K., OKUMURA, H. & WANG, T. 2017. Dimeric structure of the uracil: proton symporter UraA provides mechanistic insights into the SLC4/23/26 transporters. *Cell research*, 27, 1020-1033.
- ZEUTHEN, T., WU, B., PAVLOVIC-DJURANOVIC, S., HOLM, L. M., UZCATEGUI, N. L., DUSZENKO, M., KUN, J. F., SCHULTZ, J. E. & BEITZ, E. 2006. Ammonia permeability of the aquaglyceroporins from *Plasmodium falciparum*, *Toxoplasma gondii* and *Trypanosoma brucei*. *Molecular microbiology*, 61, 1598-1608.
- ZHANG, C., XIAO, B., JIANG, Y., ZHAO, Y., LI, Z., GAO, H., LING, Y., WEI, J., LI, S. & LU, M. 2014. Efficient editing of malaria parasite genome using the CRISPR/Cas9 system. *MBio*, 5, e01414-14.
- ZHANG, K. & BEVERLEY, S. M. 2010. Phospholipid and sphingolipid metabolism in *Leishmania*. *Molecular and biochemical parasitology*, 170, 55-64.
- ZHANG, N., YIN, Y., XU, S.-J. & CHEN, W.-S. 2008a. 5-Fluorouracil: mechanisms of resistance and reversal strategies. *Molecules*, 13, 1551-1569.
- ZHANG, W.-W. & MATLASHEWSKI, G. 2015. CRISPR-Cas9-mediated genome editing in *Leishmania donovani*. *MBio*, 6, e00861-15.
- ZHANG, W.-W., PEACOCK, C. S. & MATLASHEWSKI, G. 2008b. A genomic-based approach combining in vivo selection in mice to identify a novel virulence gene in *Leishmania*. *PLoS Negl Trop Dis*, 2, e248.
- ZOLTNER, M., CAMPAGNARO, G. D., TALEVA, G., BURRELL, A., CERONE, M., LEUNG, K.-F., ACHCAR, F., HORN, D., VAUGHAN, S. & GADELHA, C. 2020. Suramin exposure alters cellular metabolism and mitochondrial energy production in African trypanosomes. *Journal of Biological Chemistry*, 295, 8331-8347.
- ZOLTNER, M., HORN, D., DE KONING, H. P. & FIELD, M. C. 2016. Exploiting the Achilles' heel of membrane trafficking in trypanosomes. *Current opinion in microbiology*, 34, 97-103.